INVESTIGATIONS ON AUTOMATED METHODS FOR DENTAL PLAQUE DETECTION

by

LUPITA JOCELIN REYES SILVEYRA

A thesis submitted to

The University of Birmingham

for the degree of

DOCTOR OF PHILOSOPHY

School of Dentistry
College of Medical and Dental Sciences
The University of Birmingham
September 2011

UNIVERSITY OF BIRMINGHAM

University of Birmingham Research Archive

e-theses repository

Abstract

This thesis investigated different quantitative methods for dental plaque detection using digital imaging. Firstly, based on a commercially available two-tone disclosing, the concentration of the dyes in the blue disclosing solution was calculated. This blue dye was used to disclose dental plaque accumulated on natural teeth and complete upper dentures (on two different backgrounds). Digital images were acquired under visible light, in the n-IR spectrum and with a narrow band-pass interference (NIB) filter tuned to the absorption spectrum of the blue dye. The results showed that disclosing dyes and disclosed dental plaque are transparent in the n-IR spectrum whilst the NIB filter maximised the contrast of dental plaque in the images when using the blue stain. A number of computerised segmentation methods were applied to these images showed automation of dental plaque detection to identify reliable methods to quantify plaque coverage. Although minor human intervention was still required in the segmentation process, the continuous development of new software promises that full automation in plaque quantification is almost a reality. Finally, analysis of the inter- and intra-examiner reliability of the commonly used Quigley and Hein index showed moderate reliability, highlighting the need for automated, quantitative and more reproducible methodology.

DEDICATION

To my parents

ACKNOWLEDGEMENTS

With gratitude:

To my parents, my biggest support, for giving me the essentials that I needed to get where I am now, for encouraging me to never give up; for showing me that anything is possible and you can always get further when you work hard. Thank you for being a continuous source of motivation. I admire you and love you both. This degree is for you.

To my brothers, Cuau for teaching me that no matter how big the physical distance is, it can always be shortened with love. For your patience, thank you for your visits that always brought some sunshine in the rainy days. Jor you started this, with braveness you left behind the comfort of the" known" to go in the search of your own destiny. You showed me the way, thank you for being an example in my life. Your wise words, given on the day that I left home, were always with me.

To my grandparents and my big and lovely family thank you for your advice and support I know that I can always count on you. I love you all.

To Martin, thank you for looking after me when I had no time for anything else. All I can say is that you were always there to hold me up when I thought that my strengths were no more.

To my supervisors: Prof. A. D. Walmsley and Prof G. Landini thank you for your guidance through my PhD.

To Prof Gareth Price from the University of Bath for his advice with the methodological procedures in the reverse engineering experiment to separate the components of the two- tone disclosing solution (Chapter 4).

Contents

List of Figures

List of definitions and/or abbreviations

Acceptable Daily Intake (A.D.I.): It is the maximum amount of a substance (food additive, drug) that can be consumed orally everyday over a lifetime without representing a risk for the health. It is expressed in milligrams of the substance per kilograms of body mass per day.

Active contours plugin or ABS snake: It is a semi-automatic method for segmentation of fine structures. It uses an active contour or a snake that is initiated by delineating by hand the approximate contour of the object to be segmented. In dentistry the snake method has been used in different studies to segment teeth from dental casts and radiographs (Danish, 2010, Marana et al., 2011).

AE: All examiners.

Analyte: In chemistry, is the substance determined by means of an analytical procedure.

Auto thresholding methods: 16 thresholding methods were used to choose from:

− *Huang* (1995): This method determines the thresholding value based on minimizing the measure of fuzziness (blurry) in an image using the Shannon's (or Yager) entropy function. The Huang method states that with a given threshold value, the pixels that correspond to a region are identified by the absolute difference between the grey level (shade of grey in a pixel) and the average level of the region (foreground or background) where that pixel is located.

− *Intermodes* (Prewitt and Mendenlsohn, 1966): Works based on a bimodal histogram. Here, the histogram is smoothed with the running average (size=3) until only two local maxima points are found. The thresholding point is the average of two local maxima.

– *IsoData* (Ridler and Calvard, 1978): This method divides the image into foreground (object) and background by an initial threshold based on the IsoData algorithm. Then, computes the averages of the pixels a) above the threshold point and b) below or at the threshold point. These two values are averaged again and the process is repeated until the threshold value is larger than the result from the averages. This is the default method used in ImageJ.

– *Li* (Li and Lee, 1993, Li and Tam, 1998): Based on the Li and Lee algorithm which uses the histogram to minimise the cross entropy between both the segmented and the original image.

– *MaxEntropy* (Kapur et al., 1985): Applies the Kapur-Sahoo-Wong (Maximum Entropy) algorithm based on the entropy concept. The algorithm chooses the threshold in the grey-level histogram of an image for its segmentation.

– *Mean* (Glasbey, 1993): The threshold point is set using the mean of the grey levels in the image.

– MinError(I) (Kittler and Llingworth, 1986): This is an iterative (mathematical procedure that generates successive possible solutions) implementation of the Kittler and Illingworth's Minimum Error thresholding method that assumes that both the object and pixel grey level values present a normal distribution. The initial estimate of the threshold is computed using the Mean method.

– *Minimum* (Prewitt and Mendenlsohn, 1966): This method works in a similar way to the Intermodes one, as a bimodal histogram and a running average size 3 is used to smoothed it until only two local maxima points are found. The threshold **t** is: $y_{t-1} > y_t <= y_{t+1}$. Images with histograms with unequal peaks or a broad and flat valley are unsuitable for this method.

– *Moments* (Tsai, 1985): Computes the grey-level moments (quantitative measure of the shape of a set of points) of the image and then thresholds the image without modifying these moments.

– *Otsu* (1979): Uses an algorithm to separate the pixels in the grey level histogram of an image into two groups: background and foreground with the threshold separating both groups in a way that the weighted sum of their variances (intra class variance) is minimum.

– *Percentile* (Doyle, 1962): Assumes the fraction of foreground pixels to be 0.5.

– *RenyiEntropy* (Kapur et al., 1985): Similar to the MaxEntropy method but applying the Renyi's entropy.

– *Shanbhag* (Shanbhag and Abhijit, 1994): Represents a modification to the *MaxEntropy* method based on the frequency of occurrence of the pixels in the image grey level histogram.

– *Triangle* (Zack et al., 1977): Uses the Triangle algorithm (geometric method) for the images thresholding. It assumes a maximum peak (mode) near one end of the histogram and searches towards the other end, the algorithm finds on which side of the max peak the data goes the furthest and searches for the threshold within that largest range.

– *Yen* (Yen et al., 1995, Sezgin and Sankur, 2004): Implements the Yen's multilevel thresholding method to the image grey level histogram.

BinaryFilterReconstruction plugin: Removes 8-connected particles in a binary image that otherwise would disappear after n erosions. Its main difference to "morphological opening" is that preserves the original shape of the particles while "opening" smoothes them.

BinaryGeodesicDilateNoMerge8 plugin: Reconstructs a grey scale image using 8-neighbour geodesic dilations of a seed image under a mask image.

Boxcar width: This function averages the points in the graph from the spectrophotometer to create a smoother graph by reducing the noise.

CalculatorPluss plugin (Rasband and Landini, 2004)**:** Allows to add, subtract, multiply or divide the pixels in a pair of images/stacks.

CDs: Complete dentures.

ChartWhiteBalance plugin (Vander Haeghen, 2007)**:**This algorithm compensates the lighting and exposure variations in the image by scaling the colour channels to the standard RGB (Red, Green and Blue) colour space values (sRGB= 6500K) which represents the direct visualisation of the imaged scene under a blue noon sky. The program also provides the resolution of the pixels near to the chart which allowed the later measurement of both the exact distance and the area of the image.

Colour deconvolution: It is a procedure used in histology to separate two or three stains generated by colour subtraction based on pre-determined colour vectors (e.g. Haematoxylin and Eosin) but it is also possible to create new vectors and to define the vectors from a ROI in an image.

DBB: Dentures on a Black Background.

DWB: Dentures on a White Background.

FYS: Final Year Students.

ICT: Clinical images.

ImageCalculator command: Computes a new image from two single images or stacks executing not only arithmetic operations but logical ones between two images or stacks.

Both methods the CalculatorPluss and the ImageCalculator produce a new image with pixels matching (according to the operation) the corresponding pixels from both original images/stacks however the difference between both approaches is that CalculatorPluss allows scaling (re-size) of the resulting image.

Integration time: Interval in the spectrophotometer over which measurements are taken. Longer integration times allow more averaging to filter out background noise.

Jitter: Function used in scatter plots to show the density of a point. This is useful when the data contain overlapping values and it is desired to visualise how many points took that value. It adds small random offsets to the data.

K-means clustering segmentation: Classifies the pixels in an image by their proximity to its centroids (one for each cluster).

LLC: Lower Left Canine.

LLCe: Lower Left Central.

LLL: Lower Left Lateral.

LRC: Lower Right Canine.

LRCe: Lower Right Central.

LRL: Lower Right Lateral.

Macro smooth ROI3: Smoothes the coordinates of a pre-selected enclosed ROI by doing a running average of size 3 on it.

Mole (mol): Is the unit of material quantity according to the Standard International (SI). One mole is the number of atoms in 0.012 kilogram of carbon 12.

Morphological dilation: Adds pixels to the edges of the objects.

Morphological erosion: Removes pixels from the edges of the objects.

n-IR: Near-infrared.

NBI: narrow band pass interference.

nm: nanometres.

Organisation for Economic Co-operation and Development (OECD): it is an international organisation which hosts 30 membership countries: Australia, Austria, Belgium, Canada, the Czech Republic, Denmark, Finland, France, Germany, Greece, Hungary, Iceland, Ireland, Italy, Japan, Korea, Luxembourg, Mexico, the Netherlands, New Zealand, Norway, Poland, Portugal, the Slovak Republic, Spain, Sweden, Switzerland, Turkey, the United Kingdom and the United States.

Particles8 plugin: Calculates statistics measurements of 8-connected particles in an image.

PPI: Plaque Percent Index, it represents the proportion of pixels with dental plaque divided between the total pixels.

QD: Qualified dentists.

QHT: Quigley and Hein modified by Turesky index.

RGB stack: Stands for Red, Green and Blue which are the three hues of light that can be mixed to form any colour.

ROI: Region of interest.

Seeded Region Growing: Works on the principle that different set regions (seeds) are identified by the user. These seeds are then used to calculate the initial mean grey level per region and the algorithm computes which pixels belong (and which do not) to each region based on both a measure of similarity and the number or seeds.

Automatic thresholding: Refers to the separation of the pixels values in an image into classes depending on a given threshold value (e.g. object and background). There is no universal algorithm for images segmentation with many thresholding

methods available to choose from. For a review on medical image segmentation refer to Withey and Koles (2008).

ULC: Upper Left Canine.

ULCe: Upper Left Central.

ULL: Upper Left Central.

URC: Upper Right Canine.

URCe: Upper Right Central.

URL: Upper Right Lateral.

Introduction

The term "oral diseases" refers to a variety of health disorders that include caries, periodontal disease, oral cancer and lip and cleft palate among others. According to the World Health Organisation (WHO), oral diseases are considered a major health problem with caries and periodontal disease presenting the highest prevalence among them. Reports establish that approximately 5 billion people worldwide have experienced caries at some point in their life. Prevalence of caries in school children through the world ranges from 60 to 90%. Moreover, 5 to 20% of middle-aged adults worldwide suffer severe periodontal disease which may lead to tooth loss (Petersen, 2003). In the UK (excluding Scotland), two separate reports conducted every 10 to 11 years, the 2009 Adult Dental Health Survey or ADHS (The NHS Information Centre, 2011) and the 2003 Children's Dental Health Survey or CHDS (Pitts and Harker, 2005) state that there has been a reduction of the percentage of coronal caries for both children and adults. For periodontal disease, the results from the ADHS 2009 (The NHS Information Centre, 2011) showed that adults in the UK have a high prevalence (83%) of both periodontitis and its associated aetiological factors, plaque and calculus.

Treatment of oral health related problems in the population are expensive. Economically developed nations tend to allocate around 9% of their public health budget to pay these bills (OECD, 2010) while unfortunately less economically stable countries cannot afford to cover the costs of the oral health treatments. The WHO suggests that oral health programmes should be focused on the primary health care and prevention of oral diseases as by doing so the cost of the later treatment may be reduced. A healthy oral condition is also important for the general status of the

individual. Links have been established between the incidence of coronary heart disease, stroke, and pre-term low birth-weight babies in patients with periodontal diseases (Davies and Davies, 2005, Pihlstrom et al., 2005, Seymour et al., 2007). Bacterial plaque is the main causative factor in the initiation of dental caries and periodontal disease. Therefore the main purpose of oral hygiene is plaque control, to prevent its formation on the tooth or its subsequent removal. Dental plaque develops, accumulates and adheres to teeth and other objects in the mouth such as restorations and prosthetic appliances (Löe and Kleinman, 1986, Harris and Garcia-Godoy, 1999, Manson and Eley, 2000). However plaque can be removed mechanically by means of tooth brushing and flossing and chemically with the aid of mouth rinses with antimicrobial agents.

Identification of dental plaque is difficult for both the patient and the dentist because the tooth and dental plaque have similar colours. Plaque may be "seen" via the aid of disclosing agents to change its colour so that it contrasts with the tooth surfaces (Tan, 1981). Red is a popular colour for disclosing plaque used alone or in combination with a blue dye (Block et al., 1972). However, red dyes have the disadvantage that they do not present a good contrast with the soft oral tissues (Kieser and Wade, 1976).

Dental plaque indices have been created as a tool to determine the efficacy of oral hygiene methods because they allow the measurement of the amount of plaque and the area of tooth covered by it, but in general all have advantages and disadvantages. Commonly used indices evaluate the extent of the tooth area covered by plaque. However, their assessment criteria are not consistent as the scores are generally based on an examiner evaluation whilst some other indices are not

practical for clinical use (Fishman, 1986, reviewed byMandel, 1974). The search for the ideal method to measure plaque accumulation (which does not rely on subjective assessment) is still ongoing and computerised methods have been proposed to solve some of the problems that traditional plaque indices may have with the scoring methodology.

Photography has been widely used in dentistry; as a general rule, photography uses the visible part of the electromagnetic spectrum to capture images, however both infrared and ultraviolet radiation can be also used. Near-infrared (n-IR) and ultraviolet photography are useful for imaging objects and materials which cannot be discriminated by the human eye in the visible spectrum. It may have a place as an alternative method for dental plaque detection (Vetter, 1992). Digital images can be obtained in both the visible and the n-IR region however to use them as a method to measure plaque coverage, it is necessary to make adjustments in the settings and to the photographic equipment. Once the n-IR image is obtained the information from this photograph can be compared with and subtracted from the visible photograph and data can be quantified.

Chapter 1
Overview

1.1. Anatomy of the oral cavity

The oral cavity, also called the mouth, comprises of the lips, palate, tongue, floor of the mouth and portions of the throat (Fehrenbach and Herring, 2007). The mouth has a wide variety of functions that range from the vital tasks of eating, and breathing (in combination with the oro pharynx) to social interaction that includes speech, kissing or playing a musical instrument.

The lips represent the transitional zone between the skin of the face and the mucosa of the mouth and present a darker appearance than the surrounding skin. This area is called the vermilion zone, and is limited by the vermillion border (Brand and Isselhard, 1994, Fehrenbach and Herring, 2007). The upper and lower lips join at each side of the mouth at the commissures. In its middle part, the upper lip has a prominent area called the tubercle that marks the end of the philtrum. This extends up to the nasal septum (Figure 1).

The oral cavity is lined by mucosa which varies in structure depending on its location in the mouth. The thick buccal mucosa is replaced by the thin-alveolar mucosa at the muccobuccal fold. After this point the tissue becomes attached to the bone and is called gingiva. The border between the gingival and the alveolar mucosa is called the mucogingival junction (Figure 2). The two bands of connective tissue in the mid line in the buccal side of both the upper and lower jaws are called maxillary and mandibular labial fraenum respectively (Fehrenbach and Herring, 2007).

Inside the oral cavity the following structures can be found: the tongue, the maxillary (upper) and mandibular (lower) teeth and the salivary glands.
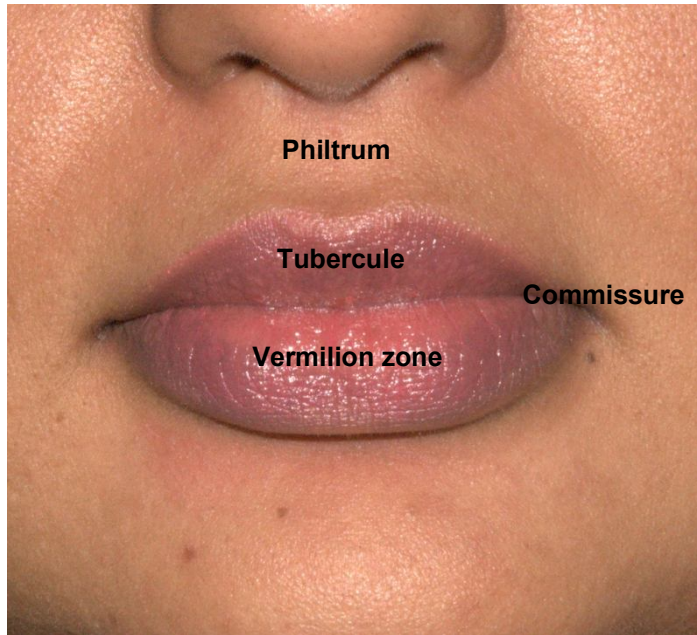
Figure 1 Frontal view of the lips.
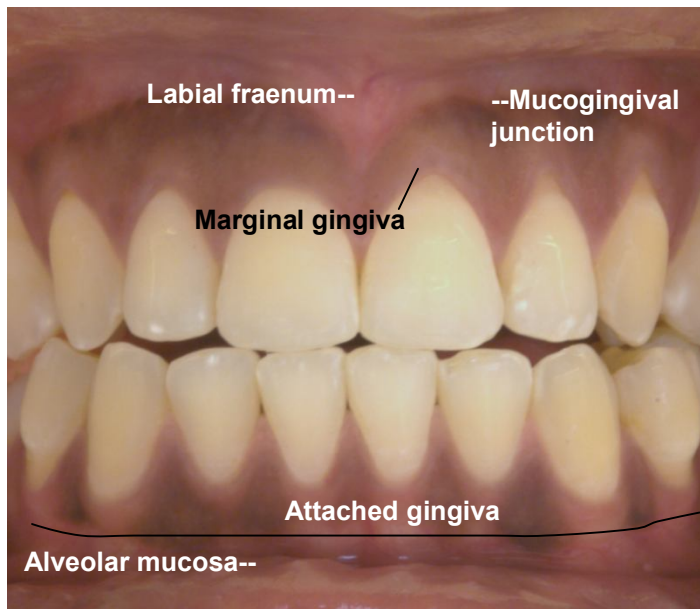
Figure 2 Gingiva and its components.

A tooth is one of 32 organs rooted in the alveoli (sockets) of the maxillary bone. In the adult there are commonly 16 maxillary (upper) teeth and 16 mandibular teeth divided into left and right central and lateral incisors, canines, first and second premolars and first, second and third molars. A tooth is formed by four tissues: pulp, dentine, enamel and cementum (Figure 3). The core of the tooth is the pulp which provides the sensorial, nutritional, defensive and reparative functions. The dentine forms the body of the tooth covering the pulp, and is protected by the enamel (the hardest tissue in the human body) in the coronal part of the tooth and by cementum in the root. The cementum also has collagen fibres that attach the tooth to the bone on one side and the gums on the other forming the periodontal ligament.

The supporting structures of the teeth form the periodontium which consists of the gingiva (free and attached), the alveolar mucosa, the cementum, alveolar bone and the periodontal ligament.

The gingiva covers the teeth and the alveolar bone. The free gingiva extends from the marginal gingiva to the base of the gingival sulcus. It is located around the tooth forming a collar and is separated from the enamel by the gingival sulcus which in healthy conditions should not be deeper than 3 mm (Carranza and Newman, 1996). The attached gingiva is the continuation of the marginal gingiva and adheres to the alveolar bone ending in the mucogingival junction. The attached gingiva is formed by many collagen fibres which connect via the cementum of the tooth to the gingiva. The colour of the gingiva is coral pink; however the pigmentation appears to be related to the melanin content of the mucosa therefore a person with darker colour skin may have darker gums. The gingiva is firm and resilient the teeth and their alignment in the arches determine its shape.

Enamel-------------

Dentine-------------

Gums-------

Pulp-------------

Periodontal

ligament---------------

Bone--------
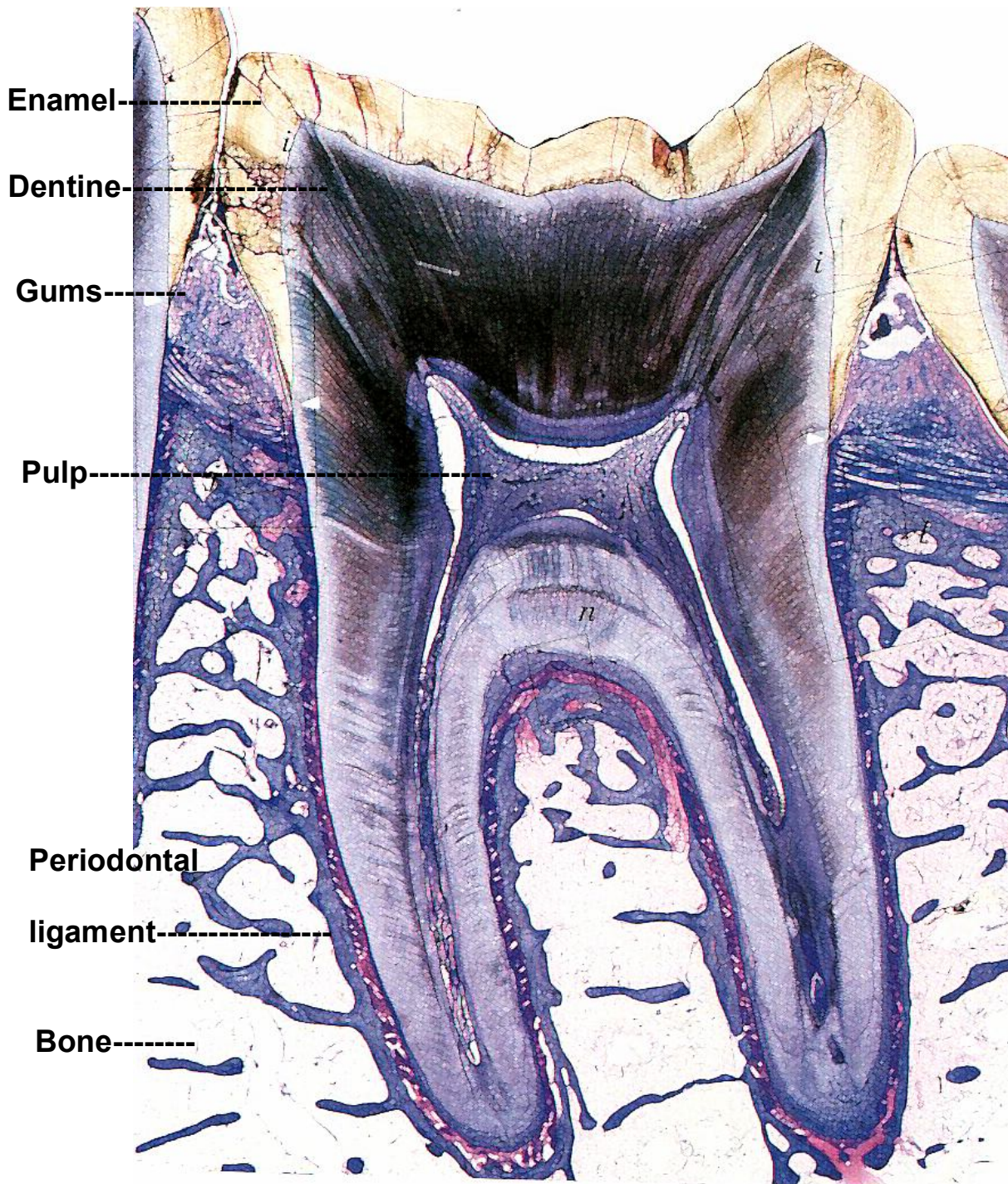
Figure 3 Anatomy of a tooth and its supporting tissues (from Urago, 1991).

The texture of the surface of the healthy attached gingiva is similar to an orange peel but this characteristic is temporarily lost when the gingiva presents with inflammation. Once the health is restored, the texture also recovers. The interdental gingiva is the gum that fills the space beneath the area of tooth-to-tooth contact. Its shape is described as a pyramidal or "col" shape but this depends on the position of the contact point between adjacent teeth (Carranza and Newman, 1996). The periodontal ligament is the connective tissue around the roots of the tooth and attaches the tooth root via the cementum to the bone. It is formed by different types of fibres and its functions are nutritive, supportive, sensorial, remodelling and formative. The bone that contains the roots of the teeth is called alveolar bone and its function is to give them mechanical support.

1.2. Oral health

Oral health refers to the disease-free condition where there is no pathology, defect or pain. The term is not only related to teeth and their supporting tissues, but covers all the structures that form both the oral cavity and the craniofacial complex. Oral disease is the state where health is compromised due to autoimmune conditions, developmental anomalies, neoplasms, infections and trauma. Tobacco use, unhealthy diet, excessive alcohol consumption and poor oral hygiene are risk factors that will lead to oral diseases such as infections and cancer. Oral health is part of general health therefore some general diseases such as haematological disorders (leukaemia, neutropenia), Sjögrens syndrome and the human immunodeficiency virus (HIV) infection may present with oral symptoms (Casiglia et al., 2009). Oral diseases may also affect the individuals' lives socially, economically and physiologically and in consequence have an impact on their quality of life (Reisine,

1985, O'Dowd et al., 2010). A study in the UK has shown that 51% out of 6,204 adults interviewed have had their lives affected by their oral condition in the 12 months previous to the application of the questionnaire. The experiences that the people in the survey reported as affecting their lives were varied and included pain, physiological discomfort, functional limitation and handicap (Nuttall et al., 2001). Dental treatments have a high demand from the population with also a high price associated. Many countries assign a large budget to deal with the cost and demand of dental treatments. Unfortunately, because of the disparities in the economical distribution, this is not always possible to achieve in poorer countries. The Organisation for Economic Co-operation and Development (OECD) reports that the average money spent for health of its 30 membership countries is 9% of their Gross Domestic Product (GDP) with 3% corresponding to public health and prevention programmes (OECD, 2010). In 2009, the UK spent 9.3% of its GDP (£1,396 trillion) to pay for the health bills (World Health Organization, 2010) with £3.30 billion allocated for dental problems (NHS and Department of Health, 2011). The United States of North America (USA) spent 16.2% of its GDP (US 14,043 trillion) on health with over 60 billion US dollars to cover the cost of oral health (US Department, 2000) whilst its total expenditure in 1999 for periodontal and preventive procedures was 14.3 billion US dollars (Brown et al., 2002). Prevention of a disease is likely to be cheaper and easier to undertake than the treatment. Therefore greater emphasis is placed on the development and application of preventive policies in dentistry.

1.3. Epidemiology of caries and periodontal diseases

The most prevalent microbial oral diseases are dental caries and periodontal disease. Reports of caries prevalence and incidence in the permanent dentition are

usually expressed using the DMFT (decayed, missed and filled per teeth) and DMFS (decayed, filled, and missed per surface) indices. The DMFT gives an accumulative number of teeth affected by dental caries while the DMFS reports the incidence or presence of new cases. Reports from the World Health Organisation (WHO) in 2004 and the OECD membership countries in 2006 showed that the global DMFT in 12 year-olds has remained the same with a value of 1.61 (Bratthall, 2005). However, dental caries has diverse epidemiological patterns in different regions of the world, with industrialised countries showing low prevalence whilst there is a high prevalence in developing countries. The reduction in caries prevalence in the industrialised countries may be related to the use of effective public health measures such as water and salt fluoridation (FDI, 1984, Petersen and Kawand, 2009). In the UK (excluding Scotland) the 2009 Adult Dental Health Survey-ADHS stated that the proportion of coronal caries in the adults participants in the survey was 29%. This number represents a reduction in the percentage of coronal caries for both England and Northern Ireland since the last survey in 1998 (Kelly et al., 2000, The NHS Information Centre, 2010). In children, the results from the Children's Dental Health Survey-CHDS (Pitts and Harker, 2005) showed that 43% of 5 year-olds had caries whilst in 8 year-olds 57% of the children had decay in at least one deciduous tooth. In the permanent dentition, the study reported the DMFT in children of three group ages. The age groups selected were 8, 12 and 15 year-olds and the caries prevalence was 14%, 34% and 49% respectively. These results show a reduction in the caries prevalence for children in the UK in comparison with previous surveys. For periodontal disease, the results from the ADHS 2009 (The NHS Information Centre, 2011) reported that only 17% of the dentate adults examined had healthy periodontal

tissues with 45% of the participants presented periodontal pockets, and 37% of them had a mild form of periodontitis with loss of attachment between 4mm and 6mm. Caries and periodontal diseases are the result of the interaction between the bacteria in the dental plaque and the host over a period of time (Marsh, 1994, Chapple and Gilbert, 2002a). Therefore oral infections can be prevented using different alternatives: increasing or modifying the host resistance (diet, dental sealants, fluoride), or by reducing or eliminating the microbial counts in the mouth. The response from the affected tissues to the lack of oral hygiene varies among individuals however clinical trials, epidemiological studies, microbiological research and immunological investigations have demonstrated that frequent professional tooth cleaning (prophylaxis) can assist to reduce dental disease (Lindhe et al., 1975, Lang et al., 1998, Manson and Eley, 2000).

1.4. Dental plaque

Dental plaque is a soft, non- mineralised, microbial biofilm, which develops, accumulates on and adheres to teeth, restorations and prosthetic appliances in the mouth (Löe and Kleinman, 1986, Harris and Garcia-Godoy, 1999, Manson and Eley, 2000, Kidd, 2005). Dental plaque is composed of salivary glycoproteins, bacteria (cocci, bacilli and filamentous forms) and their metabolic end-products arranged in matrix of extracellular material (Kidd, 2005). Clinically, thick layers of dental plaque appear as yellowish or grey deposits which can be only removed mechanically (Harris and Garcia-Godoy, 1999). Dental plaque is classified according to its location on the tooth in relation to the gingival margin, into supragingival plaque which is located above the gingival margin, and is visible in the oral cavity and subgingival plaque which is located below the gingival margin (Löe and Kleinman, 1986).

1.5. Stages in plaque formation

There are three major stages in plaque formation (Löe and Kleinman, 1986, Harris and Garcia-Godoy, 1999) with the microbial aggregation increasing in complexity over time (Page, 1986). The first stage is the **pellicle formation** or acquired saliva pellicle which is a thin, bacteria free, pellicle that protects the surface of the tooth by regulating the mineral ions exchanged between the tooth and saliva. It is formed rapidly after tooth cleaning by selective absorption of glycoproteins from saliva. The second stage is the *initial colonisation* which occurs within minutes to hours after the pellicle is deposited and it refers to the stage where the pellicle is populated with bacteria. These bacteria are predominantly gram-positive facultative (*Streptococccus sanguis, oralis and mitis and Actinomyces viscosus)*. Initially, there are a few plaque deposits which increase with time (Manson and Eley, 2000). The last stage is the development of complex flora or **plaque maturation** where the early supragingival plaque changes from simple gram-positive coccal bacteria to a complex flora with gram-positive and gram-negative rods and spirochetes (Chapple and Gilbert, 2002b). The presence of gram-positive bacteria enhances the colonisation of other species such as the gram-negative rods by co-aggregation. Plaque reaches the mature stage after 7 to14 days and becomes relatively stable around the 21st day (Harris and Garcia-Godoy, 1999). However, this is only a simple description of the bacterial composition of plaque. Location and rate of plaque formation present a broad variability between individuals as these factors are influenced by the oral hygiene habits, diet, saliva composition and the flow rate of each person. Smoking, calculus, overhanging restorations, malocclusions, and local factors such as enamel hypoplasia, cervical root resorption and cracks in the enamel, may also favour plaque

accumulation (Page, 1986). The term *Materia alba* refers to the visible yellow/white soft deposits formed by the combination between bacterial deposits and epithelial cells that can be removed by rinsing off with water. Calculus is formed by calcium phosphate and consists of the mineralised bacterial plaque. Calculus is classified depending on its location on the tooth. Supragingival calculus is usually located near to the opening ducts of the salivary glands; its surface is porous and presents a yellow-white appearance which can adopt a darker colour by extrinsic staining in consequence of smoking, consumption of red wine and tea (tannins) and the application of agents such as chlorhexidine. Subgingival calculus has a green-black colour and it is firmly attached to the root of the tooth making necessary to use scaling instruments for its removal (Seymour and Heasman, 1992).

1.6. Microorganism associated with oral diseases

The oral flora distribution is not homogenous and its presence and proportion varies depending on the site in the mouth (Mager et al., 2003). Many of the oral diseases are polymicrobial with specific microorganisms responsible for certain pathological conditions. Sometimes, these organisms are also related to the stage of the disease with changes between the acute and chronic phases (Jenkinson and Lamont, 2005, Parahitiyawa et al., 2010). Table 1 shows the typical microorganisms that are present in the oral cavity during health, and disease. It is by no means a complete list.

Table 1 Some of the microorganisms found in the oral cavity in the stages of health, caries and periodontal diseases (adapted from Marsh, 1992, Chapple and Gilbert, 2002b, Parahitiyawa et al., 2010).

Health		*Streptococcus mitis, Streptococcus oralis, Streptococcus sanguis, Actinomyces viscosus, Actinomyces naeslundi, Neisseria spp, Haemophilus spp, Fusobacterium naviforme*
Caries	Enamel	*Streptococcus mutans, Streptococcus sobrinus, Lactobacillus spp, Prevotellae* and occasionally *Candida yeasts*
	Root	*Streptococcus mutans, Actinomyces viscosus, Lactobacillus*
Periodontal disease	Gingivitis	*Streptococcus sanguis, Streptococcus milleri, Actinomyces israelii, Actinomyces naeslundii, Actinomyces viscosus, Capnocytophaga spp, Fusobacterium nucleatum, Veillonella spp, Treponema,* possibly *Bacteroides gingivalis, Eikenella corrodens, Porphyromonas gingivalis*
	Chronic periodontitis	*Porphyromonas gingivalis, Prevotella intermedia Fusobacterium nucleatum, Tannerella forsythia, Aggregatibacter actinomycetemcomitans, Selenomonas spp, Spirochaetes, Treponema denticola*
	Aggressive periodontitis	*Aggregatibacter actinomycetemcomitans, Capnocytophaga spp, Porphyromonas gingivalis, Prevotella intermedia, Tannerella forsythia, Bacteroides forsythus*

1.7. Dental caries

Dental caries is a localised disease that affects the mineralised structures of the tooth. It is a consequence of the interaction between the presence of bacterial dental plaque, fermentable carbohydrates in the diet, and a susceptible host within a period of time. The caries lesion occurs on teeth covered with plaque, where the equilibrium between the cycles of remineralisation after demineralisation is lost. The main component of the tooth (hydroxyapatite) loses more minerals (calcium and phosphate) than those it is capable of regaining. Demineralisation refers to the loss of mineral ions from the tooth when the pH of plaque falls from its normal value (pH around 7). However, the critical pH at which demineralisation occurs is variable among individuals and its dependant on the concentrations of calcium and phosphate in both the saliva and plaque. This is because higher concentrations of calcium and phosphate in the saliva and plaque require a lower pH to trigger the demineralisation process on the tooth (Dawes, 2003). Remineralisation occurs when minerals such as calcium, phosphate and fluoride are reincorporated into the tooth by the action of the saliva (Kidd, 2005, Fejerskov and Kidd, 2008). The carious process can be presented as inactive or active; however either condition can change at any time if the remineralisation and demineralisation balance is altered. When the lesion is inactive the caries lesion becomes "arrested". In the active process the bacterial invasion continues, with mineral dissolution, bacterial colonisation and cavitation of the enamel. If the demineralisation process continues the microorganisms eventually reach the dentine and the pulp, which leads to infection and death of the pulp with a subsequent spreading of the infection in the periapical tissues. The carious progress takes around 4 to 7 years for the lesion to penetrate the enamel and 4 more years to

reach the pulp (Mount, 2005, Fejerskov and Kidd, 2008). However, lesions progress faster in young age groups (Stookey, 2005). The early caries lesion or white spot is reversible up to the point where no cavitation is present on the tooth's surface (Mount, 2005) but once the continuity of the hard tissues on the tooth is lost, it is necessary to replace the damaged area with dental materials.

Many bacteria in dental plaque are acidogenic and aciduric; two specific characteristics which benefit the caries process. The former is its capacity to produce acids as a by-product from the fermentable carbohydrates (sugars) in the diet while the latter is the ability to grow in an acidic environment. Fermentable carbohydrates in the mouth are needed to produce the environment for bacterial growth however; the cariogenic ability of the diet depends on the food's adhesiveness and the frequency of its exposure on the tooth surface. Higher rates of demineralisation are more likely to occur in the presence of sticky food and with high-frequency consumption of low molecular weight carbohydrates (sugars) as these are utilised by the bacteria to form extracellular polysaccharides which creates a thicker and a stickier dental plaque. Sucrose is the most cariogenic sugar as it can be polymerised into glucans (dextran) and levans which can be used by the bacteria in the plaque to produce energy with acid as the final product of its metabolism (Kidd, 2005).

Three hypotheses have been proposed to explain the relationship between plaque and caries. The **specific plaque hypothesis** states that unique microorganisms are associated with the disease, with *Streptococcus mutans* showing the most important role. **The non-specific plaque hypothesis** relates the caries process as a result of the overall activity of all the microorganisms in plaque. Finally the **ecological plaque hypothesis** is based on the premise that the pathogenic organisms that cause the

disease are present in healthy areas and the body keeps them under control. The

disease is manifested if this equilibrium is lost by a change in the local environment.

The caries lesion can take place on any surface of the tooth with the cervical margin,

the proximal surfaces and the occlusal pits and fissures of the posterior teeth being

the most common places for its occurrence (Kidd, 2005).

Due to the multifactorial origin of caries its prevention has to involve different actions

aimed to reduce the frequency of sugar consumption from the diet (specially its

adhesive forms), incorporation of fluoride supplements and fissure sealing of the

occlusal surfaces, in addition to the traditional oral hygiene procedures for plaque

control (Anusavice, 2005). Additional activities include utilisation of antibacterial and

bactericidal agents and use of sugar substitutes like xylitol, sorbitol and mannitol.

1.7.1. Caries diagnosis

Early caries diagnosis allows for minimal intervention procedures. Traditional

methods of caries diagnosis are based on visual examination, gentle probing of the

surfaces and bitewing radiographs however, these techniques can detect caries once

the lesion has reached depths in the enamel of around 300 to 500µm (Stookey,

2005). Additional techniques include **F**ibre **O**ptic **T**rans**I**llumination (FOTI) and use of

elastic separators in the interproximal space to promote tooth separation of the area

where caries is suspected (Kidd, 2005). Once the teeth are separated, after a couple

of days, the dentist can visually examine the site or an impression of the area can be

taken looking for cavities or overhanging restorations. The FOTI consists of

transmitting visible light through the tooth with demineralised areas appearing as

shadows. However this method presents a limited sensitivity, especially in the

posterior region (Fejerskov and Kidd, 2008). New methods to diagnose caries are

focused on imaging techniques and comprise digital radiographs, quantitative light induced fluorescence (QLF), DIAGNOdent (KaVo Biberach, Germany) and electronic caries monitor or ECM (Angmar-Masson and Ten Bosch, 1987, Hall and Girkin, 2004). In QLF the tooth is illuminated with a blue-green Argon laser (peak 488nm) or with a blue 50-W Xenon arc lamp and a blue band pass filter (peak 370nm). This causes fluorescence of the sound tooth structure whilst demineralised areas look darker than the surrounding tissues. The device calculates the fluorescence loss of the carious lesion by subtracting the fluorescence of the lesion from the fluorescence of the surrounding tissues. The fluorescence is captured on a charge-coupled device (CCD) video camera. The method has been proved to be successful to detect caries with depths up to 400μm (Hall and Girkin, 2004, Stookey, 2004, Stookey, 2005, Tranæus et al., 2005, Fejerskov and Kidd, 2008). However, the readings may be affected when the diagnosis is done in the presence of saliva, dental plaque, stains or enamel fluorosis (Amaechi and Higham, 2002, Stookey, 2005).

DIAGNOdent is a portable tool that uses a red light source (peak 655nm) to measure the changes in the fluorescence intensity of the caries lesion. The device is based on the premise that under this wavelength the caries process shows an increased fluorescence. The unit gives the amount of fluorescence using a numeric display that ranges from 0 to 99 with 0 representing the minimum fluorescence. A further modification called the DIAGNOdent*pen* (KaVo Biberach, Germany) has been introduced by the same manufacturer to record interproximal changes as the original device was not able to do this. When the clinical performance of both instruments was compared, both showed an excellent sensitivity (samples correctly identified) with no differences reported between them but specificity was low (Tranæus et al.,

2005). Some factors that may affect the readings are presence of plaque, calculus and stains on the tooth surface as well as its degree of dehydration (Tranæus et al., 2005, Yang and Dutra, 2005, Fejerskov and Kidd, 2008).

The electrical impedance technique takes advantage of the high electrical resistance of the enamel to detect carious and demineralised (porous) enamel which are more conductive than normal dental tissues. The electrical conductance is measured placing an electrode on the tooth surface and closing the circuit through the patient. Extra care needs to be taken with dehydration of the tooth tissue as this may influence the results (Tranæus et al., 2005, Fejerskov and Kidd, 2008).

1.8. Periodontal diseases

Periodontal disease affects the supporting structures of the tooth and it is divided into two major categories: gingivitis as the pathology that affects only the gingival tissues and periodontal disease which damages the attachment structures of the tooth. The final diagnosis of periodontal disease is given by clinical examination supported with radiographs to identify bone loss. Saliva and biomarkers of periodontal inflammation are being investigated for future use as diagnostic tools (Pihlstrom et al., 2005), but the radiographic examination still remains the gold standard for detecting the disease.

1.8.1. Gingivitis

Gingivitis is considered the first stage of the periodontal disease and is the reversible inflammation of the gingiva with no involvement of the supporting structures (loss of periodontal attachment); therefore once the etiological factors are eliminated the oral tissues return to a healthy state. The causes of gingivitis are bacteria, hormonal imbalances, allergies nutritional deficiencies, systemic factors and drugs. Bacterial

gingivitis represents the most common type of the disease and it is developed within 3 to 4 days without oral hygiene (Carranza and Newman, 1996). Gingivitis is divided in three stages: initial, early and established (chronic). The initial stage presents only subclinical and histological changes which are manifested as an increase of the inflammatory cells and the flow of the gingival fluid. The early gingivitis is recognised by a mild inflammation of the gingiva with loss of its stippling. In the established gingivitis the inflammatory state of the gums is increased, with fibrosis as a sign of lesion healing. The gums look swollen with a red and smooth glossy appearance and an augmented facility to bleed with or without stimulus (toothbrushing). The disease may also present with an unpleasant taste and smell (halitosis) for the patient (Manson, 1986).

1.8.2. Periodontitis

Periodontitis is classified as chronic (localised or generalised), aggressive periodontitis (localised or generalised) and periodontitis as a manifestation of systematic diseases (Chapple and Gilbert, 2002b). The disease is considered generalised if it affects more than 30% of the sites in the mouth. A further subdivision of each type of periodontitis is related to the rate of progression of the disease and is expressed as mild (clinical attachment loss of 1-2mm), moderate (clinical attachment loss of 3-4mm) and severe (clinical attachment loss higher than 5mm) with the disease alternating between periods of activity and inactivity. The presence of a periodontal pocket deeper than 3mm when measured with a periodontal probe is the main indicator for the existence of periodontal disease. The disease also presents with resorption of the alveolar crest, suppuration, tooth mobility (greater than 0.2mm),

tooth migration, gingival recession, periodontal abscesses, halitosis and furcation exposure (Manson, 1986, Carranza and Newman, 1996).

1.9. Oral hygiene procedures

A healthy oral condition is also related to an adequate general status of the individual (Davies and Davies, 2005, Seymour et al., 2007). Plaque removal can be performed by the patient using different tools such as toothbrushes (electrical and manual), dentifrices, dental floss, and mouth rinses. Moreover, a professional prophylaxis is also recommended as a complement to personal hygiene (Lindhe et al., 1975, Lang et al., 1998, Manson and Eley, 2000).

An efficient toothbrushing technique has been reported to remove 65% of the plaque on the tooth surfaces (Ireland, 2006). The optimal frequency of mechanical plaque removal to prevent dental caries and periodontal disease is unclear because of their multifactorial origin although, in the case of the gingivitis it has been stated that the first subclinical changes in the tissues appear after 2 days of the oral hygiene suspension. Based on this finding, a tooth cleaning with a frequency of at least twice a day is recommended (Lang et al., 1973, Carranza and Newman, 1996, Sgan-Cohen, 2005) as most of the patients do not achieve perfect plaque removal when they clean their teeth.

The aim of this thesis is:

- To investigate quantitative methods for dental plaque detection using digital imaging.

Objectives:

- Determinate the concentration of the dyes in disclosing solutions for the creation of a disclosing product with good contrast against the oral tissues.

- Standardise the methods of obtaining photographs of stained plaque including the camera settings.

- Develop an *in vitro* study for dental plaque detection in prosthetic appliances.

- Investigate the use of n-IR photography and a narrow band pass filter (NBI) for dental plaque detection on clinical images of disclosed plaque.

- Determinate the reliability of the Quigley and Hein modified by Turesky (QHT) dental plaque index.

Chapter 2
Literature review

2.1. Dental plaque disclosing agents

The identification of supragingival dental plaque is difficult for both the patient and the dentist because of the colour similarity between the tooth surface and dental plaque. Plaque identification may be done either by screening the plaque directly from the tooth surface (Löe, 1967), changing its colour with a disclosing solution (Gillings, 1977) or using the ability of natural teeth to fluoresce under blue light (Lang et al., 1972).

Disclosing dyes work by changing the colour of dental plaque so that it contrasts with the white tooth surface (Figure 4). Dental plaque has the ability to retain a large number of dye substances which can be used for disclosing purposes. This property is related to interaction because of the polarity difference between the components of the plaque and the dyes (Gallagher et al., 1977). Particles are bound to the surface by electrostatic interaction (proteins) and hydrogen bonds (polysaccharides).

Over the years different staining agents have been used. The first chemical reported to stain plaque was Iodine (Skinner, 1914) but over the time a variety of dyes have been used including fuchsine, erythrosine, merbromin, methylene blue, brilliant blue, crystal violet, gentian violet and fluorescein (summarised by Tan, 1981). Some of these dyes can be toxic or carcinogenic at a certain concentrations while others may not provide enough contrast with the surrounding tissues (Block et al., 1972). Researchers have suggested the utilisation of food colourants for plaque detection as these substances are safe to use, widely available and in most cases cheaper than

the commercial dental plaque detectors (Kieser and Wade, 1976, Caride and Meiss, 1981).

Disclosing agents are also used to evaluate and motivate patients into oral hygiene practices and are available as chewing tablets, solutions, disclosing gels and cotton buds (Figure 5). A common disclosing colour available in the market is red (usually erythrosine or phloxine) which can be used alone or in combination with a blue dye (generally Patent Blue V or Brilliant Blue FCF) to create a two-tone dye test aiming to differentiate new or recently formed dental plaque (red) from old plaque (blue). The colour difference is related to thickness of the plaque (old plaque is thick whilst the newly formed is thin) and is explained by an easier diffusion of the blue component (Block et al., 1972, Gallagher et al., 1977). Another proposed mechanism for the differential staining is the oxidation-reduction potential of the accumulated plaque and plaque maturation; the older plaque is thought to reduce the blue dye faster than the younger plaque (Katayama et al., 1975). Some of the problems arising from the use of red dyes include prolonged persistence on the tooth and both an intense stain and poor contrast of the soft tissues. Sodium fluorescein (a dye generally used in ophthalmic angiography) was introduced to eliminate the difficulties associated with using red colourants to stain dental plaque. This dye is only visible under light sources with frequencies in the range of 200–540 nm (Cohen et al., 1972, Lang et al., 1972, Gillings, 1977) with the peak wavelength set at 490nm (Vetter, 1992).

Figure 4 Disclosed dental plaque 24 hours after cessation of the oral hygiene

methods. Picture taken by author

Figure 5 A selection of commercially available dental plaque disclosing agents.

2.2. Dental plaque indices

2.2.1. Assessment of plaque deposits

Patients and clinicians use plaque disclosing agents to verify the efficiency of the oral hygiene methods. To date four reviews on dental plaque have been published (Mandel, 1974, Fishman, 1979, Fishman, 1986, Pretty et al., 2005).

There have been a number of ways to categorise plaque accumulation however, an official classification for plaque indices does not exist. Dental plaque indices can be divided into non-quantitative and quantitative. Table 2 shows a proposed classification for dental plaque indices.

Two popular indices to evaluate dental plaque and the effectiveness of plaque removal tools, such as: toothbrushes and mouth rinses in clinical experiments are the Silness and Löe index (Löe, 1967) and Quigley and Hein modified by Turesky (QHT) index (Turesky et al., 1970). The "Simplified Oral Hygiene Index" or OHI-S (Green and Vermillon, 1964) is widely used in epidemiologic studies (Lang et al., 1998, Harris and Garcia-Godoy, 1999, Manson and Eley, 2000).

2.2.1.1. Indices to evaluate the tooth covered by plaque by surface:

      Labial/buccal and palatal/lingual surfaces

The dental plaque indices that quantify dental plaque by the extent of tooth covered by plaque are frequently used in the literature. These methods present a variable coding with the teeth-surfaces used depending on the author with most indices being designed to analyse only the labial and lingual surface of the six anterior teeth (canine to canine) which is less time consuming and facilities the data collection in large population studies expressing the results by means of ordinal codes (Lang et al., 1998).

Table 2 Proposed classification for dental plaque indices and indices that represent them.

---

1. Non quantitative indices.

    1.1. Non time depended.

        1.1.1. Tooth covered area by surface.

            1.1.1.1. Labial/buccal and palatal/lingual surfaces (including interproximal and occlusal plaque extensions): Ramfjord plaque index (1956) and its modification by Shick & Ash (1961). The Quigley & Hein plaque index (1962), the Quigley & Hein plaque index modified by: Turesky (1970), Ainamo & Bay (1975) and McCracken (2002a). The Axial Plaque Extension Index (Matthijs et al., 2001, Dombret et al., 2003), The Navy plaque index and its modifications by Elliot et al.(1972) by Rustogi et al.(1992), and Claydon & Addy (1995), and the OHI-S (Green and Vermillon, 1960).

            1.1.1.2. Other surfaces (occlusal surfaces, proximal surfaces): Carvalho et al.(1989), Addy et al. (1998), Levinkind et al.(1999) and the Proximal Plaque Extension Index (Matthijs et al., 2001).

        1.1.2. Gingival plaque thickness: the Silness and Löe index (Löe, 1967) and its modification by Van der Weijden et al.(1993).

        1.1.3. Binary indices (presence and absence): the cleanliness index (Chilton et al., 1962), the visible plaque index (Ainamo and Bay, 1975), the Patient Hygiene Performance Index (Podshadley and Haley, 1968), the Plaque Control Record by O'Leary et al.(1972), and the Plaque free score (Grant et al., 1988).

        1.1.4. Summarised indices: Plaque free surfaces(Coontz, 1983) and the Gingival Margin Plaque Index (Addy et al., 1983).

    1.2. Time dependent indices.

        1.2.1. Plaque accumulation over a period of time: The Plaque Formation Rate Index by Axelsson (2000).

2. Quantitative indices.

2.1. Dental plaque weight: Wet plaque weight: Gilmore & Clark (1975) and Trapp et al.(1975). Dry plaque weight: McCracken et al.(2006).

2.2. Planimetric indices: Plüss et al. (1974), Rekola & Shein (1977), Verran & Rocliffe (1986), Bergström (1980) and Söder et al.(1993).

2.3. Quantitative light induced fluorescence (QLF™): Coulthwaite et al.(2009), Stookey (2005) and Pretty et al.(2004, 2005).

2.4. Automated methods: Smith et al.(2001, 2004), Splieth & Nourallah (2006), Staudt et al. (2001), Sagel et al.(2000), Carter et al.(2004), and Kang et.al.(2006).

2.5. Plaque quantification using 3D co-ordinates: Yeganeh et al.(1999, 1995).

The Ramfjord plaque index, part of the "Periodontal Disease Index"-PDI (Ramfjord, 1956) was the first index to evaluate the presence of plaque. It measures six teeth (upper right first molar, upper left central, upper left first premolar, lower left first molar, lower right central and lower right first premolar) and takes into consideration the occlusal presence of plaque.

The coding values for the Ramfjord plaque index are:

code 0: no plaque

code 1: plaque present on some but not all of the interproximal and gingival surfaces of the tooth

code 2: plaque present on all the interproximal and gingival surfaces covering less than one half of the entire crown

code 3: plaque extending over all interproximal and gingival surfaces covering more than one half of the entire clinical crown

Shick and Ash (1961) introduced a modification that records plaque on the labial and lingual surfaces and scores the gingival half of the coronal surface of the teeth. The coding changes slightly as described below:

code 0: absence of dental plaque on the gingival half of the facial or lingual surface of the tooth

code 1: dental plaque covering less than 1/3 of the gingival half of the facial or lingual surface

code 2: dental plaque covering more than 1/3, but less than 2/3 of the gingival half of the facial or lingual surface

code 3: dental plaque covering 2/3 or more of the gingival half of the facial or lingual surface of the tooth

Subsequently, the Quigley and Hein (QH) plaque index (1962) was created with the purpose of giving more importance to gingival plaque formation. The scoring was limited to the labial surfaces of the anterior teeth coding plaque as:

code 0: no plaque

code 1:flecks or stains are found at the gingival margin

code 2: a definite line of plaque at the gingival margin

code 3: plaque on the gingival third of the surface

code 4: 2/3 of the surface are covered by plaque

code 5: more than 2/3 of the surface are covered by plaque

A further modification was made by Turesky et al. (1970) who suggested to record both labial and lingual tooth surfaces without considering the interproximal surfaces. This scoring still described only the extent of plaque in vertical direction, giving no attention to its mesiodistal extension. Figure 6 shows the QHT index.

Despite its inconveniences, the QHT index became very popular and underwent further modifications by Bay and Ainamo who introduced measuring the area of disclosed plaque (Bay et al., 1967, Ainamo and Bay, 1975) and recorded only the right side of the arch and then doubled the quantities to obtain a unique score per subject. The most recent attempt to improve the QH index was made by McCracken et al. (2002a) aiming to emphasise the importance of the mesiodistal extension of the plaque and the evaluation of subgingival plaque deposits. The index uses the WHO dental probe as a ruler, as it has a black-band which can be used as a marker to standardise plaque measurements. The probe is placed perpendicular to the gingival margin with the ball tip positioned sub-gingivally and swept around the tooth's surface. The index claims to evaluate both the subgingival plaque and the thickness

of the plaque in the gingival margin when the ball tip is swept sub-gingivally to identify the subgingival accumulations however no evidence is available to verify this.

The axial plaque extension index (APEI) also uses a periodontal probe to measure the extension of the accumulated plaque. The probe is held parallel to the long axis of the tooth, and the extension is measured to the closest 0.5mm starting from the gingival margin to the contact area with the adjacent tooth. Six scores are assigned per tooth, three in the buccal surface and three in the palatal one. This index has been reported to be complicated to perform and did not show advantages when compared with the visual plaque index (see 2.2.3 binary indices), the QHT index and the Navy plaque index modified by Elliot et al. (Matthijs et al., 2001, Dombret et al., 2003).

The "Navy plaque index" was created as a part of the Navy Periodontal Screening Examination (NPSE), developed at the Naval Academy to diagnose periodontal disease (Hancock and Wirthlin, 1977). This index evaluates six teeth: upper right first molar, upper left central incisive, upper left first premolar, lower left first molar, lower left central incisive and lower right first premolar. Each tooth is divided into four zones: gingival, mesial, distal and the remaining zones and a value of one is given to each zone with plaque, to give more emphasis to dental plaque in the gingival margin. The total score per tooth is obtained adding each score area. Subsequent modifications of this index were proposed to give more importance to the gingival area and to record very small changes of plaque accumulation in this zone (Elliot et al., 1972, Rustogi et al., 1992) and to attempt to move the scoring from the clinic to the laboratory using drawings and transparent grids, showing the need for some standardisation (Claydon and Addy, 1995).

31
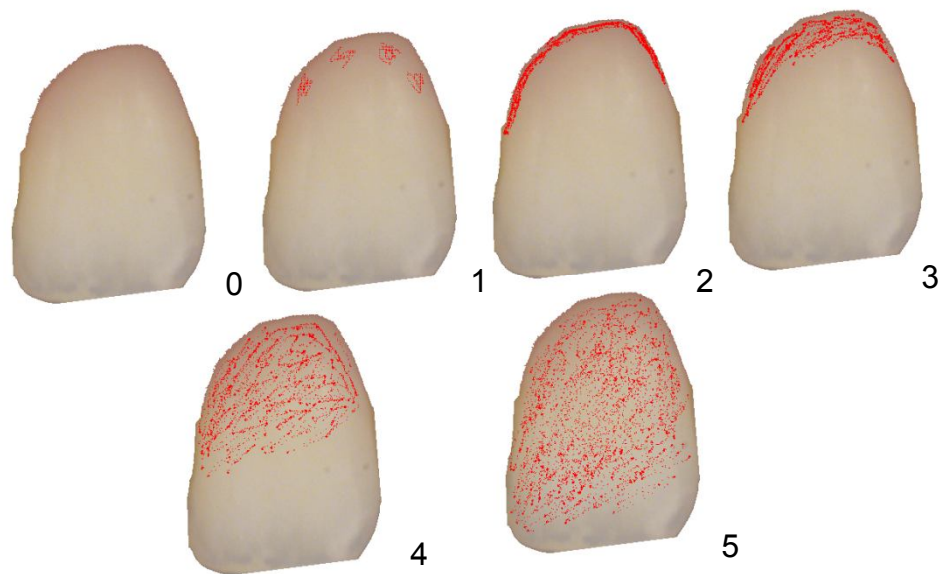
Code:

0   No plaque

1   Separate flecks of plaque at the cervical margin of the tooth

2   A thin continuous band of plaque (up to 1 mm) at the cervical margin of the tooth

3   A band of plaque wider than 1mm but covering less than one third or the crown of the tooth

4   Plaque covering at least one third but less than two thirds of the crown of the tooth

5   Plaque covering two thirds or more of the crown of the tooth

Figure 6 Scoring system for the Quigley and Hein modified by Turesky plaque index.

The "Oral Hygiene Index"-OHI (Green and Vermillon, 1960) has two components the debris index and the calculus index scoring 12 tooth surfaces each. The OHI-S is the simplified version of the OHI, because it only evaluates four posterior (first or second upper and lower molars) and two anterior teeth (upper right central incisor and lower left central incisor). The surfaces examined are the buccal surfaces of the upper teeth and the lower incisor and the palatal surfaces of the lower molar. The scoring codes for the plaque component are:

code 0: no debris or stain present

code 1: soft debris covering not more than one third of the tooth surfaces

code 2: soft debris covering more than one third but no more than two thirds of the examined tooth surfaces

code 3: soft debris covering more than 2/3 of the tooth surface

If the examiner is unsure about the scoring of one particular tooth, the lesser code value is used. The final plaque score is calculated by the sum of the scores for all teeth divided by the number of surfaces analysed. The final score ranges from 0-6, with 0.1-1.2 representing a good hygiene, 1.3-3.0 a fair oral hygiene and 3.1-6 a poor hygiene (Green and Vermillon, 1960, Green, 1967).

One advantage of non quantitative indices that measure the extent of tooth covered area by surface is the use of numerical indexing which is quick and easy. However, these indices are not sensitive enough for clinical studies because they cannot record differences in plaque removal before and after toothbrushing. This is related to the fact that the codes are expressed in ordinal values which make it difficult to analyse the difference between scores, therefore a code 2 is not always double the amount of plaque of code 1. Also the plaque patterns presented on a certain tooth

when the analysis is performed may not fit any of the set criteria in the code leaving it to the examiner to take the decision on how to code it, which in turn leads to a subjective index. Furthermore, the results from scoring non quantitative indices give ordinal data for the statistical analysis. To solve the subjectivity on plaque measurement the utilisation of dental probes as a marker (Matthijs et al., 2001, McCracken et al., 2002b), mathematical formulas and more complicated methodology beyond just a qualitative code were proposed (Harrap, 1974, Addy et al., 1983, Coontz, 1983). However, these indices were never very popular and their utilisation is limited. This is one of the reasons why many researchers carry on using the simple and better understood methods such as those of Silness and Löe (Silness and Loe, 1964) or QHT (Turesky et al., 1970).

2.2.1.2. Other surfaces: occlusal and proximal surfaces

Some indices are specifically designed to evaluate plaque on the occlusal surfaces (Carvalho et al., 1989, Addy et al., 1998, Levinkind et al., 1999). However, the evaluation of the occlusal surfaces is often difficult and requires operator training to achieve accuracy. In Carvalho's method (Carvalho et al., 1989), the distribution of the occlusal plaque on the four first permanent molars was assessed visually and with a detailed mapping on standardised drawings following occlusal surface morphology. The visual examination was recorded using four criteria ranging from:

code 0: no visible plaque

code 1: hardly detectable plaque restricted to the groves and fossae

code 2: plaque easily detectable in groves and fossae

code 3: occlusal surface partially or totally covered with heavy plaque accumulation

The distribution of plaque on the drawings was transformed into numerical indices ranging from 0 for no plaque to 2 for thick plaque accumulation. The results of this non-quantitative method indicated a relationship between the stage of eruption and plaque accumulation in specific anatomical sites in the first molars (Carvalho et al., 1989).

The index by Addy et al. (1998) evaluated the occlusal surfaces of premolars and second molars and recorded both the area (scored from 0 to 5) and units of area extent on drawings of the occlusal surfaces obtained from a tooth atlas. Plaque was measured with a graphics tablet and a pen attached to a microcomputer.

The index by Levinkind et al. (1999) evaluated plaque on un-restored upper and lower premolars and molars. The occlusal surface of each tooth was divided into four zones for the first lower premolar, into six zones for the upper premolars and second lower premolar and into nine zones for the molars,. The evaluation of the occlusal surfaces was reported to be difficult and training of the operator was required to achieve accuracy.

Plaque removal from the interproximal surfaces is often difficult; therefore indices are required to determinate interproximal plaque accumulation and removal. There are some approximal surface indices described in the literature (Wolffe, 1976, Wong and Wade, 1985, Fishman et al., 1987, Benson et al., 1993, Saxer and Yankell, 1997, Matthijs et al., 2001, Dombret et al., 2003) but these have not shown wide acceptance in clinical applications. The lack of acceptance may be related to the difficulty to assess the proximal areas making necessary to have some training is in its utilisation to achieve accuracy in addition to a time consuming application.

2.2.2. Gingival plaque thickness

The "Gingival Index"-GI (Silness and Loe, 1964) measures two variables (plaque and calculus) and can be used to evaluate the surfaces of either all teeth, or on individually selected teeth. A final score is given to represent the general status of the gums. The score is expressed in mild, moderate and severe inflammation and it is obtained by adding up the individual scores. The plaque component of the GI index is represented by the "Silness and Löe dental plaque *index" (*Löe, 1967*) and* evaluates the amount of undisclosed plaque at the gingival margin under direct visual examination by running a dental probe across the tooth surface. The evaluated teeth are dried using compressed air and no importance is given to the coronal extension of plaque. The criteria to quantify plaque are:

code 0: no plaque

code 1: plaque in the free gingival margin (recognised only by running the probe along the tooth)

code 2: moderate plaque accumulation identified by the naked eye

code 3: abundance of dental plaque on the gingival margin

Figure 7 synthesises the examination for recording the index. The examination starts with the upper right second molar continuing through the mid line to the upper left second molar. The distal, buccal and mesial surfaces are evaluated and after crossing the midline the evaluation changes in a reverse order. Once the mesial, buccal and distal surfaces are evaluated in the upper teeth, it is the turn for the assessment of the palatal surfaces starting with the upper left second molar finishing on the upper right second molar. The distal, buccal and mesial surfaces of the lower maxillary teeth are evaluated starting with the lower right second molar using the

same methodology as for the upper teeth. The surfaces in the right side are evaluated in the follow order: distal, buccal and mesial for each tooth while after crossing the midline the evaluation changes in a reverse order. Finally the lingual surfaces are scored starting with the lower left second molar.

The "Silness and Löe dental plaque index" together with the GI is used to provide evidence of the causal relationship between plaque and gingival inflammation (Manson and Eley, 2000). However, the correct visualisation of plaque without a disclosing agent is complicated.

A lesser used modification of this index made by Van der Weijden et al. (1993), analyses six surfaces in each tooth (buccal, lingual, mesial and distal, from the buccal and lingual side), thus giving more emphasis to the proximal surfaces and allowing the use of disclosing solutions for the scoring.

Evaluation order
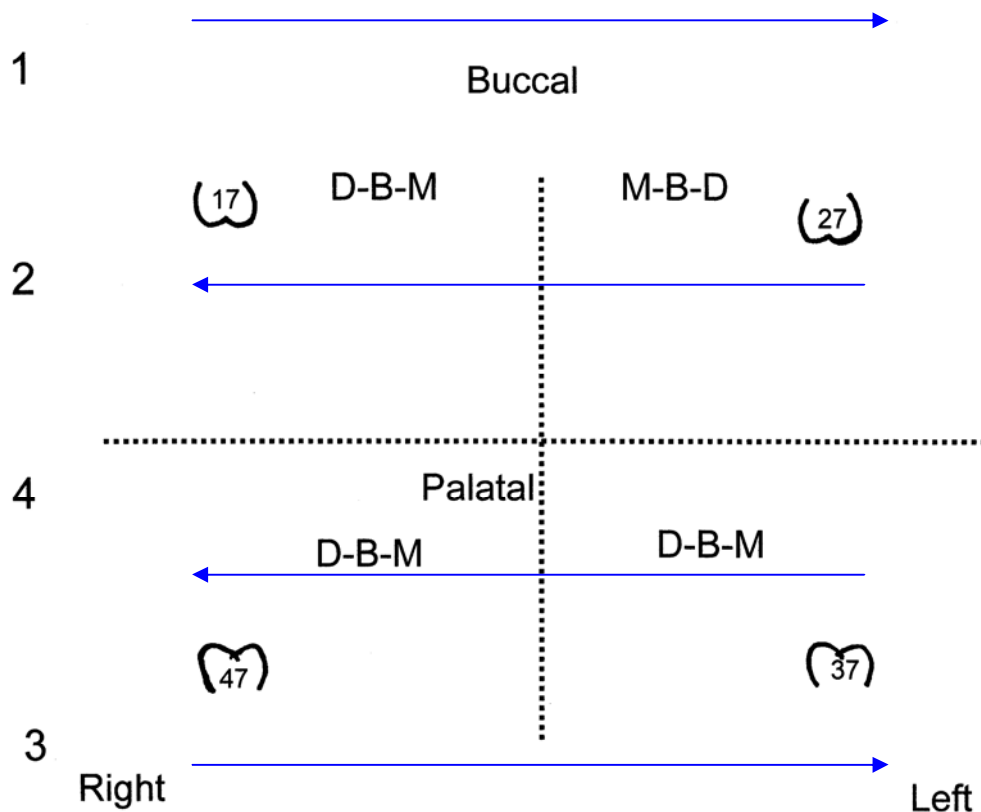
Figure 7 Diagram describing the Silness and Löe index plaque evaluation. The examination starts with the upper right second molar (1), assessing the distal, buccal and mesial surfaces continuing through the mid line where the evaluation changes in a reverse order, to the upper left second molar. Then, the palatal surfaces are evaluated starting on the upper left second molar finishing on the upper right second molar (2). The lower teeth are evaluated starting with the lower right second molar using the same methodology as for the upper teeth (3). Finally the lingual surfaces of the lower teeth are scored starting with the lower left second molar (4).

2.2.3. Binary indices

These indices, also known as "dichotomous", evaluate the presence or absence of plaque without considering its extent or quantity. The "Cleanliness Index" was the first index reported to measure the presence or absence of plaque. The examiner assigns a value from I to III depending on the amount of plaque remaining on the teeth after rinsing with a disclosing solution (Chilton et al., 1962). No further description is given on the way the coding method was done. Later on, the visible plaque index or VPI (Ainamo and Bay, 1975) attempted to make the patients aware of their oral health condition and motivate them to improve their oral health care. The VPI measures the presence of plaque without using disclosing agents and measures only the right side of the dentition to make the scoring system faster.

The "Patient Hygiene Performance Index" or PHP (Podshadley and Haley, 1968) was created to evaluate the patients' hygiene performance and their ability to follow toothbrushing instructions. It uses the same tooth surfaces as the OHI-S (described in page 33) but these are divided into five parts (Figure 8).

In the "Plaque Control Record" of O'Leary et al. (1972) dental plaque is recorded in a chart form where each tooth in the dentition is represented. Each tooth is divided in mesial, distal, buccal and palatal surface. Presence of plaque is registered filling the corresponding surface in the chart. It is suggested that this is done with red ink and missing teeth are crossed by a diagonal line. The number of surfaces with plaque is divided by the total number of tooth surfaces evaluated and multiplied by 100 to obtain a percentage. According to the index parameters 10% or less of plaque is a suitable goal for the patient (Figure 9).

Index 1   Index 2   Index 3

Index 4   Index 5
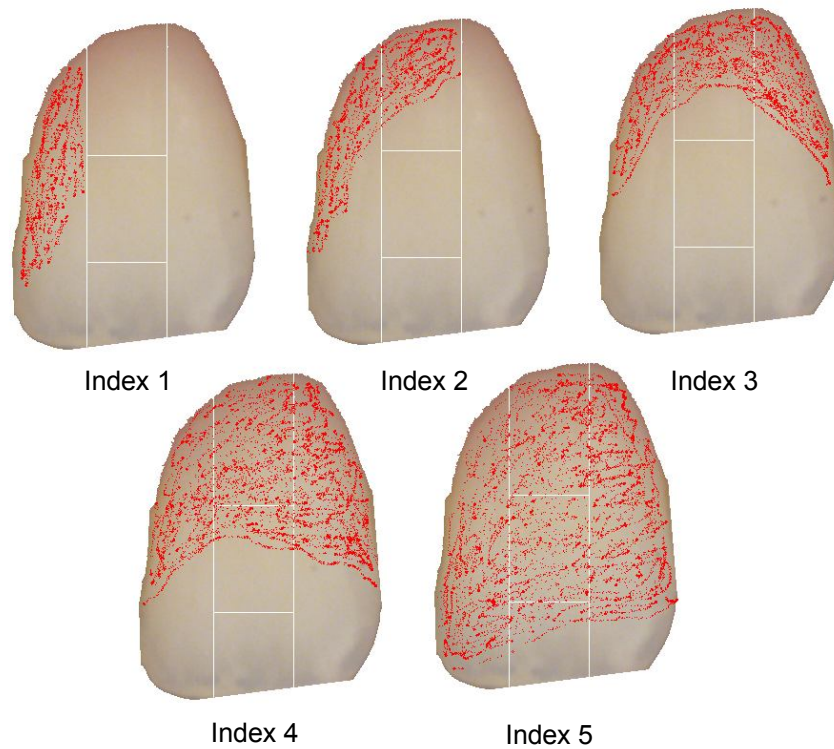
0   No debris or questionable

1   Debris definitely present

Figure 8 Representation of the division for the tooth's surface in the Patients Hygiene Performance index and the illustration of the different codes that a tooth can have. The tooth is divided into five parts (white lines). The examiner codes dental plaque as present (code 1) and absent (code 0). The sum of the surfaces with plaque corresponds to the index per tooth.
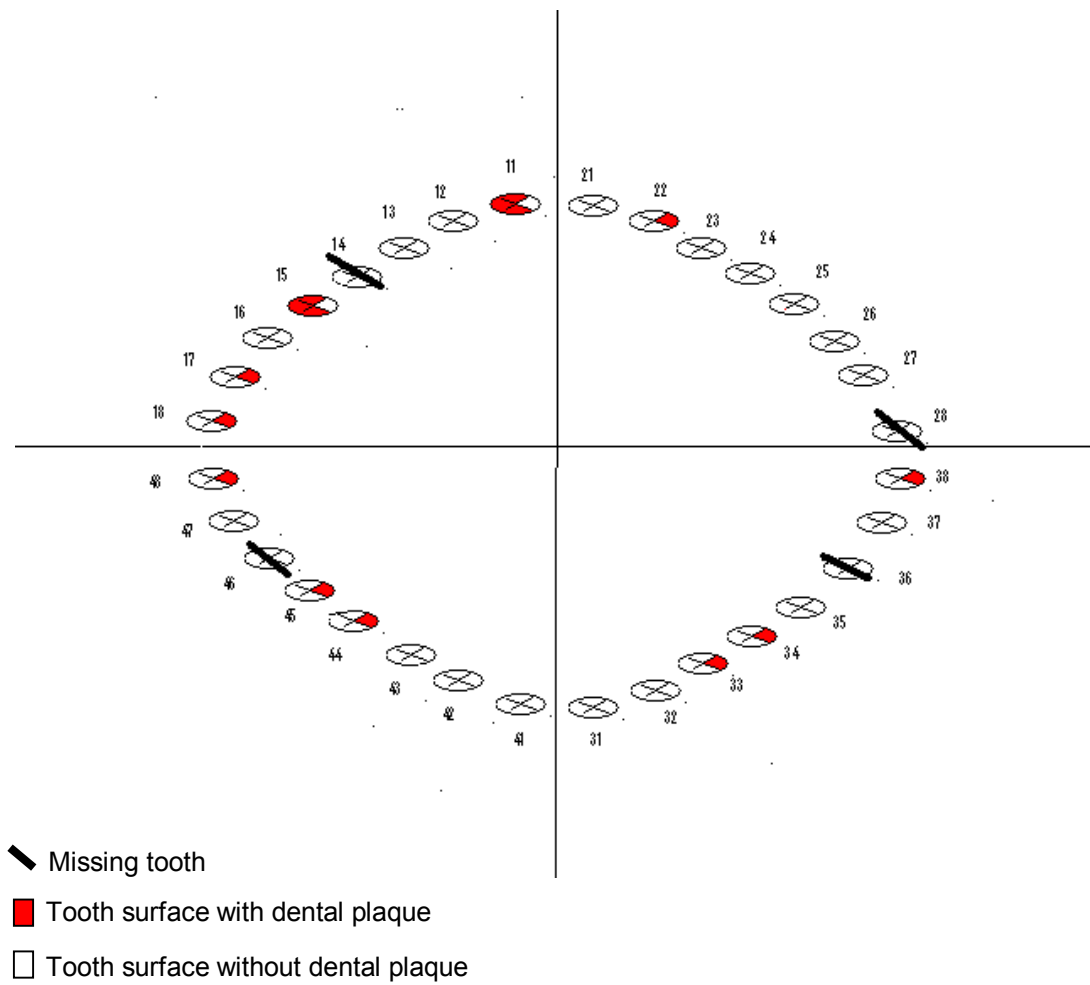
Figure 9 Representation of the O'Leary index plaque scoring system. Here, the examiner uses the chart to register the corresponding tooth surfaces (mesial, distal, buccal and palatal) where the patient presents dental plaque.

The "Plaque Free Score" only scores the presence and absence of plaque in a chart using red ink. However, this index expresses the results as the surfaces free of plaque (Grant et al., 1988).

Binary indices do not quantify the amount of plaque, but recording is easy and the final result is simple and understandable for both the professional and the patient. The results can be expressed as percentage of teeth with plaque, surfaces free of plaque or surfaces with plaque.

2.2.4. Summarised indices

The "Plaque Free Surfaces" (Coontz, 1983) and the "Gingival Margin Plaque Index"-GmPI (Harrap, 1974, Addy et al., 1983) were developed to measure small areas covered by plaque. The plaque free surface index divides each tooth into six surfaces: mesial, middle, distal in both the buccal and lingual sides. The presence of plaque on any surface was given a score of 1. The percentage of plaque free surfaces was calculated by multiplying the number of teeth by the number of total surfaces per tooth. The GmPI was expressed as $(x/y)*100$, where x is the surfaces covered with plaque and y is the total surfaces. This represents the percentage of the length of the buccal gingival margin and its visible proximal extension covered with plaque. Disclosed plaque is measured only on the buccal surfaces of all teeth (except second and third molars). Results for each tooth are averaged to obtain a plaque score for the whole dentition. These indices are not very popular and their utilisation is limited.

2.2.5. Time-dependent indices

These indices evaluate plaque accumulation over a period of time. The "plaque formation rate index" or PFRI describes the accumulation of disclosed dental plaque

24hrs after a professional dental cleaning in all but the occlusal tooth surfaces. The patient is instructed to avoid any dental hygiene procedures for the next 24 hrs. After this time the teeth are examined for adherent plaque according to the percentage of surfaces affected. A five points score is given according to the percentage of surfaces affected. The percentage ranges from a score 0 or absence of plaque (0%) to a score 5 (over 40%) which is related to a very high amount of plaque (Axelsson, 2000).

2.2.6. Quantitative indices

Quantitative measurements include: microbiological counts, carbohydrate and nitrogen content on dental plaque (Hotz et al., 1972) dental plaque weight, planimetric indices, quantitative light induced fluorescence (QLF) and computerised methods.

2.2.6.1. Dental plaque weight

Various attempts have been made to weigh dental plaque both wet and dry. Results from weighing wet plaque (Gilmore and Clark, 1975) are prone to inaccuracies because the evaporation of water affects the final outcome. Weighing dry plaque represents a challenge. As an attempt to collect dental plaque, Trapp et al. (1975) placed intraorally, a removable insert for the buccal surface of full-veneer gold crowns. Dental plaque was left to accumulate for periods of 3 and 5 days, giving instructions to the volunteers to suspend the oral hygiene (in the crown's area) for that period. Plaque weight was calculated as the difference between the weight of the crown before and after its insertion in the mouth. The plaque was left to dry at room temperature before weighing (Trapp et al., 1975). McCracken et al. (2006) weighed dry plaque collected from target sites of the proximal surfaces of six teeth. These

results were compared against the Turesky modification of the Quigley and Hein index. It was found that there were no advantages of weighing dry dental plaque in clinical trials and that determining plaque weight is a complex and time consuming process.

2.2.6.2. Planimetric indices

Planimetric indices were created as an attempt to automate the plaque evaluation process and avoid subjective judgement by operators. These methods are based on images of the teeth and the evaluation is done using the plaque percentage index (PPI), which represents the percentage of tooth surface covered with disclosed plaque (Pretty et al., 2005).

A photograph of the teeth is taken and the image is magnified to calculate the area, which is traced by hand onto a planimeter (millimetrical transparent paper) and projected onto a surface to count the number of involved grid units (Plüss et al., 1974) or digitised for further computer analysis (Rekola and Scheinin, 1977). One of the planimetric plaque index modalities involved the utilisation of the "Magiscan" television camera to display an image on a television screen connected to a computer (Verran, 1986). A further proposal was to use a special camera system consisting of a stereomicroscope with two cameras; obtaining right and left images simultaneously. To make this possible, it is necessary to have reference points in which the positions do not change (object points, surface of teeth) and the object is fixed to a holder in a well focussed position. It is suggested that the results obtained with the photogrammetric method present a linear relationship with the total score obtained with the QHT index (Söder et al., 1993).

Planimetric methods have several advantages: the determination of plaque quantity is made in an interval scale and it can quantify small differences in plaque accumulation. However, as plaque is measured in a two-dimensional image only plaque extension is assessed without considering its thickness. Human judgement is required to hand trace the area of interest making the method time consuming. Additionally standardised procedures while taking the photographs are needed to achieve accuracy and reproducibility.

2.2.6.3. Quantitative light induced fluorescence for plaque detection

QLF is defined as a "dental diagnostic tool for *in vivo* and *in vitro* quantitative assessment of dental caries lesions, dental plaque, bacteria activity, calculus, staining, and tooth whitening" (Angmar-Mansson and ten Bosch, 2001, Coulthwaite et al., 2009). Under QLF illumination dental plaque appears orange while teeth appear green. Fluorescence of dental plaque is thought to be related to the presence of porphyrins in certain bacterial species (Stookey, 2004, Stookey, 2005). For dental plaque quantification, QLF is used in combination with the planimetric methodology based on pixel counts to calculate the Plaque Percent Index or PPI. The patient is positioned using a head rest and the fluorescence from the oral tissues is captured on a CCD video camera. Image analysis is performed using computer software (Pretty et al., 2004, Stookey, 2005, Pretty et al., 2005).

The advantage of using QLF is that a small camera (without flashlight) is used to access the mouth which gives a live image enabling immediate review. However, visualisation of small amounts of plaque are difficult due to the short focal depth of cameras and fluorescence makes difficult to distinguish the borders of dental plaque which need to be outlined by the operator (Coulthwaite et al., 2009).

2.2.6.4. Computerised methods

Computerised methods take advantage of the imaging technological advances, and propose solutions to problems with the traditional methods for plaque quantification, such as the indices subjectivity related to the examiner intervention when coding the presence of plaque. Modern methods quantify plaque using computers and digital photographs whereas early computerised methods had to digitalise the printed photographs after these were taken. The method used for plaque quantification usually requires software that supports the application of masks which aids in the image analysis.

In imaging, a mask is a duplicate of an original image that is used to address specific information. For example, a binary mask contains only those pixels (set as foreground) that are of interest or fulfil certain criteria in the original image, whilst the rest of the pixels are set to the background value. The creation of masks enables the use of Boolean logical operations between the original image and the mask to extract the pixels of interest from the original without user intervention. The result is expressed as the number of pixels in the image counted as disclosed plaque to obtain the percentage of tooth area or Plaque Percent Index (PPI).

The advantages of the computerised methods for dental plaque quantification are: an increase in the sensitivity of the index, a reduction in the examiner subjectivity when recording plaque, the storage of the information for future analysis or re-evaluation and the presentation of the results on a continuous scale. The application of computerised methods for plaque detection has also brought new challenges such as the need for image standardisation including the positioning of the patient, camera's equipment used and the creation of contrast disclosing solutions recognisable by the

computer. Attempts have been made to standardise the acquisition of plaque images from the patient both intraorally and extraorally by using head and camera positioning devices, intraoral "positioners", scales or individual splints (Smith et al., 2001, Smith et al., 2004).

Computerised methods are commonly applied to photographs of the anterior teeth because these pictures are easier to obtain. Some studies have also tried to reproduce the position of the patient while taking images from the lingual and occlusal surfaces with the aid of mirrors (Staudt et al., 2001, Smith et al., 2004, Splieth and Nourallah, 2006). Measurement of dental plaque on lingual surfaces has been questioned as it has been shown not to increase the sensitivity of the system (Smith et al., 2004) and plaque measurement of the anterior teeth being representative of all the dentition (Lang et al., 1973). However, specific situations may need either a full dentition assessment or recording dental plaque on specific areas. A more rigorous plaque control regime is necessary when the patient presents an altered local oral environment (xerostomia) or systemic diseases (diabetes, cancer) as well as in patients who are under periodontal treatment or those who present an increased risk for caries development (Smith et al., 2001, Smith et al., 2004, Smith et al., 2006). Digital image acquisition for dental plaque quantification can be done using either a digital Single Lens Reflex (SLR) camera or an intra-oral camera. Smith et al. (2006) found that digital SLR cameras perform better because, even though intra-oral cameras can reach less accessible areas in the mouth, they present a limited depth of field (8-40mm) due to a fixed aperture. Therefore, the intra-oral cameras need to be positioned in close proximity to the object which results in an image that only covers two teeth in each measurement.

Many of the computerised methods used a red colourant (erythrosine) to disclose dental plaque, whilst others used fluorescein (FDC yellow No. 8) which is only visible under ultraviolet illumination with plaque appearing in a yellow-green colour (Hefferren et al., 1971). One study that combined the use of fluorescein to stain dental plaque with a digital image system to determinate the amount of disclosed plaque found that it was difficult to define the plaque borders in the tooth to calculate the area covered with plaque (Sagel et al., 2000). The amount of disclosed plaque was calculated according to the number of pixels corresponding to the disclosed plaque area.

2.2.7. Automated methods

A common problem that the automated methods face is that in some cases, human intervention is still required to "guide" the software in the analysis to quantify dental plaque. This can include locating the area that corresponds to dental plaque or isolating regions of interest. A few non-operator dependent methods aiming to automate plaque measurement have been reported including the studies by Carter et al. (2004) and Kang (2006, 2007). In the former, the investigators created a reference database to identify the Hue, Saturation and Intensity (HSI) colour space values of the colour components of the tooth, gingiva and disclosed plaque from digital pictures, of the six anterior teeth, on 25 volunteers. Methylene blue was used to disclose plaque and the image analysis was undertaken by using a computer imaging software. The authors also highlighted the option to use this method to quantify dental plaque on gingival tissues whilst in the latter; a Cellular Neural Network (CNN) technique was used to segment the images. The segmentation was done by analysing the histograms of digital images where a programme was used to

locate the thresholding point (minimum valley) of the histogram of grey scale values in images of teeth with plaque. These values where used to calculate the number of pixels representing plaque and teeth (Kang et al., 2006). A further modification of this study was made by combining the use of the CNN segmentation method with a fuzzy c-means clustering algorithm on HSI colour space images. The results were reported as the percentage of area covered by plaque (Kang et al., 2007).

Although important technological advances occurred, computerised methods are still being developed. Difficulties to undertake include problems related to the complexity of the methods, cost of the equipment, standardisation of the imaging techniques and accessibility to the areas in the mouth.

2.2.8. Plaque quantification using 3D co-ordinates

The oral structures and dental plaque are three-dimensional (3D) entities whilst digital images only represent them in two-dimensions, therefore as an attempt to measure dental plaque on the exposed root surface of a 3D tooth replica, a pilot study was developed by Yeganeh et al. (1995, 1999). A cast of the dentition was used to build an individual jig for the tooth to be analysed. On a subsequent visit of the patient, two vinyl siloxane impressions of the selected tooth were taken before and after plaque disclosing using a specially designed positioner to secure that the area impressed was the same. Casts of the tooth impressions were digitalised to visualise in 3D by recording its surfaces' co-ordinates using a laser probe mounted in a Co-ordinate Measuring Machine (CMM). Both replicas (before and after) were matched and superimposed to determine plaque thickness at the gingival margin. The results were from the 3D measurements were compared with the Silness and Löe plaque index (see 2.2.2). The results from the study showed a good correlation

between the Silness and Löe Plaque index and the 3D method, with thicker and more abundant presence of dental plaque near the gingival margin. However, this method only analysed the plaque at the gingival margin with no reference to the coronal extension. It must be also emphasised that to obtain the samples several steps are involved which may disrupt plaque formation, influencing the final result (e.g. high dependence of the quality of the sample on the impression material). At this stage of research, is still not possible to obtain a full intra-oral 3D scan of the dentition.

Chapter 3
Digital intraoral imaging

3.1. Introduction

The pinhole photography (camera obscura) represents the first attempt to capture images. The basic principles behind the camera obscura can be traced back to the 5th century BC (Hammond, 1981). Later, in the 19th century with the invention of the daguerreotype, the use of chemicals to record pictures started. Photography techniques went through rapid changes and for a long time relied on the reactions between chemicals in the presence of light to produce a photographic record until technology was developed to capture light in a photo-sensitive electronic device. This led to the replacement of the photographic films and the emergence of the digital image age. Today, classic film cameras are starting to be withdrawn from the market with some manufacturers not producing them anymore.

Digital cameras use a light-sensitive chip in the form of either a Charged-Coupled Device (CCD) or a Complementary Metal-Oxide Semiconductor (CMOS) which is attached to a lens. Digital images are formed by an arrangement of dots or pixels (picture element) in a rectangular grid. The lens quality and the numbers of pixels determine the sensor maximum image resolution. A higher number of pixels increase the image detail which leads to a bigger file size.

In comparison with classic film cameras, the digital ones present some advantages especially related to the large capacity of storage in memory cards and ability to view the image immediately after it has been captured. Moreover images can be transferred without the need for a dark room to process them (Bengel, 2002). Compact cameras tend to be aimed for general users who want a simple and

practical solution to take pictures. These cameras are usually easy to operate and to carry around due to their compact size however their functionality and features are limited. In contrast, professional digital single-lens reflex cameras (DSLR) work on the principle that a mirror reflects the light that comes from the lens through a separate optical viewfinder. DSLRs produce high quality photos due to large image sensors and allow a greater variety of image capture because the flexibility of the cameras to accept different lenses and external lighting (Hutchinson and Williams, 1999, Wall et al., 1999).

The exposure (amount of light that enters into the camera sensor) of an image is controlled by the combination of three factors: the aperture of the diaphragm in the lens, the shutter speed and the ISO sensitivity (International Organisation for Standardisation). The aperture relates to the diameter of the diaphragm at the time of exposure. It is represented by an "f-number" which ranges from 2.8 (aperture fully open) up to 32 (aperture at smallest opening) in standard lenses. Smaller apertures (larger numbers) increase the depth of field (Figure 10). The shutter speed is given in seconds or fractions of a second. It refers to the time that the film or sensor is exposed (Maheshwari and Kumar, 2011). The ISO is based on the old film system and determines the film sensitivity to light. In digital cameras, the ISO refers to a signal amplification of the photo sensor. Higher ISO numbers allow a faster shutter speed and larger aperture. ISO values higher than 400 are more prone to introduce noise to the image although many manufacturers have included noise reduction features in their cameras.

.
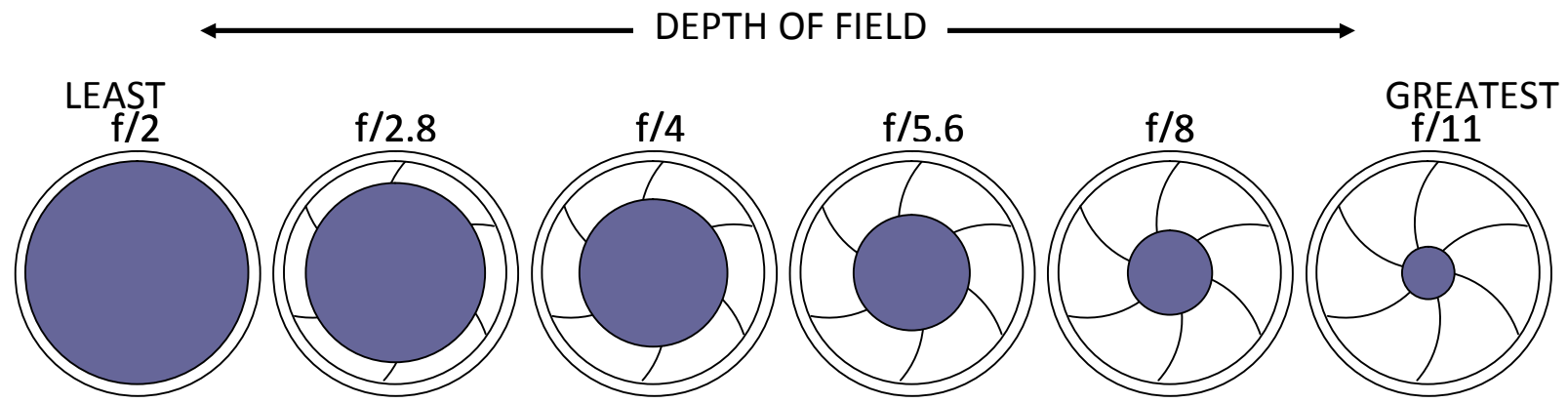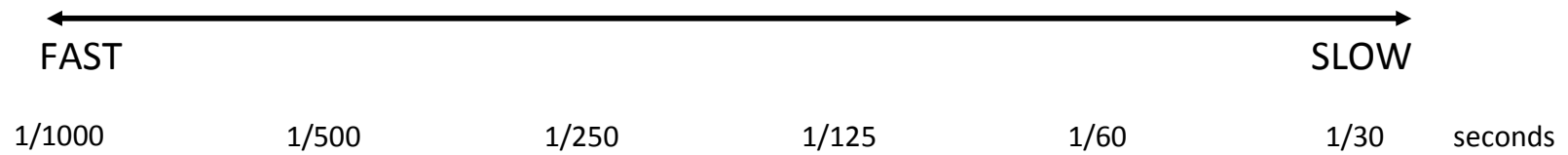
Figure 10 Relationship between the aperture and the shutter speed in a camera used to obtain a correct exposure.

In order to calculate the correct exposure of a picture the camera uses a photometer. There are several options for camera metering. In average metering the camera averages all the light that is coming into the metering cell. The reference values can be taken from the entire frame or sampling different subareas (matrix). The centre-weighted metering gives more emphasis to the values in the centre of the frame, and the spot metering acts in a similar manner to the centre- weighted metering. The difference being the measurement is taken from only a small area of the total frame. This area corresponds to the site that the user wants to emphasise (Coe and Weston, 2010).

The camera presents different exposure programmes, which include fully-automated settings, like program mode (P) where the best settings for the exposure are calculated automatically. Among the semi-automated programs there is an aperture (A) priority mode, where the camera selects the shutter speed according to the f/number set by the user. This is helpful when the user requires control of the depth of field (e.g. the object in focus with the background slightly out of focus). The shutter priority mode (S or TV) is the option where the user selects only the shutter speed and the camera selects the aperture. This mode is best for imaging moving objects. The manual (M) mode is the option where the user has complete control over the camera settings.

3.2. File formats

Once transferred to the computer, there are a large variety of formats to store digital images whereas three of the most popular ones are JPEG, TIFF, and RAW. The Joint Photographic Experts Group (JPEG) format is characterised by its compression properties where the final result is obtained by changing the colour details of the

pixels using algorithms which depend on the compression ratio. This format is useful for easy handling images on the Internet, emailing or for storing large amounts of images in a compact camera. The main disadvantage is that due to the compression of the image, valuable information is lost and the quality of the image decreased. Tagged Image File Format (TIFF) files are usually uncompressed but support compression without sacrificing the information from the image. It is a common option to store digital images because small size files contain large amount of information related to the image such as the dimensions or colours (Wootton et al., 1995) which reduce the time that the computer takes to process the images and making the archiving easier. The format also offers flexibility as it supports different compression schemes and can be used with different applications and formats (Burger and Burge, 2008). Finally, RAW files refer to the non processed (raw) data. This format stores all the information available when taking the image and allows its processing afterwards, however once this has been done the file needs to be saved under another file format (usually TIFF). RAW format is becoming the preferred option for digital photography.

3.3. Digital intraoral photography

Photography in dentistry is used within all its clinical specialities as well as in research. In the former, photography helps to document all the phases of the treatment including its progress and review after treatment as well as the self assessment of the quality of the treatment provided to the patient (Bengel, 2002). In the latter, records, illustrates and measures the changes that occur with the investigation. The basic dental photographic equipment includes a DSLR camera,

lenses, illumination (ring flash), lip and cheek retractors, and intraoral mirrors. The preferred lens for intraoral images is the 105mm macro (Williams, 1984).

3.4. Ultraviolet and infrared photography

The electromagnetic spectrum is formed by a continuous range of wavelengths but the human eye is only capable of visualising wavelengths between 400 to 700nm. The region located beyond the blue end is the ultraviolet (UV) whilst above the red end the infrared (IR) region is found. Images of UV, visible and IR can all be displayed in the visible range via filters (if the film or sensor is sensitive to these wavelengths). While the photoreceptor cells in the human eye can only react to in the visible part of the spectrum to some extent, both the films and sensor in the cameras can be sensitive to both the IR and the UV wavelengths. The sensors in many digital cameras are triggered by both the UV and IR radiation with the electronic device recording these signals and spilling the data into the visible range thus allowing its visualisation by the human eye.

3.4.1. Ultraviolet photography

The UV spectrum covers radiation with wavelengths from 100-400nm divided into three regions: UVA (315-400nm), UVB (280-315nm) and UVC (280-100nm). Most of the UV radiation that reaches the Earth's surface is composed of UVA rays with a small percentage (10%) of UVB. UVC is completely filtered by the ozone layer. Exposure to small amounts of UV radiation are needed to produce vitamin D, however in excess it can damage the skin (sunburn), the eyes (photokeratitis) and the immune system due to molecular and cellular changes that may modify or destroy cellular DNA by penetration of the UV energy into the eyes and the skin (Young, 2006). In photography only the wavelengths from 320nm to 400nm

wavelengths or near-ultraviolet (n-UV) can be captured due to the camera sensitivity. Some specialised film-based cameras are sensitive to record wavelengths from 250nm (Vetter, 1992). Recording any type of UV radiation requires care because the operator will not perceive its presence but still the radiation may represent a danger. The sources of UV radiation are diverse ranging from the sun, to electronic flashes, xenon lamps fluorescent tubes (black light) or mercury vapour lamps (Diffey, 2002).

Fluorescence refers to the characteristic of some objects which have the ability to "glow" once excited under a certain radiation source. It is the result of a change in the wavelength on the incident light (absorbed) once the object reflects it. Fluorescence radiation uses only UV light to illuminate the subject with no extra light present. Two filters are used, a transmission filter in front of the light source to promote fluorescence and an UV absorbing filter in front of the lens to block all the UV radiation from reaching the sensor. As a result this method records only visible fluorescence (Williams and Williams, 2002).

Ultraviolet photography has many applications in a variety of fields. In dentistry, dental tissues have the natural ability to fluoresce under UV radiation (QLF works on this principle) with teeth taking on a green colour; dental plaque is orange whilst calculus fluoresces with a yellow-orange colour. Some anomalies also present with a distinctive fluorescence pattern. For example enamel pigmentations appear as dark zones whilst tetracycline stains presents a yellow fluorescence. Hypoplastic enamel, cracks in the enamel and early caries lesion are more obvious under UV radiation (De Ment and Culbertson, 1951, Hefferren et al., 1971). Artificial fluorescence of dental plaque can be provoked by applying, sodium fluorescein (FDC yellow No. 8) which results in dental plaque glowing when illuminated under UV light. Other

applications for UV photography include dermatology for detection of changes in pigmented lesions, microscopy and microbiology where fluorescent markers are used to quantify bacteria and forensics where UV imaging can enhance detection of fingerprints and footprints. When combined with dentistry, reflected UV radiation has been used to assist the analysis of bite marks (Vetter, 1992).

3.4.2. Infrared photography

The IR is the part of the electromagnetic spectrum that comprises of wavelengths above 700nm to 1mm (Young, 2006) and it is divided into near, medium and far IR radiation. Of these three, only near-infrared (n-IR) wavelengths can be used in digital photography, as cameras are only sensitive to wavelengths up to 900nm. Reflected n-IR photography is based on the principle that the subject is illuminated with any radiation source including n-IR. An infrared transmission filter is attached to the front of the camera lens to block all the wavelengths except n-IR. Some examples of the filters available for n-IR photography are the Hoya R-76, R72 (Hoya Corporation, Japan), the Schott RG 715, RG 780, RG 830 (Schott AG, Germany), the Tiffen 87 (Tiffen Manufacturing CO., USA) and the Kodak Wratten 87 and 87C (Eastman Kodak, USA).Near-IR radiation is produced by the sun, tungsten sources, quartz iodine lamps and electronic flashes which can also be modified to produce only n-IR radiation.

Infrared luminescence refers to the photographic technique where luminescence from the object is recorded. Luminescence is a type of fluorescence where the object produces light in the IR region after being exposed to either visible or UV radiation. In the IR luminescence the photograph needs to be taken in absence of light. Two filters are needed, a blue-green on top of the light source (blue-green light) and an opaque

filter on the lens. The filter on the light blocks the infrared radiation that reaches the object whilst the filter on the lens allows only the produced IR radiation (from the object) to reach the sensor. The main disadvantage of this technique is the long exposure times (Williams, 1984, Vetter, 1992, DeBroux et al., 2007). Some tissues and objects have shown to have a strong luminescence such as chlorophyll, teeth, and healthy skin (Williams, 1984).

Generally all sensors in digital cameras are sensitive to IR radiation and this may reduce the quality of the image on the visible photography. To eliminate this problem, the manufacturers mount an IR blocking filter (hot mirror) in front of the sensor. However, in IR photography this produces long exposure times. Another inconvenience with IR imaging is that by mounting an IR filter in front of the lens, to block visible light, the visibility in the view finder is nil. Therefore framing and focusing of the object needs to be done before the filter is placed on the lens. To solve both problems an option is to eliminate the hot mirror from the camera, although this will make the camera shoot constantly in IR without the flexibly of swapping between visible and IR spectrums (Annaratone and Ruscello, 2006). Infrared photography must be differentiated from thermal photography which is related to heat generation (wavelengths at the far end of the IR spectrum) and studies the IR radiation emitted from an object or subject (e.g. the body temperature and night vision).

Infrared can penetrate the skin to a depth up to about 3mm (Williams, 1984) therefore it can be used to identify abnormalities in the venous pattern such as varicosities, thrombosis, and for early breast cancer detection (Gibson, 1973). In dentistry, n-IR radiation has been used to evaluate the soft tissues that have undergone radiotherapy (McCarty, 1976), intraoral ulcerative lesions (Wilson et al., 1992) and

venous patterns. One study reported the differences between images of extracted teeth taken under IR, UV and visible light with sound enamel and the cementum presenting almost the same tone whereas enamel appeared darker than dentine. *In vitro* demineralised enamel had a lighter appearance than the surrounding sound tissue (De Ment and Culbertson, 1951). A more recent application for the n-IR radiation is the early caries detection on the occlusal surfaces (Bühler et al., 2005, Fried et al., 2005).

Some other fields for IR photography application are astronomy, ophthalmology, and archaeology. Infrared is also a useful tool to track modifications in paintings, letters and documents since some dyes are transparent therefore it is possible to see through them. Conversely some inks and stains (blood) are only visible under IR, an ability that is exploited (Vetter, 1992).

3.5. Digital image processing

The term image processing refers to the procedures used to manipulate images. These actions have two principal aims: image editing which consists on improving the appearance of the images to the viewer or setting the basis for the detection, measurement and description of the structures in the image (Russ, 1995, Berry, 2008, Burger and Burge, 2008).

There is a wide range of free source and commercial software used to process images. The software used will depend on the skills of the user, the tasks to perform, the language preferred (C[++], Java, Matlab) and the operating system from which the software will be run.

For medical applications, ImageJ is a programme written in Java programming language, created by Wayne Rasband at the National Institute of Health (NIH) in

Bethesda, Maryland, USA. It is an open source programming and is characterised for its compatibility which allows it to work with a variety of operating systems and file formats. It is also very flexible as it is possible to write commands via macros or plugins. A macro is a set of simple instructions (commands) that are part of an application which executes them whilst a plugin is software that is installed into an application to perform different specific tasks. Different plugins are available by contributors (Burger and Burge, 2008).

Image processing involves a series of steps starting with the image acquisition. Extra caution needs to be taken in the selection of the light source for the acquisition of colour images. This is because the colours in the image vary depending on the light used. Therefore for scientific applications the lighting condition must be calibrated. Digital images are formed by a set of pixels. Each pixel occupies a different position in the image. In RGB colour images each pixel has three values (red, green and blue) while in monochromatic or grey scale image it only has one value. The simplest image is a binary image with the pixels taking only two values either 0 or 1 (black or white). Grey scale images use only one channel with depths of 8, 10, 12, 14, 16 or 32 bits per pixel with 8 bits images being quite common. An 8-bit image takes intensity values ranging from 0 (black) to 255 (white). Colour images can take depths of 24, 36, 32 and 48 bits per pixel with the 24 bits image (8 bits per channel) being the most common one. In both cases (grey scale and colour images) higher depth values are used when a better quality image is needed (Burger and Burge, 2008).

After an image has been taken it might be necessary to correct or enhance it prior to further analysis with binary images or masks often needed to support such operations. Examples of image pre-processing include histogram equalisation (which

expands the pixels and distributes them in the whole range from 0 to 255), noise reduction (Bankman, 2000), Boolean logic operations (e.g. AND, OR, XOR), and erosion and dilation of pixels around the borders in an image. Enhancement can be achieved by modifying the values of a group of pixels in the image using different filters such as mean, median, minimum and maximum (Wootton et al., 1995). When analysing a series of images it usually becomes necessary to detect the differences between them (e.g. stages of the treatment). But before this can be done the images need to be aligned and this procedure is called "image registration". Registration can be manually, semi-automatic or fully automatic by means of different algorithms (Wootton et al., 1995). Segmentation refers to the partition or grouping of an image into smaller areas that share characteristics in common. There are different ways to perform the segmentation including histogram-based methods (thresholding), edge detection, clustering, region-growing, statistical pattern recognition, snakes and graph-cut. The thresholding of the grey levels represents one of the simplest options (Withey and Koles, 2008). Analysis is the final step in the image processing. In this step takes place the measurement (area, length, volume) and classification of the information (particles), with the results usually expressed in numerical units.

Chapter 4
Spectrophotometry of dyes for disclosing dental plaque

4.1. Introduction

Dental plaque can be disclosed by using its characteristic of retaining dyes. To provide a good contrast with both the surrounding tissues and the tooth, an alternative possibility would be to use either a blue or a green dye. Unfortunately, green dental dyes are not available in the market and the blue dental dyes come as gel, tablets or in a solution combined with red dye. An alternative could be to use blue or green food dyes for the same purpose or to create a single tone solution taking as a reference what is already available in the market. However there is not enough information from the manufacturers about the dye concentration used in both food dyes and dental disclosing solutions.

4.1.1. Dental dyes

Some dental dyes use the same additive as the ones found in certain food colourants. Likewise, food colourants may be used for plaque detection, as these substances are safe to use and in some cases cheaper than the commercial dental plaque detection agents (Kieser and Wade, 1976, Caride and Meiss, 1981). Dental plaque disclosing dyes change the colour of dental plaque so that it contrasts better with the white tooth surface. In general they are red, blue or the mixture of both to create a two-tone disclosing agent aiming to differentiate recently formed dental plaque (stained in red) from older plaque in blue (Block et al., 1972).

4.1.2. Food additives

A food additive is the name of a chemical substance that modifies the properties of the food, possibly to increase the appeal to the consumer. This is achieved in a number of ways including colour enhancement, improving its flavour, texture and consistency and helping its preservation (Consumers' Association and Hodder & Stoughton, 1988). Additives are divided into the following categories: colours, preservatives, antioxidants, emulsifiers, stabilisers, thickeners, sweeteners, solvents, mineral hydrocarbons, modified starches, and gelling agents (Hanssen, 1984).

The Food Standards Agency in the European Union regulates and recognises the additives that are safe for human consumption for the member countries. An "E" number is given to food additives to classify them. Outside Europe, the most popular classification is the number given by the Federal Food, Drug and Cosmetic Act (FD&C), enacted by the Congress of the United States of America. As a result, the label on a product may show the same additive with two different names e.g. brilliant blue FCF is E 133 in Europe and FD&C 1 in the USA. A third organisation that regulates colour additives is the Japanese Ministry of Health and Welfare (MHW). Its classification is, however, more widely used in Asian countries. Each of the above organisations has its own regulations with discrepancies between them and only a few additives are permitted in common by all three (The European Commission for Food Safety, 1994, Freeman and Oeters, 2000).

4.1.3. Colour additives for food, drugs and cosmetics

The colour additives for human consumption can be classified into three groups.

1) Dyes for food colouring, including all the colourants that are safe for external application in cosmetics and for staining either foods or medicines that will be ingested (must be arsenic and lead free).

2) Dyes for external application in cosmetics and consumption only. In medicines or cosmetics which may be ingested but only sporadically.

3) Dyes that cannot be ingested but are used for staining of medicines and cosmetics which are applied only externally (Freeman and Oeters, 2000).

According to the European Parliament and Council directive 94/36/EC (1994) a food colourant is a substance that adds or restores colour in a food. Colours may have a natural origin, nature-identical or synthetic. Natural food colours come from plants and animal pigments such as: carotenoids, chlorophyll, anthocyanins, and flavonoids, whilst many synthetic dyes are derived from aromatic hydrocarbons, benzene, toluene, xylene, naphthalene, anthracene or aniline (Consumers' Association and Hodder & Stoughton, 1988, The European Commission for Food Safety, 1994). A number of synthetic food dyes are azo-dyes, but anthraquinone and triphenylmethane [$(C_6H_5)_3CH$] compounds are also used. Azo-dyes, are characterised by the presence of one or more Azo (-N=N-) groups in their formula, Other uses for food dyes include colour indicators, drugs and bacteriological stains (Venkataraman, 1952).The E numbers for colour additives are grouped by their colour in a numeric range between the numbers 100 and 199 (Table 3). There are 42 colours approved in the United Kingdom (Gedling, 2009). A detailed description of the red, blue and green colour additives can be found in Table 4a-c (Hanssen, 1984, The European Commission for Food Safety, 1994, Food Additives and Ingredients Association and Centre., 2008, Food Standards Agency, 2010).

Table 3 Colour additives classification, E numbers and an example of each group.

E-Number	Colour	Example
100-109	Yellow	E102 Tartrazine
110-119	Orange	E110 Sunset Yellow FCF
120-129	Red	E127 Erythrosine
130-139	Blue and violet	E131 Patent blue V
140-149	Green	E142 Green S
150-159	Brown and black	E150a Plain caramel
160-199	Others colours, different than the listed above.	E163 Anthocyanins

Table 4a Main characteristics of red dyes (Hanssen, 1984 , Food Standards Agency, 2010).

E number	Name(s)	Description	Used in	Precautions
E120	Cochineal, Carminic acid, Carmines	Natural red colour, extracted from insect scales	Alcoholic beverages, carbonated drinks, soups, deserts	N/A
E122	Azorubine, Carmoisine	Synthetic red azo colour	Powdered soups, sauces, yoghurts, confectionery	N/A
E123	Amaranth	Dark purple synthetic colour	Powdered soups, jams, ice creams, instant gravy	N/A
E124	Ponceau 4R, Cochineal Red A	Synthetic red colour	Powdered soups, tinned fruits, jelly, salami	N/A
E127	Erythrosine	Synthetic cherry-pink/red coal tar dye	Jars of cherries, chocolates, tinned meat, biscuits, Scotch eggs, strawberries, pre-packed Swiss roll, canned fruit, custard mix, sweets, bakery, snack foods, biscuits, dressed crab, garlic sausage, luncheon meat, salmon spread, paté, stuffed olives & packet trifle mix. Dental plaque disclosing tablets	Contains iodine, which can increase the levels of thyroid-hormone. Causes: Hyperactive behavioural disorders in children. Banned in Norway & USA
E129	Allura red AC	Synthetic red colour	Soft drinks	N/A

Table 4b Main characteristics of blue dyes (Hanssen, 1984 , Food Standards Agency, 2010).

E number	Name	Description	Used in	Precautions
E131	Patent blue V	Dark bluish-violet synthetic coal tar dye	Scotch eggs, diagnosis of lymph vessels and dental plaque disclosing tablets	Should be avoided by people with allergy reactions. Banned in Australia, USA & Norway
E132	Indigotine, indigo carmine	Blue synthetic colour	Confectionery	N/A
E133	Brilliant blue FCF	Blue synthetic colour	Processed peas, dairy products, sweets & drinks. Can produce green hues in combination with tartrazine	Banned in Austria, Belgium, Denmark, France, Germany, Greece, Italy, Norway, Spain, Sweden, & Switzerland

Table 4c Main characteristics of green dyes (Hanssen, 1984 , Food Standards Agency, 2010).

E number	Name(s)	Description	Used in	Precautions
E140	Chlorophyll Chlorophyllin	Green pigment extracted from plant sources (photosynthesis)	Confectionery, jams, soups, chewing gum, medicines, fats, oils, soaps	N/A
E141	Copper complexes of chlorophyll & chlorophyllin	Green-colour derived from chlorophyll (E140)	Green vegetables & fruits preserved in a liquid	N/A
E142	Green S	Synthetic coal tar dye	Processed peas, instant gravy, packet cheesecake mix, packet breadcrumbs, gravy granules, mint jelly sauce, ice cream & sweets	Hyperactivity, asthma, urticaria & insomnia. Banned in Canada, Finland, Japan, Norway, Sweden & USA

4.1.4. Spectrophotometry

Spectrophotometry is the study and measurement of the radiation produced or absorbed by a specimen at different wavelengths (Nassau, 1998). The electromagnetic spectrum covers a range of energies with radio waves (long) at one extreme and gamma-rays (short) at the other (Figure 11). The type of energy is determined by its wavelength which is the linear distance between successive maximum and minimum of a wave. Spectrophotometers measure the transmittance or reflectance of solutions and solids at specific wavelengths. The part of the electromagnetic spectrum that a spectrophotometer can measure depends on the manufacturer specifications related to the sensitivity of the equipment. The regions used for spectroscopic analysis are: nuclear magnetic resonance (NMR), electron spin resonance (ESR), microwaves, IR, visible, UV, x-rays and γ-rays (Skoog et al., 1994).

Spectrophotometry is used widely in many scientific areas including chemistry, biochemistry, pharmaceutics, physics, photography and molecular biology for applications that range from colour testing, visual colourimetry and analysis of the vitamin content (Thomas, 1996, Pavia et al., 2001).

Transmittance is the amount of light at a specific wavelength that passes through a sample whilst absorbance is the amount of light that a sample absorbs at a particular wavelength Absorbance increases whilst transmittance decreases (Figure 12).
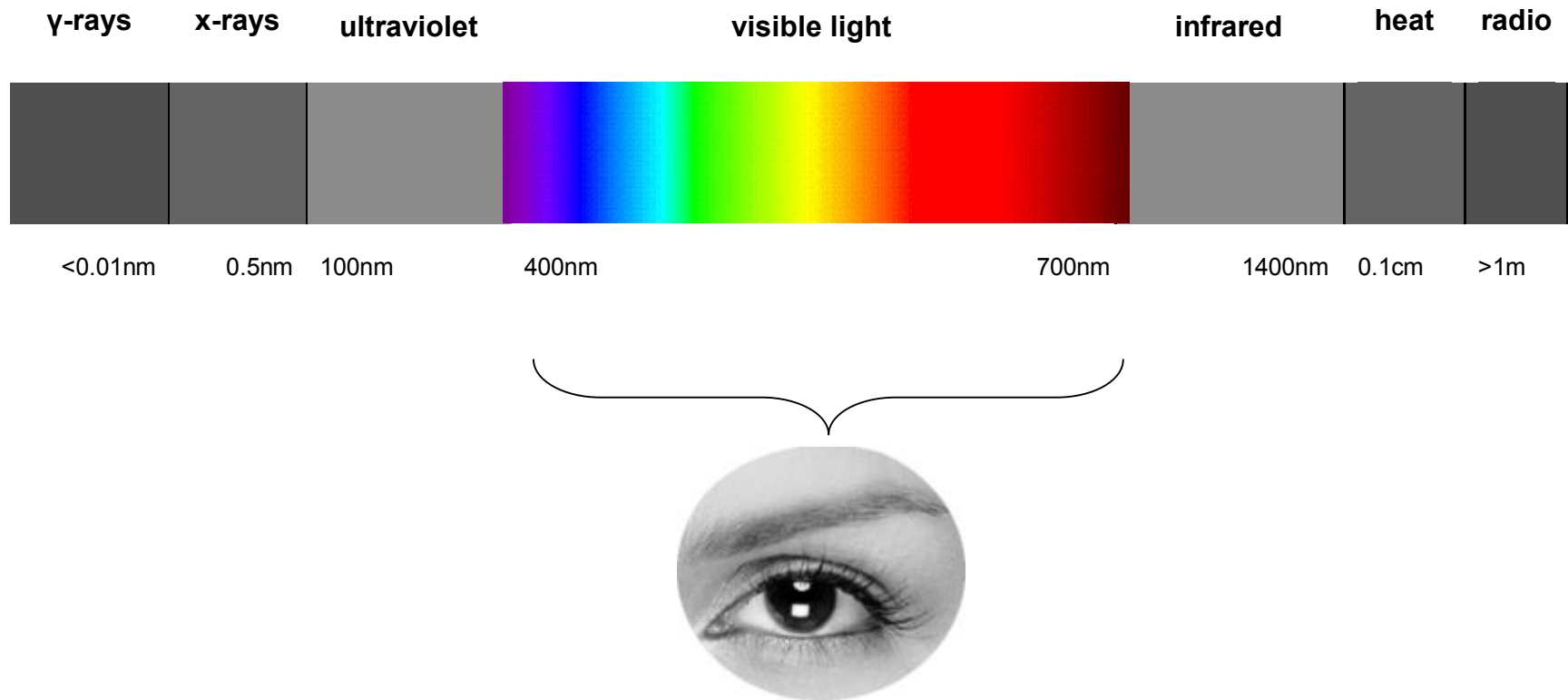
Figure 11 The different wavelengths and regions of the electromagnetic spectrum. The visible region is comprised between 400nm to 700nm.
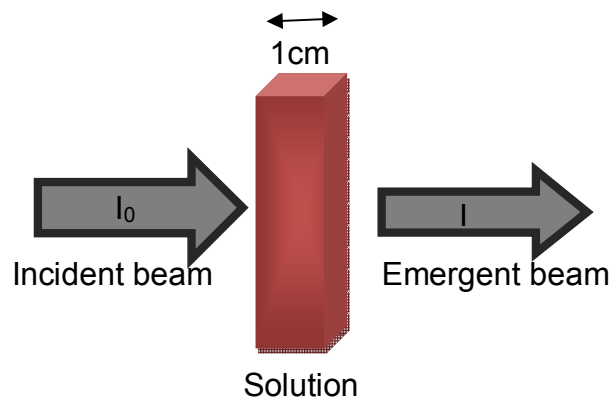
Figure 12 Attenuation of a beam of radiation by an absorbing solution (based on Skoog et al., 1994). The light intensity of the beam when it passes through a solution is related to the concentration of the compound. Then, if a solution presents a high concentration it absorbs more light. This relationship is established by the Beer-Lambert law which is useful to determine the unknown concentration of a given solution.

Absorbance is represented by the negative logarithm of the transmittance (Dorland's, 1988) by the following equation:

$$A = -\log_{10}(I_0/I) \qquad \text{[Eq. 4.1]}$$

The equation for transmittance is:

$$T = I_0/I \qquad \text{[Eq. 4.2]}$$

Where,

A= absorbance

I= light intensity after it passes through the sample

I_0= initial light intensity or other reference solution.

The observed colour of a substance is given by the interaction between the light frequencies that it reflects/transmits (wavelengths that are not absorbed) given by the energy levels of the molecules or atoms that make up the substance. There are two ways for a material to produce the perception of a particular colour. Either, the substance absorbs all the wavelengths but the ones from the perceived colour or the substance presents a strong absorbance in the region of the complementary colour with a direct relationship between the absorbed and observed/reflected colour (Figure 13). For example, in the first option an observed yellow coloured object will absorb all the wavelengths but the ones in the yellow region whilst in the second way, a yellow substance will absorb blue radiation (wavelength 380-470nm) to reflect the yellow colour (Brown, 1980, Pavia et al., 1996).
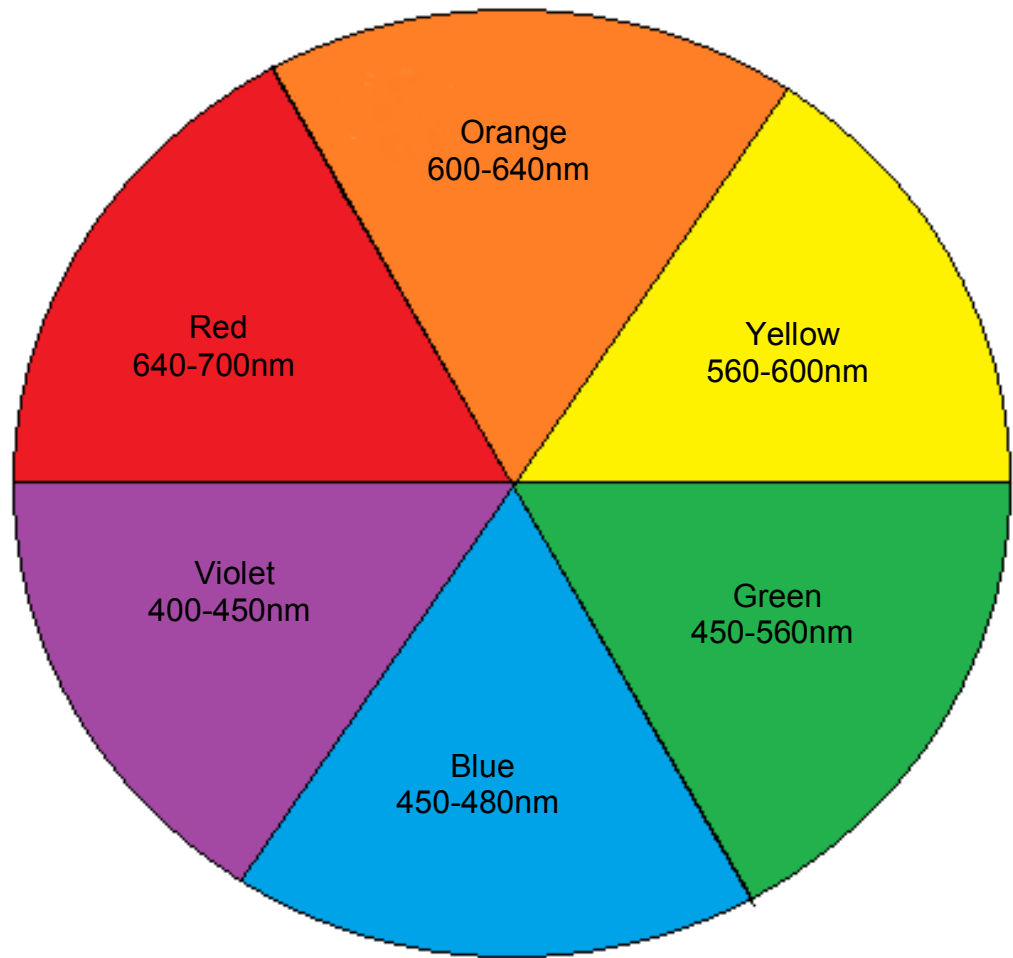
Figure 13 Representation of the observed colour with its approximate wavelength values.

The Beer-Lambert law represents the linear relationship, between the solute concentration (molar concentration) and the intensity of the transmitted light or absorption value. It is useful to determine the concentration of an analyte in solutions using its absorbance as a reference. This law is expressed by the following equation (Brown, 1980):

$$A = \varepsilon c l \qquad \text{[Eq. 4.3]}$$

Where,

ε = molar absorption expressed in L mol-1cm-1

c = molar concentration of the compound solution, expressed in mol/L or mol/dm-3

l = path length of cuvette or container in which sample is contained.

The Beer-Lambert law presents some limitations which can be due to chemical or instrument factors that produce deviations from the linear relationship between the solution and the absorption. Such restrictions include: the difference on the absorptivity coefficient of solutions with high concentrations (>0.01mol) due to electrostatic interactions of molecules in close proximity. Other limitations include scattering of light due to particles within the sample, fluorescence or phosphorescence of the sample and changes in refractive index at high analyte concentration.

In analytical chemistry, to determine an unknown concentration of a substance in a sample, a calibration curve and the Beer-Lambert law, are used. Absorbance is measured with a spectrophotometer as the light passes through a sample and a curve is plotted to compare the absorbance results of the unknown solution with those of samples with known concentrations. The precision of the calibration curve is improved by increasing the number of measured points. By rule the calibration curve

deviates with absorbance values higher than 1, although some authors allow a maximum value of 1.5.

4.1.5. Aim of this investigation

The aim of this experiment was to determine, by spectrophotometry, the dye concentration in three different solutions: a two-tone dental disclosing solution, a green food colourant agent and a blue food colourant for the creation of a dye suitable to be used as dental plaque disclosing solution.

4.2. Material and Methods

First, a paper chromatographic identification of the colour components of five dyes: three dental dyes and two food colourants was done. Then, from these five colourants three products (one dental disclosing solution and two food colourants) were further analysed by spectrophotometry to determine their dye concentration. Only both green and blue dyes in a solution presentation were selected to be further investigated because a dye with a good contrast against the oral tissues was desired. Because both food dyes and dental plaque disclosing solutions have already been approved for human consumption these products were used as a reference in the creation of a new dental plaque disclosing solution.

4.2.1. Chromatographic identification of the colour components of five dyes by paper chromatography

A qualitative preliminary experiment to identify the colour components of five different dyes by means of paper chromatography was done. The dyes used are shown in Table 5. Two of the dental dyes were presented as tablets. Each tablet was ground into powder and mixed with 25ml of distilled water. Five circles, with a diameter of 2.4

cm (Figure 14), corresponding to each of the colourants, were drawn on qualitative filter paper (Whatman international Ltd, Maidstone England). A smaller circle with a diameter of 0.6cm was drawn inside the big circle to use it as reference when placing the colourant. A drop of each colourant (10 µl) was placed into a separate circle. Five millilitres of each solvent (either distilled water or 70% ethanol) were placed on individual plastic trays. The filter paper was held vertically for 5 minutes with its lower border in contact with the solvent on the tray allowing capillary diffusion of the solvent onto the filter. The results were recorded by visual examination depending on the colour separation in the samples.

4.2.2. Determination of the amount of colour added to dyes

This investigation involved preparing stock solutions and the measurement of the dyes' maxima light absorption wavelengths with a spectrophotometer. A calibration curve was produced for each one of the components of the dyes to be analysed using the powder presentation of the dyes. In the second part, the absorbance values from the original dyes (two-tone dye and the two food colourants) were obtained. The dyes analysed in this part of the investigation were as follows:

- Two-tone disclosing solution, plaqsearch (Oraldent Ltd, UK)

- Blue food colourant (Super cook, UK)

- Green food colourant (Super cook, UK)

Table 5 Five dyes used in the paper chromatography and their characteristics.

Dye	Commercial name	Manufacturer
Two food dyes:		
Green food colourant	Green food colourant	Super cook, UK
Blue food colourant	Blue food colourant	Super cook, UK
Three dental dyes:		
Two-tone disclosing solution	Plaqsearch	Oral dent Ltd., UK
Red dental tablet	Endekay (was Ceplac)	Manx Pharma limited, UK
Blue dental tablet	Disclosing tablets	Boots company PLC, UK
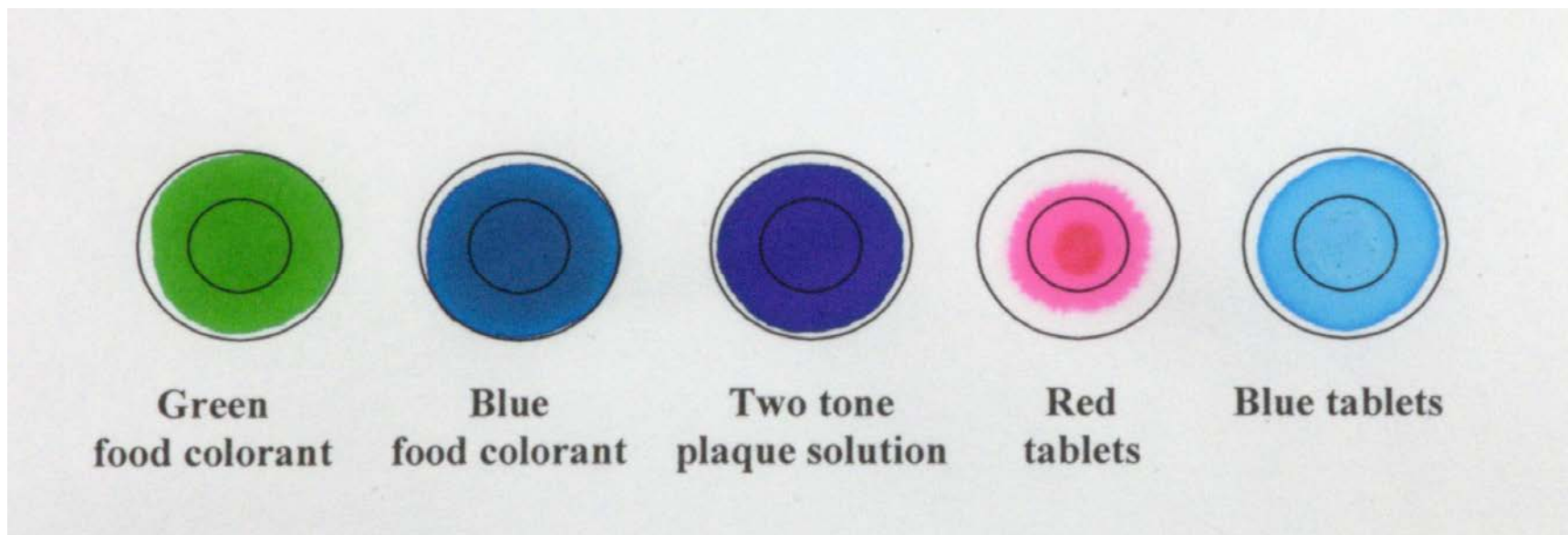
Figure 14 Pattern produced by the colourants placed on the chromatography paper before their immersion in solvent.

4.2.3. Preparation of the stock solutions and calibration curve for both components of the analysed substances

Each of the three dyes analysed was composed of the combination of two colours. The E numbers for each of the colours in the solutions were determined by checking the labels of the products and matching their components with the list of the Food Standards Agency. This allowed ordering one powder, from Sigma-Aldrich (USA), for each of the components in the dyes (Table 6). The blue component, in the blue food colourant and the two-tone dye, was the same. Two stock solutions were prepared for each of the five powders (n=10). The first solution was made with a concentration of 2×10^{-4} mol/ dm^{-3} (stock solution A), and the second with a concentration of 1.5×10^{-4} mol/ dm^{-3} (stock solution B) both, made up to a total volume 100ml. The molecular weight for each of the powders is shown in Table 7.

The stock solutions were prepared at concentrations described above in order that the quantity of powder used could be measured within the accuracy limits of the analytical balance (Ohaus Analytical Plus balance, USA) used in this experiment (readability of 10^{-5}g). A broad range of concentrations with an absorbance below 1.5 allowed for the creation of a calibration curve.

The formulas to calculate the concentration in moles were as follows:

$$\text{Moles= mass (g)/RMV} \qquad \text{[Eq. 4.4]}$$

$$\text{Concentration= moles/volume } (1\times10^{3}\text{dm}^{-3}) \qquad \text{[Eq. 4.5]}$$

Where:

RMV is molecular weight or formula weight

Table 6 Dyes used in the spectrophotometry and its characteristics (The European Commission for Food Safety, 1994, Nordic, 2002).

Name	E No.	CI	Description	Other names	Chemical formula	Max. level (drinks)	Max. level (solid foods)	A.D.I.
Erioglaucine	133	42090	Reddish-blue powder	Acid blue 9, Alphazurine No.1, Acid Blue 9, Alzen, Erioglaucine Food Blue 2; D&C Blue No 1; D&C Blue No 4; FD&C Blue No. 1 Brilliant Blue FCF	$C_{37}H_{34}N_2Na_2O_9S_3$	100mg /L	50-500mg/kg	10mg/kg/bw
Phloxine B	N/A	45410	Red acid dye (fluorescein)	Acid Red 92, Eosin 10B, Cyanosine, D&C red 28, red 104	$C_{20}H_2Br_4Cl_4Na_2O_5$	N/A	N/A	1.25mg/kg/day
Carmoisine	122	14720	Synthetic mono-azo dye	Azorubine, Food Red 3, Azorubin S, Brilliant Carmoisine O, Acid Red 14, D&C red 10, Food Red 3; Acid Red 14, D&C, Food Red 5	$C_{20}H_{12}N_2Na_2O_7S_2$	50mg/L	50-500mg/kg	4mg/kg/bw
Lisamine Green	142	44090	Triarylmethane synthetic coal-tar dye.	Acid Green 50, Food Green 4; Brilliant Green BS; Food green S; Wool Green S 50, wool green S	$C_{27}H_{25}N_2NaO_7S_2$	100mg/L	50-500mg/kg	5 mg/kg/bw
Tartrazine	102	19140	Synthetic mono-azo dye	Acid yellow 23, FD & C Yellow no. 5, yellow no. 4	$C_{16}H_9N_4O_9Na_3O_9S$	100mg/L	50-500mg/kg	7.5mg/kg/bw

Table 7 Molecular weight of the two colour components of the two-tone disclosing solution, the blue food colourant and the green food colourant.

Dye	Component		Molecular weight
Two-tone dental disclosing solution	Blue component	Erioglaucine	792.84*
	Red component	Phloxine B	829.64
Blue food colourant	Blue component	Erioglaucine	792.84*
	Red component	Carmoisine	502.44
Green food colourant	Blue component	Lisamine Green	576.62
	Yellow component	Tartrazine	534.37

*Same substance

Ten serial dilutions were made from stock solution A, while seven serial dilutions were made from stock solution B (Figure 15). The procedure was repeated for each of the working solutions of the two colour components, of the two-tone disclosing solution, the blue colourant and the green colourant, to obtain of 95 samples. The dilution factor used for all the dilutions was 1:2.

The wavelength of maximum absorbance (λmax) or wavelength peak for each solution was identified from the Sigma-Aldrich specification sheet. A second reference was taken from the Commission directive 2008/128/EC for the purity criteria concerning colours for use in food. The λmax for each solution is described in Table 8. Because the dyes analysed were composed of the combination of two colours, two maxima light absorption wavelength values at λ_{max} (λ1 and λ2) were found for each dye (Figure 16).

The spectral reflectance (wavelengths and absorption spectra) was determined using an USB 4000 modular fibre-based spectrometer (Ocean Optics, USA) and the Spectra Suite Java-based software platform (Ocean Optics, USA). The balanced Deuterium-Tungsten-Halogen light source (DH 2000-BAL, Ocean Optics, USA) was used with an output between 210 to1700 nm. This was connected by two 600μm diameter quartz optic fibres to an external cuvette holder (Hellman optics, USA). Disposable plastic cuvettes with 1cm path length and 4ml volume (Labtech, UK) were used.

The spectrometer was warmed up for 40 minutes (minimum of 20 minutes for Tungsten-Halogen and 40 minutes for Deuterium) according to the manufacturer's instructions. The parameters used were: Integration time: 70 milliseconds and scans to average: 25.

Stock solution B	5ml colour + 5ml distilled water	5ml colour + 5ml distilled water	5ml colour + 5ml distilled water	5ml colour + 5ml distilled water	5ml colour + 5ml distilled water	5ml colour + 5ml distilled water	5ml colour + 5ml distilled water
	dilution 1	dilution 2	dilution 3	dilution 4	dilution 5	dilution 6	dilution 7
Sample 1	Sample 2	Sample 3	Sample 4	Sample 5	Sample 6	Sample 7	Sample 8

Figure 15 General procedure used to obtain the working solutions, from the stock solutions B.

Table 8 Wavelength of maximum absorbance (λ_{max}) for each colour component for the two-tone dental disclosing solution, the blue food colourant and the green food colourant analysed in this experiment.

Colourant	Component	Common name	λ_{max} Wavelength
Two-tone dental disclosing solution	Blue	Erioglaucine	630nm
	Red	Phloxine B	539nm
Blue food colourant	Blue	Erioglaucine	630nm
	Red	Carmoisine	516nm
Green food colourant	Blue	Lisamine Green	632nm
	Yellow	Tartrazine	426nm
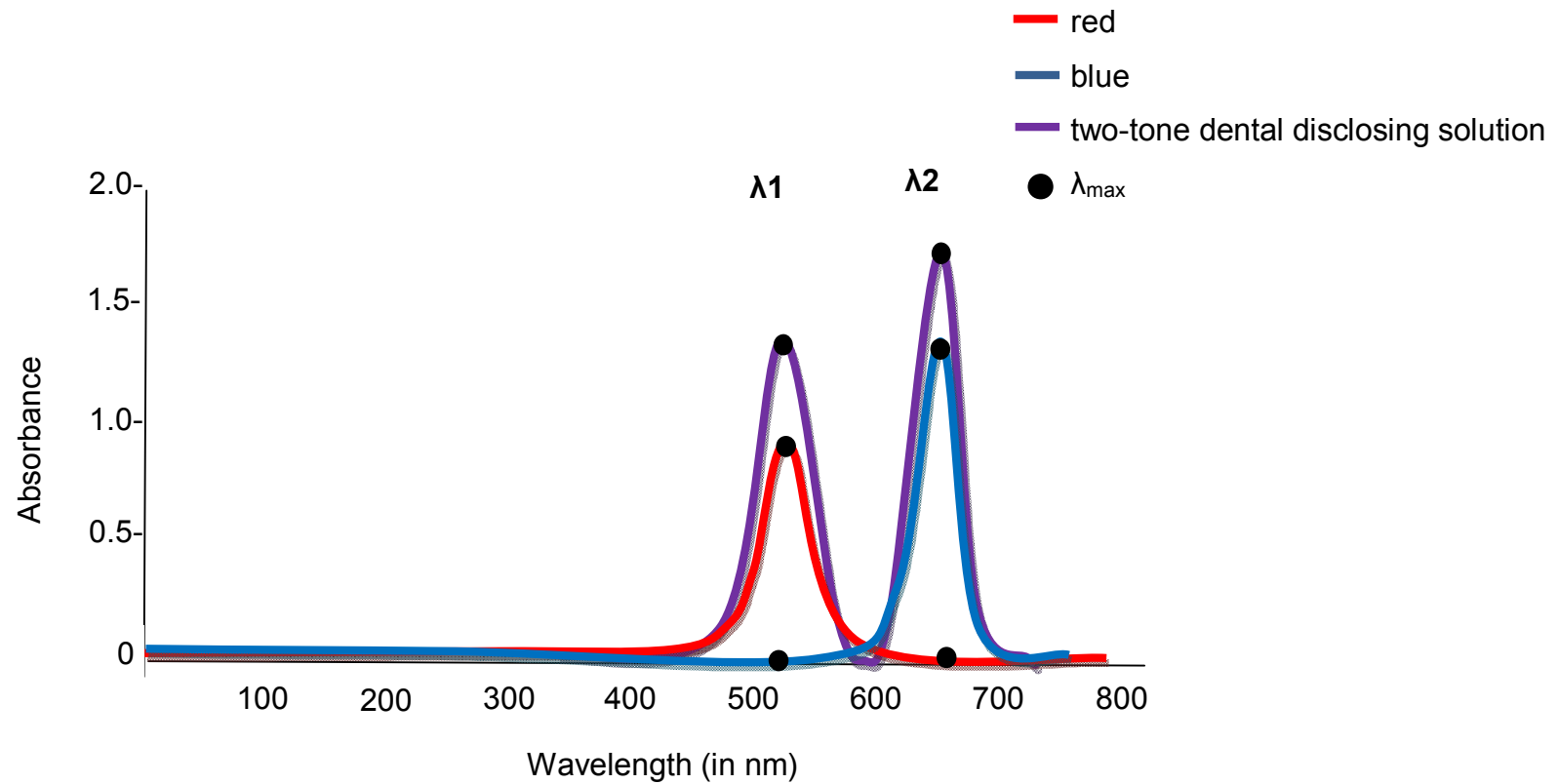
Figure 16 Localisation of the values of maxima light absorption wavelength (λ1 and λ2) for the two-tone dental disclosing solution

and its two components: phloxine B and erioglaucine. Because the two-tone dental disclosing solution was formed by two

colours, two absorbance values at λ_{max} are marked (one for each colour).

The spectrometer was calibrated by using distilled water in a plastic cuvette. This was cleaned and dried thoroughly between readings and discarded when signs of wearing were present. The set up was re-calibrated whenever a new cuvette was used. The absorbance was measured three times for each sample. The obtained data was plotted in Excel and a calibration curve (absorbance vs. concentration) obtained for all colours using only the linear part of the graph.

4.2.4. Measurement of the absorbance of the original dyes (two-tone dye and two food colourants)

The solutions analysed were diluted to measure their absorbance. The dilution was prepared with 0.1ml (100µl) of the original solution mixed with distilled water to make a 100ml solution. The maxima light absorption wavelength at λ_{max} (λ_1 and λ_2) was measured for each sample following the same procedure as described above. Once the absorbance was obtained, the molar extinction coefficient for each of the five dyes was determined with the following formula:

$$A_{\lambda 1} = C\varepsilon_{\lambda 1} \qquad\qquad \text{[Eq. 4.6]}$$

$$A_{\lambda 2} = C\varepsilon_{\lambda 2} \qquad\qquad \text{[Eq. 4.7]}$$

Where:

$A_{\lambda 1}$ = absorbance $_{\lambda 1}$

C = concentration

$\varepsilon_{\lambda 1}$ = molar extinction coefficient $_{\lambda 1}$

$A_{\lambda 2}$ = absorbance $_{\lambda 2}$

$\varepsilon_{\lambda 2}$ = molar extinction coefficient $_{\lambda 2}$

The concentration was already known from the amount of powder used when the solutions were mixed.

To obtain the total absorbance, the dyes were matched with the corresponding pair within the substance and the following formula was used:

$$A_{Tot}= A_{component\ 1\ (e.g.\ blue)} + A_{component\ 2\ (e.g.\ red)} \qquad \text{[Eq 4.8]}$$

Finally, to calculate the amount of the dye in the unknown solution the following formula was used:

$$A_{\lambda 1}=C_{blue}\varepsilon_{\lambda 1}+ C_{red}\varepsilon_{\lambda 1} \qquad \text{[Eq 4.9]}$$

$$A_{\lambda 2}= C_{blue}\varepsilon_{\lambda 2}+ C_{red}\varepsilon_{\lambda 2} \qquad \text{[Eq 4.10]}$$

4.3. Results

4.3.1. Colour components of five dyes by paper chromatography

The pattern obtained by the paper chromatography technique of the colourants after 5 minutes immersion into alcohol and water, is shown in Figure 17. The paper chromatography provided a visual display of the composition in the analysed dyes. Three out of the five dyes were the result of the combination of two colours: the green food colourant (yellow and blue), the blue food colourant (blue and red) and the two-tone dental disclosing solution (blue and red) whereas both the red and blue tablets showed only one colour pattern. All the analysed dyes showed a better diffusion when using water as solvent rather than alcohol.
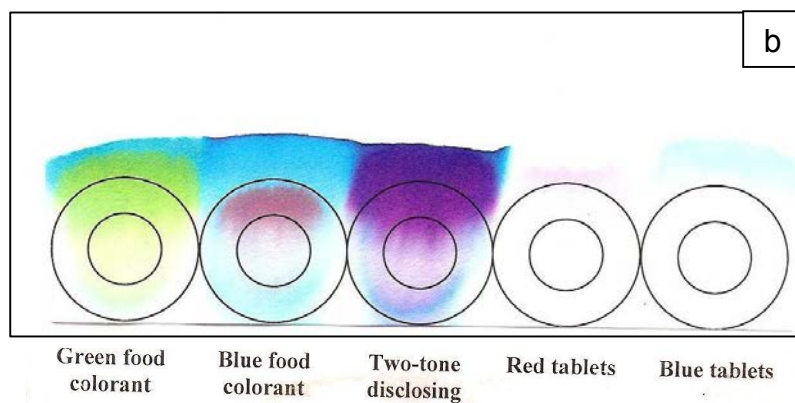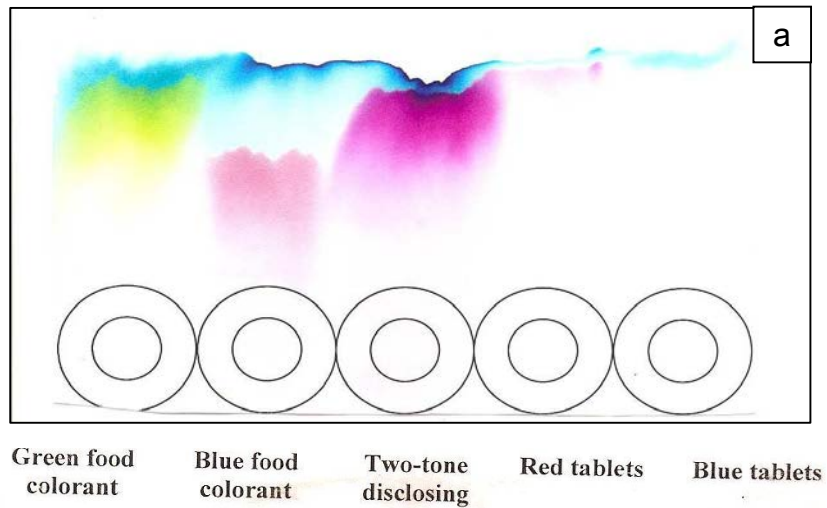
Figure 17 Paper chromatography showing the separation of the colour compounds, for the five dyes analysed, after five minute immersion in: a) water and b) alcohol.

4.3.2. Determination of the amount of colour added to dyes

The values used to plot the calibration graphs including the concentration, absorbance, mean and standard deviation values at the maxima light absorption wavelength (λ1 and λ2) for both components of each of the dyes analysed: the blue component: erioglaucine and red component: phloxine of the two tone solution. The blue component: erioglaucine and red component: carmoisine for the blue food colourant and the blue component: Lisamine green and yellow component: tartrazine for the green food colourant are in Appendix I.

4.3.3. Calibration curve

The calibration curves showing the linear relationship of absorbance against concentration as well as the R^2 values for each of the regression lines are presented in Figure 18-20. Figure 18 shows the absorbance against concentration for erioglaucine and phloxine B at the maxima light absorption wavelength (λ1 and λ2) of the two-tone solution. It can be seen that the absorbance at a wavelength of 630nm for λ2 for phloxine B is 0. Figure 19 shows the absorbance against concentration for erioglaucine and carmoisine at the maxima light absorption wavelength (λ1 and λ2) of the blue food colourant. The graph shows that the absorbance at a wavelength of 630nm for λ2 for carmoisine is 0. The absorbance against concentration lisamine green and tartrazine at the maxima light absorption wavelength (λ1 and λ2) of the green food colourant is shown in Figure 20. The absorbance at a wavelength of 632nm for λ2 for tartrazine is 0.
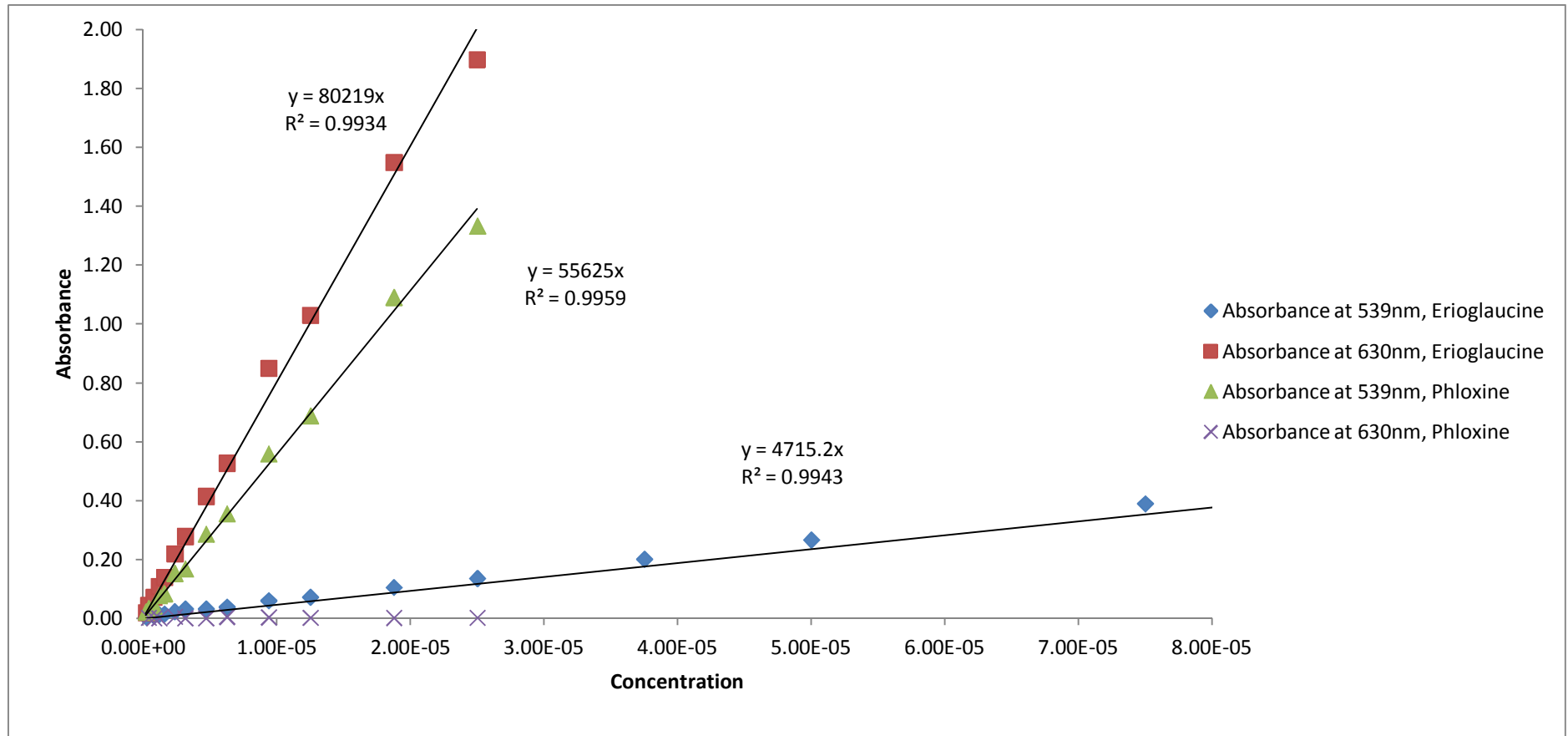
Figure 18 Absorbance against concentration at the maxima light absorption wavelength for the working solution and dilutions of the two tone solution's blue component (erioglaucine at λ1 and λ2) and red component (phloxine B at λ1 and λ2).
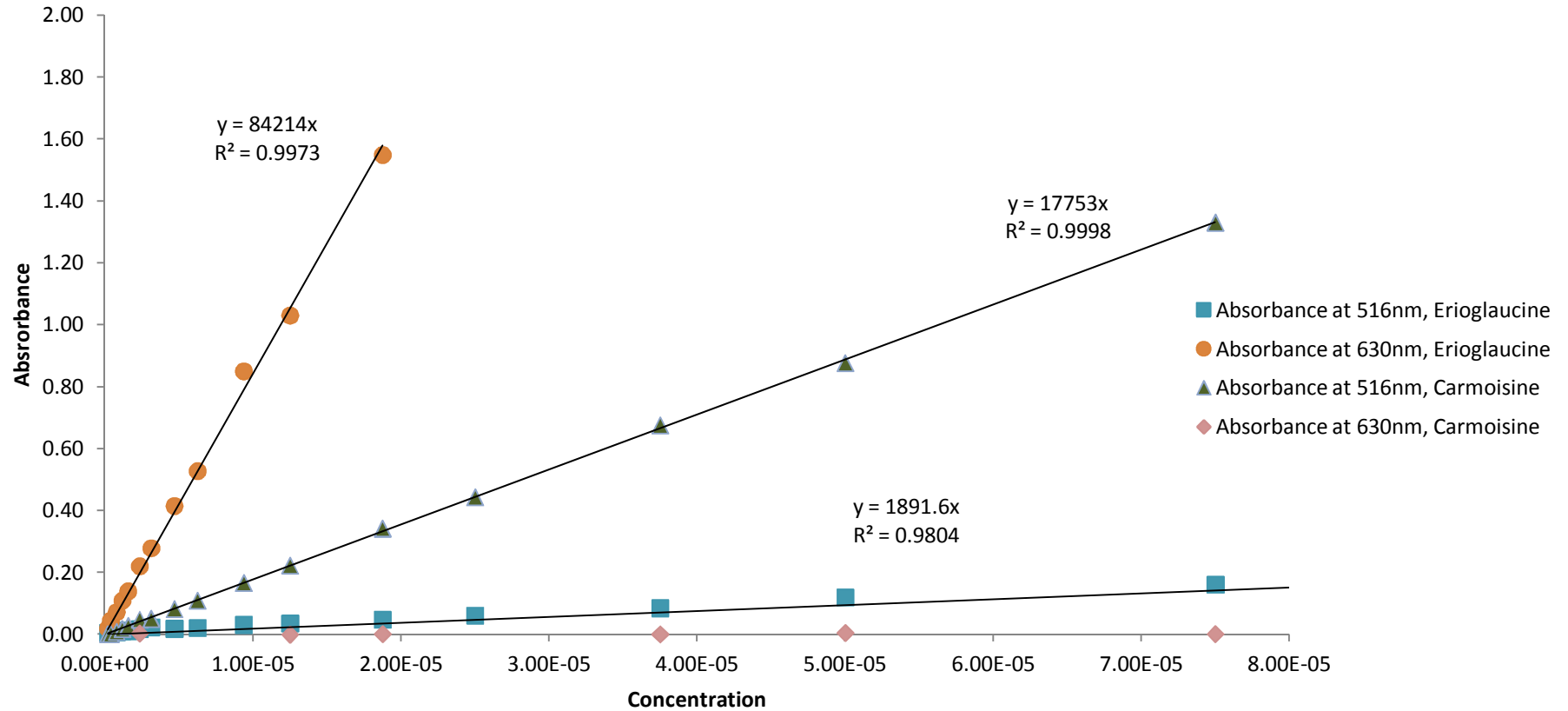
Figure 19 Absorbance against concentration maxima light absorption wavelength for the working solution and dilutions of the blue food colourant's blue component (erioglaucine at λ1 and λ2) and red component (carmoisine at λ1 and λ2).

Green food colourant

$y = 81414x$
$R^2 = 0.9996$

$y = 23076x$
$R^2 = 0.9946$

$y = 5303.4x$
$R^2 = 0.9898$

◆ Absorbance at 426nm, Lisamine
■ Absorbance at 632nm, Lisamine
▲ Absorbance at 426nm, Tartrazine
✕ Absorbance at 632nm, Tartrazine
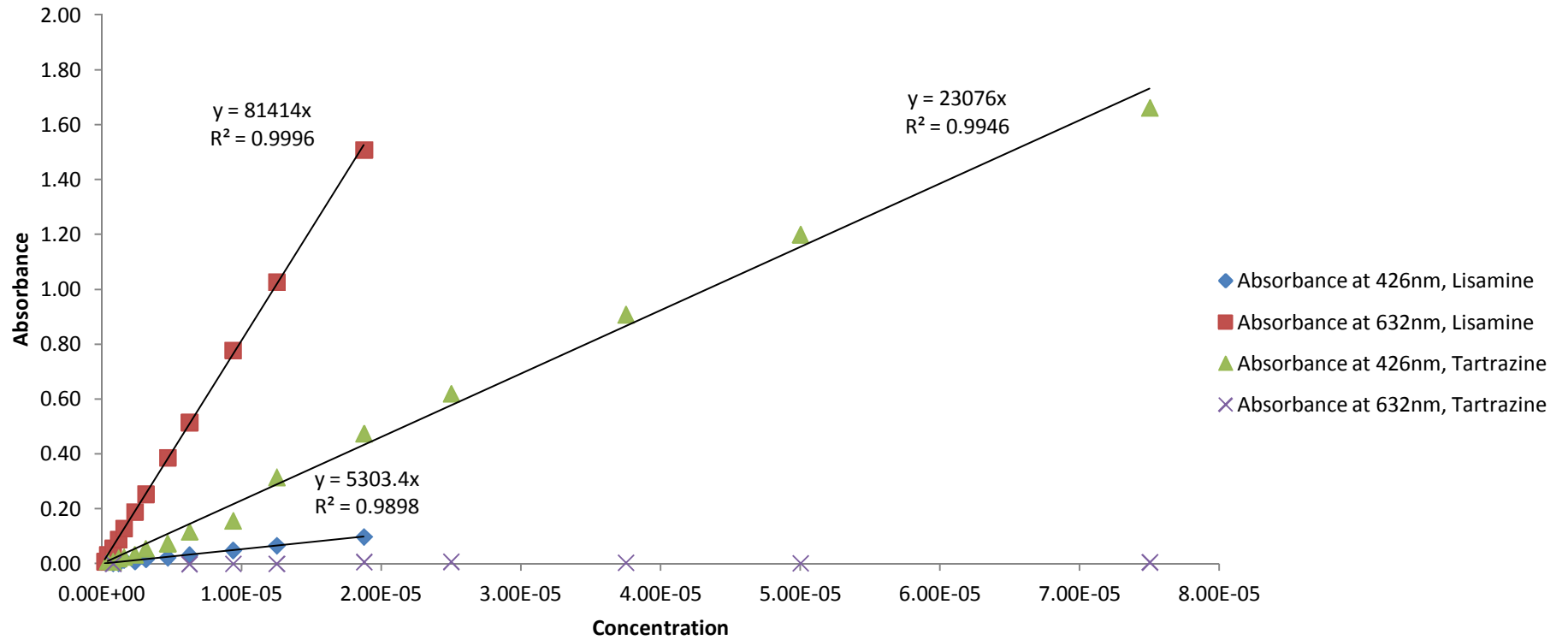
Figure 20 Absorbance against concentration at the maxima light absorption wavelength for the working solution and dilutions of the

green food colourant's blue component (lisamine green at λ1 and λ2) and yellow component (tartrazine at λ1 and λ2).

4.3.4. Measurement of the absorbance of the original dyes (two-tone dye and two food colourants)

The absorbance values for the two-tone solution, blue food colourant and green food colourant are shown in Table 9-11. The average absorbance for the red component of the two-tone dye was 0.76 at 539nm maxima light absorption wavelength (λ_{max}) whilst its blue component at 630nm λ_{max} had an average absorbance of 0.85 (Table 9). For the blue food colourant, its red component had an average absorbance of 0.05 at 516nm λ_{max} whilst its blue component had an average absorbance of 0.49 at 630nm λ_{max} (Table 10). Finally, the absorbance values at λ_{max} wavelength for the green food colourant are shown in Table 11. At a 426nm wavelength λ_{max} the average absorbance was 0.14 and at a 632nm λ_{max} the average absorbance was 0.13.

Once the dye concentrations were obtained, the amount of the substance in grams was calculated (the mathematical formulas used and the procedures followed are in appendix II). The concentration of each component, the grams of colourant per litre and the ratio between the components is shown in Table 12. To obtain the concentration of the original dyes (two-tone dental disclosing solution, blue food colourant and green food colourant), the final result was multiplied by 1000 as the original solutions were diluted to measure their absorbance. The amount of dye per litre of solution as found in the market is shown in Table 13.

Two-tone solution

Table 9 Absorbance for the two-tone solution at 539nm (red component) and 630nm (blue component).

TWO-TONE DYE=Phloxine B (red 28) + Erioglaucine (E133)

Maxima light absorption wavelength: 539nm (red 28) and 630nm (E131)

Absorbance at 539nm					
Wavelength	Measurement 1	Measurement 2	Measurement 3	Average	S.D.
539.00	0.76	0.76	0.76	0.76	0.00

Absorbance at 630nm					
Wavelength	Measurement 1	Measurement 2	Measurement 3	Average	S.D.
630.00	0.85	0.85	0.85	0.85	0.00

Blue Food colourant

Table 10 Absorbance for the blue food colourant at 516nm (red component) and 630nm (blue component).

BLUE FOOD COLOURANT = Carmoisine (E122)+ Erioglaucine (E133)

Maxima light absorption wavelength: 516nm (E122) and 630nm (E133)

Absorbance at 516nm					
Wavelength	Measurement 1	Measurement 2	Measurement 3	Average	S.D.
516.13	0.05	0.05	0.05	0.05	0.00

Absorbance at 630nm					
Wavelength	Measurement 1	Measurement 2	Measurement 3	Average	S.D.
630.08	0.49	0.49	0.49	0.49	0.00

Green food colourant

Table 11 Absorbance for green food colourant at 426nm (yellow component) and 632nm (blue component).

GREEN FOOD COLOURANT = Lisamine green (E142) + Tartrazine (E102)

Maxima light absorption wavelength: 426nm (E142) and 632nm (E102)

Absorbance at 426nm					
Wavelength	Measurement 1	Measurement 2	Measurement 3	Average	S.D.
426.10	0.14	0.14	0.14	0.14	0.00

Absorbance at 632nm					
Wavelength	Measurement 1	Measurement 2	Measurement 3	Average	S.D.
632.17	0.13	0.13	0.13	0.13	0.00

Table 12 Concentration, grams of colourant per litre and ratio between the components for each of the analysed dyes.

Dye	Component	Concentration	Grams of colourant per litre	Ratio
Two-tone disclosing solution	Blue component	1.06×10^{-5} mol / dm^{-3}	8.40×10^{-3} g/dm^{-3}	44.2%
	Red component	1.28×10^{-5} mol / dm^{-3}	1.06×10^{-2} g/dm^{-3}	55.8%
Blue food colourant	Blue component	5.8×10^{-6} mol / dm^{-3}	4.60×10^{-3} g/dm^{-3}	80.6%
	Red component	2.20×10^{-6} mol / dm^{-3}	1.11×10^{-3} g/dm^{-3}	19.4%
Green food colourant	Blue component	1.5×10^{-6} mol / dm^{-3}	8.65×10^{-4} g/dm^{-3}	22.1%
	Yellow component	5.72×10^{-6} mol / dm^{-3}	3.06×10^{-3} g/dm^{-3}	77.9%

Table 13 Concentration and grams of colourant per litre for each of the components for the analysed dyes as are sold in the market.

Dye	Component	Concentration	Grams of colourant per litre	In the bottle
Two-tone disclosing solution	Blue component	1.06×10^{-2} mol/dm^{-3}	8.40g/dm^{-3}	0.13g (15ml bottle)
	Red component	1.28×10^{-2} mol/dm^{-3}	10.6g/dm^{-3}	0.14g (15ml bottle)
Blue food colourant	Blue component	5.8×10^{-3} mol/dm^{-3}	4.60g/dm^{-3}	0.17g (38ml bottle)
	Red component	2.20×10^{-3} mol/dm^{-3}	1.11g/dm^{-3}	0.04g (38ml bottle)
Green food colourant	Blue component	1.5×10^{-3} mol/dm^{-3}	0.87g/dm^{-3}	0.03g (38ml bottle)
	Yellow component	5.72×10^{-3} mol/dm^{-3}	3.06g/dm^{-3}	0.12g (38ml bottle)

4.4. Discussion

Plaque detection is necessary due to the relationship between presence of bacterial dental plaque in the initiation of both dental caries and periodontal disease. This link is dependent on the interaction between the host response and the period of time the plaque has been on the tooth (Lang et al., 1973, Harris and Garcia-Godoy, 1999). It also helps patients maintain and monitor their oral health acting as a learning process which provides feedback on whether their oral hygiene techniques are effective. Dental plaque disclosing agents can be administrated as tablets, solutions or gels. The solutions are generally preferred to the others as they allow better administration in the oral cavity. Gels may disrupt plaque when they are applied to the surface and patients may prefer the tablet presentation. No studies appear to be available regarding the preferences of patients or clinicians in relation to these presentations of the plaque disclosing agents. Red is a very popular colour for disclosing plaque; however it is not clear why this is the preferred colour. It may be related to its large accessibility in the market and its traditional place in the literature. The two-one solution plaqsearch attempts a different approach offering a selective staining by differentiating old and newly formed plaque. Recently formed plaque appears red whilst older plaque stains blue. There is no clear limit between both colours which results in a mixture of different hues when applied to the tooth. It is suggested that the staining mechanism of the two-tone solution is related to the plaque thickness but there is no clear evidence of the length of time needed to distinguish old from new plaque (Block et al., 1972, Gallagher et al., 1977). Therefore a patient who tends to accumulate plaque quicker may present the same staining pattern as a patient who accumulates plaque at a slower rate. It is an area that requires further research.

Furthermore, no studies were found that compare the superiority that may exist between a two tone disclosing solution over a single tone. Perhaps using a two tone solution is not as relevant for the patient or the clinician because the end result is the total amount of plaque formed followed by removal from the surface.

The ideal characteristics of a dental plaque disclosing product should be cheap, non toxic with an acceptable taste, easy to use and to remove by rinsing, capable of producing a good contrast with the teeth and soft tissues without staining the restorations permanently (Gillings, 1977, Caride and Meiss, 1981). Researchers have remarked that dental plaque visualisation was difficult without a disclosing agent with a strong contrasting colour (Ambjørnsen et al., 1982). For this project, a plaque disclosing agent that provided a good contrast between disclosed plaque on the teeth and the surrounding tissues was needed. Therefore the work concentrated on either blue or green as preferred colours. It was decided that the vehicle to be used to deliver the agent should be a water based solution which would cause minimal alteration to the plaque. The first option was to use a dye already available commercially such as the blue disclosing tablets but as stated before, this research required a solution for an easier and improved handling which in turn would make administration more accurate. A second option was to use methylene blue as it is widely used in medicine and it has proved to be a disclosing solution that provides a good contrast (Lovato et al., 2002, Carter et al., 2004) however; Material Safety Data Sheet reports show that the compound may cause adverse reactions if swallowed due to the presence of a methyl ring (Safety officer in physical chemistry, 2010).

4.4.1. Paper chromatography

The results from the paper chromatography allowed the identification and separation of the components of each of the dyes analysed. It revealed that only the red and blue tablets were pure, as no other colour was found in its structure whilst the food colourants and the disclosing solution were a combination of two colours. Mixing of dyes operates by subtraction of the wavelengths of the primary colours from white (Nassau, 1998) and relies on the reflection (or absorption) of the wavelength of each colour as the colour of an object is the result of the light that is reflected or transmitted (in case of a transparent object) by it. The subtractive primary colours are cyan, magenta and yellow. Cyan reflects green and blue (absorbs red), yellow reflects red and green (absorbs blue) and magenta reflects red and blue (absorbs green). The combination of two subtractive colours produces a colour that is the result of the wavelength that none of the subtracted colours absorbs. For example yellow (absorbs blue) and magenta (absorbs green) allow only red to be seen by the human eye (Figure 21). Ideally, the combination of the three subtractive primary colours in the subtractive colour system results in black.
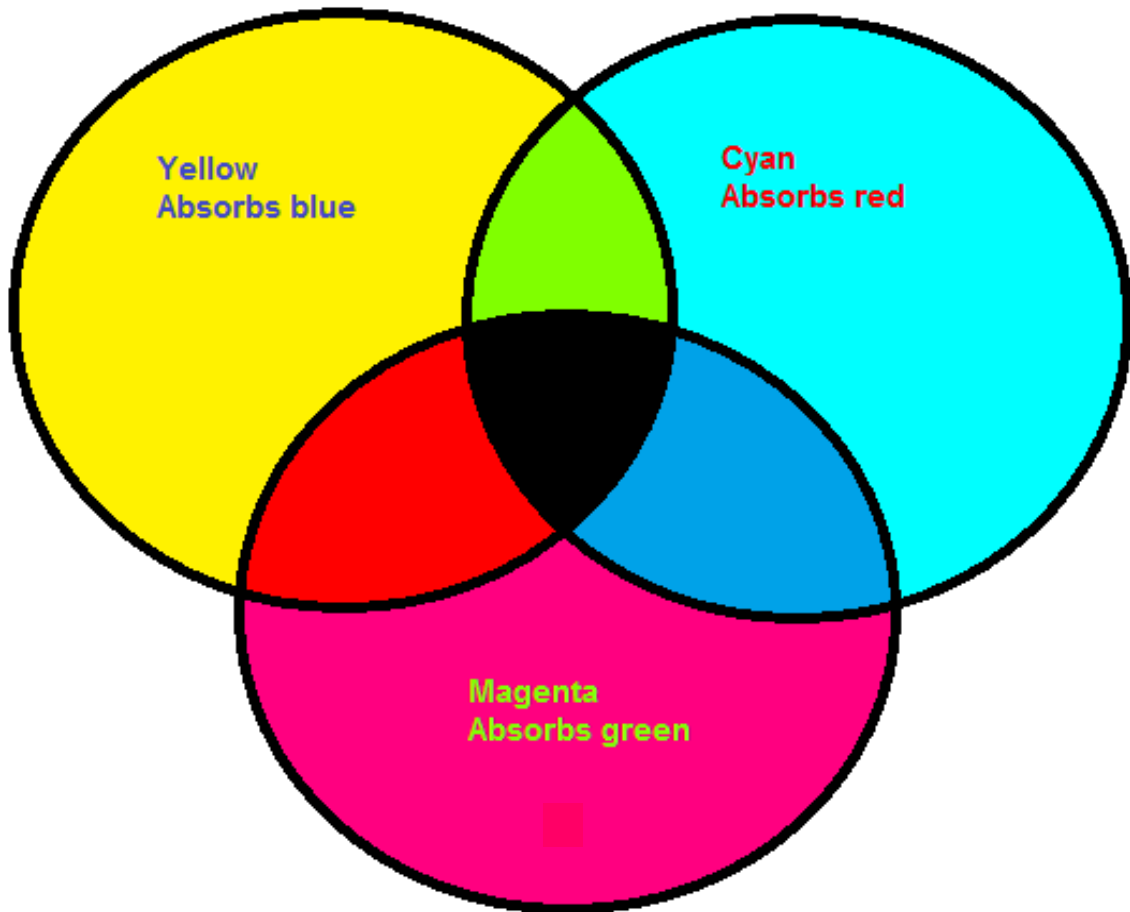
Figure 21 Primary colours and the subtractive colour mixing.

In this study, the components of the dyes were separated because they were able to dissolve well in the solvent. However, when comparing the solvents used in the paper chromatography it was seen that all the analysed dyes had a better diffusion when using water, rather than alcohol. This was corroborated with a higher migration of the substances in the paper imbibed in water. The water solubility of the plaque disclosing dyes is a desired characteristic, as the dye needs to be able to diffuse into voids and porosity in the plaque matrix (Marsh, 2003, Hope and Wilson, 2006, ten Cate, 2006).

4.4.2. Spectrophotometry

For this study, due to the characteristics of the machine used, only the visible spectrum of the dyes was analysed. Further research is required to analyse the dyes appearance in both n-IR and UV regions of the spectrum to determine whether they are transparent or not under these wavelengths.

Each dye has a unique wavelength pattern which can be considered as its fingerprint. The absorption spectrum of a dye can be used to determine its components or to corroborate the presence of a dye in an unknown solution. This is done by comparing the location of the peaks of the maximum absorbance of the unknown solution against a known pattern. If the peaks match, then the dye is considered to be the same. In this experiment, each of the substances analysed presented two peaks that corresponded to the absorbance peaks reported by the manufacturer. This confirmed the presence of the substances as marked in the labels.

The concentration of a solution does not affect where the peak is located in the spectrum. A higher concentration will only modify the peak height. In this experiment,

this principle was applied as the three solutions examined presented a high concentration. To measure their absorbance, several dilutions were made (different concentrations) until the spectrophotometer was able to register the absorbance. Figure 22 shows the observed colour for the dyes analysed and the position in the spectrum where its absorbance is located. The blue dye absorbs in the orange-red region (550-700nm), the red dye absorbs in the green region (490-560nm) while the yellow dye absorbs in the blue region (440-490nm).

4.4.3. Food dyes and phloxine B

All the colourants used in this experiment except phloxine B are azo dyes and have approval from the Food Standards Agency in the European Union to be used as food colourants. Carmoisine and lisamine are not permitted in either USA or Japan (Freeman and Oeters, 2000).

Phloxine B is a halogenated fluorescein dye (xanthene) with a molecular formula similar to dyes such eosin and erythrosine. At the moment, this substance has only approval to be used either in medicines or in cosmetics (except for the eye area) but not as a food dye therefore does not have an "E" number (Freeman and Oeters, 2000). This may be related to the lack of evidence available about their side effects in humans. One study conducted in rats in 2003, proved that phloxine B is safe to use as a dye at concentrations up to 0.5% during four weeks (Hagiwara et al., 2003). However, the safety specifications from manufacturer's Sigma-Aldrich and Mallinckrodt Baker Inc, have labelled it with a hazard warning on the possible harm if swallowed, inhaled or absorbed through skin but this has not been proved in humans.
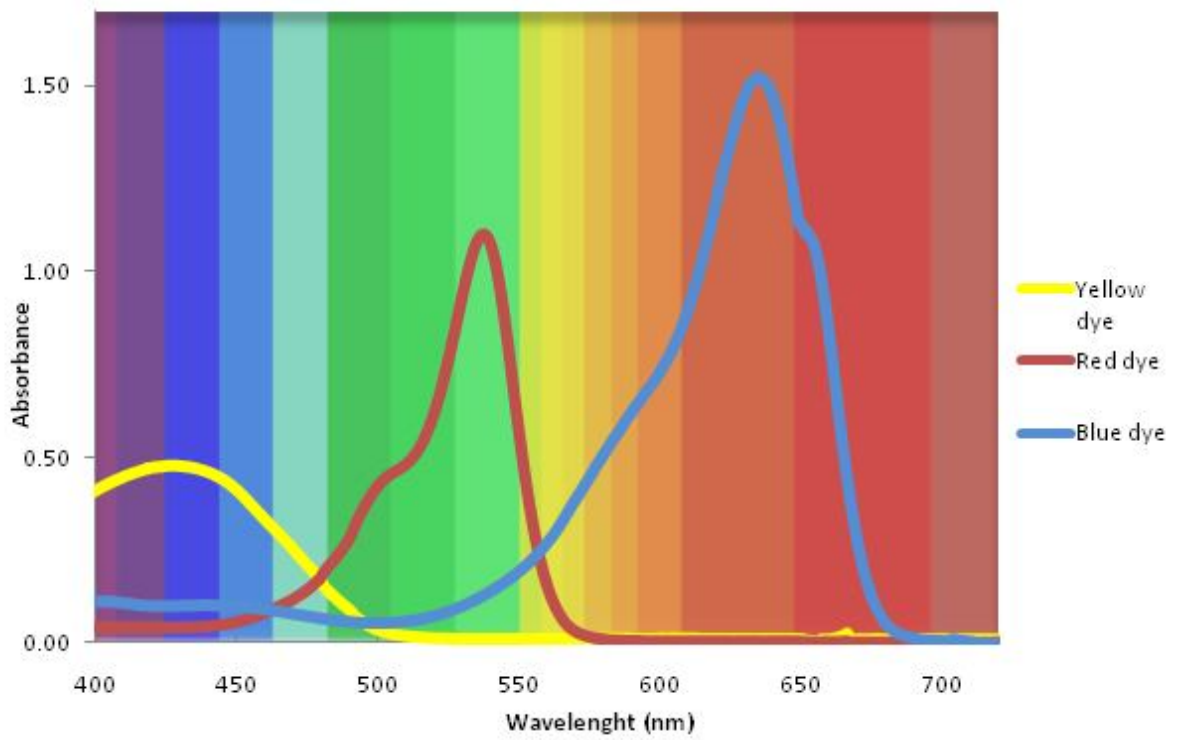
Figure 22 Spectral analysis for the colours: red, blue, yellow, and the position in the spectrum where its absorbance is located.

Toxicological reports state that the lethal values in mice and rats with a LD50 (lethal concentration 50 percent kill) of 310mg/kg. Unintentional ingestion is not thought to be cause for concern; however adverse reactions such as nausea, hives, vomiting and anaphylactic shock may happen. These responses are not specific to phloxine B. Food additive consumption may also cause urticaria, eczema and allergic reactions. However these are very rare and the literature is not clear about these reactions being caused by the dye itself or in response to the food that contains the dye. No reports were found on adverse reactions to dental plaque disclosing agents (Simon, 2003).

Phloxine B has a variety of applications. It is added as an inactive ingredient to the antibiotic amoxicillin. In histology, it is used for different stain procedures (Rasooly, 2007) and more recently, researchers have found that phloxine B has a bactericidal effect on *Streptococcus aureus* and on gram-positive and gram-negative bacteria (Rasooly, 2005, Waite and Yousef, 2009). Further research is needed to verify if these antimicrobial properties can be exploited when this dye is used for plaque disclosure.

When comparing the food colourants against the dental disclosing solution, the food dyes presented a lower concentration of the dye. This may be related to health and safety regulations where the risk to a person of intoxication is higher if the colourant is used as a food dye. This can be also associated with poorly controlled distribution and handling. More precaution is expected when dental professionals use a disclosing agent. Following a controversial discussion, a report was published on the association between food colourants and the Attention Deficit Hyperactivity Disorder (ADHD) in children (McCann et al., 2007). Therefore, both carmoisine and tartrazine

additives used as part of the red component in the blue colourant, and the yellow component in the green one were replaced at the beginning of 2011. In the blue dye carmoisine was completely removed from the contents in the food colour, leaving brilliant blue as the only component whilst the green food colourant tartrazine was replaced with copper chlorophyllin.

4.4.4. Comparison of the colour content of the two-tone disclosing solution, the blue food colourant and the green food colourant

When comparing the amount of the colourant added to the different products analysed in this experiment, it is apparent that the disclosing solution contains larger amounts of both the composing dyes. The blue component is almost double the amount of the same dye in the blue food colourant. The red component has around 6 times more red dye (phloxine B) than the red component in the blue food colourant (carmoisine). It may be that the dental disclosing solution is classified for medical use and therefore its application does not involve its ingestion whilst when using the colourant in food it implies it. However, the amount of both dyes in the dental disclosing solution is still within prescribed safety values. The green food colourant presented with the lowest concentrations, for both its blue and yellow components. Both the blue and the green food colourants presented dye concentrations below the maximum level allowed for drinks, which is set to a 100 mg/L for erioglaucine, lisamine green and tartrazine and 50mg/L for carmoisine.

Comparing the ratios for the components in the blue food colourant and the two-tone disclosing solution, the latter had a similar ratio between the blue and red components (44.2% vs. 55.8% respectively) while the former presented a higher concentration of the blue component (80.6% vs. 19.4%). This may be the

requirement of the manufacturer who aims for a solution that looks and stains blue. The red component may be added to make the colour darker. In the case of the dental solution, as its name indicates, a two tone solution is desired.

In the market, it is possible to find blue and red plaque disclosing tablets. The blue tablets contain 3mg of blue V per tablet, while the red tablets contain 6mg of erythrosine per tablet. This compares to 0.13g of blue and 0.14g of red in 15ml per bottle for the disclosing solution. In this study it has been shown that the concentration in the tablets is higher.

During the course of this study the manufacturer has expanded their products range for plaque disclosure and now has tablets and disclosing buds. However both systems use the same colourants as the solution. A future topic for research would be to compare which of the three systems has the best results for plaque disclosure. The results from this investigation allowed us to create our own blue dye in a solution. The blue colour for plaque disclosing presents a better contrast with the surrounding oral tissues. All traces of red are eliminated when our own solution was created and the concentration is safe to use within the safety limits.

4.5. Conclusions

The results from this investigation present a dental plaque disclosing dye that satisfies most of the characteristics of an ideal disclosing product. Using a commercially available two-tone disclosing solution as a reference, a blue solution for dental plaque detection was created. This dye had the following characteristics: cheap, easy to use, easily removed by rinsing, capable of producing a good contrast with the oral tissues and with a concentration within the safety limits for its consumption.

Chapter 5
Near-infrared photography in dental plaque detection

5.1. Introduction

In clinical and experimental research dental plaque measurement allows evaluation of the oral hygiene performance of different devices with toothbrushing as the principal method by which individuals control plaque-related diseases. There is also commercial interest in assessment of dental plaque removal as many manufacturers express the efficacy of their products in terms of amount of plaque removal. Once dental plaque is detected, a reproducible, sensitive and specific dental plaque index can be used to quantify the amount of plaque. However many of these plaque indices are represented in ordinal scales that make difficult to record small differences within these coding systems. Therefore an automated method to measure and quantify dental plaque will eliminate subjective intervention increasing the reliability of the measurements allowing comparisons between data obtained by different investigations. Carter et al.(2004) reported on the use of a fully automated method based on digital imaging. Images were assessed using the hue (H), saturation (S) and intensity (I) colour space to distinguish automatically between three colours, disclosed dental plaque (blue), tooth structure (white) and the soft tissue (red). Whilst this study showed potential, it had the disadvantages that there was no standardisation or calibration of the light. There was no standardisation of the volunteers' position and the results of this study only focused on the investigation of the HSI colour space method and did not attempt to evaluate the extent of plaque by

tooth but identify stained areas. Nevertheless, the study did demonstrate that automation of the assessment of dental plaque is possible.

Prosthetic appliances or dentures, like natural teeth, can accumulate plaque on their surface. Salivary glycoproteins are responsible for the initial bonding of bacterial deposits to the denture (Abelson, 1981). Complete dentures (CDs) are made from polymethyl methacrylate (PMMA) which when processed is a strong and robust material. However the PMMA is porous and does allow the growth of microorganisms to take place, especially if the denture is not cleaned well. The lack of denture cleaning together with dental plaque accumulation is an ethological factor for denture stomatitis (candidiasis) and malodour (Nikawa et al., 1998). Therefore denture cleansing and dental plaque removal is an essential procedure for oral health to be maintained (Tarbet, 1982). Oral hygiene procedures for dentures generally require the use of soap and water with a scrubbing brush which removes the plaque by mechanical action. However chemical denture cleansers and disinfectants containing either sodium peroxidise, hypochlorite and enzymes are also available on the market (Budtz-Jørgensen, 1979).

5.2. Pilot study

The aim of this study was to investigate a novel approach for dental plaque detection using near IR imaging.

5.2.1. Material and Methods

Two web cameras (Philips SPC900NC PC USB Web Cameras, Amsterdam, Netherlands) and a 35 X 35 cm beam-splitter mirror (NT 45325, Edmund optics Inc, NJ, USA) were used to capture two images of a lower complete denture (CD). The two cameras were located at an angle of 90 degrees to each other. One camera

recorded the image in the visible spectrum whilst the second camera recorded in the n-IR region. To be able to take a picture in the n-IR radiation spectrum, one camera was modified by removing the infrared filter on the back of the lens. The beam-splitter mirror was used to assist in the photography as follows. When the incident side of the mirror was housed with a dark chamber it split the incident light into two. One face reflected the objects whilst the opposite surface allowed light transmission. Only the n-IR camera and the mirror were kept in darkness and the mirror was positioned at a 45^oangle to the intersection of the cameras allowing that one image to be reflected and the other transmitted. Therefore, one visible and one n-IR image were captured with the beams being split simultaneously. The arrangement is shown in Figure 23. The n-IR camera was activated first to take the initial picture and was immediately followed by the visible light spectrum camera. All pictures were taken on the same day, under natural daylight conditions.

Both cameras and the beam-splitter mirror were mounted and fixed on to a holder. The side of each camera had a metallic arm attached to a base. The metallic arm allowed vertical displacement whilst a second screw on the base of the camera's metallic arm allowed horizontal adjustments along a rail made on the base. The beam-splitter mirror was also able to move horizontally by means of a rail in the base. The cameras were connected to a computer (Dell Inc, USA), via USB and the Philips Video Lounge software was used to capture and visualise the images.

A complete lower denture was used as a mock patient. Coloured starch was applied to the cervical and medial third of all labial surfaces of the denture's teeth to simulate stained dental plaque (Figure 24).
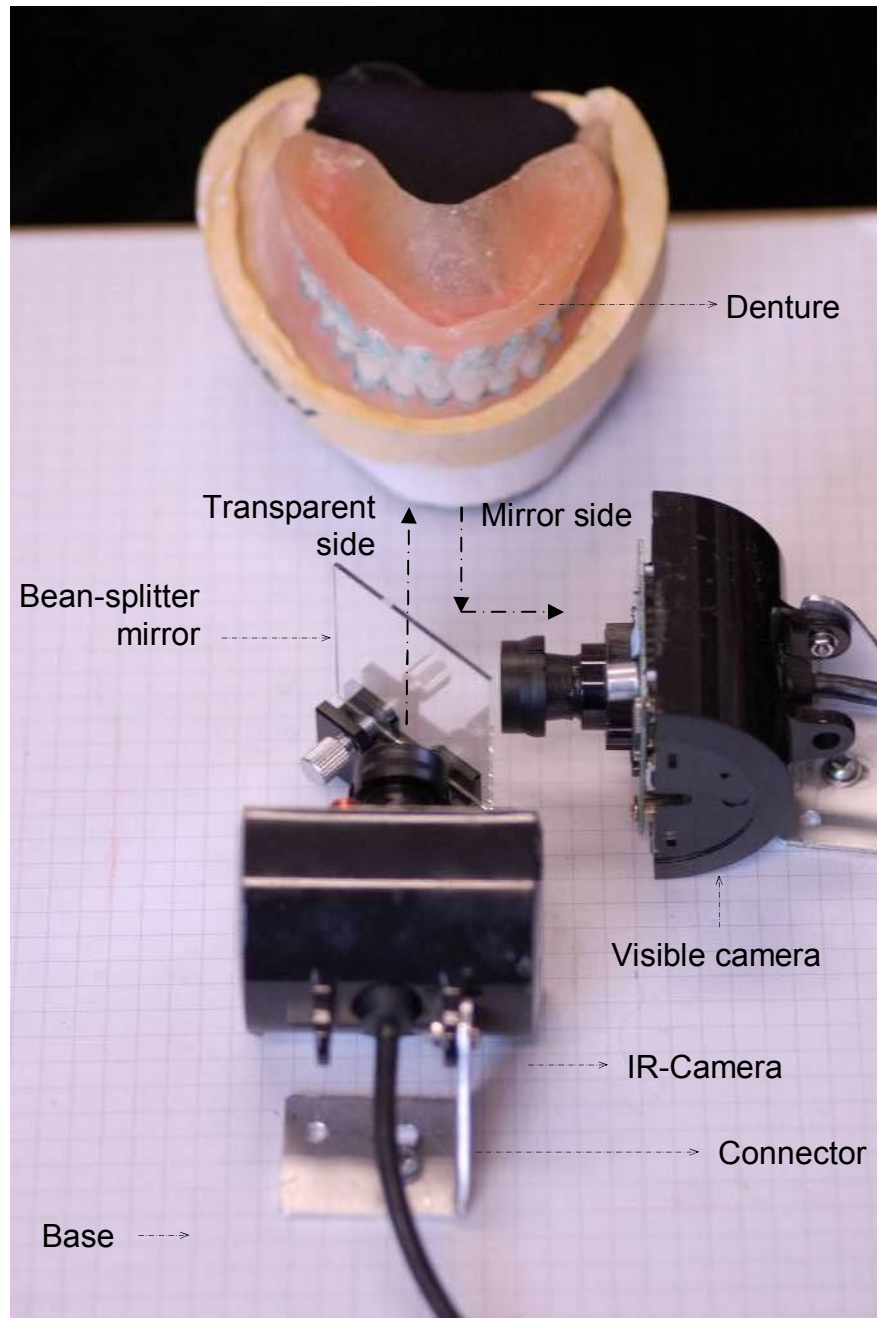
Figure 23 Web cameras and beam-splitter mirror set up.

Figure 24 Complete lower denture with the coloured starch applied on the labial

surface. The starch shows up as blue contrasts with the teeth (white) and

denture base (pink).

The artificial dental plaque consisted of a mixture of 1g of starch and 5ml of distilled water. The mixture was mixed up and boiled to achieve a sticky consistency. After cooling down, the starch was coloured with one drop (100µl) of one of the various disclosing solutions. Five disclosing agents were used to stain the artificial plaque, two food colourants: green (Supercook, UK) and blue food colourant (Supercook, UK) together with three dental plaque disclosing agents: two-tone disclosing solution (Oral Dent Ltd. UK), Endekay erythrosine tablets (Manx Healthcare Ltd. UK) and blue disclosing tablets (Boots, UK). The tablets were ground into powder and mixed with 25ml of distilled water to create disclosing solutions. Two images (n-IR and a visible light) of the denture were obtained for each disclosing solution.

5.2.2. Results

An example of the images obtained for both the visible spectrum and under n-IR radiation is shown in Figure 25. Artificial dental plaque was invisible in the n-IR images of the five disclosing agents used. The n-IR image also had poor focus with diffuse and poorly defined borders especially near the gingival margin. A detailed view of the anterior area of the denture under a) visible light conditions and b) near IR radiation following the use of blue food colouring to disclose the artificial dental plaque is shown in Figure 26.
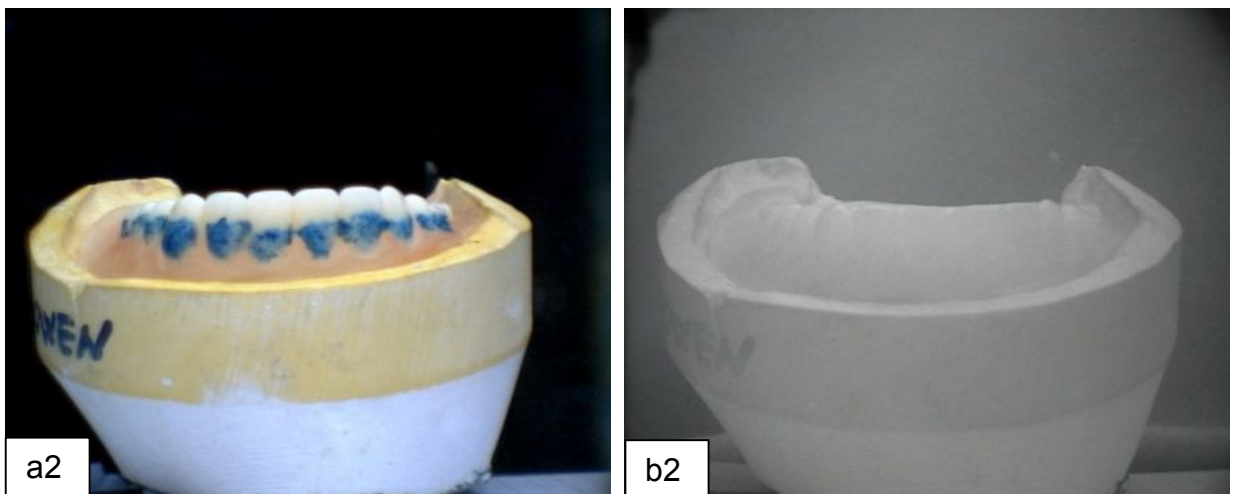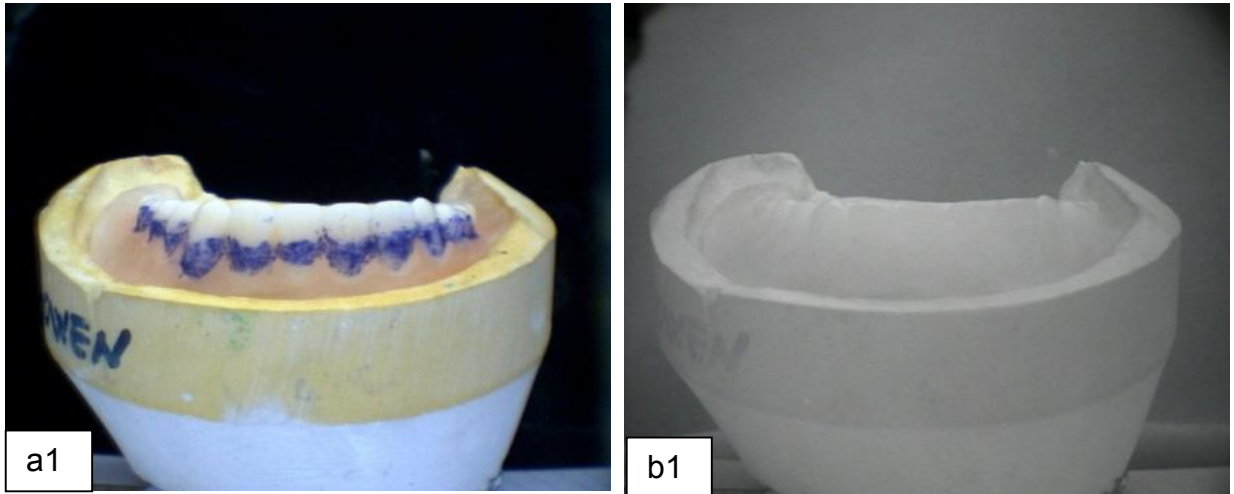
Figure 25 Lower denture with artificial dental plaque stained with 1) two-tone disclosing solution and 2) blue food colourant imaged under a) visible light and b) near IR radiation. Note that in the near IR image the artificial dental plaque is invisible and that the gingival margin has lack of detail.

Figure 26 Close up view of the denture with the starch stained with blue food colouring solution under a) visible light conditions and b) near IR radiation.

5.2.3. Discussion

The artificial dental plaque on the teeth of the denture of the images taken with the n-IR camera was invisible, therefore the concept showed promise as an alternative method for dental plaque quantification as dental plaque is "not seen" in the n-IR image this image can be used as a baseline. Moreover, the stained and non-stained images of the same subject can be combined to compute plaque coverage with minimal changes to the imaging setup. However the images obtained with the two web-cameras were not clear. The n-IR image was diffused, with poorly defined borders. This may be due to the camera lack of sophisticated optics combined with a low resolution of web cameras sensor (Vetter, 1992). This absence of focus for n-IR photography has been reported previously in the literature (DeMent and Culbertson, 1951).Somewhat improved images were obtained when a close up photography was done.

Infrared photography is useful to record objects which cannot be seen by the human eye and in this preliminary experiment the artificial dental plaque was not detected under n-IR radiation with any of the disclosing solutions used. The results from this experiment show that such a novel approach may prove useful to aid in the quantification of dental plaque by providing a control image at the same time that a disclosed image acquisition. However, further research is needed as the use of web cameras is not particularly sensitive to produce detailed pictures. The use of a more sensitive digital camera is required.

5.2.4. Conclusion

This technique shows a new digital method to quantify dental plaque. It is possible to acquire two images simultaneously of the stained and unstained structures, which

118

may be used for comparison of teeth and to quantify plaque accumulation. It overcomes problems of capturing images before/after plaque disclosure which may generate inaccuracies due to the repositioning of the head between images.

5.3. Determination of the camera settings of digital camera for n-IR imaging

A Nikon D40 digital SLR camera (Tokyo, Japan) with a Sigma 105mm F2.8 EX DG macro lens (Kanagawa, Japan), fixed on a tripod (Velbon PH-656Q, China) was set up in a dark room. This allowed it to be used under different continuous light sources (discussed in section 5.3.1). The shooting mode was set in single mode with "A" priority aperture (the camera determining the shutter speed according to the f-number chosen), the metering was matrix mode (the camera averages the exposure from the viewfinder frame), and the image files were saved in RAW format. No exposure compensation was used and the images were focused manually. A lower CD was used as a mock patient and dental plaque was simulated with blue coloured starch applied on the labial surface of teeth as described earlier.

Images were taken in sets of three, using the following sequence:

1. Visible light with Gretag Macbeth colour checker mini-chart (Munsell Colour, Michigan, USA) was used as reference for further illumination and colour standardisation (Figure 27).

2. Close up under visible light. The same settings and illumination as in the first sequence were used. The colour chart was eliminated and a close up of the canine-to-canine region was selected as the area of interest.

3. n-IR photograph. This image was taken with a Hoya R 72 n-IR filter screwed onto the lens.

The distance from the denture to the camera focal plane was measured and registered before taking each image.

5.3.1. Light sources tested for image capture

Three light sources were tested:

1. A ring flash (Nikon SB-400 ring flash, Japan) mounted on the camera's accessory shoe (Figure 28).

2. Two 50W fluorescent lamps (92014 tabletop lighting kit, Smick trading, UK).

3. Two 100W tungsten incandescent lamps (SupaLite 100W, 427125, UK).

The white balance setting in the camera (flash, incandescent and fluorescent modes) was modified to match the type of light source used each time. The lamps were placed at a 45º angle to the object as illustrated in Figure 29.

To reduce reflections on the tooth surfaces in the images taken under visible light, two polarised filters were used: a 58mm Hoya circular filter (Tokina Co., Ltd., Japan) on the lens and a pair of linear filters on top of each light source (Figure 30). The circular filter was manually rotated until minimum reflections were present. A series of images were taken to evaluate variations in the f-number and the shutter speed when the polarised filters where placed on the lens in combination with the n-IR filter, giving three different options.

1. All the filters were in place: The circular filter was screwed on the camera lens with both linear filters in front of the lamps. The n-IR filter was placed onto the circular filter.

2. The circular filter screwed on the lens with the n-IR filter on top (removing the linear filters from the lamps).

3. None of the polarised filters in place, with only the n-IR filter attached.

Figure 27 Gretag Macbeth colour checker mini-chart used to standardise the light

and colours in the image.

Figure 28 Ring flash mounted on the camera.
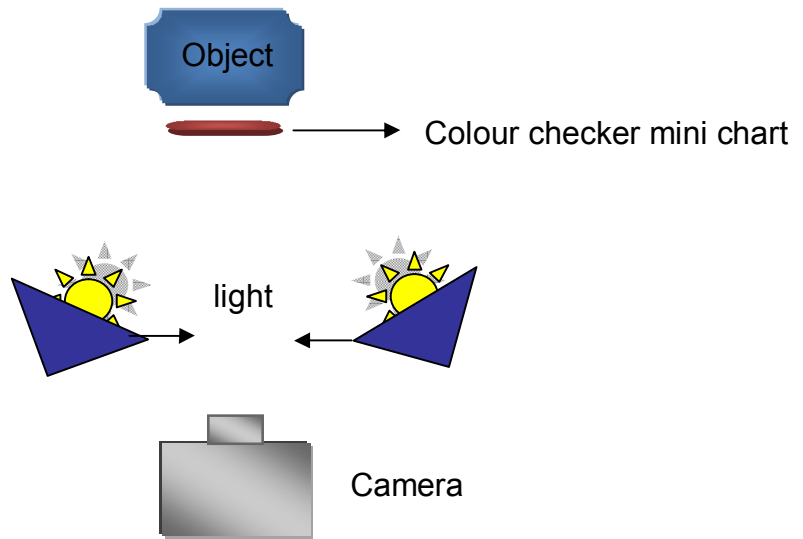
Figure 29 Scheme of the position of the light source in relationship with the camera,

the object and the colour checker mini chart.
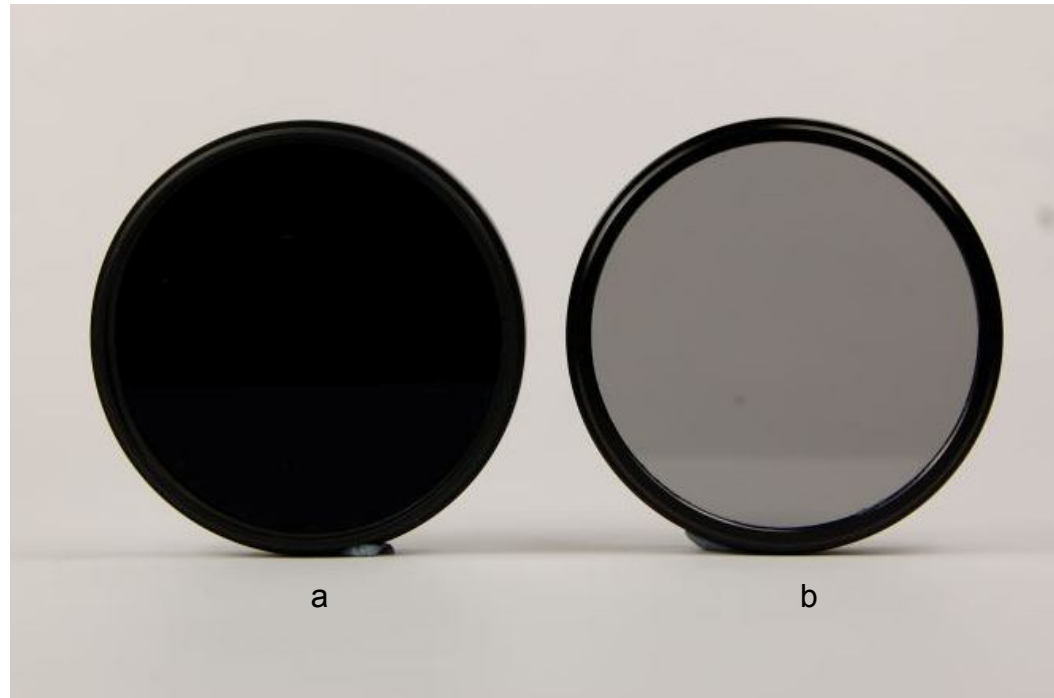
Figure 30 n-IR filter (a) and circular polarised filter (b) used to eliminate the reflections from the teeth surfaces.

To determine an appropriate sensitivity ISO setting (200, 400, 800, 1600 or 3200), the camera was set to an f/ 22.

5.3.2. Light spectrum of the light sources

The light spectra for the fluorescent lamp, the incandescent lamp and the flash were recorded with an USB 4000 modular fibre-based spectrometer (Ocean Optics, USA) and the Spectra Suite Java-based software platform (Ocean Optics, USA). The output of both the fluorescent and incandescent lights was also measured when the polarised filters (linear and circular) and the n-IR filter were covering the light source.

5.3.3. Focus shift

Because of the wavelength difference the n-IR images are formed at different focal lengths (closer distances) than the visible light ones. Series of images were taken with and without the n-IR filter to record the focal distances to determinate the point of optimum focus in the n-IR. A plastic scale was attached around the lens barrel and a piece of wire was used to mark the measurements (Figure 31). The lens barrel was rotated manually until an optimal image (i.e. in focus) was obtained.

5.3.4. Results

Figure 32 shows an example of the images obtained under a) visible light, b) the magnification of the anterior (canine to canine) area and c) n-IR radiation. The distance (measured with a metric tape) from the denture to the focal plane was between 52.0 cm and 54.0 cm when the Macbeth colour chart was framed whereas the distance for both images, the canine-canine magnification under visible radiation and under the n-IR filter was between 37.6 cm and 42.2 cm.

Figure 31 Location of the plastic scale attached around the lens barrel in the camera and the piece of wire used to register the focus

shift.
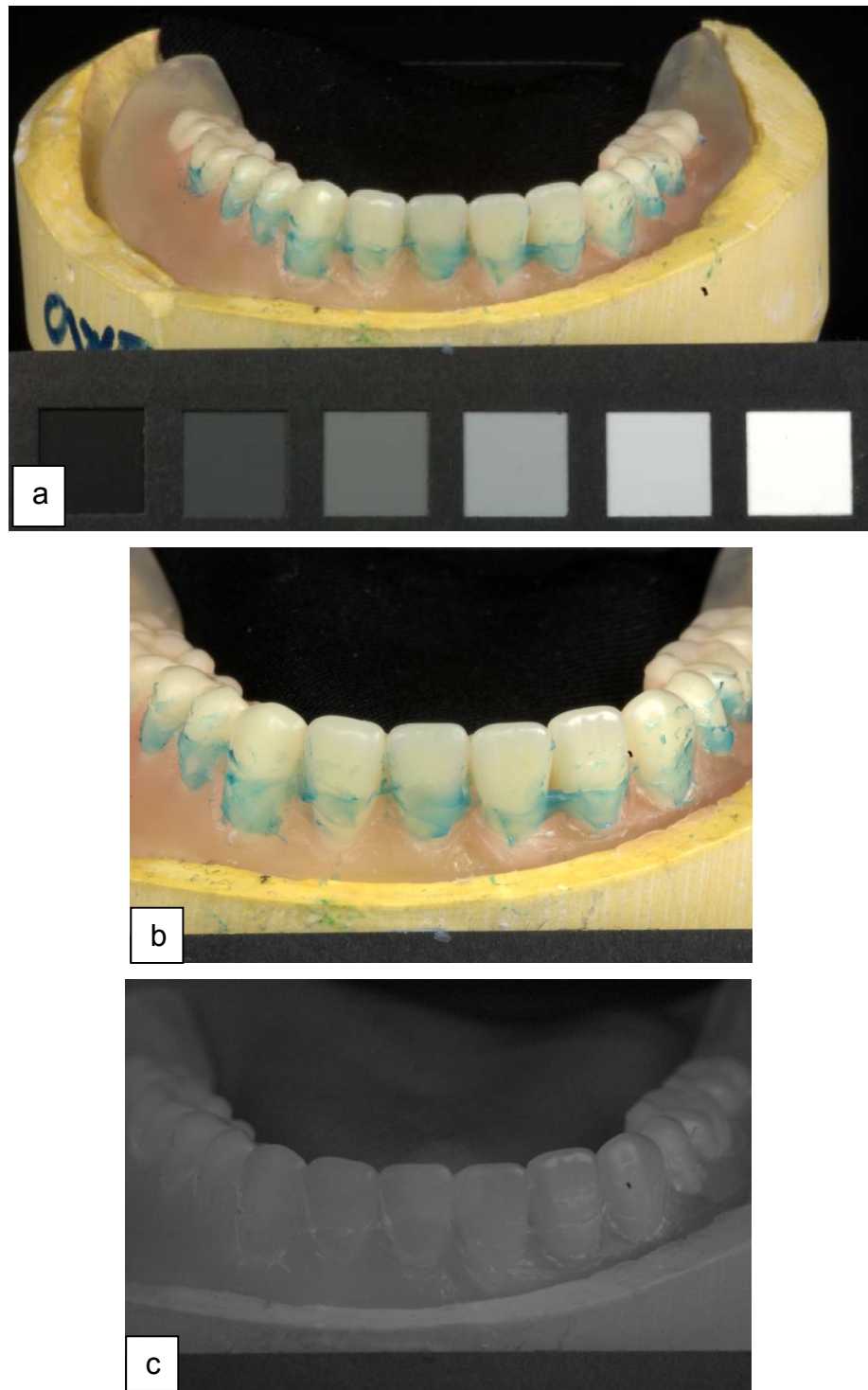
Figure 32 Example of the images sequence used in this investigation: a) visible light image, b) close up of the visible light image and c) n-IR image.

5.3.4.1. Light source

Table 14 lists the advantages and disadvantages of the light sources used in this experiment. The fastest shutter speed was recorded with flash light for both images visible light and n-IR. The longest shutter speed was recorded when using the incandescent lamps for the visible images. For the n-IR images, the longest shutter speed was recorded when fluorescents lamps were used. Figure 33 shows the shutter speed differences for the three light sources under visible light; whilst Figure 34 shows the shutter speed differences for the three light sources under n-IR light.

5.3.4.2. Light spectra of the light sources

The light spectra for the flash, fluorescent and incandescent lamps are shown in Figure 35 to Figure 37. The output when both types of polarised filters were used to cover the light source is also shown. The output of the fluorescent and the incandescent lamps when the n-IR filter was used is shown in Figure 38.

5.3.4.3. Shutter speed with and without the polarised filters

The n-IR filter was used in combination with both polarised filters on, only the circular filter on, and without both polarised filters (Figure 39). The shutter speed differences for the visible images between an ISO 200 and 400 for incandescent light and fluorescent light are shown in Table 15 and Table 16. The shutter speed was faster under ISO setting 400 than for ISO 200 for those images taken under visible light. The exposure time was as expected longer when all the filters (both polarised and n-IR filter) were used under both incandescent and fluorescent light sources. The exposure time was reduced when the n-IR filter was used without any of the polarised filters was the fastest option.

Table 14 Advantages and disadvantages of the light sources used.

Light source	Advantages	Disadvantages
Incandescent light:	Good source of n-IR radiation therefore the shutter speed is faster than with the fluorescence lights	The shutter speed for the visible light shoot is the slowest, produces heat and under high f-numbers there is a hot spot in the image
Fluorescent light:	The shutter speed for the image under visible light is fast, there is no heat production	Bad source of n-IR radiation therefore the shutter speed is long
Flash	The shutter speed for both images is fast, there is no heat production is a good source of n-IR radiation and is practical to use	No control on the reflections on the teeth's surfaces. Hot spot present when high f-numbers are used

Light source Two 100W lamps
White balance Incandescent
f-number 22
Shutter speed 8 seconds
ISO: 200

Light source Two 50W fluorescent lamps
White balance Fluorescent
f-number 22
Shutter speed 2.5 seconds
ISO: 200

Light source Flash
White balance Flash
f-number 22
Shutter speed 1/60 seconds
ISO: 200

Figure 33 Shutter speed differences for the three light sources under visible light for a) incandescent lamps, b) fluorescent lamps and c) flash. The Incandescent lamps resulted in the longest shutter speed whilst the flash gave the shortest.

Light source Two 100W lamps
White balance Incandescent
f-number 22
Shutter speed 30 seconds
ISO: 400
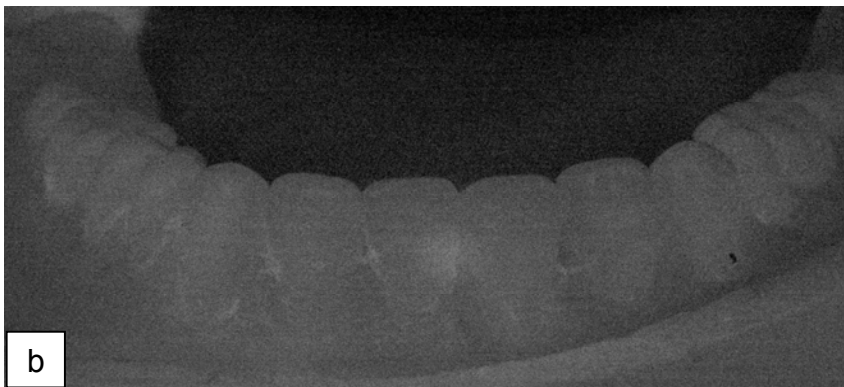
Light source Two 50W fluorescent lamps
White balance Fluorescent
f-number 22
Shutter speed 32 seconds
ISO: 400

Light source Flash
White balance Flash
f-number 22
Shutter speed 1/60 seconds
ISO: 400

Figure 34 Shutter speed differences for the three light sources with the near IR filter on: a) incandescent, b) fluorescent and c) flash. Note the increase in the shutter speed when incandescent and fluorescent lamps were used as well as the hot spot in the former and the noisier appearance of the latter.
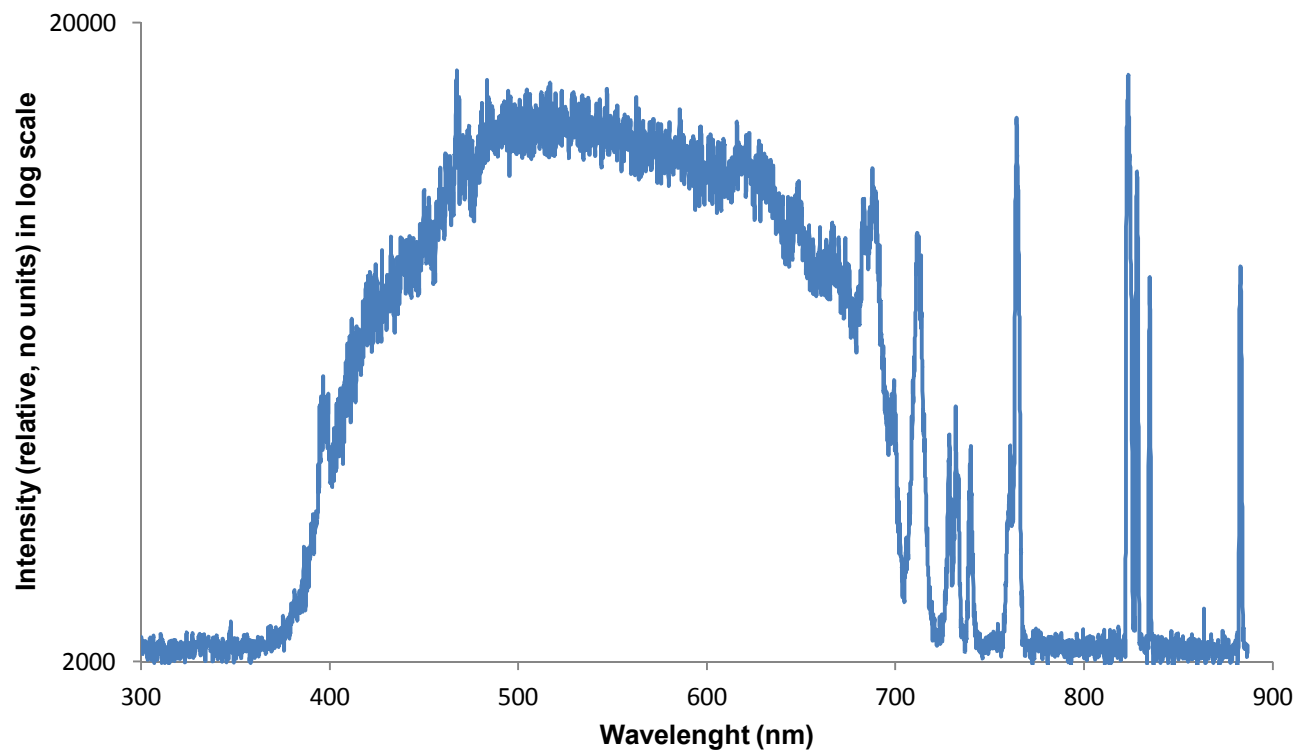
Figure 35 Light spectrum of the Nikon SB-400 ring flash.
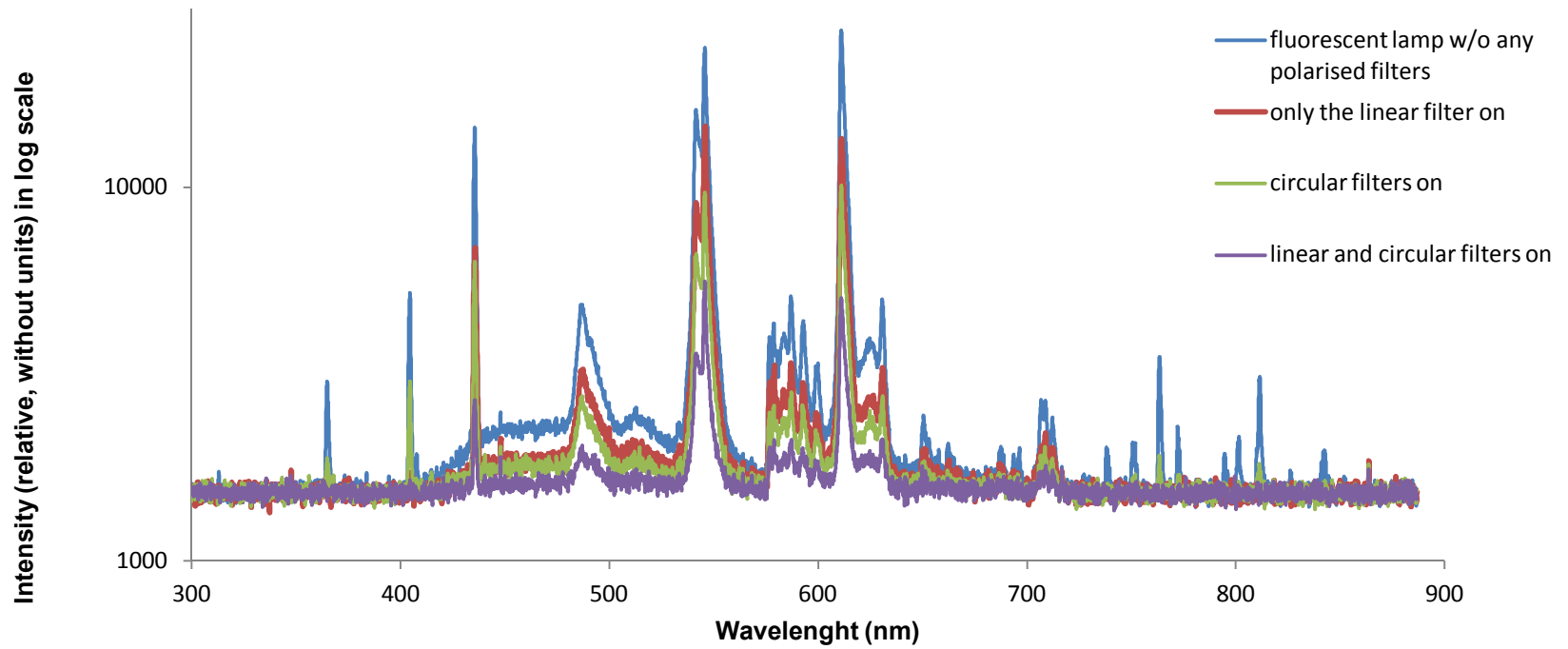
Figure 36 Light spectra for the fluorescent lamp with and without the polarised filters.
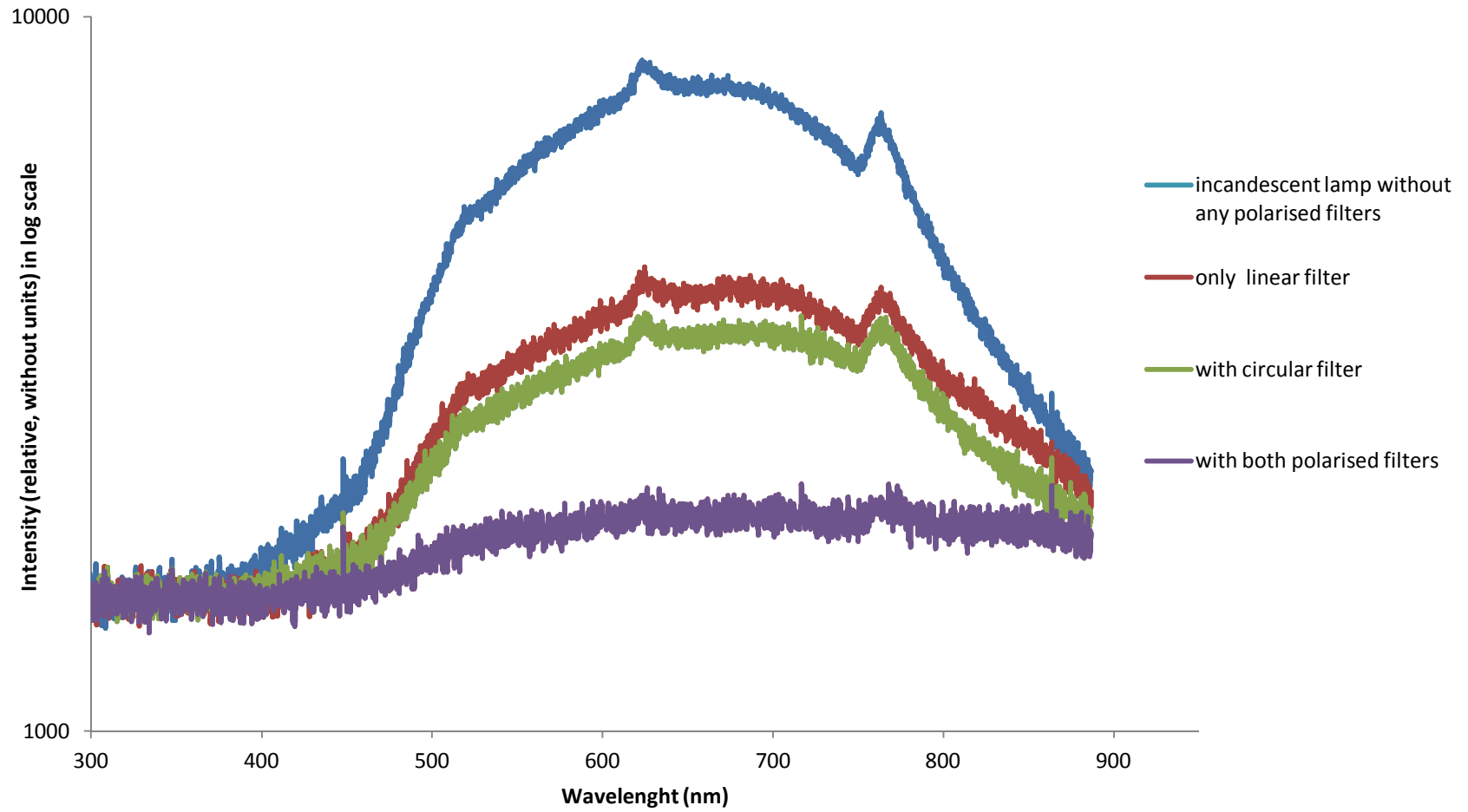
Figure 37 Light spectra for the incandescent lamp with and without the polarised filters.
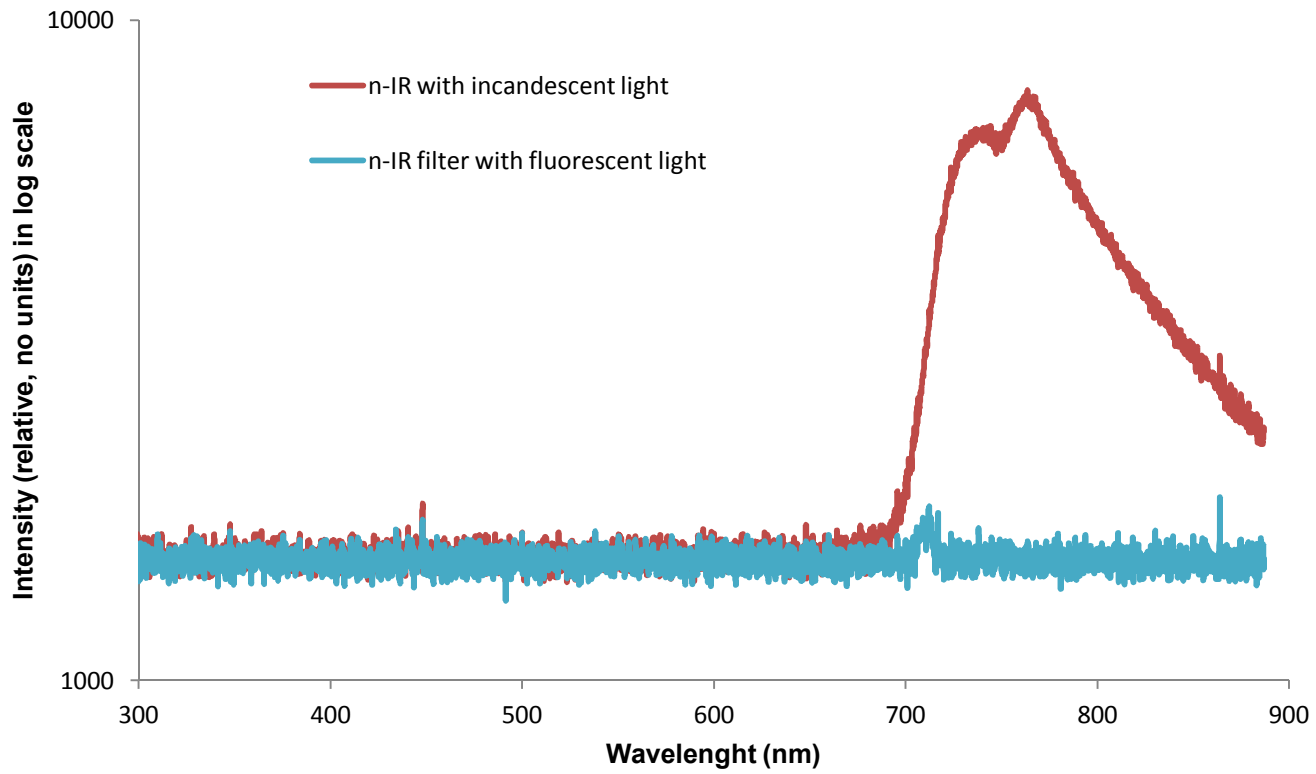
Figure 38 Light spectra for the incandescent and the fluorescent lamps when the light source is filtered with the Hoya R 72 n-IR filter.
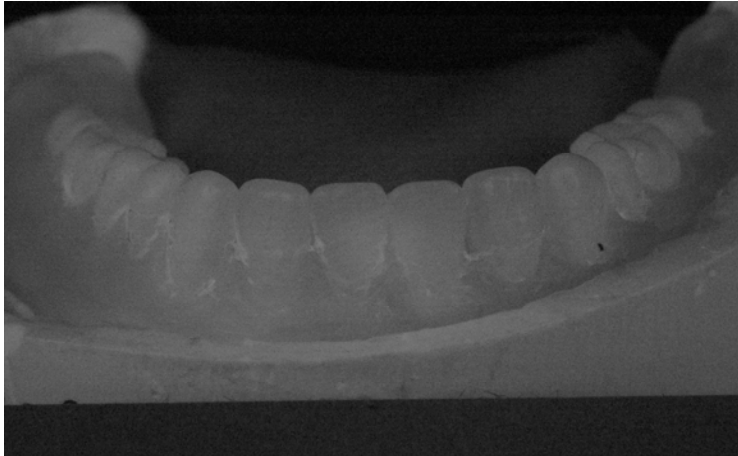
Light source Two 50W fluorescent lamps
White balance Fluorescent
f-number 14
Shutter speed 32 seconds
ISO 400
Polarised filters Both filters on
n-IR filter On

Light source Two 50W fluorescent lamps
White balance Fluorescent
f-number 14
Shutter speed 8 seconds
ISO 400
Polarised filters linear filters off, circular filters on
n-IR filter On
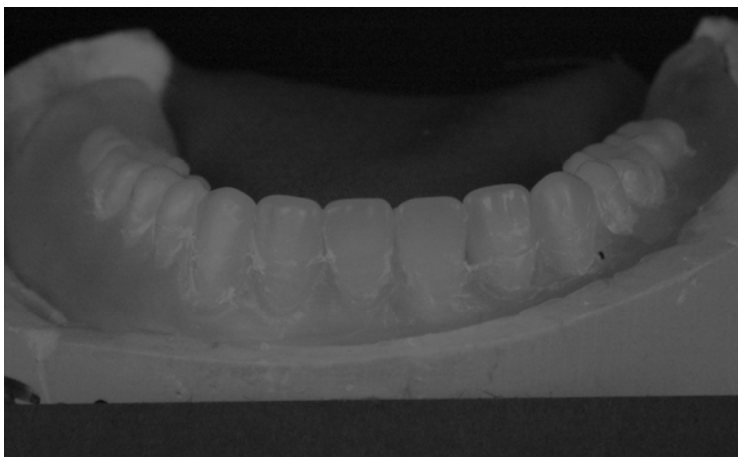
Light source Two 50W fluorescent lamps
White balance Fluorescent
f-number 14
Shutter speed 8 seconds
ISO 400
Polarised filters both filters off
n-IR filter On

Figure 39 Images obtained with and without the polarised filters for the near-IR images: a) both filters on, b) only the circular filter on, and c) both filters off. It can be seen the shutter speed increases with the addition of both polarised filters.

Table 15 Shutter speed of visible and n-IR images (ISO 200 and 400) and the f-numbers using polarised filters and a fluorescence light source.

	f- number	Visible light ISO 200	Visible light ISO 400	n-IR filter + Both polarised filters	n-IR filter + Circular filter on, linear off	n-IR filter + Both polarised filters off
Shutter speed	22	1.3s	1/1.6s	Lo (32s)	25s	20s
	20	1s	1/2s	Lo (32s)	20s	15s
	18	1/1.3s	1/2.5s	Lo (32s)	13s	13s
	16	1/1.6s	1/3s	Lo (32s)	10s	10s
	14	1/2s	1/4s	Lo (32s)	8s	8s
	13	1/2.5s	1/5s	Lo (32s)	6s	6s
	11	1/3s	1/6s	21s	5s	5s
	10	1/4s	1/8s	18s	4s	4s
	9	1/5s	1/10s	13s	3s	3s
	8	1/6s	1/13s	13s	2.5s	2.5s
	7.1	1/7.1s	1/15s	8s	2s	2s
	6.3	1/10s	1/20s	7s	1.6s	1.6s
	5.6	1/13s	1/25s	6s	1.6s	1.3s
	5	1/15s	1/30s	4s	1.3s	1s
	4.5	1/20s	1/40s	3s	1s	1/1.3s
	4	1/25s	1/50s	3s	1/1.3s	1/1.6s
	3.5	1/30s	1/60s	2s	1/2s	1/2s
	3.2	1/40s	1/60s	2s	1/2.5s	1/2.5s
	2.8	1/50s	1/80s	1.5s	1/3s	1/2.5s

Table 16 Shutter speed of visible and n-IR images (ISO 200 and 400) and the f-numbers using polarised filters and an incandescent light source.

f- number	Visible light ISO 200	Visible light ISO 400	n-IR filter + Both polarised filters on	n-IR filter + Circular filter on	n-IR filter + Both polarised filters off
22	10s	4s	Lo (32 s)	25s	25s
20	8s	3s	30s	20s	20s
18	5s	2.5s	20s	15s	13s
16	4s	2s	15s	13s	10s
14	3s	1.6s	13s	10s	8s
13	2.5s	1.3s	10s	8s	6s
11	2s	1s	8s	6s	5s
10	1.6s	1/1.3s	6s	5s	4s
9	1.3s	1/1.6s	5s	4s	3s
8	1s	1/2s	4s	3s	2.5s
7.1	1/1.3s	1/2.5s	3s	2.5s	2s
6.3	1/1.6s	1/3s	2.5s	2.0s	1.6s
5.6	1/2s	1/4s	2s	1.6s	1.3s
5	1/2.5s	1/5s	1.6s	1.3s	1s
4.5	1/3s	1/6s	1.3s	1s	1/1.3s
4	1/4s	1/8s	1s	1/1.3s	1/1.6s
3.5	1/5s	1/10s	1/1.3s	1/1.6s	1/2s
3.2	1/5s	1/10s	1/1.3s	1/2s	1/2s
2.8	1/6s	1/13s	1/1.6s	1/2.5s	1/2.5s

Shutter speed

An example of the variations in the images obtained under fluorescent lamps for three different apertures (f's) under an ISO 200 and 400 are shown in Figure 40. The shutter speed under f/22 with different ISO numbers (200 to 3200) for the visible and n-IR pictures are shown in Table 17

5.3.5. Discussion

This study showed that it was possible to obtain clinical n-IR images using a Hoya R 72 infrared filter. This filter allows radiation above 720nm through the lens and has the advantage of simplicity compared to converting the camera to n-IR by removal of the IR filter from the camera sensor. However, one disadvantage is that the filter is opaque at visible wavelengths and once in place, it is not possible to focus or frame the picture. As a solution, the camera was focused visually under visible light without the near-IR filter in place, followed by its quick threading over the lens before the shot.

5.3.5.1. Light source

All three light sources proved to be a suitable choice for photographing dentures in the visible spectrum however, for n-IR imaging it was necessary to have an equivalent n-IR radiation source present. The greatest source of n-IR radiation is daylight which by its very nature is difficult to control. In this investigation, all the pictures were taken inside a dark room using only the light sources described (incandescent, fluorescent and flash) to avoid light contamination.

f/32 shutter speed 2.5s ISO 200

f/32 shutter speed 1.3s ISO 400

f/10 shutter speed 1/4s ISO 200

f/10 shutter speed 1/8s ISO 400

f/2.8 shutter speed 1/50s ISO 200

f/2.8 shutter speed 1/80s ISO 400

Figure 40 Example of the difference in the shutter speed under an ISO 200 (left) and 400 (right) for an a) f/32, b) f/10, and c) f/2.8 for visible light images under fluorescence light. It can be seen a diminution on the depth of field with smaller f stops. The images taken with an ISO 400 had a faster shutter speed.

Table 17 Shutter speeds under different ISO numbers for an f/22 under visible light and n-IR radiation. As expected the shutter speed decreased under higher ISO, however the images with an ISO above 400 were also noisier.

ISO	F-number	Shutter speed	
		Visible light	n-IR
200	f/22	1/1.3s	8s
400	f/22	1/1.6s	4s
800	f/22	1/3s	2s
1600	f/22	1/6s	1s
Hi 1	f/22	1/13s	1/1.6s

Incandescent lamps are a good source of n-IR radiation, but produce large amounts of heat as light is generated from a heated tungsten filament. The electronic flash with xenon tubes emits enough infrared radiation to take the images under small apertures and is practical to use with short exposure times. However, the main inconvenience when using the flash was the difficulty in adjusting the position of the circular polarising filter in relation to the linear polarised filters on the light source. Fluorescent lamps produce light with little n-IR energy (Williams, 1984, Tetley and Young, 2007) which makes them suitable for the images under visible light but not for the n-IR ones.

5.3.5.2. Light spectra of the light sources

The light source spectra were recorded to identify their relative wavelength peaks therefore all the measurements are in arbitrary units. The output spectrum of the flash was mainly in the visible region, with a few sharp peaks in the IR region (above 700nm) which suggested that flash light could be used in n-IR image acquisition. No outputs of the flash were possible to be obtained when the polarised filters or the n-IR filter were in front of the light source due to the complexity of registering the flash spectrum by the spectrophotometer. The speed at which the light was produced did not provide enough time for the present system to record it.

The fluorescent light output was formed by the combination of peaks along the UV, visible and n-IR electromagnetic regions of the spectrum with the majority of the output in the visible area (400nm to 700nm). This may explain why fluorescent sources are not the best sources for n-IR radiation.

The output of the incandescent lamp gave a bell shaped output which consisted of both the visible and IR regions in the electromagnetic spectrum. The incandescent

lamps provide a constant production of energy within the infrared spectrum with a second peak located in the region around 760nm.

As expected, when the polarised filters were used, there was a reduction on the height of the spectral peaks. This was related to the filters blocking about one half of the incident light. The reduction was more pronounced when both filters (linear and circular) were placed in front of the light source (Figure 37). This corresponds with the results obtained when testing the relationship between shutter speed and the polarised filters of the camera. Finally, when the n-IR filter was placed in front of the light sources using the incandescent lamp as a light source, the output registered a peak in the n-IR region whilst the output for the fluorescent lamp was almost linear with only a small amount of n-IR energy registered at a wavelength of approximately 720nm (Figure 38).

5.3.5.3. Shutter speed

When capturing images under both visible light and n-IR the fastest shutter speed recorded was when the flash was used. With the camera set in flash mode the shooting speed was 1/60 seconds and this does not take into account either the ISO or the f-numbers. Therefore, when the f-numbers were decreased (f/22) in order to obtain a greater focus depth the quality of the image was altered. A better control on the settings was achieved when the fluorescent and tungsten lamps were used but this led to an increase in the shutter speed. To deal with longer exposure times the camera was mounted on a tripod. When fluorescence lights were used for n-IR images the shutter speed was extended and resulted in dark images due to the lack of n-IR radiation produced. To correct this, the f-number was reduced; however values lower than f/11 added noise to the image. Therefore the selected option was

to use the incandescent lamps as a light source as they provided more n-IR radiation.

5.3.5.4. Shutter speed and the polarised filters

Testing different combinations of the n-IR filter and the polarised filters was done to determinate if there were any interactions between the filters and the shutter speed. The exposure time was longer when both polarised filters were left on place with the n-IR filter on top. This shows that the use of polarised filters increases the f-stop by two steps in the camera therefore blocking out about one half of the light. However, the differences in the shutter speed between images produced without the filters and those where the linear filter was removed were less than 5 seconds. Therefore, the selected option was to use both the polarised filters in combination with the n-IR filter with a bigger aperture (e.g. f/7.1).

5.3.5.5. ISO and f-number

The ideal ISO for visible light images was either 200 or 400 with little difference between them whilst ISO values higher than 800 added noise to the images. The ISO 400 gave faster shutter speeds therefore it was the preferred option. The ideal ISO for n-IR light images was set at 400, because although higher ISO values gave shorter shutter speeds, the resulting images had noticeably more noise.

5.3.5.6. Focus shift

This refers to the difference in the focus distance between the visible and the n-IR images. The pictures taken under n-IR filter appear out of focus mainly in the anterior region which agrees with the findings of Williams (1984). The focus shift occurred specifically in the region of the central incisors (Figure 41). The focus shift was found to be 2-3mm closer to the object for the n-IR image.

Visible light.

n-IR image without focus shift.
Central incisors out of focus
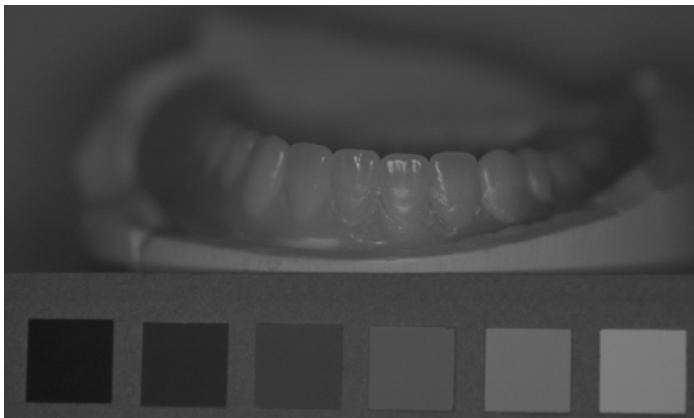
n-IR image adding the focus shift compensation.
Central incisors in focus

Figure 41 Image taken under visible light and the n-IR images with and without the focus shift. It shows that the focus shift in the IR is shorter than in the visible with the central incisors out of focus. When adding the focus shift compensation the central incisors are in focus.

5.3.5.7. Hot spot

A hot spot is a bright round disc that appears in the centre of the n-IR image because of a reflection pattern in the lens. It is related to the lens coating, which is designed for visible light (as most IR radiation would not normally reach the sensor). Due to the characteristics of the lens, a hot spot appeared in the middle of the image when incandescent lamps were used in combination with large f-numbers (small apertures). This also sometimes occurred when using flash. It was noticed that the smaller the aperture the brighter and smaller the spot became (Figure 42), however small apertures resulted in a lack of depth of field. There are two possible solutions to eliminate the hotspot from the images. One is to remove the IR blocker to convert the camera for infrared photography. The other option is to frame the object off centre to the viewer either below or above it. A decision was made to use the second approach because of its simplicity.

5.3.6. Conclusion

Near-infrared photography is useful to reveal certain differences in objects that cannot be seen by the human eye. This work demonstrated that it was possible to use n-IR imaging to create a baseline image to be compared against visible light images. The summary of the camera settings for the visible and the n-IR images produced are in Table 18. The ideal illumination source for visible photography was fluorescent lamps whilst for image capture with n-IR, incandescent lamps were the best.
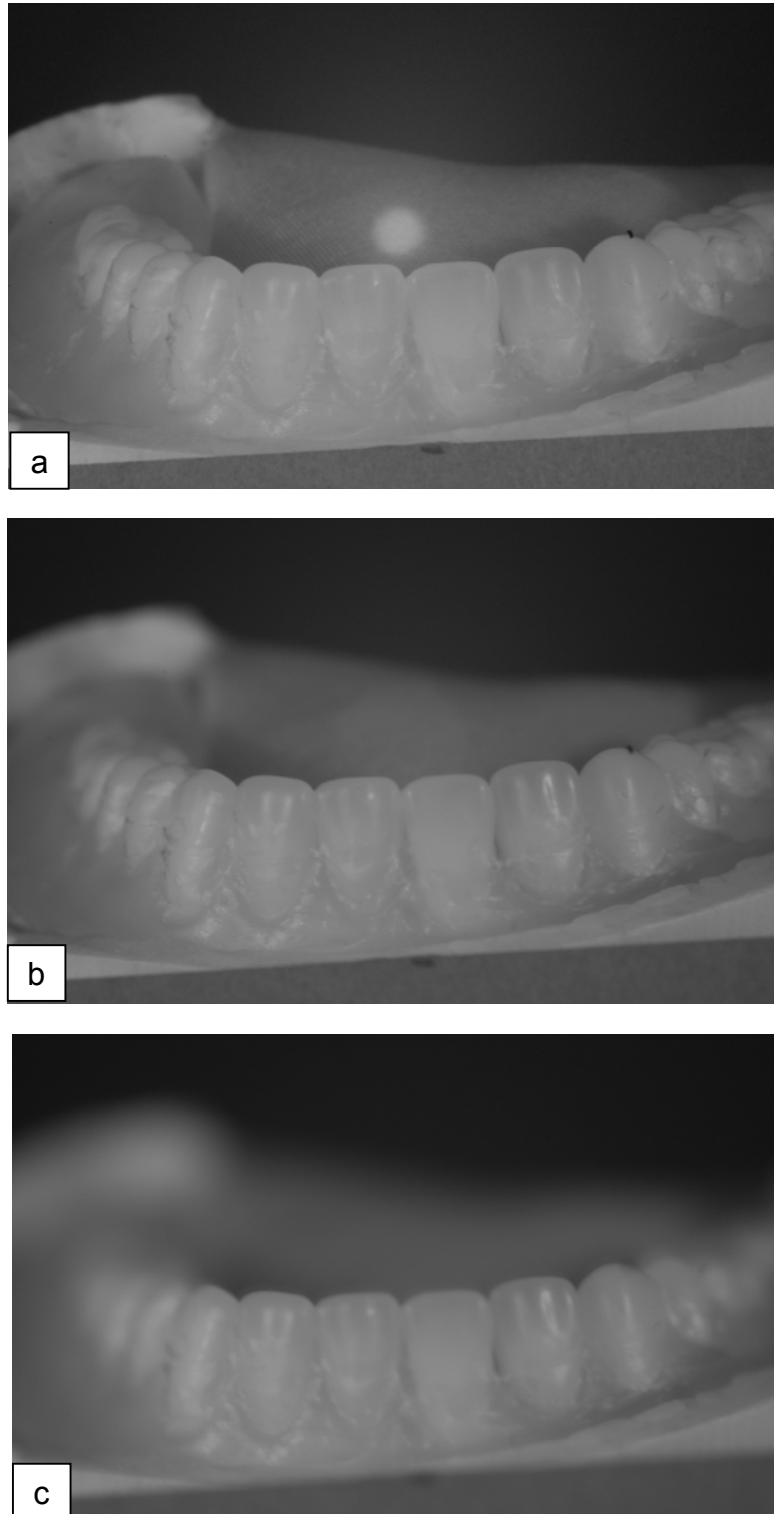
Figure 42 Hot spot behaviour when incandescent is used as a light with an a) f/22, b)

f/9, and c) f/2.8. The hot spot was brighter when small apertures (f/22) were

used. Longer apertures (f/2.8) reduced the depth of field.

Table 18 Camera settings (white balance, ISO, Shooting mode, metering, f-number and light source) for the visible light and n-IR

images resulted from this experiment.

Radiation		White balance	ISO	Format	Shooting mode	Metering	f-number	Light source
Visible light		Incandescent, Fluorescent & Flash	200	RAW	Single	Matrix	f/22	
n-IR	Incandescent	Incandescent	400	RAW	Single	Matrix	f/16	Two 100W incandescent lamps
	Fluorescent	Fluorescence	400	RAW	Single	Matrix	From f/7.1 or lower (there is noise)	Two 50 W fluorescent lamps
	Flash	Flash	400	RAW	Single	Matrix	f/22	Ring flash

Chapter 6
Clinical application of near-infrared photography in dental plaque detection

The aim of this part of the thesis was to investigate the feasibility of automated quantification of plaque coverage on digital images (from both CDs and clinical images) using n-IR imaging and narrow band pass interference (NBI) filter.

6.1. Sample collection

6.1.1. Images of complete dentures

Patients who attended the Prosthetics clinic at the Birmingham Dental Hospital between February and July 2010 underwent routine clinical oral hygiene instruction of their CDs. As part of this hygiene instruction, their complete upper dentures were stained to identify the presence of plaque and digital images were taken. There were no inclusion/exclusion criteria other than the patient wore an upper CD. Due to the routine nature of the procedure no ethical issues were required to address. Details of the methods used and frequency to clean the denture, as well as the length of time that the patient had been using dentures were recorded.

The dentures were removed from the patients' mouth and rinsed for 5 seconds with tap water to eliminate food debris. A dye solution (brilliant blue) at a concentration of 8.3×10^{-2} mol/dm^{-3} (6.6g/L) was used to disclose dental plaque (for more details see appendix III). Two drops of the dye were applied with a 3ml plastic pipette on a) right, b) middle and c) left buccal denture surfaces (pink acrylic) and on d) right, e) middle and f) left teeth surfaces (acrylic teeth). Only one drop of the dye was applied on both the base and fitting denture surfaces. The denture was rinsed with tap water for 15 seconds to remove the dye excess. The stained denture was placed on a piece of

absorbent paper to eliminate excess water and placed on top of a disposable plastic base. A photographic frame with an incorporated tripod mount for the camera was used to take the images in a known position (Figure 43). For cross infection control, the photographic frame was wiped with SaniCloth70 (PDI, USA) and the disposable plastic base was replaced between patients. Once the photographic session was finished and before returning the denture to the patient, it was disinfected by immersion in 0.2% hypochlorite for 60 seconds and brushed with soap and water. If remnants of the dye were still visible, the denture was taken to the laboratory to polish any remaining plaque/debris or dye.

Two tungsten incandescent lamps in an angle of 45° were used as a light source inside a room where the blinds were closed. Light reflections on the surface of the dentures were minimised by using a circular polarised filter on the lens and a pair of linear filters on top of the light sources. The dentures were photographed on two different backgrounds black and white. The camera settings used to obtain the images of the upper CDs are detailed Table 19.

Each denture was imaged with six views: right, left, frontal and posterior as well as the occlusal surface and the fitting surface. Each view of the digital images was taken three times under the following sequence:

1. Visible light image: the row with the white, grey and black shades of the Gretag Macbeth colour checker mini-chart was included in the frame and in front of the denture, as reference for further illumination/colour standardisation.

2. Photography with a 636nm NBI filter (Edmund Optics, USA).

3. Near-infrared image with a Hoya R 72 n-IR filter.
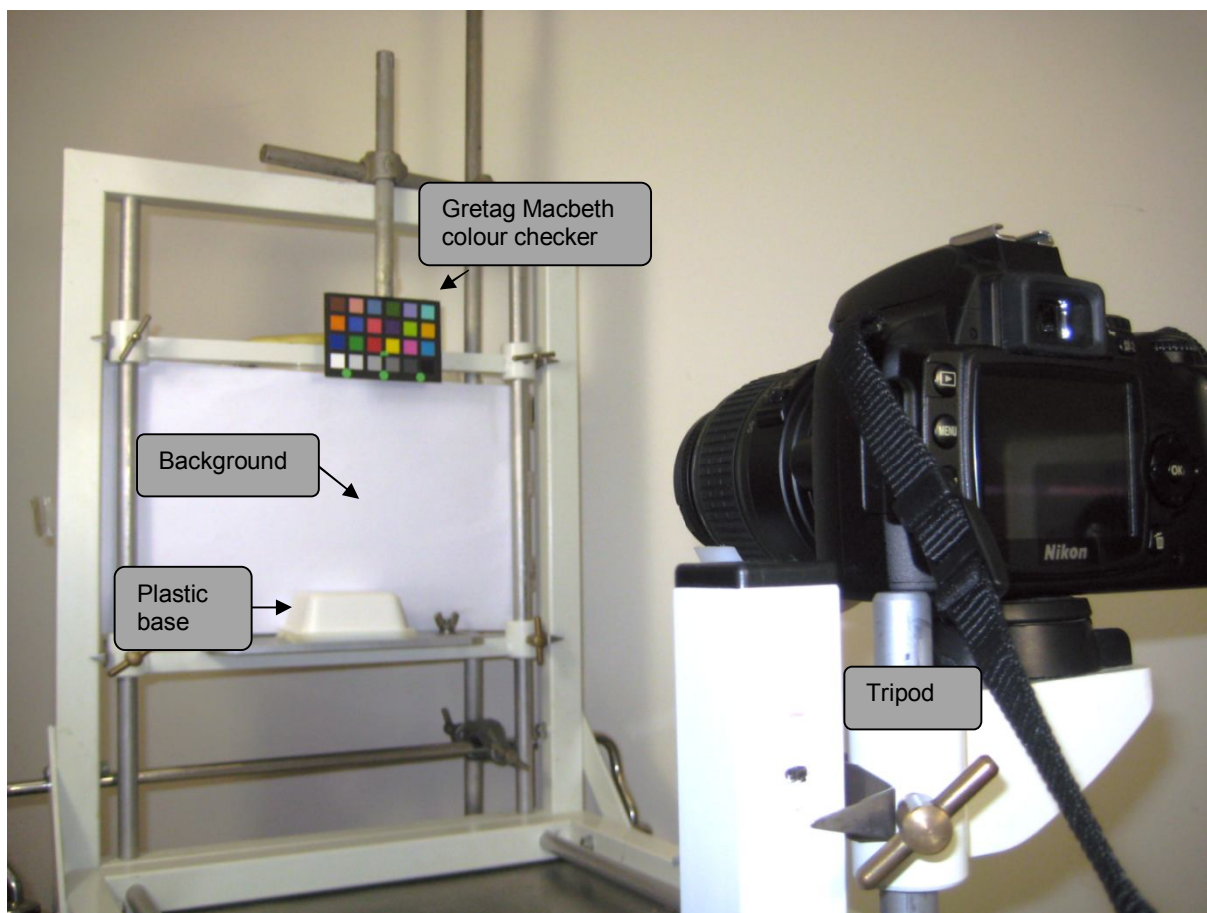
Figure 43 Adjustable photographic frame and incorporated tripod used to take the pictures of the complete upper dentures. The image shows the set up for the camera, the disposable plastic base and the position of for the images taken on a white background.

Table 19 Camera settings used to obtain the images of the upper complete dentures for the visible, narrow band interference filter and n-IR filter images.

Photograph	White balance	ISO	Program	Shooting mode	Shutter speed	Metering	f-number	Programme	Focus shift
Visible light	Incandescent	400	RAW	Single	Auto	Matrix	f/22	A	n/a
Narrow band interference	Incandescent	400	RAW	Single	5s	Matrix	f/22	M	n/a
n-IR	Incandescent	400	RAW	Single	15s	Matrix	f/16	M	2mm (closer to object)

Although all six views of the images were corrected, only the frontal view of the images was further analysed, for an easier handling of the data. The analysis of the rest of the views will be done as future work.

6.1.2. 636nm NBI filter

The disclosing dye (Brilliant Blue) used in this study had its greatest absorption at a wavelength of 630nm. A NBI filter was incorporated in front of the lens of the camera to photograph blue-stained dental plaque with the highest possible contrast (Figure 44).

6.1.3. Clinical images

This part of project took place at the Birmingham Dental Hospital which is part of the South Birmingham Primary Care Trust. Twenty-five volunteers (students at the School of Dentistry at the University of Birmingham) were recruited for the trial. Ethical approval (NHS-REC reference 10/H1207/5) was obtained from the National Research Ethics Committee (Appendix IV). The inclusion criteria for participants who were willing to participate in the trial having understood, signed and read the consent form were: to have intact natural teeth in the upper and lower anterior region from canine to canine, without evidence of any prosthetic (bridges/dentures) work, to be older than 18 years old and a student at the School of Dentistry. The main exclusion criterion was pregnancy, due to the documented ability of the hormonal changes (experienced in this state) to predispose the gingival tissues to inflammatory alterations (Barak et al., 2003, Laine, 2002).
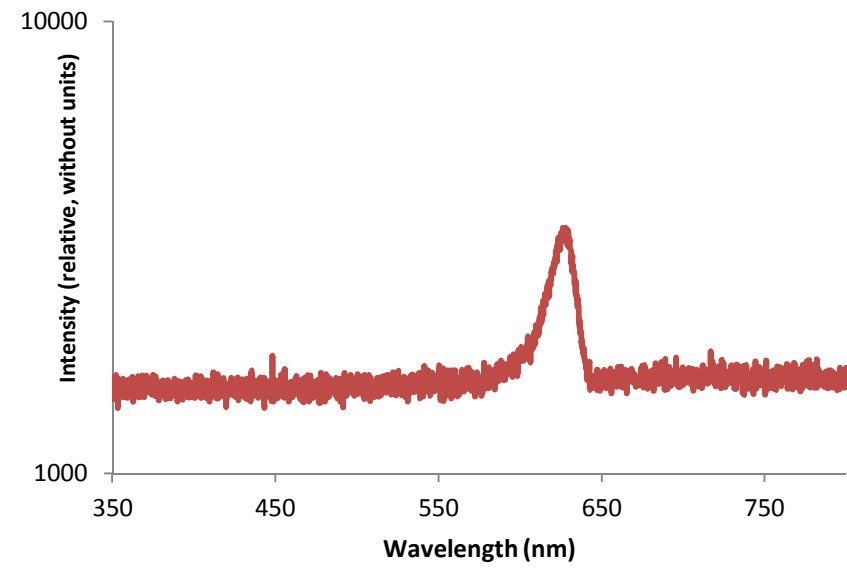
Figure 44 636nm narrow band interference filter and its spectral absorption.

The volunteers were asked to attend the clinic on two occasions. On the first visit, the volunteers brushed their teeth for 3 minutes using the Bass technique (Bass, 1954) with a fluoride containing toothpaste (Aquafresh, GlaxoSmithKline, UK) and a standard medium-head toothbrush (Oral B Advantage, Procter & Gamble, USA). After this, they were then instructed to position themselves in the frame of an adjustable photographic head holder frame that allowed the images to be taken at a known position and on how to use the cheek retractors. A facial mirror was placed in front of the subjects to assist them in their positioning in the frame. Figure 45 shows the subject position in the photographic head holder frame. A sheet of beauty wax was used as a biting plate to ensure the front teeth of the volunteers obtained an edge-to-edge position. The wax was softened with a water bath and cut into two halves. Each half was then folded to produce a narrow strip that was converted in the biting plate. Three intraoral images of the anterior region of their dentition were taken following the same sequence as for the images from the complete upper dentures (visible light, NBI filter and n-IR photography). At the end of the session, the volunteers were asked to refrain from any form of oral hygiene for 48hrs to allow plaque to accumulate. The volunteers were allowed to use mints as a mouth freshener if they felt that their breath was affected by the lack of hygiene, however chewing gum and mouth rinses were not allowed as they could disrupt plaque formation. The biting plate was disinfected according to the protocol followed in the prosthetics clinic by immersing it in 0.2% hypochlorite for 60 seconds and stored in a plastic bag that contained the volunteers' identification details. This was reused for repositioning at the next session.
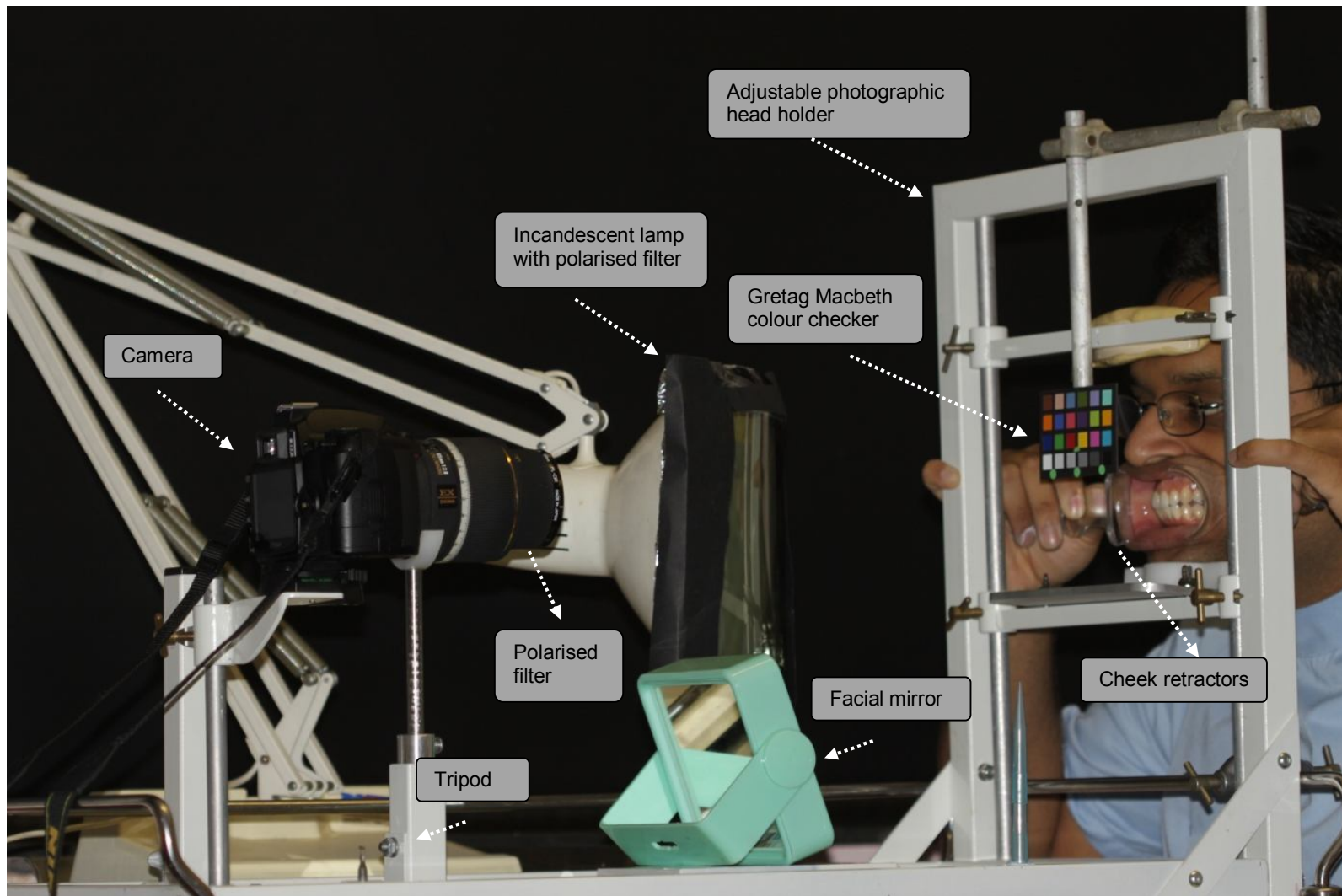
Figure 45 Subject position in the photographic head holder frame when taking the intraoral images.

The patients were asked to come back after 48hrs. A routine clinical procedure to disclose plaque was undertaken. Two drops of brilliant blue solution, at a concentration of 8.3×10^{-2} mol/dm^{-3} (6.6g/L), were placed under the volunteer's tongue, with a 3ml plastic pipette. The volunteer was asked to rinse to eliminate the excess of the dye following which the biting plate and the cheek retractors were given to the subject and the same images as in the first session were taken. Once the images were obtained, the volunteers were free to remove the stained plaque deposits. The light source, camera settings and the illustration room used to obtain the images were the same as the setting used to image the upper CDs discussed previously.

6.1.4. Image processing

All the images obtained were transferred to a computer (Dell Precision M4500, Dell Inc., USA) and ImageJ "v1.45f9" was used for their correction and analysis. The RAW files from the camera were decoded and opened with the DCRaw reader "v1.2.0" plugin (Coffin, 1997) without white balance. The decoded data was saved as a TIFF to be used as a "working" image whilst the original, unmodified, RAW image was kept as a backup. Macros were created whenever this was possible, using the ImageJ Macro Recorder function as a guide in the writing procedure, to simplify the analysis of the images. Specific plugins, part of the ImageJ software package, were also used. A more detailed description of the plugins described in the following sections can be found in the list of definitions at the beginning of the thesis whilst the macros used in the analysis of the images are in appendix V.

6.1.4.1. Image colour correction

The images were obtained from three different sources: Images from CDs on a white background (**DWB**), images from CDs on a black background (**DBB**) and clinical images (**ICT**). Due the differences in the image background, different methods were taken to correct them prior to their analysis. The ICT were corrected in a similar way as the DWB images. Therefore the description of the colour correction is mainly focused on the procedure followed to correct both DWB and DBB images, indicating any difference in the correction of the ICT. These procedures were repeated for all six photographic views. Figure 46 summarises the procedures followed in the image correction whilst Figure 47 is an example of the DWB and DBB images after their correction.

a) Visible light images

The light balance of the visible images of the DWB DBB and ICT images was calibrated using the Chart White Balance plugin by drawing a line from the black tile to the white one (right to left) on the image with the Macbeth colour checker mini chart.

b) Images taken with the 636nm NBI filter

The NBI images for the DWB, DBB and ICT were converted into RGB stack and its red channel was duplicated, converted into 8bits (grey level) and saved under the name of "red". Only the red channel of the image was used because no information was recorded in the remaining channels (blue and green).
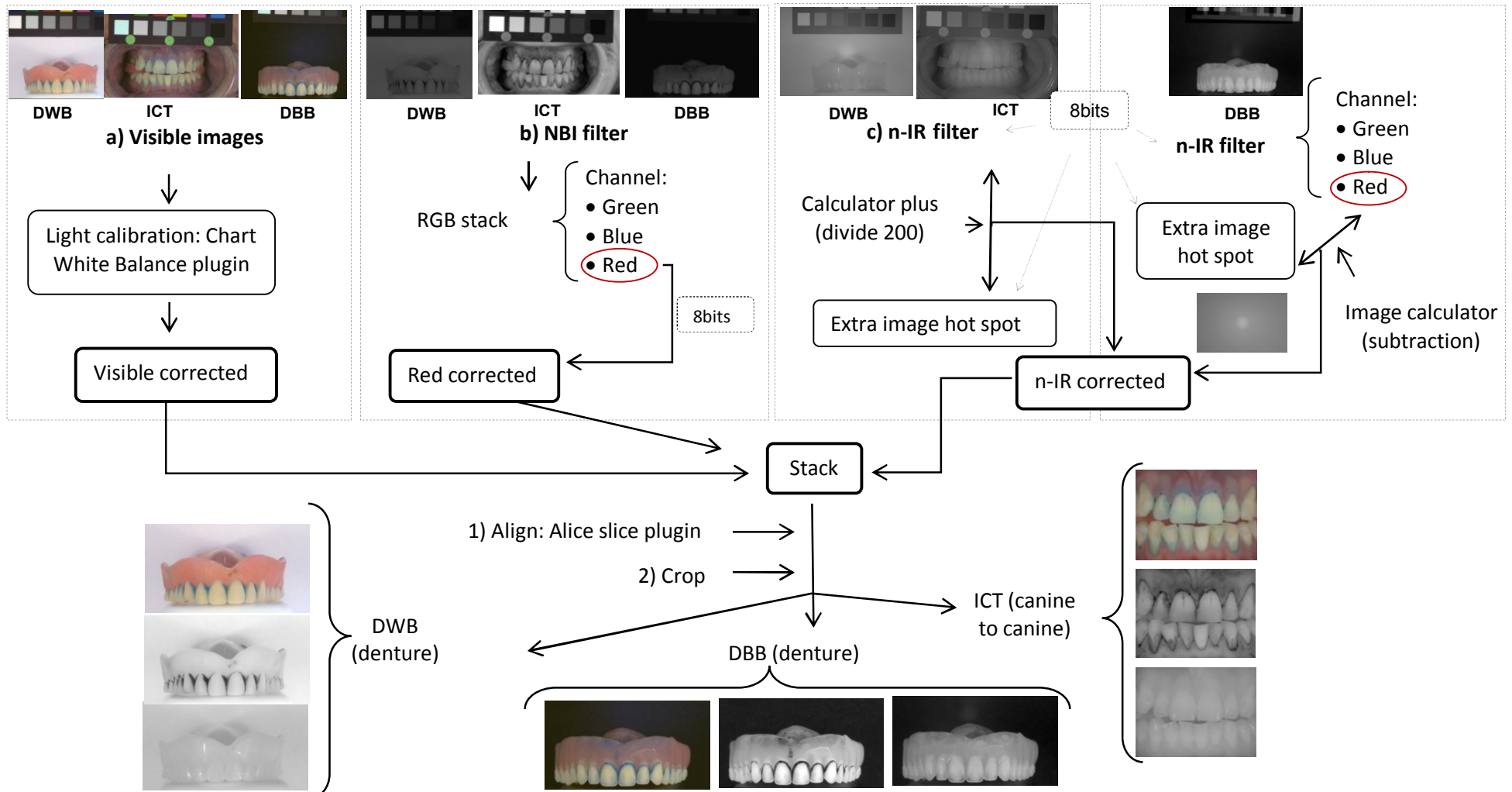
Figure 46 Summary of the procedures followed for the correction of the DWB, DBB and ICT images in the a) visible light images, b) NBI images and c) n-IR images.
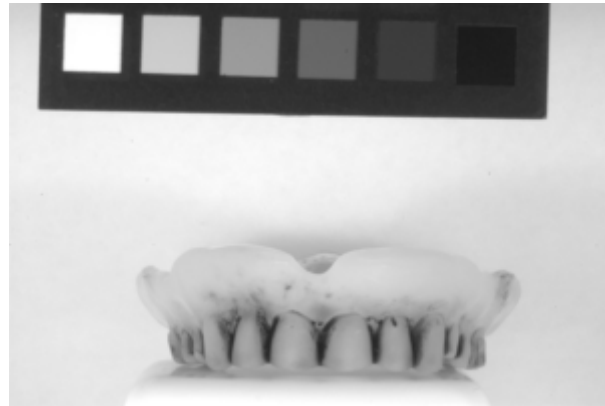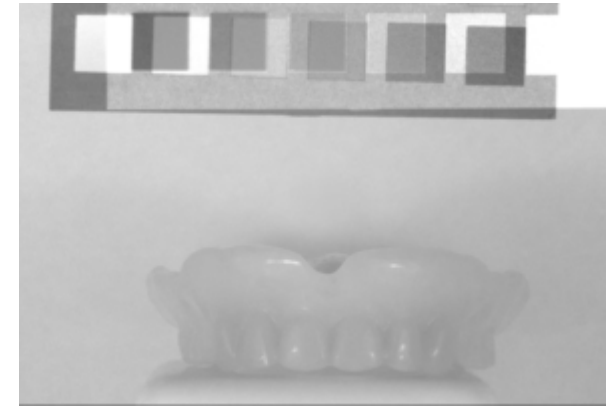
| Visible light image | Photography with the narrow band-pass filter | Near-infrared image |

| Visible light image | Photography with the narrow band-pass filter | Near-infrared image |
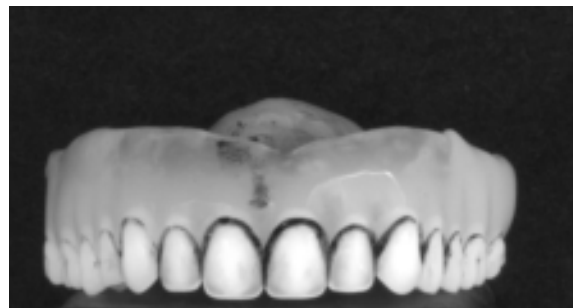
Figure 47 DWB and DBB images after their colour correction. The upper row shows the DWB images with the Gretag Macbeth

colour checker mini-chart whilst the lower row presents the DBB images once the cropping was done.

c) Near-Infrared images

All n-IR images presented a hot spot in the centre of the image (Figure 48).

Therefore the correction of these images was focused on the hot spot elimination. An

additional photograph without the dentures present (to capture only the hot spot to

appear in the centre of the frame) was taken under both black and white

backgrounds with the same camera's setting as for the n-IR images. Both images

(the hot spot only and with the denture) were converted to 8bits. After this point, the

correction of the DWB images was slightly different from the DBB images.

The correction of the DWB images (and ICT) was done dividing the n-IR-8bits image

between the 8bits-hot spot image and scaling it by 200 (CalculatorPluss plugin). The

resulting image was re-named "n-IRcorrected" and saved. The DBB images were

corrected by subtracting the hot spot image from the red channel of the n-IR image

(ImageCalculator command). The resulting image was also saved under the name

"n-IRcorrected".

6.1.4.2. Image analysis

In general, the images were segmented into regions of interest: dental plaque, teeth,

denture base and background. To do this, different methods were tested, such as the

analysis of the Hue, Saturation and Intensity, calculation of the excess of the colour

(blue and red) and via analysis of the histograms of the images. Colour segmentation

techniques including colour deconvolution, seeded region growing and K means

clusters were also investigated. The final method, (the one that produced the best

results), comprised of a combination of several procedures therefore only the

description of the final methodology is presented.
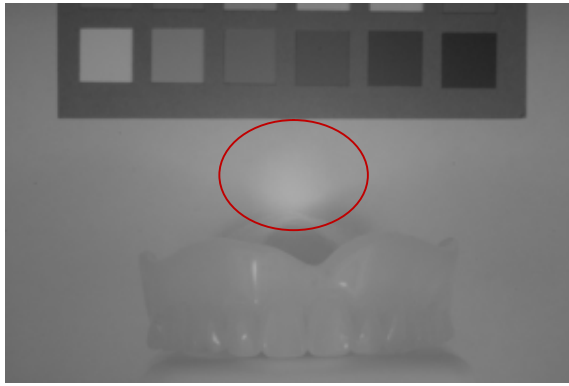
DWB
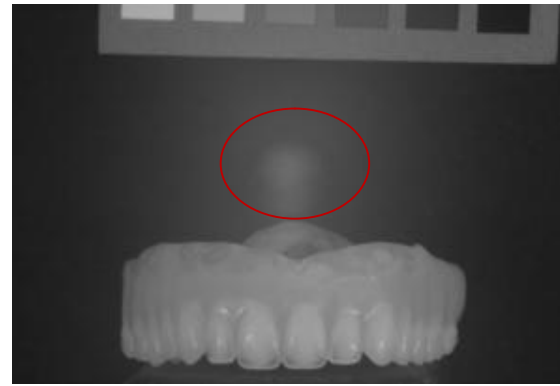
DBB
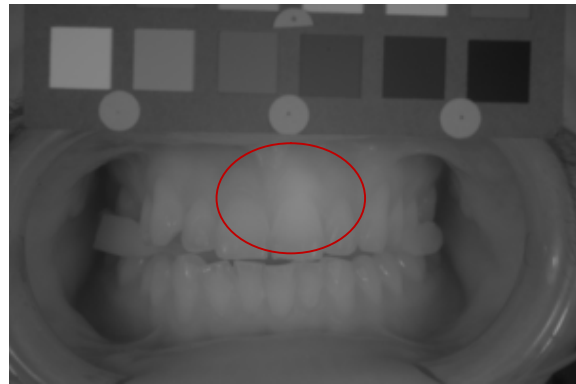
ICT

Figure 48 DWB, DBB and ICT images with a hot spot (encircled) in the centre of the image.

a) Images of dentures on a white background

The approach taken for the segmentation of the DWB images was different to the DBB images, as they were analysed using the denture as the unit and no partition of the teeth into units was attempted because the human intervention during the segmentation of the denture from its background introduced undesirable subjectivity into the design of an intended fully automated method (for more detail see discussion 6.3.2). The denture (in the visible images) was segmented by outlining its border by hand with the freehand tool. The resulting area was selected and its ROI was added to the SRG plugin to be used as the foreground. The ROI for the background was the result of a sample taken by drawing by hand a square that represented this region. The resulting image was converted into a mask and saved as "denture mask" (Figure 49).

Dental plaque was thresholded from the red image using the MaxEntropy method and the image was saved under the name "plaque mask". Unfortunately when using this method, extra pixels belonging to the surface where the denture rested on were also segmented as dental plaque, therefore to eliminate these, the denture mask image was combined logically using the Boolean AND operator (Image Calculator-AND) to the plaque mask. The resulting image contained the extra pixels was called "excess" and was subtracted from the plaque mask to obtain the plaque total extent (Figure 50). The region from canine to canine was cropped manually and the quantity of pixels for both dental plaque and area total were obtained from the histogram (white pixels) of each image for canine to canine and all teeth.
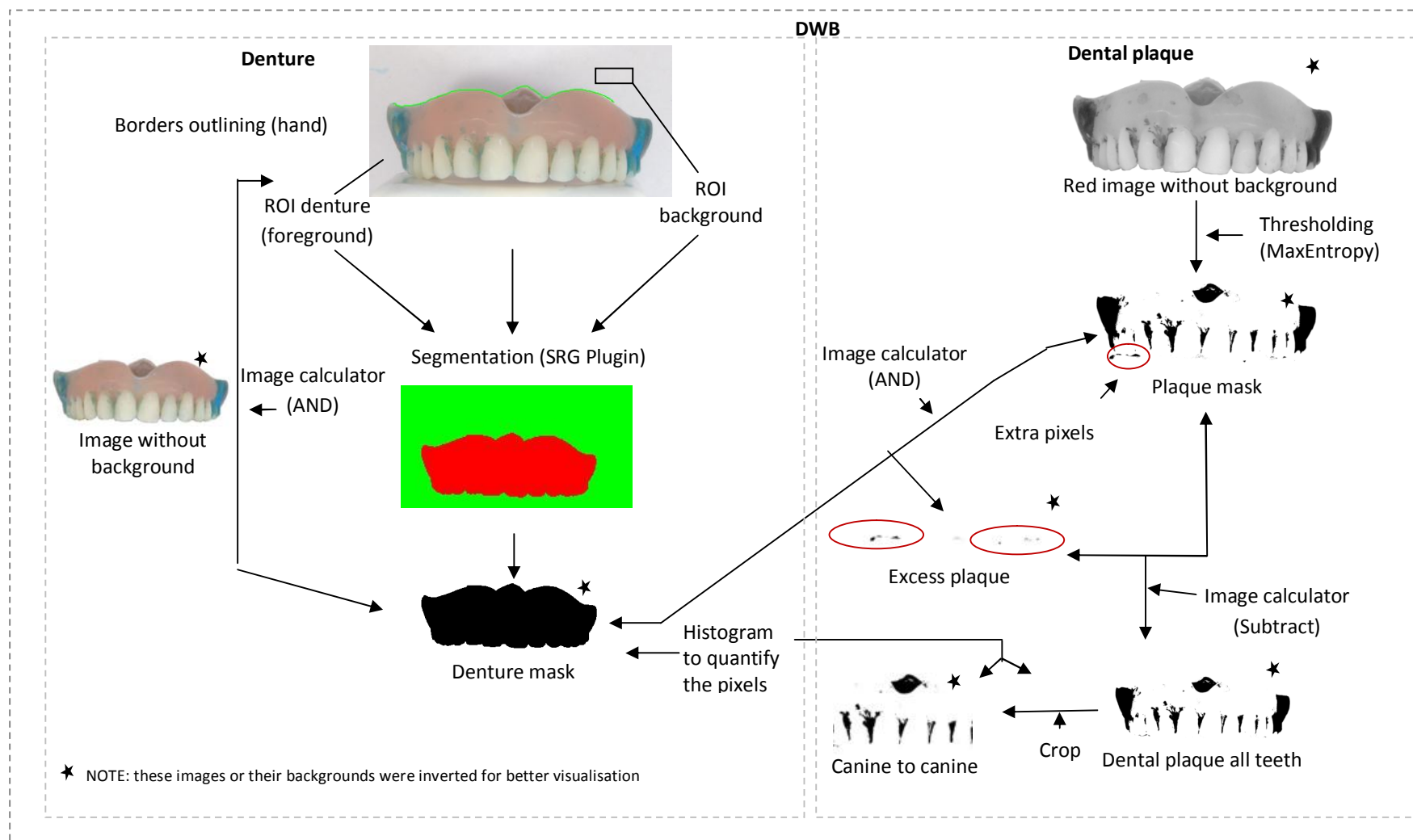
Figure 49 Summary of the procedure followed to segment DWB images.

a) Plaque mask with extra pixels

b) Plaque mask without extra pixels

✴ NOTE: these images or their backgrounds were inverted for better visualisation

Figure 50 Images showing the localisation on the DWB images of the dental plaque excess (a) and the final appearance of the mask once the extra pixels were eliminated (b).

164

b) Images of dentures on a black background

The process comprised five main stages: background extraction, separation into teeth and denture base, teeth area segmentation, separation of teeth into units and dental plaque segmentation.

i. Background extraction

A stack was created with both the blue and the green channels of the visible image, the red image and the n-IR corrected image (Figure 51). To reduce the noise in the image a median filter (radius=4) was applied to the stack. This filter works replacing each pixel in the image with the median value of the nearby neighbouring pixels. A pixel-based segmentation called k-means clustering, with three clusters corresponding to a) background, b) denture base and c) teeth, was applied to the stack and a single image consisting on each of the clusters (denture, teeth and background) was obtained. The Huang (Huang and Wang, 1995) auto thresholding method was used to separate the denture from its background and isolated particles were removed from the thresholded image with the BinaryFilterReconstruction (erosions=10), followed by a filling hole function. This image was renamed "Clusters". Ten cluster images presented extra pixels in the surface were the denture rested on (Figure 52), due to shadows between the denture and the disposable plastic base (its elimination is discussed in section iii-teeth area segmentation). The background was extracted individually in each set of images by adding (ImageCalculator plugin-AND) the Clusters image to the visible light, the red and the n-IR corrected images. The resulting images, consisting of the denture without the background, were saved adding the tag "no-background" to their name (Figure 53).
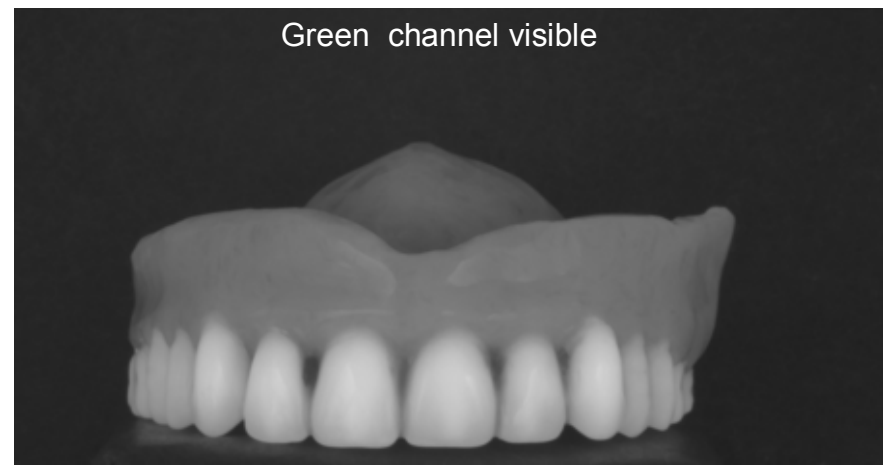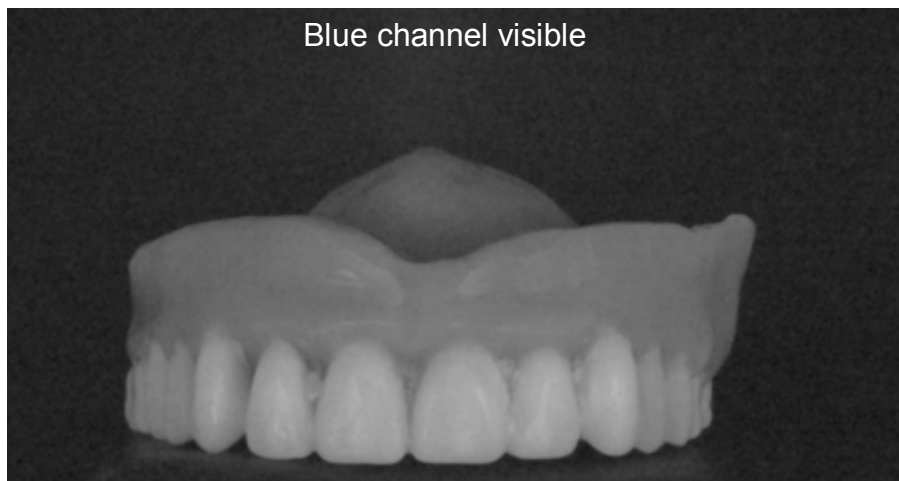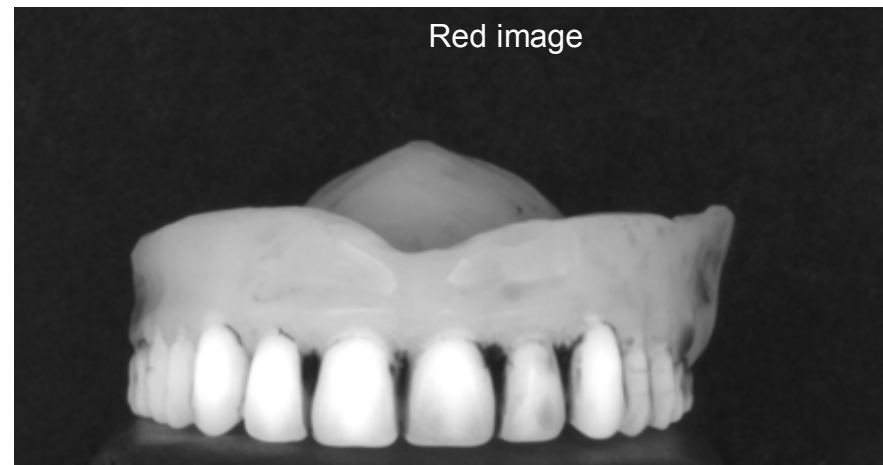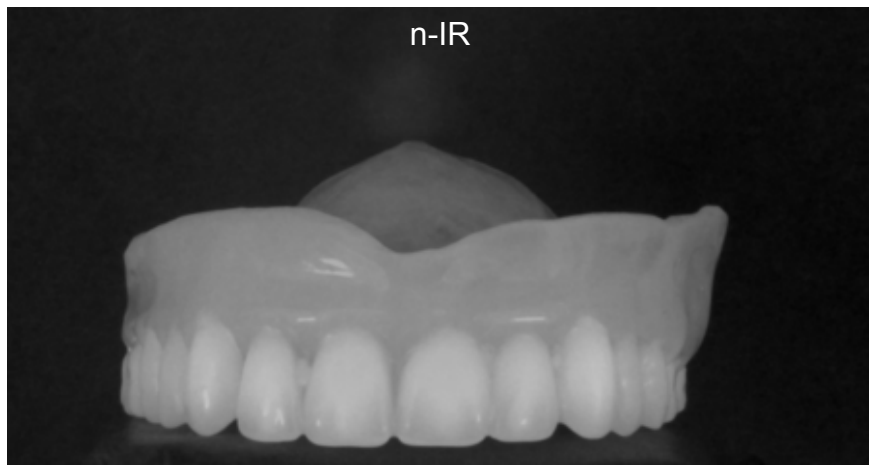
Figure 51 Individual images used to separate the denture from the background in the DBB images. Note the "absence" of dental plaque in the n-IR image and its increased contrast in the red image.

Clusters image with excess
pixels

Visible image without background
presenting excess pixels

✦ NOTE: this image or its background was inverted for better visualisation

Figure 52 Excess pixels in the area of the base of the denture in the cluster image due to shadows between the denture and the

disposable plastic base.
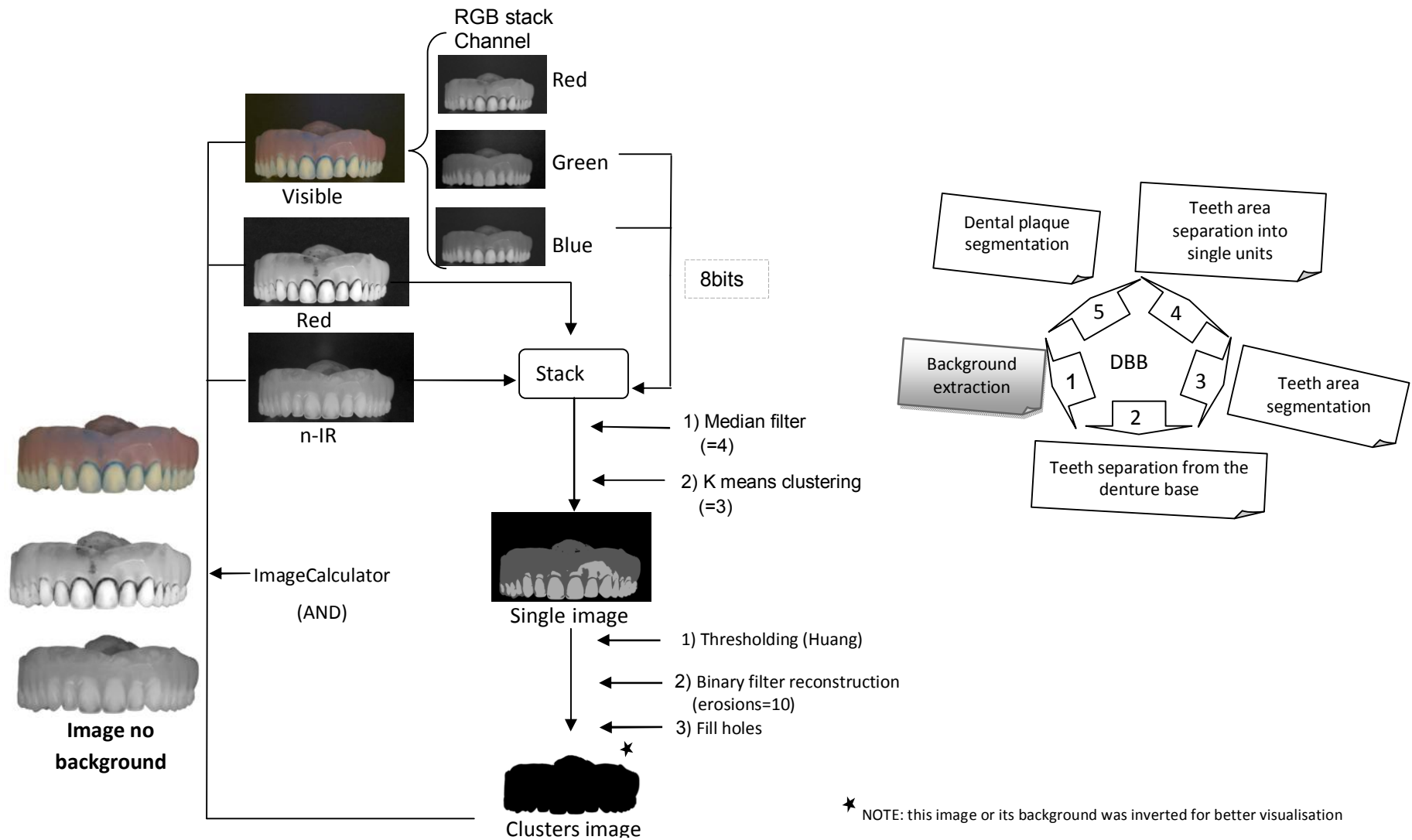
Figure 53 Summary of the steps followed for the background extraction of the DBB.

ii. Separation of the image into teeth and denture base

The next step in the segmentation procedure was to separate the image into the regions: teeth and denture base (Figure 54). A sample of the teeth was taken manually by drawing a rectangle from the visible no-background image to obtain its Region Of Interest (ROI). This area was selected and filled using the colour threshold and then highlighted with the wand tracing tool to represent the ROI of the teeth. The segmentation of the image into teeth and background was done with the technique called Seeded Region Growing (SRG) which works on the principle that different set regions (seeds) are identified by the user. Both the ROI of the teeth (seed 1), and a single ROI for both the denture and the background (seed 2) were loaded into the SRG plugin (Adams and Bischof, 1994, Jarek, 2011) which resulted in a segmented image composed by teeth and background. The teeth were selected and their ROI was restored (transferred) to the clusters image. The teeth area was filled in black and the clear outside function was used. This step separated the denture from the teeth leaving only an image of the denture. The gingival margins of the denture were further smoothed and rounded (macro smooth ROI3), the holes were filled and the large particles (if needed) were eliminated ("Clear Outside" function). This image was saved with the name "denture-base" (Figure 55).

Visible image no-background

ROI denture & background

ROI teeth

1) Manual selection of the teeth

2) Region selection & filling ⟶ Threshold Colour plugin

Transfer

3) Highlight (wand tracing tool)

Segmentation (SRG Plugin)

Teeth selection

Teeth segmented

Dental plaque segmentation

Teeth area separation into single units

Background extraction

DBB

Teeth area segmentation

5 4
1   3
2

Teeth separation from the denture base
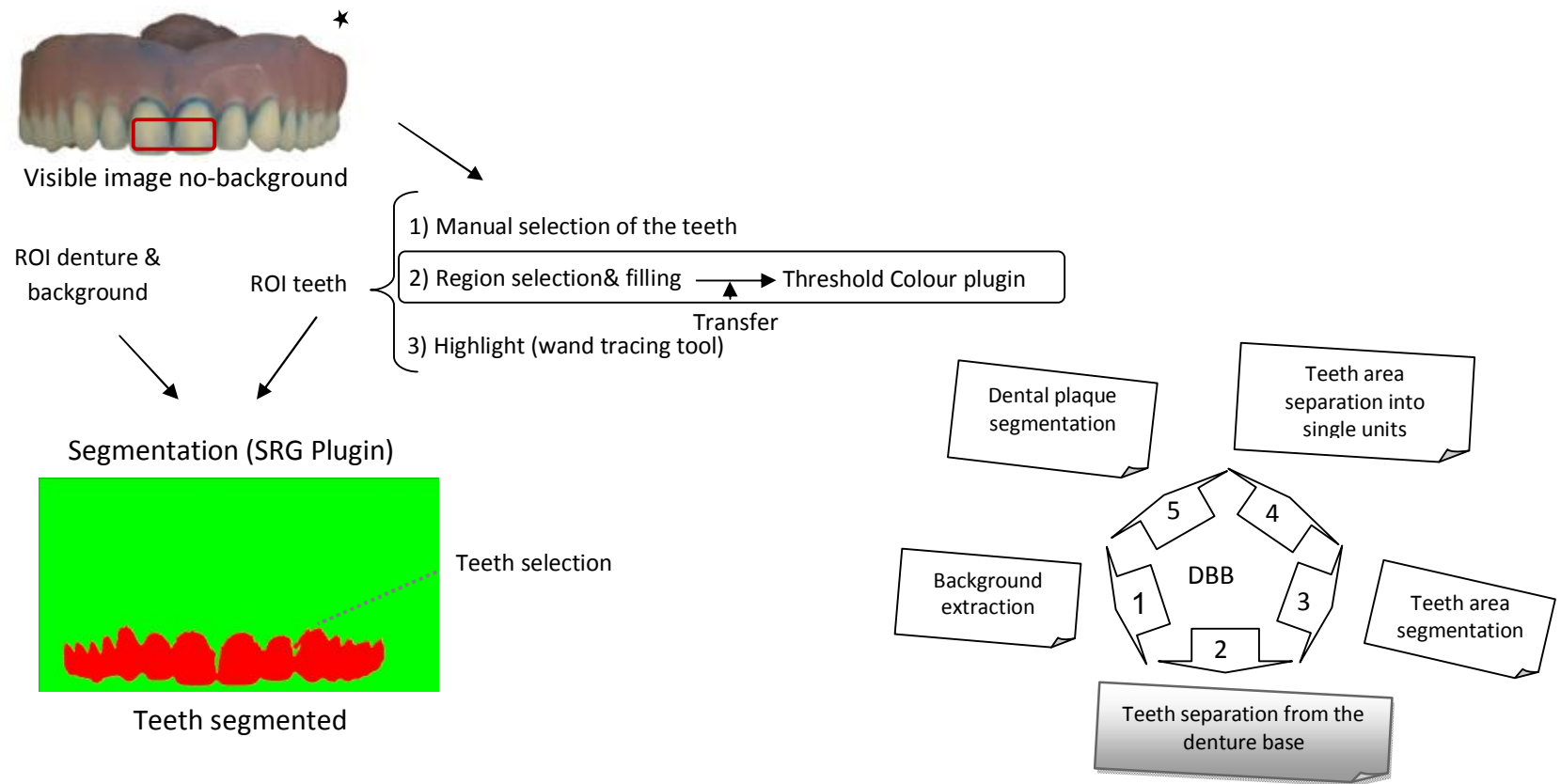
✦ NOTE these images or their backgrounds were inverted for better visualisation

Figure 54 Summary of the steps followed to segment the DBB images into teeth and denture base (part 1).

170

Teeth selection

Teeth segmented

ROI Transfer

Clusters image

1) Teeth filled

2) Clear outside

1) Gingival margins
smooth & round
(Macro ROI3)

2) Fill holes

Denture base

Dental plaque segmentation

Teeth area separation into single units

Background extraction

DBB

5   4

1   3

2

Teeth area segmentation

Teeth separation from the denture base

✶
NOTE: these images or their backgrounds were inverted for better visualisation

Figure 55 Summary of the steps followed to segment the DBB images into teeth and denture base (part 2).

171

iii. Teeth area segmentation

The procedure used to extract the teeth also allowed the excess of the denture margins to be cleared. Figure 56 contains the steps followed to extract the teeth and to eliminate the excess of pixels in the DBB images. To isolate only the region of the teeth in the denture, the denture-base image was inverted and added to the n-IR-no-background image (ImageCalculator-AND), and the resulting image was thresholded with the Intermodes method (Prewitt and Mendenlsohn, 1966). Big particles (binary filter reconstruction-BFR-erosions=10) and the isolated pixels were eliminated (morphological erosion followed by a dilation) and the holes were filled. This image was saved as "teeth-mask" and added (ImageCalculator-AND) to both the visible and the n-IR no background images and the resulting images were used to later segment the teeth into units.

iv. Teeth area separation into single units

The separation of the teeth area into single units was achieved using the 8bits version of the visible image of the teeth (Figure 57). Two copies of the same image were required. The first copy was used as a mask whilst the second image was used as a seed. The seed image was in the centre of the teeth (as the interdental spaces were always darker) sliding the upper thresholding bar until no contact points were observed between the teeth. Two images (8, 16) presented two teeth were the contact points could not be broken automatically. After sliding the upper thresholding bar they were still joined by a small band of pixels, which had to be eliminated by hand. The thresholding values used to seed each image are shown in Table 20. The result image was corrected filling the holes and eliminating the remaining loose particles with the BFR (erosions=10). Once the seeds were produced, the final teeth

segmentation was done redirecting both the seed and the mask to the BinaryGeodesicDilateNoMerge8 plugin. The resulting image was first saved as "each-tooth" mask and then duplicated to crop it from canine to canine.

v. Dental plaque segmentation

The portions of the image corresponding to stained dental plaque were extracted using a procedure called colour deconvolution (Ruifrok and Johnston, 2001) on the visible image that contained only the teeth. The vectors for the ROIs corresponding to a) teeth and b) stained dental plaque were hand selected. A third component is determined automatically as the complementary of the other two colours. This process resulted in three 8-bit images with colour look up tables representing the optical density for each of the deconvolved colours (Figure 58).

The area of dental plaque coverage was determined by thresholding using the MaxEntropy method (Kapur et al., 1985) on the image of the dental plaque (blue stain).

The estimation of both the area covered with plaque and the teeth dimensions per tooth were calculated by redirecting the binary image (mask) of the teeth to its corresponding image with dental plaque using the Particles8 plugin (Figure 59). The results were originally expressed in pixels but the conversion factor in area/mm^2 was calculated with the following formula:

$$\text{Area in mm}^2 = ((\text{image width in mm}) * (\text{image width in pixels}))^2 \qquad \text{[Eq. 6.1]}$$

The final results were expressed in a) area/mm^2 and b) Percentage of Plaque Index (PPI) which is the proportion of pixels with dental plaque divided between the total pixels. One DBB image had one tooth missing (denture 1, URC) which was considered as missing in the statistical analysis.
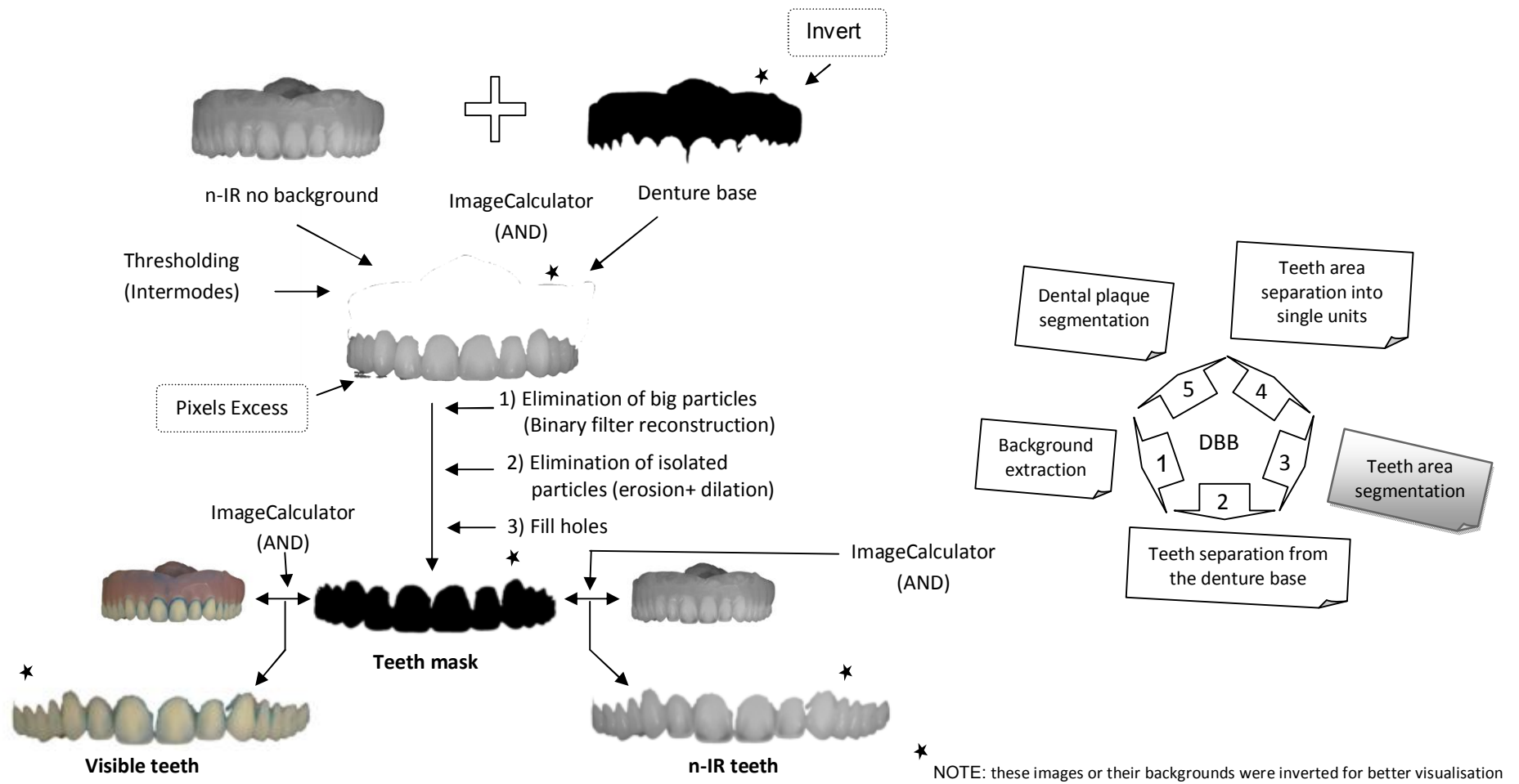
Figure 56 Summary of the steps followed to segment the teeth area and to eliminate the excess of pixels in the DBB images.
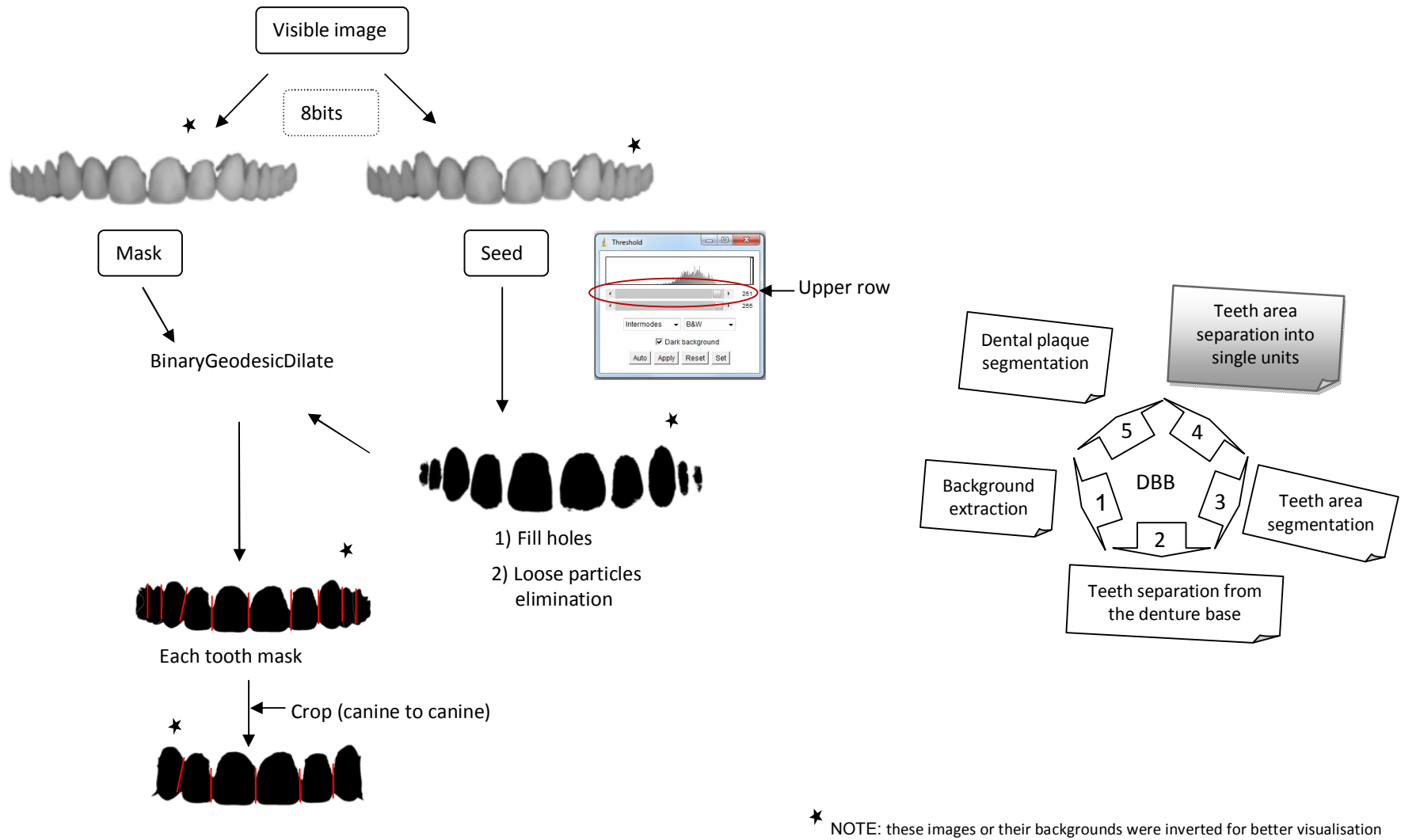
Figure 57 Summary of the procedure followed to separate the teeth area into single units in the DBB images.

Table 20 Thresholding values per image used to produce the seeds to segment the teeth into units. The images in bold represent the ones where the contact points between the teeth had to be broken by hand.
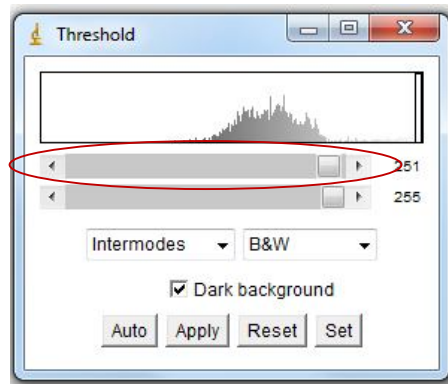
Image number	Thresholding point
1	154
2	157
3	147
4	142
5	151
6	145
7	170
8	**158**
9	147
10	142
11	154
12	155
13	150
14	151
15	156
16	**147**

Visible teeth

Colour deconvolution

Vectors:
1. teeth
2. plaque
3rd component

1. Teeth

3rd component

2. Plaque

Thresholding
(MaxEntropy)

Redirect

Mask

Canine to canine

Dental plaque segmentation

Teeth area separation into single units

Background extraction

DBB

5 4

1 3

2

Teeth area segmentation

Teeth separation from the denture base
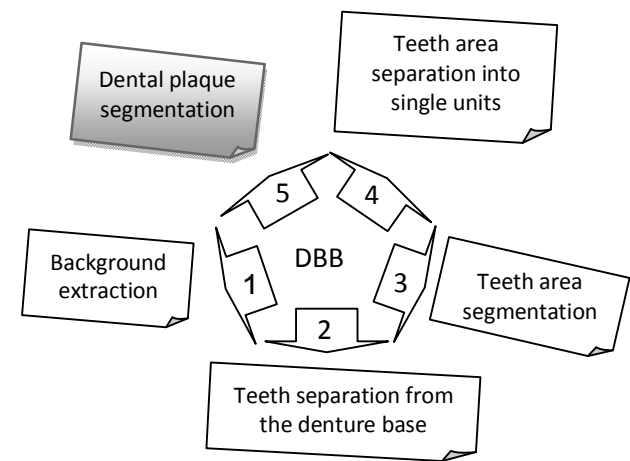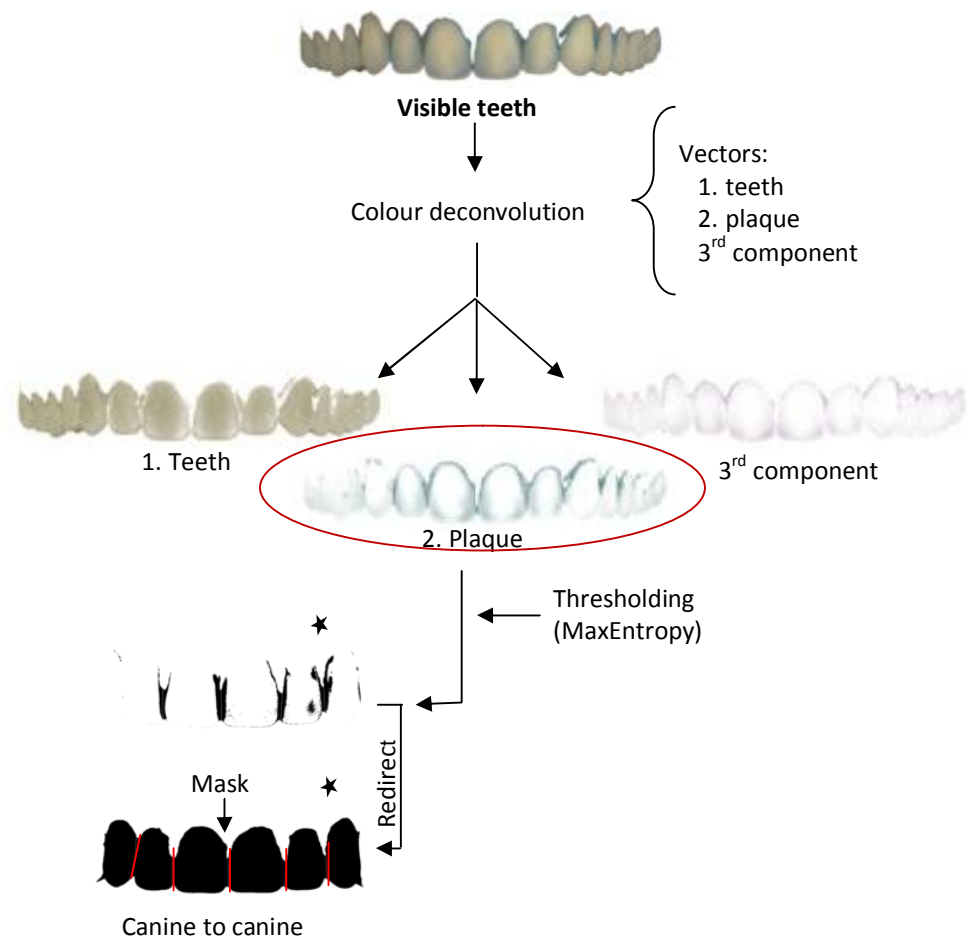
★ NOTE: these images or their backgrounds were inverted for better visualisation

Figure 58 Steps in the segmentation of dental plaque in the DBB images.

Six teeth- dental plaque

Plaque mask

Redirect
Particles8

Teeth mask
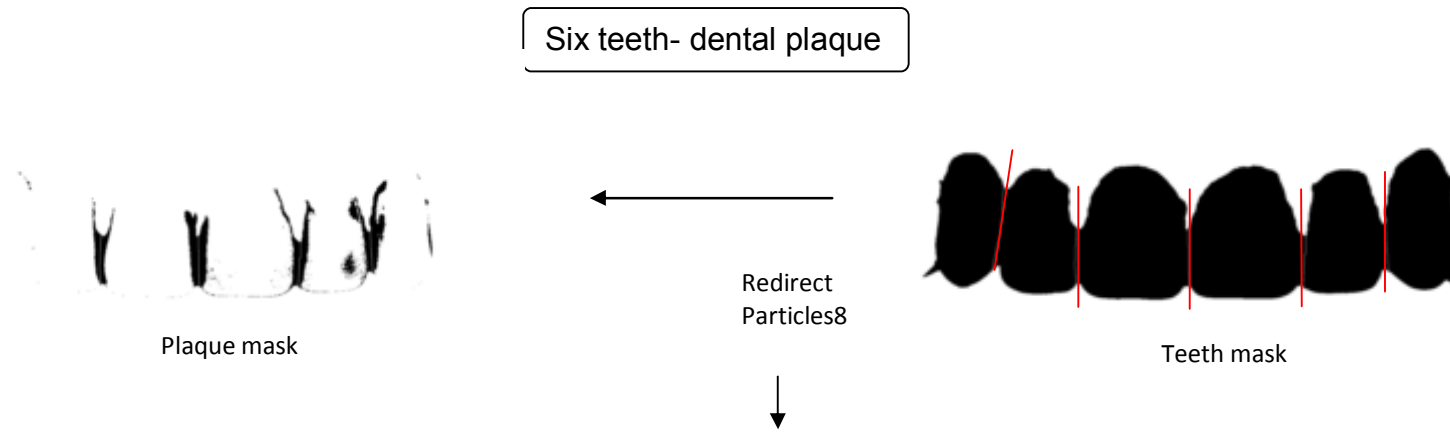
Results:
1. area covered with plaque
2. teeth dimensions

✶ NOTE: these images or their backgrounds were inverted for better visualisation

Figure 59 Procedure to calculate the area covered with plaque and the teeth dimensions per tooth in DBB images.

The means for a) tooth area and b) PPI for each tooth were grouped per tooth type (central, lateral, etc) for all the dentures and its normality was assessed. The distribution of the means for the PPI was skewed therefore the data was normalised using a square root transformation. Comparisons between teeth means for a) tooth area and b) PPI were analysed with one way ANOVA. A Bonferroni post hoc test (1937) was used to evaluate the differences between matching pairs of teeth (left vs. right).

c) Clinical images

The ICT were segmented into three areas teeth, plaque and gingiva using the colour deconvolution plugin. The vectors used for the segmentation were created taking samples (from the same area) from 25 cropped (canine to canine) visible images in three different areas of three regions: a) soft tissues (gingiva between centrals, between lower incisors and in the region of the upper left central), b) teeth (middle third of the upper right central, incisal edge of the lower left central incisor and gingival third of the upper right canine) and c) dental plaque. The samples for both teeth and gingiva were taken from the images in which no staining was used whilst the samples for dental plaque came from matching images where the dye was applied. The sets of samples were grouped into three big stacks, one for each vector (gingiva, teeth and dental plaque) and the average, maximum, median, and minimum intensity of the pixels from each stack were obtained (Z-projection macro). These results were used to assign the values of the vectors in the colour deconvolution procedure, so vector number one was the soft tissues, number two the teeth surface and number three was the stained dental plaque (Figure 60).

Once these vectors were obtained, to separate the teeth from the gingiva, the visible image was blurred (radius 5) to reduce any noise in the image (thus improving the result of the segmentation method) and segmented applying the colour deconvolution plugin. Three colour look up table corresponding to the respective vector colours were obtained: a) gingiva, b) teeth and c) dental plaque (Figure 61).

Both thresholding methods Huang (Huang and Wang, 1995) and the Intermodes (Prewitt and Mendenlsohn, 1966) were applied in the image with the vectors for the soft tissues (a) on 6 images (1, 3, 10, 18, 19, 23) and 19 images (2, 4, 5. 6, 7, 8, 9, 11, 12, 13, 14, 15, 16, 17, 20, 21, 22 24, 25) respectively. Two methods were used because although under visual examination no differences were found between thresholding methods for some images. There were others that had differences- which occurred specially in the gingival margin (Figure 62). Therefore it was decided to classify the images into two groups according to the method that worked the best for each one. After the thresholding, the loose particles in the images were eliminated with a dilation (radius=1) followed by binary filter reconstruction white (radius=40) and black (radius=5) in the images where the Huang method was used. Due to thresholding differences with a wider gingival margin, the images where the Intermodes method was used, an extra erosion (radius=1) was needed at the beginning of the procedure. In both cases, the gingival margins were smoothed and rounded (macro ROI3), and the images were save as "teeth mask. The teeth segmentation was done by adding (ImageCalculator-AND) the teeth mask to both a) the visible image and b) the 8bit-green channel of the visible image. The latter was saved under the name "teeth visible" whilst the former was called "teeth green".
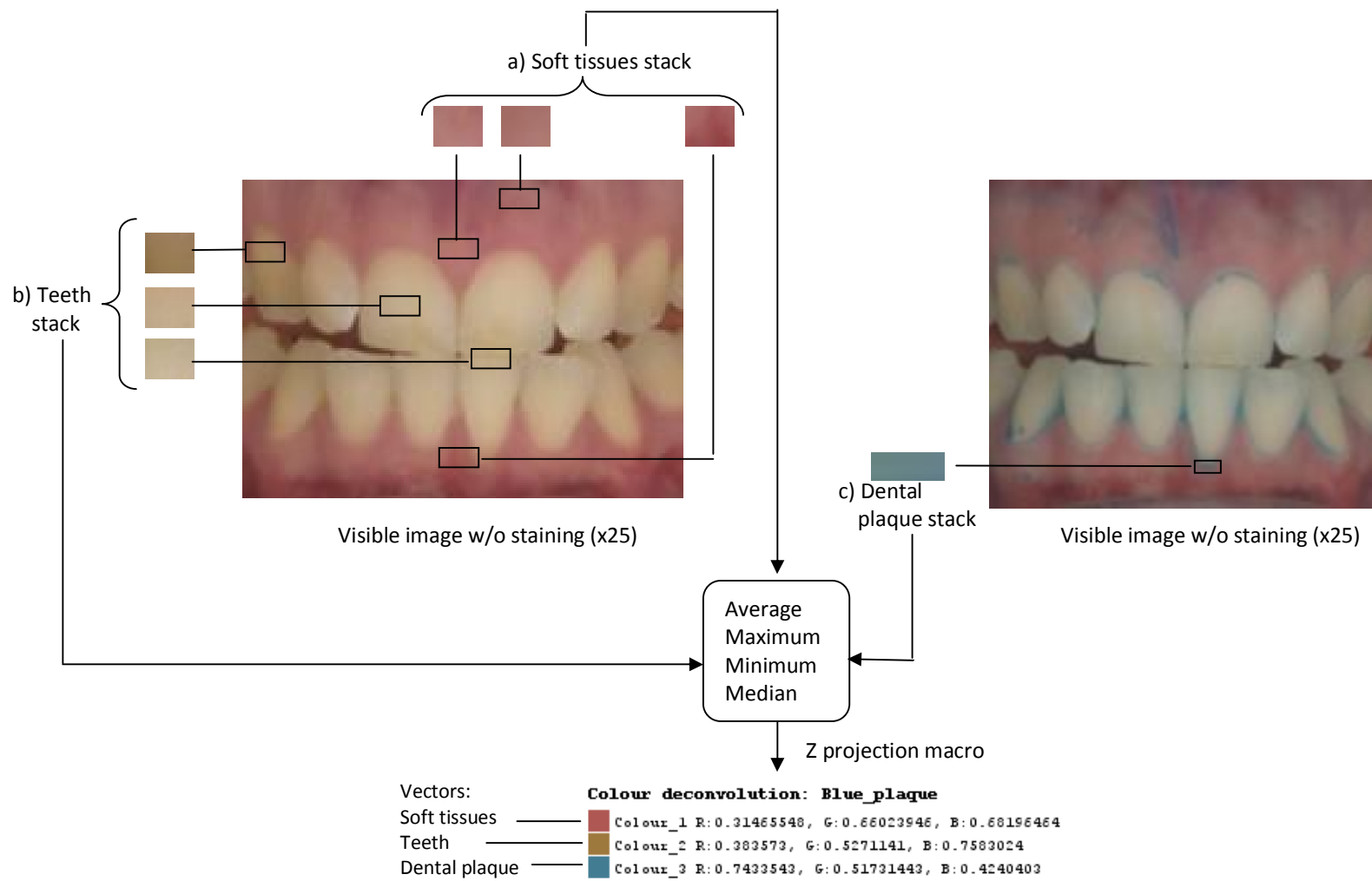
Figure 60 Places in the ICT where the samples were taken to create the vectors for the colour deconvolution segmentation.

Colour deconvolution: Blue_plaque

Colour_1 R:0.31465548, G:0.66023946, B:0.68196464
Colour_2 R:0.383573, G:0.5271141, B:0.7583024
Colour_3 R:0.7433543, G:0.51731443, B:0.4240403

a) Soft tissues

b) Teeth

c) Dental plaque

Figure 61 Vectors created (soft tissues, teeth and dental plaque) to perform colour deconvolution on the ICT.

a) Huang thresholding method
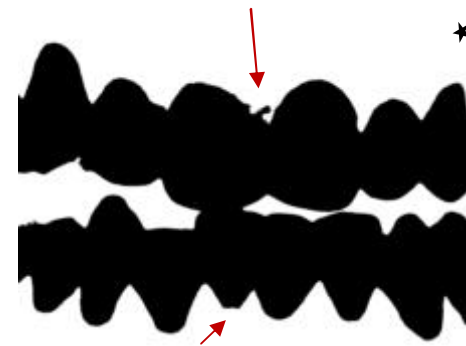
b) Intermodes thresholding method

✦NOTE: these images or their backgrounds were inverted for better visualisation

Figure 62 Example of the differences (red arrows) between the Huang (left) and Intermodes (right) thresholding methods to separate the teeth from the gingiva in the ICT.

The separation of the teeth into units (tooth) was achieved using a semi-automatic segmentation method called ABS snake or Active Contours Plugin (Andrey and Boudier, 2006) on the teeth "green" image. This image was used because it provided the required image of the teeth without (strong) stained dental plaque. Moreover, originally the n-IR image was going to be used for this purpose as stained dental plaque is not shown, but the lack of definition in the teeth borders (especially in the gingival area) made their identification more difficult and thus segmentation by the ABS snake plugin (Figure 63). The contour of the snake had to be initiated by drawing approximately the contour of each tooth by hand (close to the border) and stored in the ROI manager which is a tool that allows working with multiple selections within the image or from different images. The ROIs stored were then used to activate the ABS snake plugin (Figure 64). One ROI was selected each time and the plugin initiated, then it would determine more precisely the final ROIs position. The final segmented tooth was filled alternating colours in either white or grey to differentiate them from each other. Figure 65 illustrates the steps explained above to segment the ICT images. The teeth dimensions were determined with the Particles8 plugin and the final result is expressed in mm^2 which results from multiplying the area per tooth (in pixels) by its conversion factor in mm^2.

6.1.5. Dental plaque segmentation in the clinical images

To investigate the most effective method to threshold dental plaque on the ICT images, two different approaches were used: a) colour deconvolution and b) high pass filter.
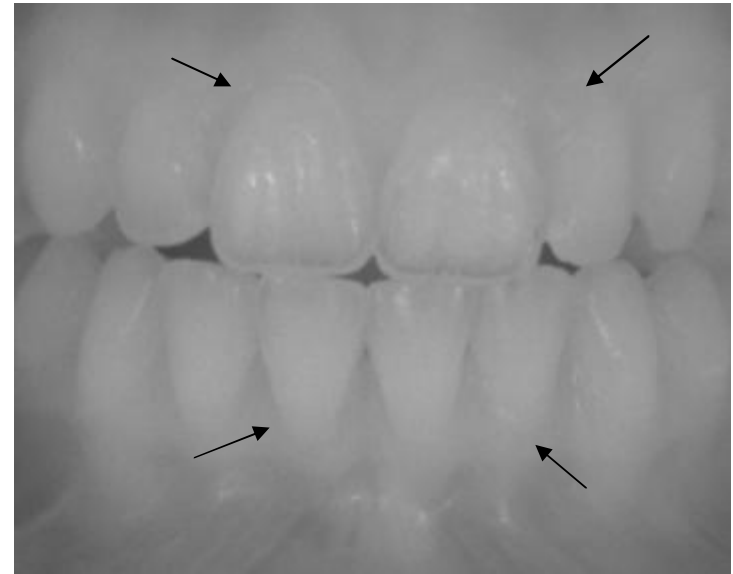
Figure 63 Original image (above) with its green (left) and n-IR (right) image where stained plaque is NOT visible. Note the reduced definition in the teeth borders in the n-IR image (arrows).
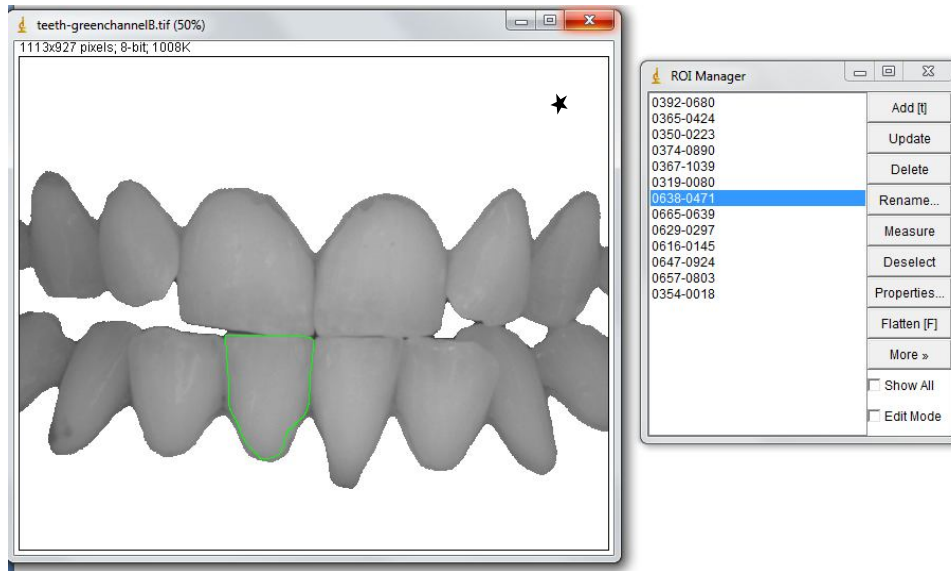
Teeth green

Teeth segmented into
units (ABS snake)

✦ NOTE: these images or their backgrounds were inverted for better visualisation

Figure 64 Example of the use of the ROI manager with the contour of a snake drawn around a tooth (left). This was used to activate the teeth segmentation into units. The image on the right shows the image once all teeth were segmented.
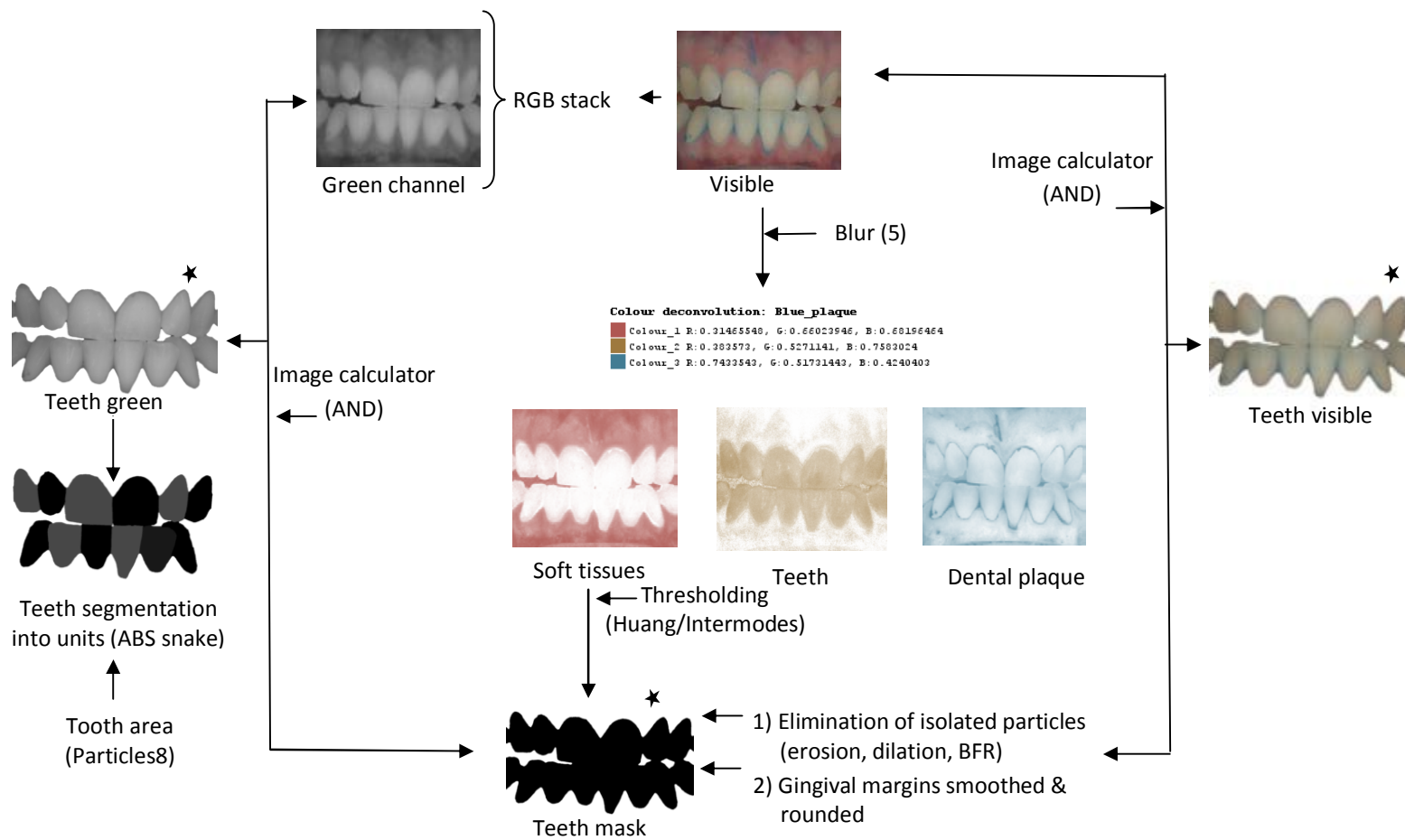
186

Figure 65 Method followed to segment the teeth from the gingiva and to segment the teeth into units in the ICT.

a) Method 1: Colour deconvolution

The image with the vectors for dental plaque (image 3) was thresholded using three methods: MaxEntropy (Kapur et al., 1985), RenyiEntropy (Kapur et al., 1985) and Yen (Yen et al., 1995, Sezgin and Sankur, 2004). Although all the thresholding methods (n=16) were tested only these methods were the ones that under visual examination managed to threshold dental plaque. To obtain only dental plaque on the teeth surfaces each of the three thresholded images were added (ImageCalculator-AND) to the teeth mask image and the resulting images were re-named "ROI+ the thresholding method" and saved (Figure 66).

b) Method 2: High pass filter

To enhance the contrast of the stained areas in the ICT where dental plaque was thresholded, the low frequency components (those that change slowly) in the image where reduced by the application of a high pass filter. A copy of the red image was blurred with a value of 30 to reduce its detail and then, divided (CalculatorPluss 255) by the red image obtaining a new one where the stained dental plaque appeared black and the teeth and gingiva appeared white. This image was called "BG corrected". All sixteen automated thresholding methods from ImageJ were tested in the BG corrected image but only the results from seven methods: Default, IsoData, Li, Moments, Otsu, RenyiEntropy and Yen were further analysed as these methods were the ones that under visual examination, were able to threshold plaque (Figure 67). The thresholded images presented extra pixels corresponding to the gaps between the upper and lower arches related to the edge-to-edge position adopted when taking the photograph (Figure 68). To eliminate these pixels a new image was created from the combination (ImageCalculator-ADD) between the visible image and

the mask from each method. The values that represented the extra pixels were located in the threshold colour plugin moving the Hue and Brightness bars. These values were incorporated in a macro that thresholded the visible image with the excess and a second image without the extra pixels was obtained. This image was given the name of "no-excess+ the thresholding method used" (e.g. "Default no excess").

6.1.6. Analysis of the methods used to threshold dental plaque in the clinical images

The best method to threshold dental plaque was determined calculating the negative and positive values, and the sensitivity and specificity between three images in which the dental plaque area was hand outlined (gold standard) and their matching images where automatic dental plaque thresholding methods were used. To achieve this a mask with values or 0's and 1's was created for the images where dental plaque was outlined by hand whilst a mask with values of 2's and 4's was created from the images from the automatic thresholding methods where:

0= Background image hand outlined

1=Detected dental plaque image hand outlined

2=Background image automated thresholding

4=Detected dental plaque image automated thresholding

These two masks (hand outlined and automatic method) were combined (ImageCalculator-ADD) and a new image was obtained with pixel values from 2-5 (Figure 69).
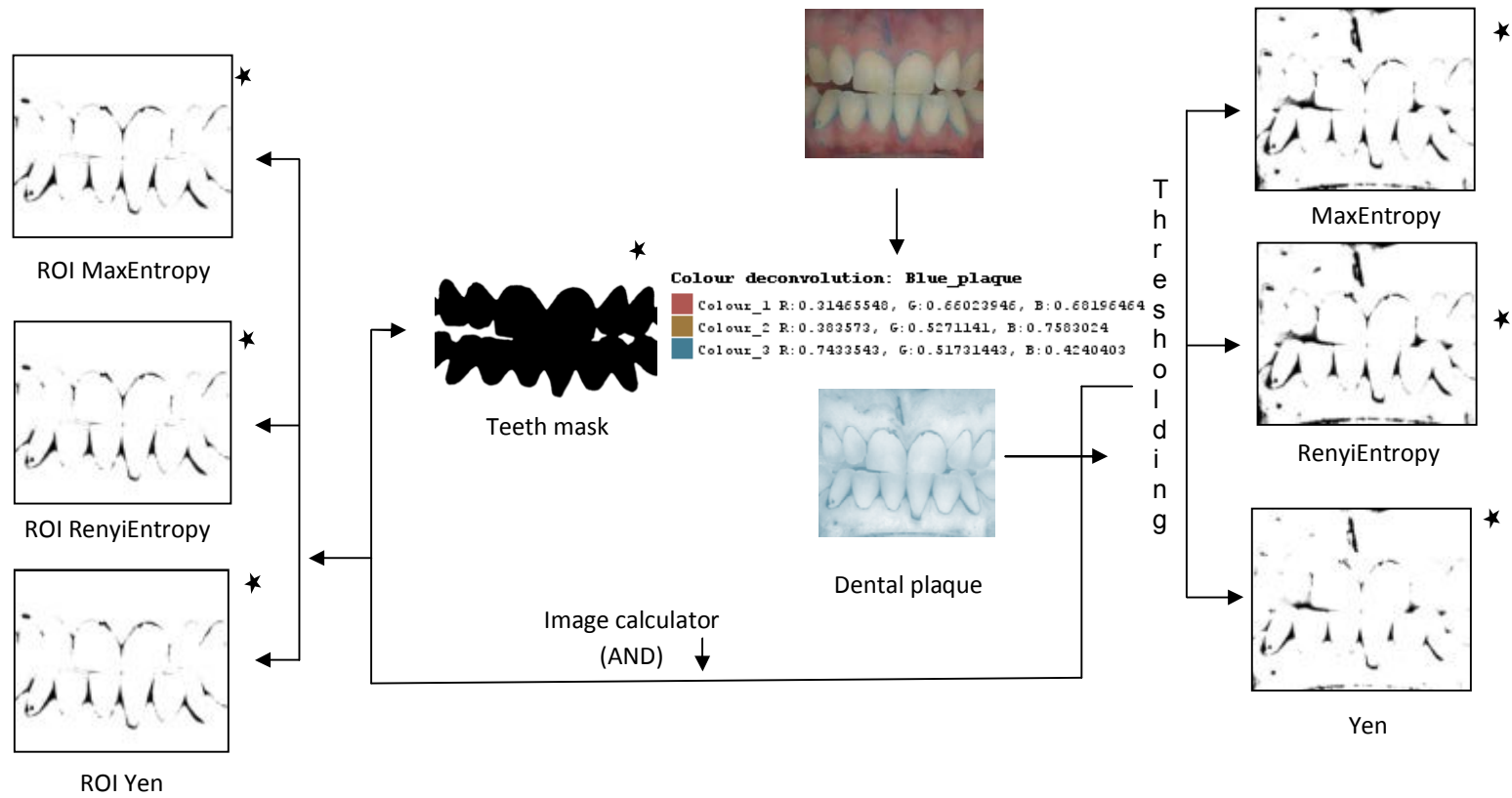
Figure 66 Procedure for the dental plaque segmentation of the ICT images using the colour deconvolution approach.
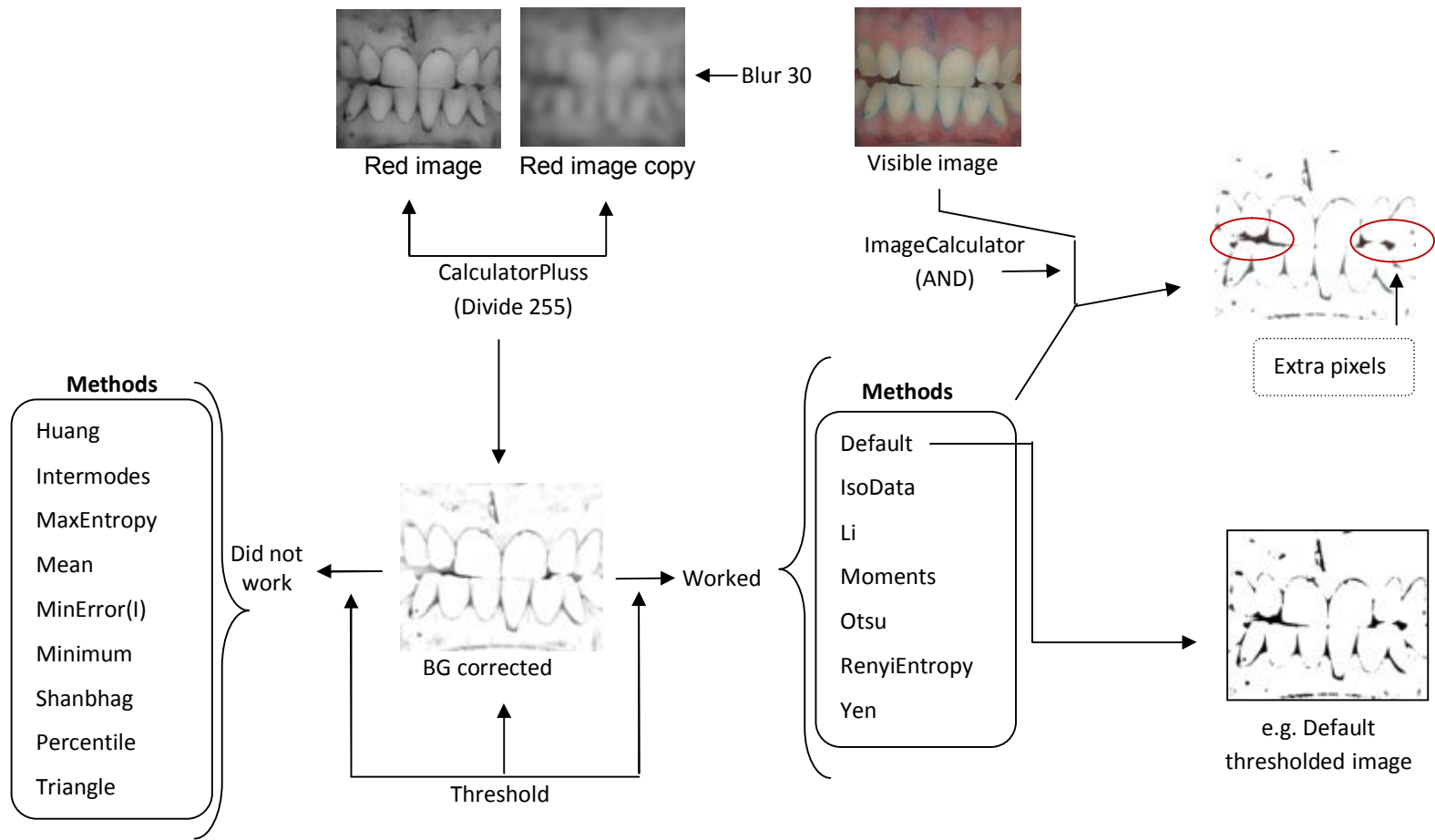
Figure 67 Procedure for the dental plaque segmentation of the ICT images using the high pass filter approach and the elimination of

the extra pixels.
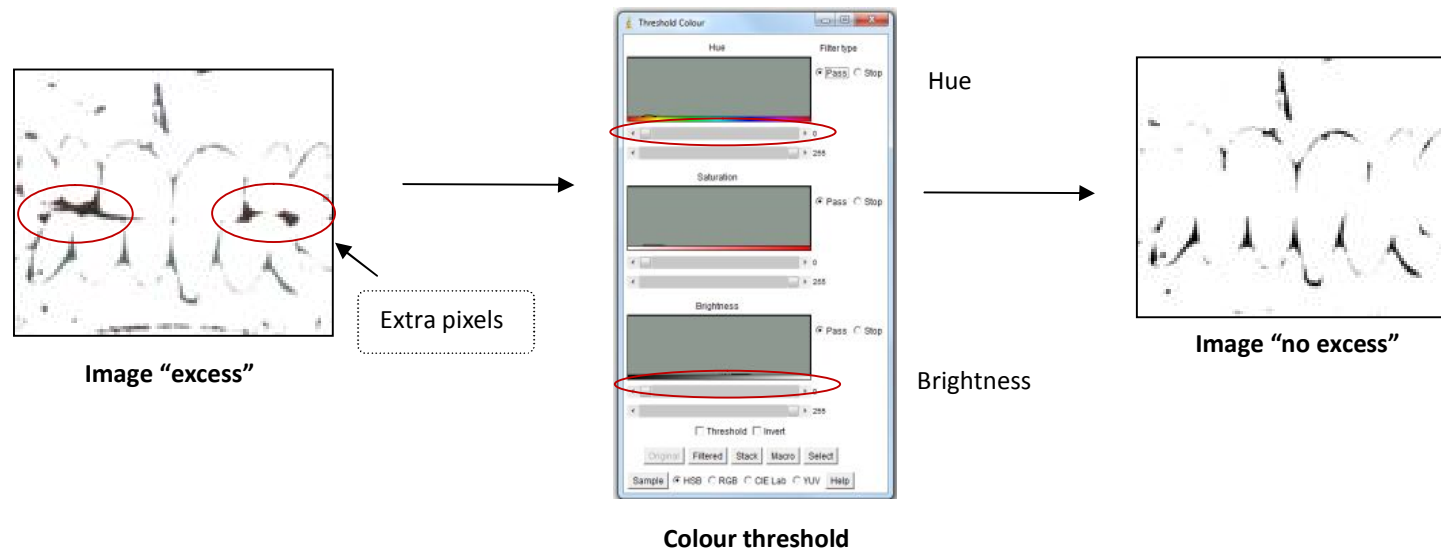
Figure 68 The extra pixels (left) registered (at the time of thresholding dental plaque) in the gaps between the upper and lower arches due to the teeth's edge to edge position adopted when taking the photograph were located in the colour threshold (centre) and eliminated moving the Hue and Brightness bars (right).
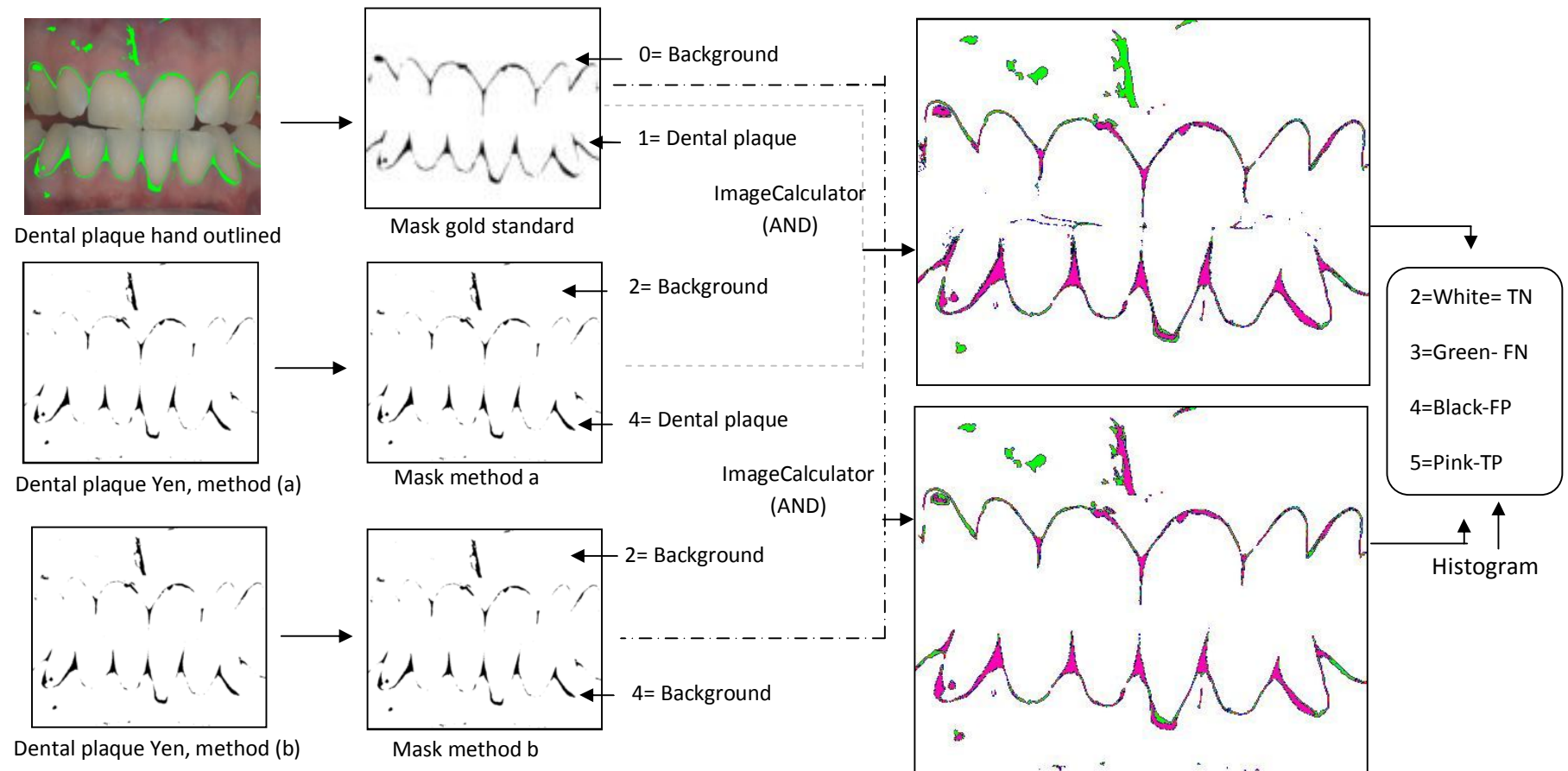
Figure 69 Procedure used to create the masks of the images where dental plaque was outlined by hand (gold standard) and thresholded with the automated methods.

The histogram of the resulting images was used to generate a 2X2 contingency table (Figure 70) and these values were then used to a) plot sensitivity vs. specificity graphs and b) calculate the Euclidean distance d to the ideal (given by the case when sensitivity=1 and specificity=1) for each thresholding method using the formula:

$$d= SQRT(((1-Sensitivity)^2) +((1-Specificity)^2)) \qquad [Eq.6.2]$$

If the distance to ideal is seen as the distance between two points x (sensitivity) and y (specificity) following the Pythagorean formula, the ideal distance is equal to 0.

6.1.7. Intra-observer reliability of determination of dental plaque

To determine the intra-observer reliability to outline dental plaque by hand a single image was outlined five times (leaving at least one day between examinations). The coloured areas were converted into masks and the number of pixels obtained from their histograms. The values per pixels were converted into mm^2 by multiplying the pixels for dental plaque by the conversion factor of that image. The results were analysed with the coefficient of variation with the formula:

$$CV= (S.D./Mean)*100 \qquad [Eq. 6.3]$$

The Coefficient of Variation measures the precision (degree to which repeated measurements under unchanged conditions show the same results) of the operator during a set of repetitive individual tests.

6.1.8. Comparison between automated and manual methods of dental plaque segmentation

Fifteen DWB images were randomly selected to outline dental plaque by hand using the pencil tool and a contrasting (green) colour. A single examiner (the author) did the outlining. Dental plaque was segmented by taking a sample of the coloured area and thresholding it to obtain a mask (8bits) which was then subtracted

194

(ImageCalculator-Subtract) from the original image. Figure 71 illustrates the

procedure followed to threshold dental plaque by hand outlining.

The agreement between the automated and the manual methods was assessed first

by visual examination with the Bland-Altman method (Altman and Bland, 1983, Bland

and Altman, 1986) and then with a paired samples t-test.

6.1.9. Distortion in the anterior region

To measure the amount of distortion, occurred in the canine to canine region due to

the curvature of the dental arches, a strip of graph paper (with blue squares) was

attached to the front of an upper denture, so that the strip followed the curvature of

the arch. A photograph was then taken and transferred into ImageJ. The blue

squares were used as the known measurement to calculate the distortion by

projection in the canine to canine region (Figure 72).

6.1.10. Analysis of the differences in plaque accumulation

The mask with plaque (1) and the mask for individual tooth (2) in the ICT were used

to obtain a the percentage of plaque accumulation (PPI) in mm^2 and the tooth area

(mm^2) per tooth by redirecting (Particles8) the individual tooth mask to the mask with

dental plaque (Figure 73). The results in pixels were multiplied by the scale

conversion factor in mm^2. The mask with dental plaque used in the analysis, was the

image where dental plaque was segmented with the method 1: colour deconvolution

using Yen as the thresholding method.

Gold standard result (hand outlined images)

Automated thresholded methods		Dental plaque 1	Background 0	Total
	Dental plaque 4	True Positive TP 5	False Positive FP 4	TP+FP
	Background 2	False Negative FN 3	True Negative TN 2	Value FN+TN
	Total	TP+FN	FP+TN	

2= TN	4=FP
3= FN	5=TP
Sensitivity= TP/(TP+FN)	**Specificity=** TN/(FP+TN)

Figure 70 Contingency table used to calculate the negative positive values and the sensitivity and specificity of automated thresholding methods compared to hand outlined (gold standard).
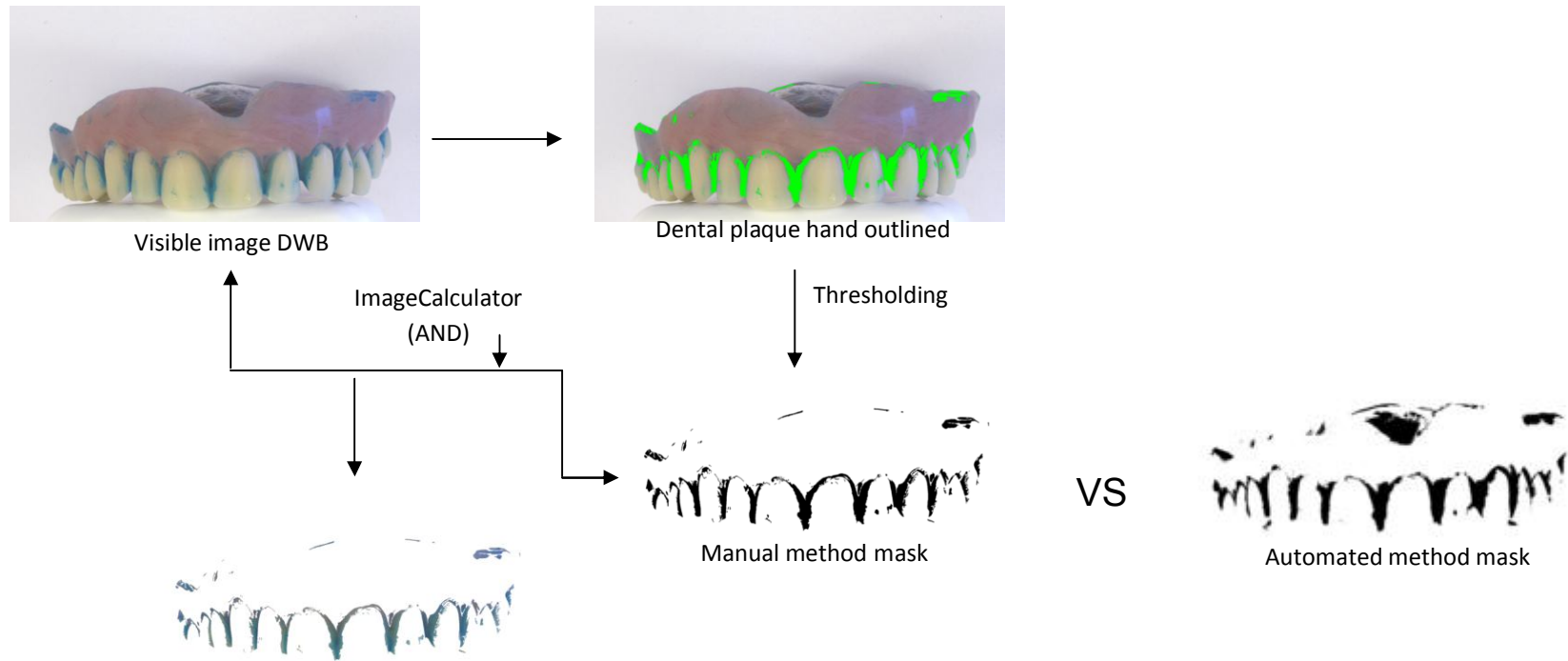
Figure 71 Procedure to threshold dental plaque by hand outlining.
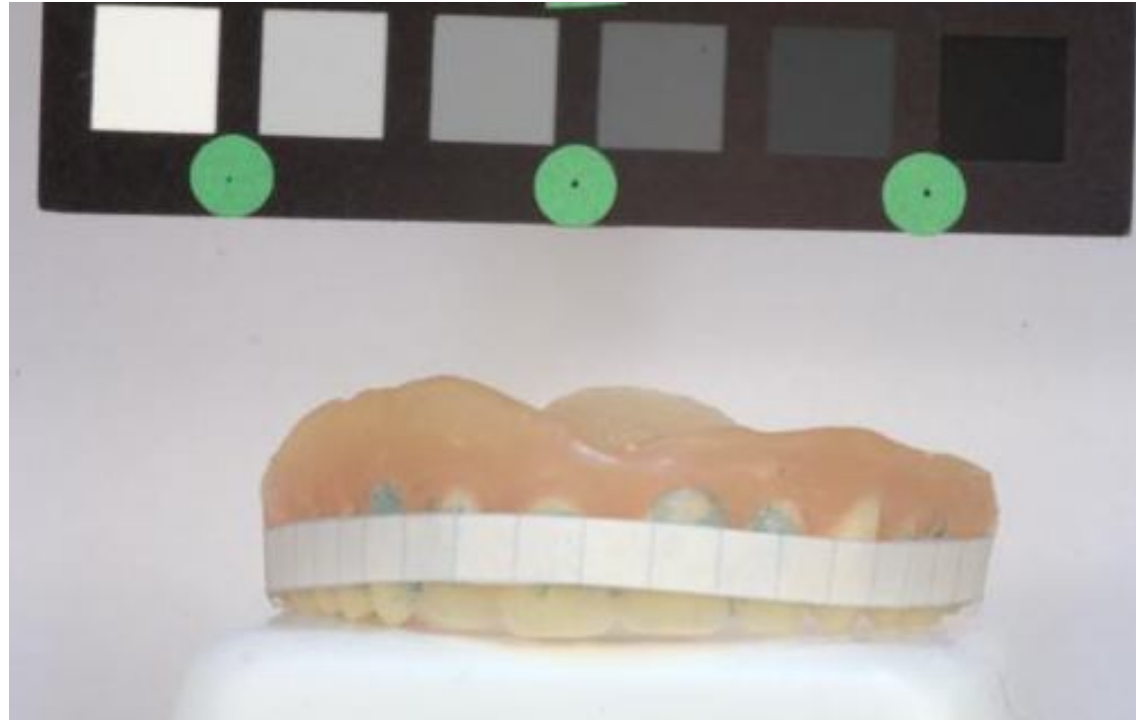
Figure 72 Image showing the strip of graph paper (with blue squares) glued in front of a denture to measure the distortion in the anterior region in the dentures.

Teeth segmented into units (ABS snake)

Redirect (Particle8)

Colour deconvolution Yen

PIXELS
1) PPI
2) Tooth area (mm^2)

Conversion factor mm^2

1) PPI
2) Tooth area (mm^2)
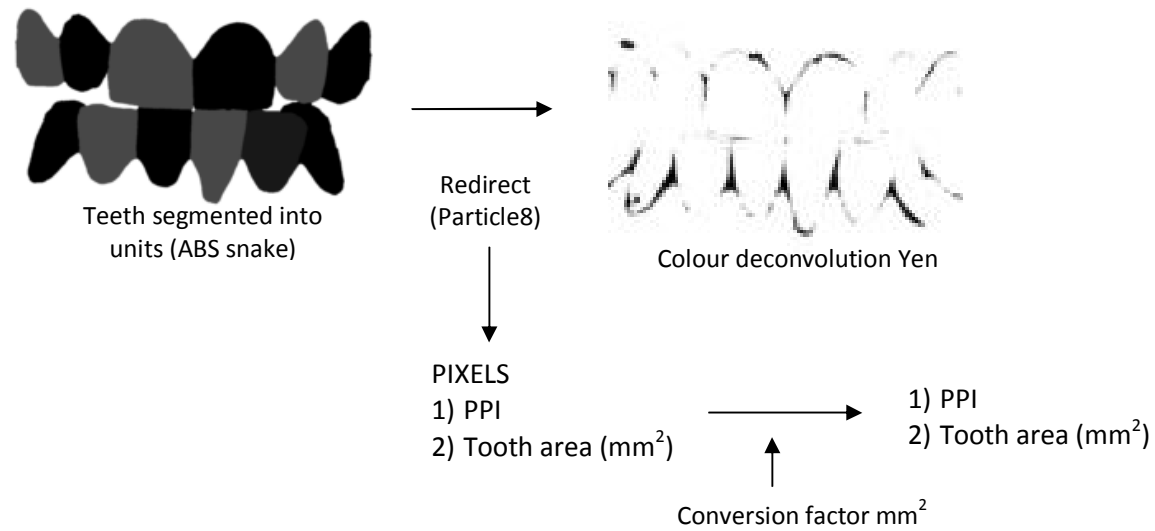
Figure 73 Procedure followed to obtain the PPI and tooth area in the ICT.

A paired samples t-test was applied to compare a) the individual PPI distribution per tooth in matching pairs (right versus left), and b) per tooth by gender. Comparisons per patient were calculated for a) the general PPI per patient, b) between the mean PPI per patient for the upper arch vs. the lower arch and c) the mean PPI per patient of the 6 teeth in the right side vs. those on the left side. ANOVA was used to analyse the mean PPI distribution differences among subjects.

6.2. Results

6.2.1. Images of complete dentures

During the five months that the sample collection lasted, 60 DWB images and 16 DBB images were obtained. Regarding to the denture cleaning the results showed that the use of Steradent with brushing (28.6%) or without it (21.4%) was the preferred method. Sixty-eight percent of the patients reported to clean their denture with a frequency of at least once a day with the night cleaning (35.7%) showing higher values than the morning (32.9%) cleaning (Figure 74). The denture wearers have had their denture for an average of 8.8 years.

6.2.2. Images of dentures on a white background

Five images (out of 60) the method to threshold dental plaque did not segment the image therefore only the results from 55 images are presented. The denture area (mm^2), dental plaque area (mm^2) and the PPI, in addition to their mean and standard deviation, for all teeth and from canine to canine are presented in Table 21.

How is the denture cleaned. All dentures

Legend:
- steradent only (no brushing)
- bleach & brush
- steraden & brushing & soap
- steradent & brushing
- steradent & brushing & paste
- only toothbrush & water
- toothbrush & soap
- toothbrush and paste
- dentural
- tothbrush & dentural
- nothing

Values shown: 21.4%, 1.4%, 4.3%, 1.4%, 4.3%, 28.6%, 5.7%, 5.7%, 2.9%, 21.4%, 2.9%
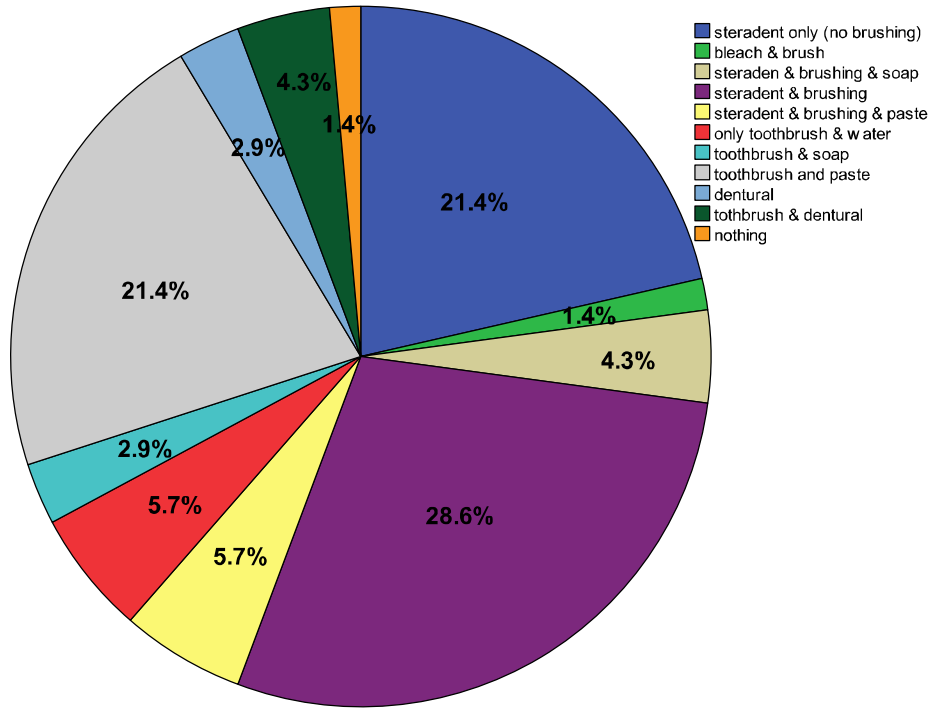
How often is the denture cleaned. All dentures

Legend:
- never
- once a week
- once a day (morning)
- once a day (night)
- twice a day or more (with meals)
- every third day

Values shown: 1.4%, 2.9%, 32.9%, 35.7%, 22.9%, 4.3%
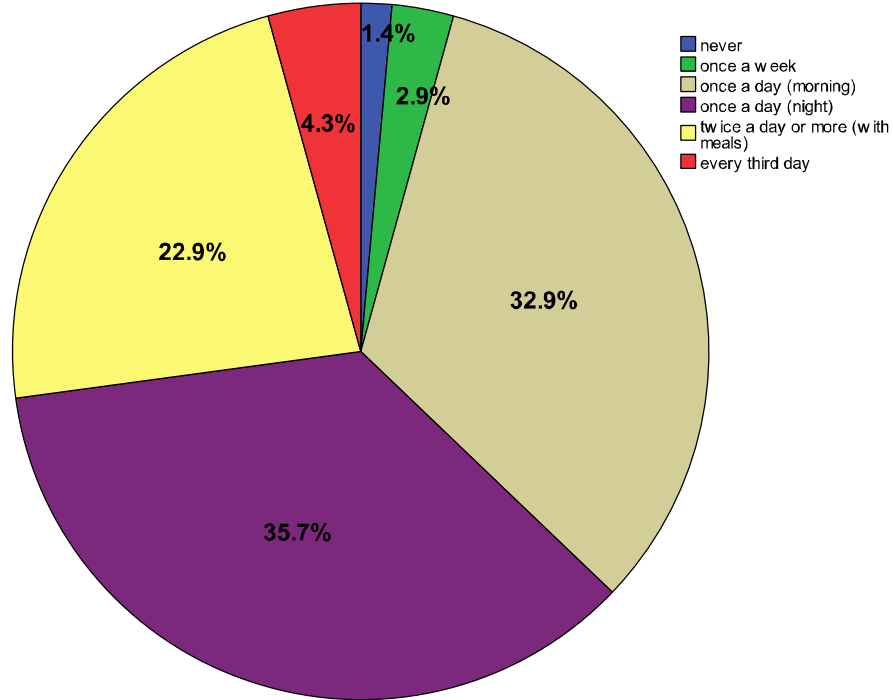
Figure 74 Methods and frequency of the cleaning procedures used to clean the upper complete dentures (both backgrounds).

Table 21 Plaque area (mm^2) and denture area (mm^2) for all teeth and canine to

canine for the DWB.

	All teeth		Six teeth	
image	Denture area (mm^2)	PPI % (plaque/denture)	Denture area (mm^2)	PPI % (plaque/denture)
1	1038.77	11.76	757.35	13.21
3	914.44	16.33	694.71	12.67
4	1112.74	4.75	810.32	4.91
5	1122.26	0.45	838.63	0.61
6	940.05	15.51	732.87	10.74
7	1129.53	8.65	871.46	8.54
8	1096.58	14.85	801.76	15.97
9	798.58	5.86	591.39	6.75
10	1014.86	19.09	771.45	22.06
11	925.74	3.60	665.78	3.48
12	998.60	4.66	809.73	5.60
13	1106.41	27.51	825.66	29.78
14	900.44	6.19	660.11	6.45
16	1106.44	5.28	852.71	6.01
17	865.05	17.84	620.99	10.07
18	773.95	3.49	451.99	4.39
19	1003.59	37.51	761.03	36.25
20	1446.95	75.79	1202.22	77.09
21	934.98	11.51	662.57	11.35
22	769.11	14.04	579.83	12.65
23	1188.00	4.59	869.43	4.94
24	1120.80	5.53	730.42	7.20
25	917.03	14.10	670.56	12.61
26	1128.50	7.03	824.16	7.93
27	1058.19	0.58	756.83	0.08
28	1142.36	16.65	819.54	17.14
29	1148.31	7.02	843.19	7.94
30	1094.77	1.00	858.03	1.06
31	935.66	5.66	642.49	3.44
32	761.74	1.30	559.60	1.71
33	968.62	18.56	794.60	20.88
35	1060.92	3.05	787.43	4.10
36	1188.31	16.05	880.92	15.33
37	1090.77	4.72	808.94	4.56
38	819.77	5.67	572.04	5.04
39	936.40	19.14	687.42	18.68
40	970.81	4.43	744.72	4.50
41	839.92	0.90	612.15	0.36
42	1326.49	10.57	1014.73	12.58
43	953.39	4.95	677.81	6.03
44	1083.07	3.55	885.14	4.02
45	1024.60	0.85	764.50	0.05
46	978.28	23.97	662.66	24.79
47	856.44	7.10	596.65	8.27
48	1172.99	2.06	820.00	0.98
50	1120.45	6.60	804.87	7.57
51	948.96	4.06	743.04	4.38

52	1400.97	12.11	983.68	11.01
53	1013.57	17.46	752.26	19.36
54	1289.90	4.02	883.16	3.55
55	968.72	6.01	728.28	5.39
57	1221.00	9.94	838.45	13.73
58	1190.14	12.69	835.91	17.59
59	839.91	11.30	609.20	14.58
60	1200.82	14.04	848.96	11.42
Mean	1035.63	10.76	761.35	10.93
S.D.	154.17	11.63	126.29	11.83

6.2.3. Images of dentures on a black background

Table 22 shows the percentage of plaque coverage and the area total per tooth in each denture. It shows that the PPI ranged from 0.03% (tooth-11) image 6 to 53.5% (tooth-12) image 4 (Figure 75). The one way ANOVA did not find significant differences between the mean plaque PPI per tooth type (central, lateral, etc) at the p<0.05 [$F_{(5,89)}$=0.64, p=66] however there were statistical significant differences in the teeth size (area) at p<0.05 [$F_{(5,89)}$=0.35.5, p=0] (Figure 76). The largest teeth in the dentures were both the right and left central incisors (Figure 77). Moreover, when comparing the teeth size (area) on the left side of the dentition against its matching pair on the right no statistical significant differences were found (p=1.0 in all cases) with p<0.05.

6.2.4. Clinical images

The sample comprised the upper and lower natural teeth from canine to canine of 25 right handed volunteers (18 female and 7 male) with an average age of 24.5, (S.D. 3.5 years). The tooth area in mm^2 from canine to canine (upper and lower), per image are presented in Table 23. The underlined numbers represent the female population. The t-test did not find statistical significant differences for the mean teeth area between matching teeth (left vs. right) for all the population (Table 24) nor for gender (Figure 78).

6.2.5. Methods used to threshold dental plaque in clinical images

The results when using colour deconvolution to threshold dental plaque were better than those when the high pass filter technique was used.

Table 22 Tooth area (mm^2), plaque area (mm^2), and percentage of plaque coverage (%) per denture of the DBB images.

Image	Teeth	Tooth area (mm^2)	PPI % (plaque/area)	Image	Teeth	Tooth area (mm^2)	PPI % (plaque/area)
1	13		missing	9	13	42.00	26.32
	12	24.14	17.63		12	51.80	6.69
	11	50.92	2.53		11	73.18	23.97
	21	60.37	3.00		21	66.82	33.11
	22	38.38	12.85		22	52.97	14.12
	23	33.06	6.22		23	32.60	13.80
2	13	50.82	3.11	10	13	50.68	7.41
	12	60.83	7.16		12	58.04	11.23
	11	96.16	5.94		11	85.92	10.41
	21	90.03	5.23		21	89.45	8.84
	22	54.27	6.59		22	57.37	11.99
	23	51.10	5.35		23	47.27	9.14
3	13	38.05	0.28	11	13	35.94	11.38
	12	42.77	4.75		12	46.10	20.15
	11	65.42	9.65		11	72.92	10.49
	21	65.83	10.44		21	74.29	8.33
	22	43.92	18.44		22	41.94	12.01
	23	43.04	12.37		23	32.60	20.13
4	13	50.42	38.65	12	13	48.85	1.09
	12	51.54	56.53		12	36.29	1.62
	11	94.97	37.91		11	55.76	1.67
	21	98.74	12.10		21	58.95	3.60
	22	56.74	10.24		22	40.58	4.66
	23	46.93	0.89		23	43.49	2.37
5	13	41.19	1.49	13	13	41.88	5.66
	12	51.58	4.71		12	41.20	11.50
	11	77.44	3.16		11	70.20	19.02
	21	77.70	10.85		21	67.76	15.80
	22	37.69	32.42		22	43.73	14.14
	23	34.74	33.26		23	49.85	13.97
6	13	41.23	0.09	14	13	52.09	2.51
	12	35.55	0.09		12	58.68	11.97
	11	63.47	0.03		11	79.75	2.57
	21	62.62	0.05		21	80.58	4.22
	22	35.30	0.56		22	55.24	2.36
	23	37.27	0.06		23	43.66	0.14
7	13	33.74	34.19	15	13	27.96	13.43
	12	39.19	31.24		12	42.92	12.87
	11	78.75	11.25		11	59.65	8.21
	21	76.77	1.67		21	59.85	8.32
	22	41.52	11.47		22	14.75	10.85
	23	38.51	8.81		23	35.31	16.66
8	13	24.24	3.03	16	13	37.31	3.24
	12	41.19	25.56		12	36.69	14.82
	11	78.12	28.37		11	64.52	12.88
	21	81.92	21.23		21	61.23	13.76
	22	58.81	15.66		22	37.93	8.86
	23	45.96	10.55		23	39.85	4.56
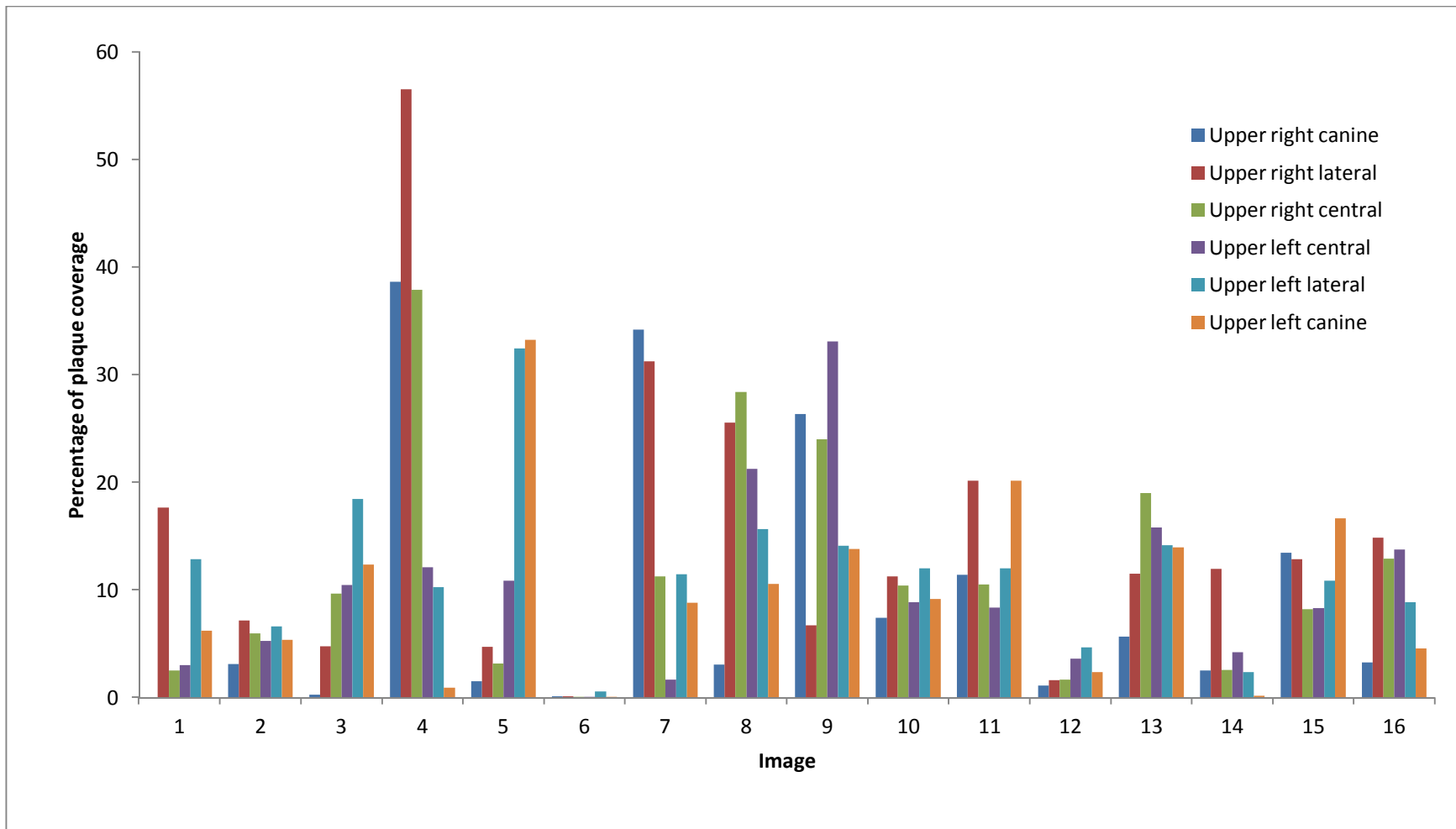
Figure 75 Percentage plaque coverage (PPI) per tooth in the dentures in the DBB images.
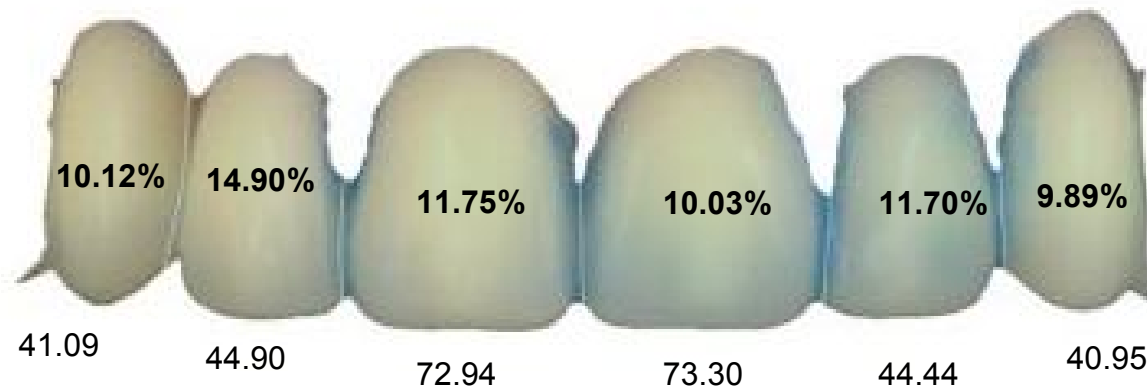
Figure 76 Mean PPI per tooth (bold) and mean area (mm^2) tooth area for all the DBB (before the square root transformation).
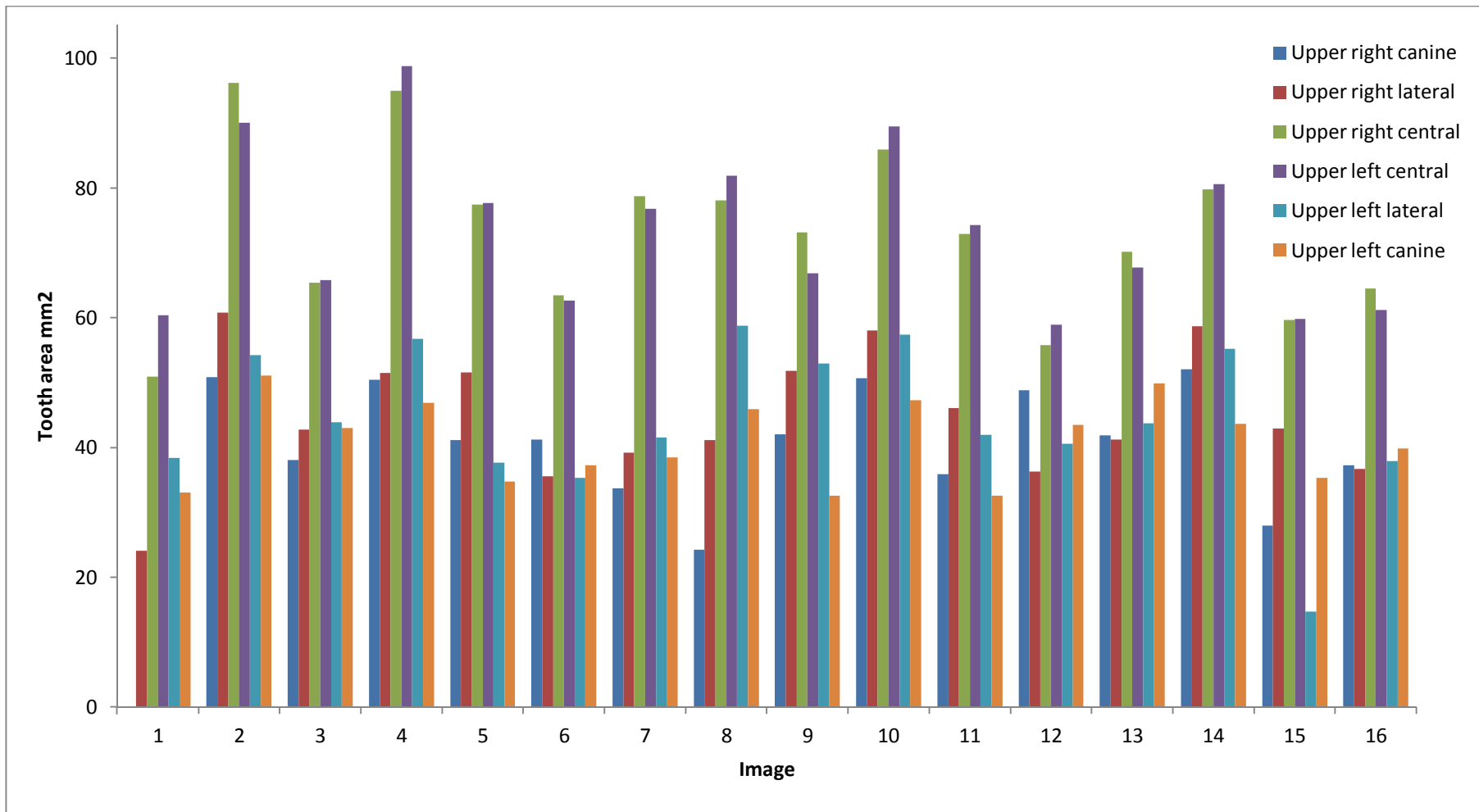
Figure 77 Tooth area (mm^2) per tooth, per image, for the DBB images.

Table 23 Tooth area (mm^2) from canine to canine (upper and lower) per image for all the ICT. The underlined numbers show the women.

Image						Tooth (area mm^2)						
	URC(13)	URL(12)	URCe(11)	ULCe(21)	ULL(22)	ULC(23)	LLC(33)	LLL(32)	LLCe(31)	LRCe(41)	LRL(42)	LRC(43)
_1_	35.81	34.60	55.25	54.04	27.10	23.85	29.62	26.71	29.59	25.09	31.65	27.38
_2_	21.79	23.17	50.22	47.72	25.61	22.27	21.50	31.93	30.56	28.21	30.29	22.32
_3_	32.21	23.05	47.92	45.89	31.08	31.29	32.05	29.49	29.76	28.34	26.38	29.67
_4_	22.73	20.57	43.68	43.48	23.09	23.09	14.76	22.65	21.68	23.34	23.25	21.85
_5_	23.14	33.17	54.69	56.19	31.46	28.74	25.26	26.60	29.79	27.36	26.52	27.19
_6_	22.84	29.47	62.07	58.02	23.44	19.87	21.26	30.84	32.93	31.61	33.37	25.47
_7_	25.19	26.15	60.08	61.36	26.34	22.46	27.96	29.39	33.63	34.06	30.51	23.94
8	24.74	30.94	59.97	58.26	33.49	31.63	26.12	29.68	25.97	23.26	33.40	31.95
9	17.39	21.18	42.34	45.70	24.30	18.96	22.48	23.72	26.45	26.49	22.89	23.37
_10_	31.81	35.42	62.44	54.74	27.57	24.42	27.76	22.87	29.24	32.29	32.22	31.32
_11_	22.36	31.40	54.95	58.16	36.19	25.02	27.28	28.78	28.44	27.22	27.66	26.87
12	26.77	30.97	53.40	53.89	31.66	24.97	32.46	27.13	28.20	21.78	30.42	30.32
_13_	43.26	34.89	70.59	70.41	35.76	39.98	34.95	26.69	33.61	30.75	34.42	37.78
_14_	31.04	38.06	66.89	61.37	35.81	27.68	30.50	27.19	27.62	27.55	26.43	31.58
_15_	22.73	25.07	47.61	45.37	25.63	17.95	25.03	23.57	23.62	24.34	25.71	22.67
_16_	27.97	39.57	71.61	67.23	40.69	29.20	29.23	36.06	38.23	32.18	39.24	31.28
_17_	33.56	34.36	62.58	64.49	34.41	31.19	33.90	33.56	36.58	32.46	35.00	31.20
_18_	24.16	23.84	52.08	52.34	27.53	22.85	27.62	27.44	23.81	23.03	25.15	26.89
19	30.47	34.96	57.26	57.93	35.85	32.10	34.45	35.81	31.64	35.00	24.90	28.02
_20_	25.76	34.37	60.26	63.21	39.50	27.80	34.58	31.29	32.21	30.40	29.37	28.78
_21_	22.00	26.46	44.93	44.66	28.76	22.57	26.58	23.66	23.40	24.07	21.57	25.18
_22_	38.21	30.80	55.91	54.02	26.73	34.35	34.35	34.45	29.33	30.45	33.02	35.59
23	27.22	22.50	51.32	51.86	22.62	25.42	35.66	28.75	20.25	26.04	25.19	30.81
24	28.29	34.47	61.03	61.64	39.35	25.82	34.25	27.17	27.80	26.66	28.88	39.57
25	25.88	33.56	56.41	61.53	41.82	34.36	38.11	37.15	34.46	31.99	32.61	35.44
Mean all	27.49	30.12	56.22	55.74	31.03	26.71	29.11	28.90	29.15	28.16	29.20	29.06
S.D. all	5.92	5.59	7.77	7.40	5.93	5.35	5.55	4.20	4.51	3.78	4.40	4.77

Table 24 Results of the paired samples t test when comparing the right vs. the left mean tooth area (mm^2) scores per tooth for the entire sample. Note that no statistical significant differences were found at p<0.05.

		Upper						Lower					
Tooth		Canine		Lateral		Central		Central		Lateral		Canine	
		Right	Left	Right	Left	Right	Left	Right	Left	Right	Left	Right	Left
Tooth area (mm^2)	Mean	27.50	26.71	30.12	31.03	56.22	55.74	28.09	29.22	29.18	28.93	28.77	29.39
	SD	5.91	5.35	5.58	5.93	7.77	7.40	3.88	4.41	4.43	4.17	5.39	4.94
Left vs. right	p	0.37		0.28		0.42		0.05		0.76		0.39	

Figure 78 Mean tooth projected area (mm^2) for the upper and lower teeth per gender (W=women, M=male). No statistical differences were found per gender at p<0.05 (the S.D is in brackets).

a) *Method 1: Colour deconvolution*: The reliability measures from comparing the masks of the three dental plaque auto thresholding methods using dental plaque traced by hand as the gold standard for ICT are shown in Table 25. These results were then used to plot the graphs in Figure 79 and Figure 80. When comparing the three thresholding methods, both the graph and the plot illustrate that all methods had similar values with a high specificity (mean 0.97 ± 0.02) and regular sensitivity (0.69 ± 0.18). The results also showed that variations occurred between images, with the image 25 recording the highest sensitivity and specificity which can be corroborated in Figure 80 as this image presented the shortest distance to the ideal.

b) *Method 2: High pass filter*: The reliability results when comparing the masks of the images of dental plaque thresholded with the automated methods (Default, IsoData, Li, Moments, Otsu, RenyiEntropy and Yen) against the masks of the dental plaque traced by hand (gold standard) for the ICT are shown in Table 26. These values were used to plot the sensitivity against specificity per image and method (Figure 81) and their averages (Figure 82). It can be seen that the specificity for all the methods was high (mean 99 ± 0.01) whilst the specificity was no higher than 0.56 (mean 0.54 ± 0.08). Otsu, IsoData and Yen presenting the highest values and the shortest distances to the ideal (Figure 83). Of the three images used the image 25 presented the highest sensitivity and specificity and therefore the shortest distance.

6.2.6. Intra-observer reliability of determination of dental plaque

Table 27 shows the area of plaque for the five images traced by hand. The coefficient of variation for the intra-examiner reliability was 3.55%.

Table 25 Reliability measures of the three auto thresholding methods and dental plaque traced by hand for the ICT when using

colour deconvolution.

Method/image	TN	FP	FN	TP	**TNR**	**TPR**
MaxEntropy-02	983438	6759	20039	21515	0.99	0.52
RenyiEntropy-02	983951	6246	20400	21154	0.99	0.51
Yen-02	983951	6246	20400	21154	0.99	0.51
MaxEntropy-18	978144	18654	18304	34834	0.98	0.66
RenyiEntropy-18	979406	17392	18585	34553	0.98	0.65
Yen-18	979406	17392	18585	34553	0.98	0.65
MaxEntropy-25	867052	40827	13924	114837	0.96	0.89
RenyiEntropy-25	848257	59622	9405	119356	0.93	0.93
Yen-25	842632	65247	8500	120261	0.93	0.93
mean					0.97	0.69
average					0.02	0.18

Code: *TPR*-Sensitivity *TNR*-Specificity *TN*-True Negative *TP*-True Positive *FP*-False positive *FP*-False negative
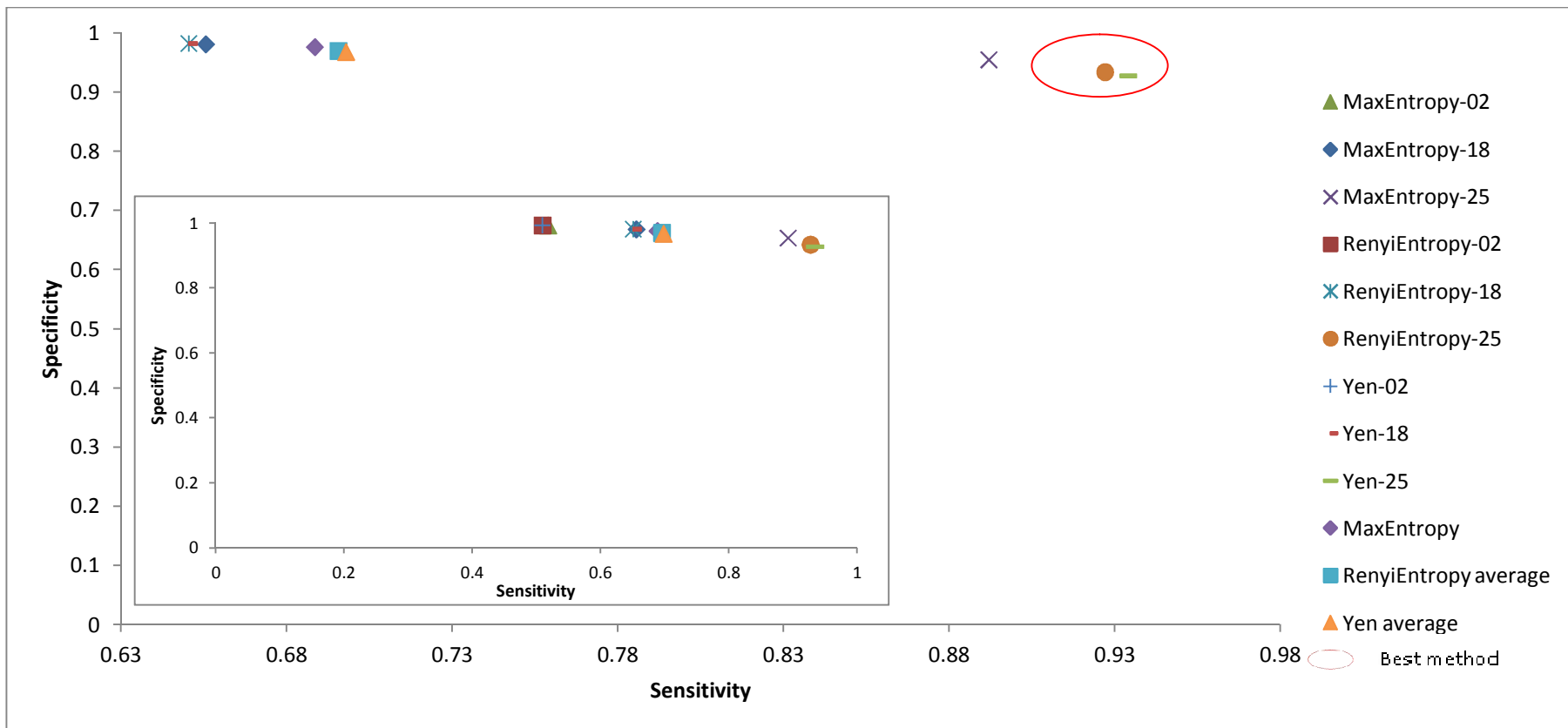
Figure 79 Sensitivity vs. specificity when comparing the masks of the images where dental plaque was traced by hand against the masks of the images where colour deconvolution was used to segment dental plaque. The small graph on the left presents the full scale from 0 to 1 for both the X and Y axes whilst the bigger graph presents smaller range of the Y axis. The circle represents the "best" method.
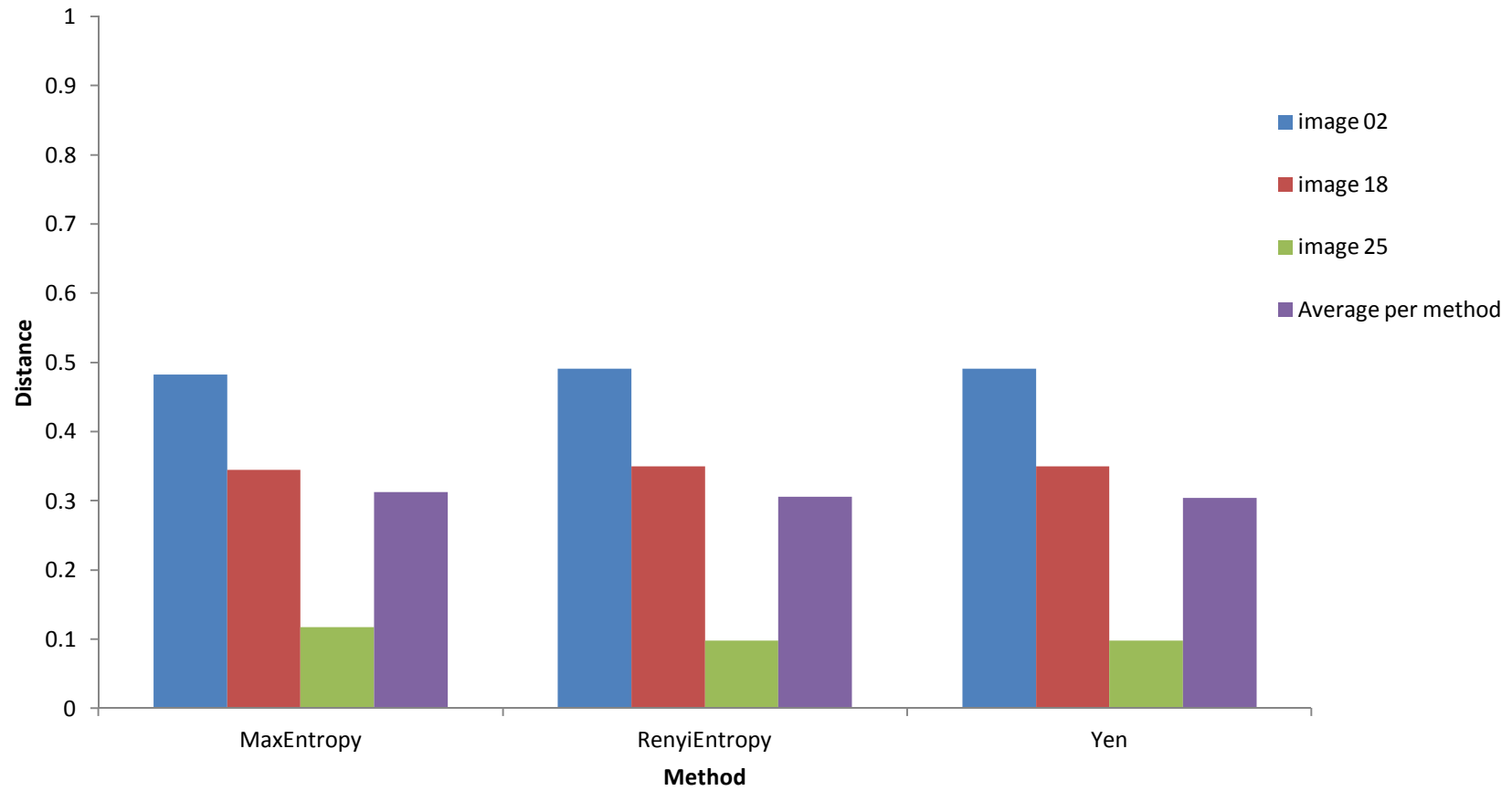
Figure 80 Distance to the ideal when comparing the masks of dental plaque in the images traced by hand and the three auto

thresholding methods for ICT using colour deconvolution.

Table 26 Reliability measures of the seven auto thresholding methods for the ICT and dental plaque traced by hand when using high pass filter approach.

	TN	FP	FN	TP	**TNR**	**TPR**
Default-02	987882	2315	18334	23220	0.998	0.559
IsoData-02	986464	3733	16906	24648	0.996	0.593
Li-02	986922	3275	17266	24288	0.997	0.585
Moments-02	987383	2814	17706	23848	0.997	0.574
Otsu-02	986228	3969	16771	24783	0.996	0.596
RenyiEntropy-02	988850	1347	20290	21264	0.999	0.512
Yen-02	988691	1506	19884	21670	0.999	0.522
Default-18	993100	3698	31650	21488	0.996	0.404
IsoData-18	991030	5768	28072	25066	0.994	0.472
Li-18	993439	3359	32443	20695	0.997	0.390
Moments-18	991394	5404	28630	24508	0.995	0.461
Otsu-18	990883	5915	27798	25340	0.994	0.477
RenyiEntropy-18	991856	4942	29390	23748	0.995	0.447
Yen-18	991394	5404	28630	24508	0.995	0.461
Default-25	897216	10663	57827	70934	0.988	0.551
IsoData-25	894047	13832	49339	79422	0.985	0.617
Li-25	896979	10900	57145	71616	0.988	0.556
Moments-25	896979	10900	57145	71616	0.988	0.556
Otsu-25	894047	13832	49339	79422	0.985	0.617
RenyiEntropy-25	891594	16285	43615	85146	0.982	0.661
Yen-25	889171	18708	38502	90259	0.979	0.701
Mean					0.99	0.54
S.D.					0.01	0.08

Code: *TPR*-Sensitivity-*TNR*-Specificity *TN*-True Negative *TP*-True Positive *FP*-False positive *FP*-False negative
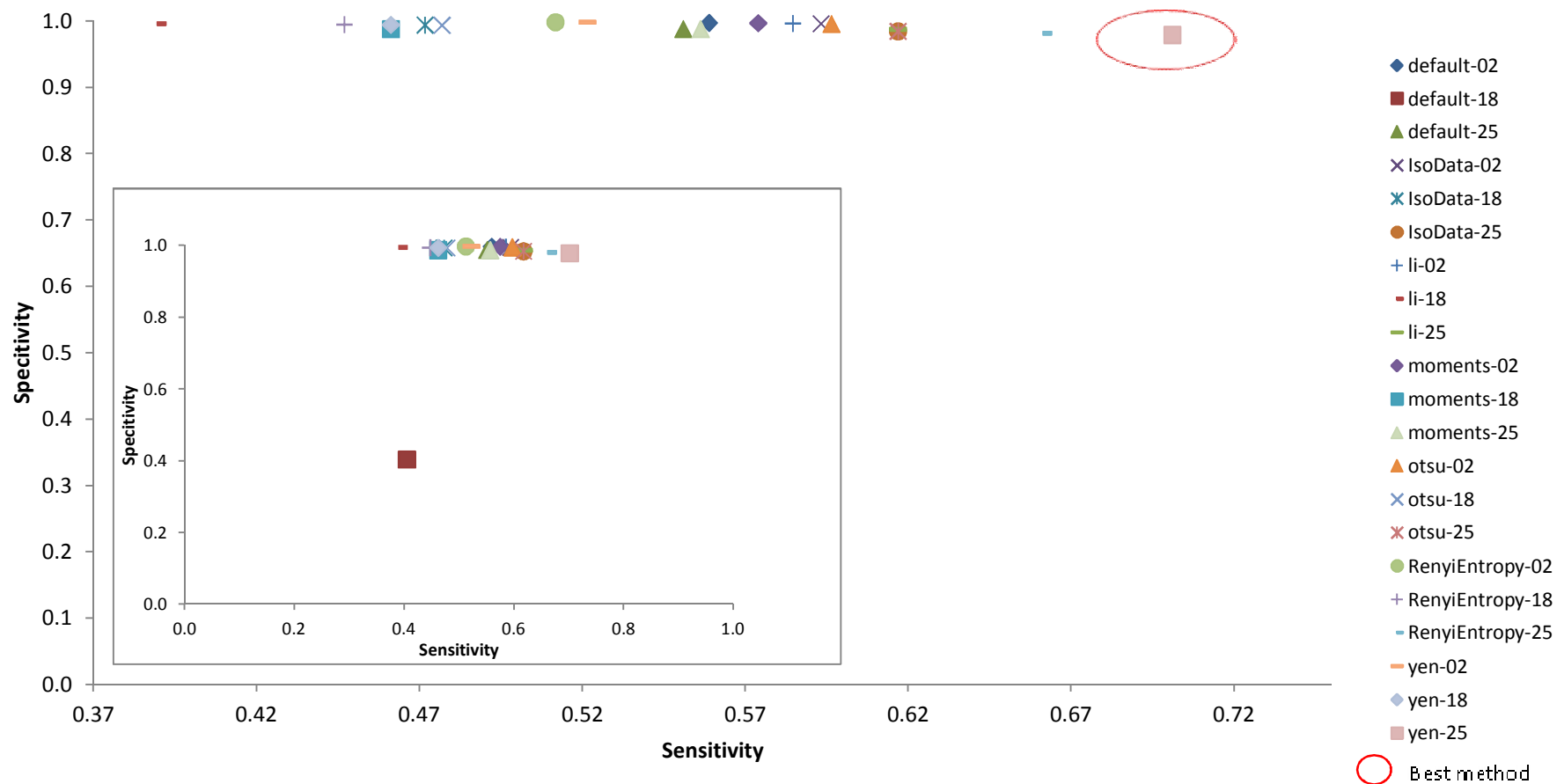
Figure 81 Sensitivity vs. specificity when comparing the masks of the ICT images where dental plaque was traced by hand against the masks of the images where <u>high pass filter</u> was used to segment dental plaque. The small graph on the left presents the full scale from 0 to 1 for both the X and Y axes whilst the bigger graph presents smaller range of the Y axis.
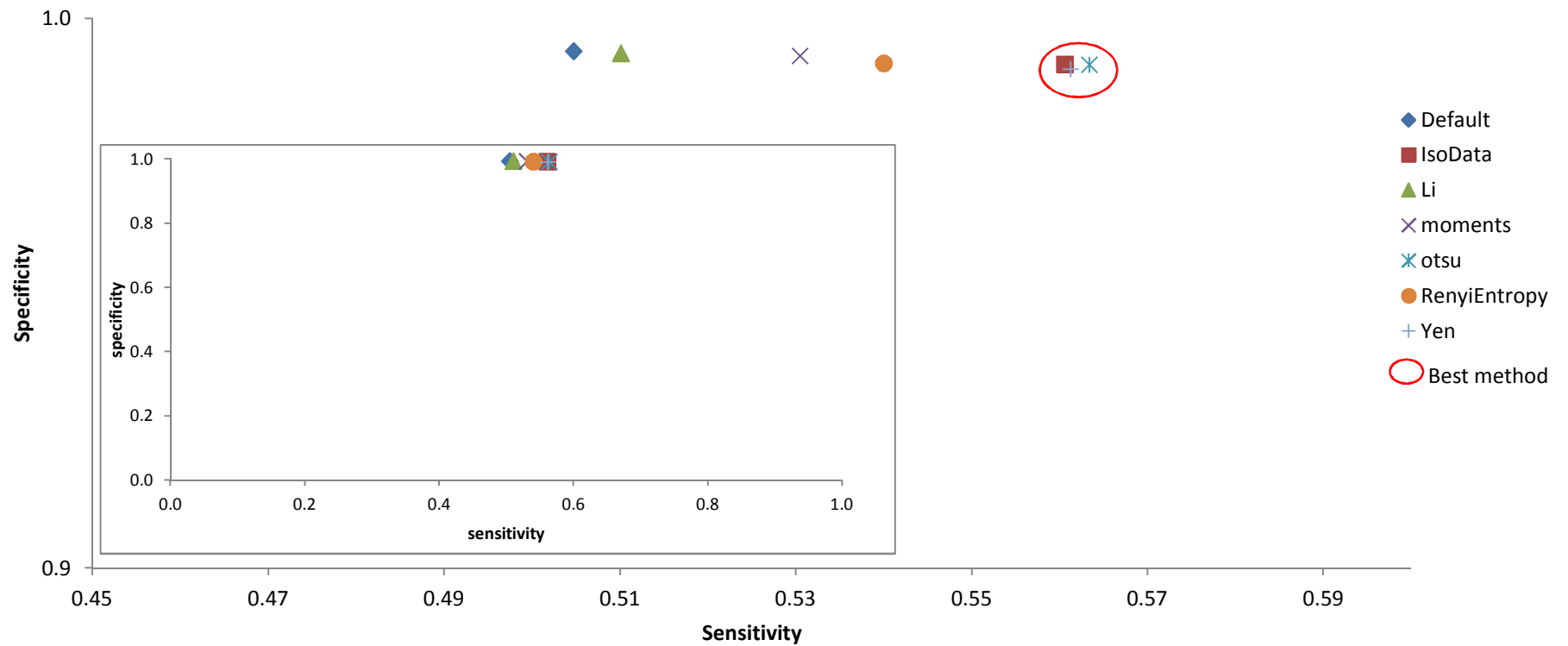
Figure 82 Average sensitivity vs. average specificity per method for the ICT when comparing the masks of where dental plaque was traced by hand against the masks of the images where high pass filter was used to segment dental plaque. The small graph on the left presents the full scale from 0 to 1 for both the X and Y axes whilst the bigger graph presents smaller range of the Y axis.
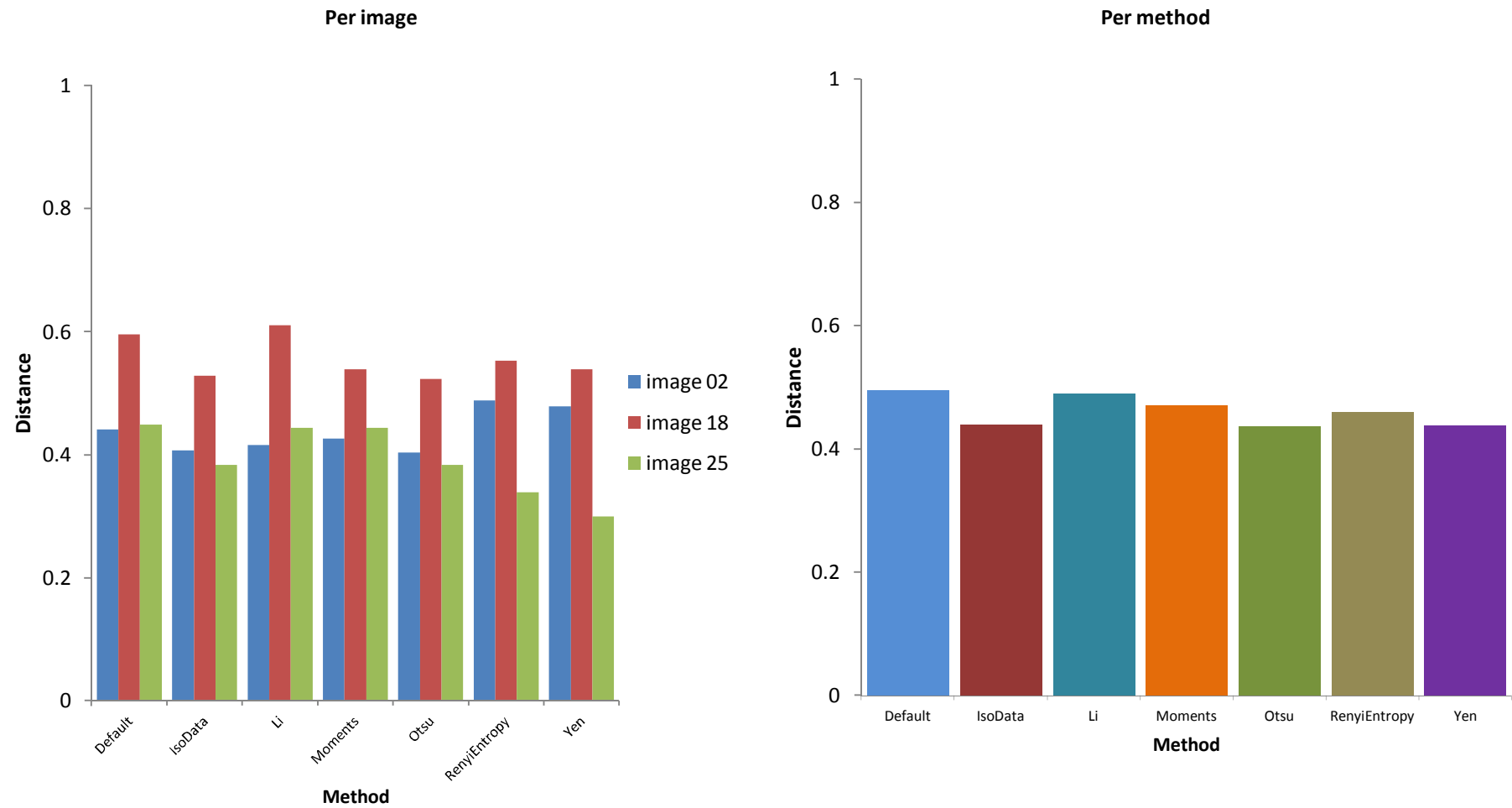
Figure 83 Distance to ideal when comparing the masks of dental plaque in the images traced by hand and seven auto thresholding methods (and average) for the ICT using the high pass filter approach.

Table 27 Pixels with plaque and its equivalent in area (mm^2) for the five images where dental plaque was highlighted by hand.

Image	Area of plaque mm^2
1	96.26
2	99.33
3	92.77
4	101.99
5	96.83
Mean	97.44
S.D.	3.46
CV	**3.55%**

6.2.7. Comparison between automated and manual methods of dental plaque segmentation

The Bland-Altman test shows that only one point (6.7%) out of 15 is outside the limits of agreement (Figure 84). which is consistent with the results from the paired t-test where no statistical significant differences were found in the scores for the automated (M=101.89, SD=56.99) and manual (M=87.89, SD=52.9) methods for plaque segmentation *t*(14)=1.04, *p* 0.31.

6.2.8. Distortion in the anterior region

The amount of distortion in the canine to canine region was 0.65mm for the right side and 0.53mm for the left (Figure 85).

6.2.9. Differences in plaque accumulation

No statistical differences were found with the paired samples t-test for the PPI between a) left and right individual paired teeth, b) per tooth by gender (Figure 86), the c) the mean PPI for the upper teeth (M=12.39, S.D=12.74) vs. the lower ones (M=11.72, S.D=11.89) t(149)=0.62, p 0.53 and d) the mean PPI for the 6 teeth in the right side of the arch vs. the 6 teeth in the left and. However statistical significant differences were found between the mean PPI for the upper and lower teeth (Table 28). The mean PPI between patients showed significant differences with the one way ANOVA (*F*(24,275)=12.72, p=<0.01) at p<0.05.
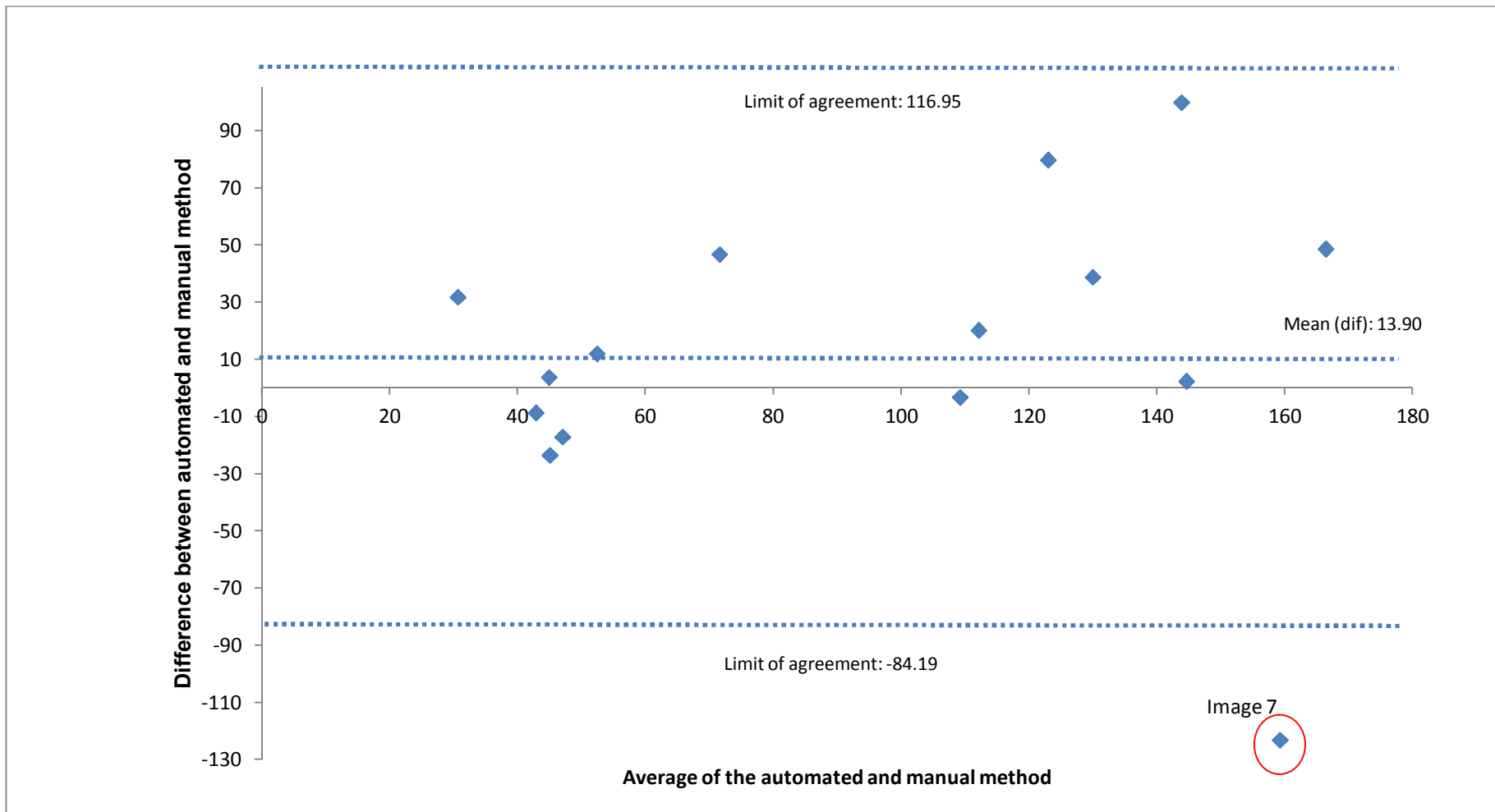
Figure 84 Bland-Altman plot: difference against mean of the automated and manual methods to segment dental plaque on the DWB images.
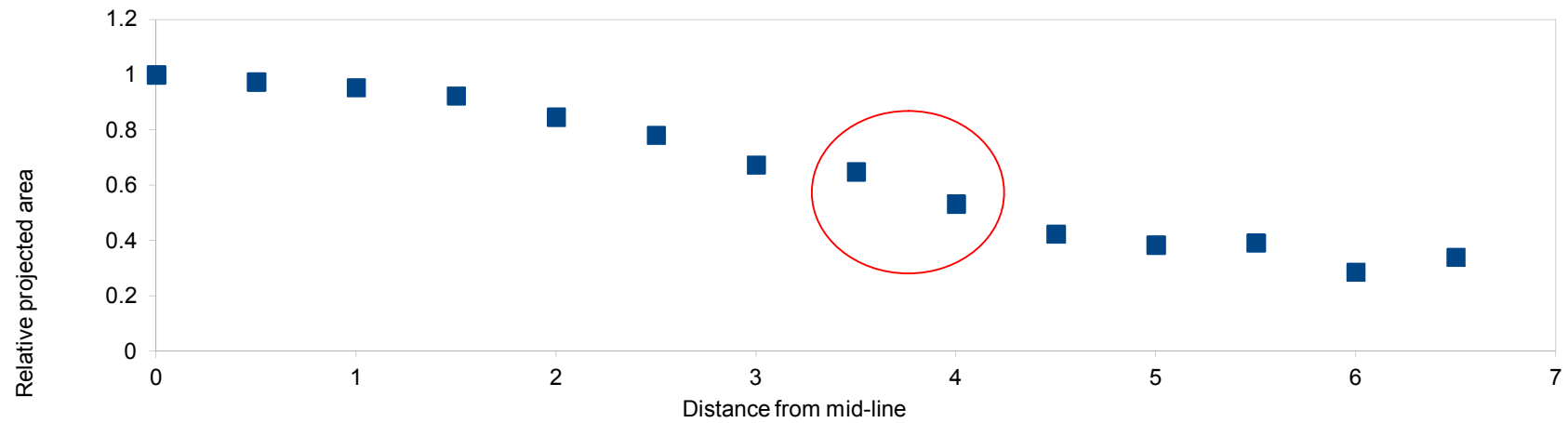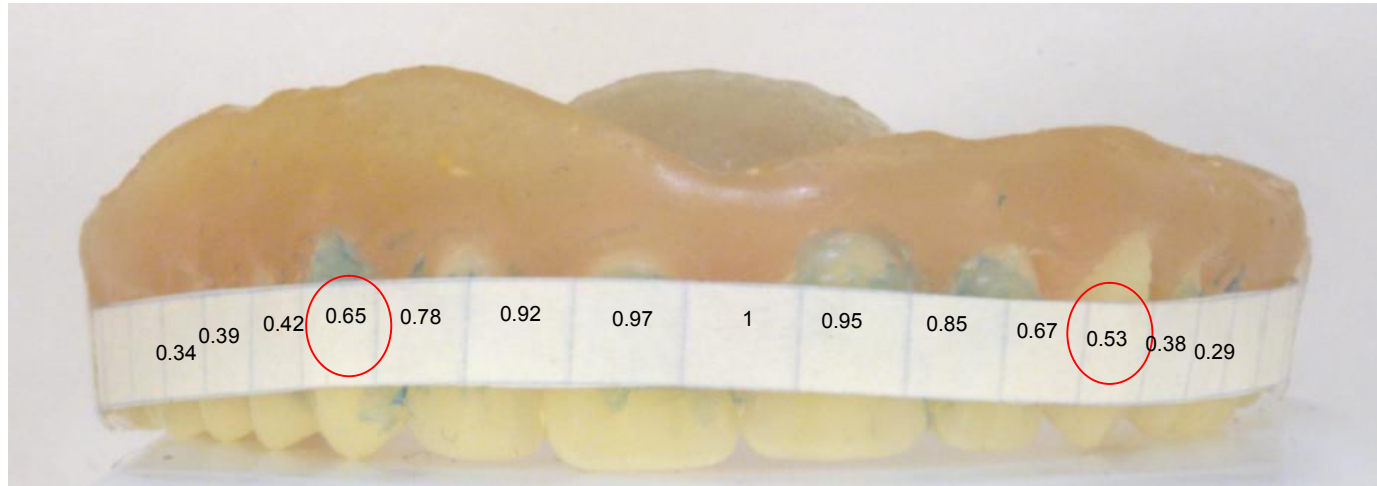
Figure 85 Distortion (in mm) of the anterior region due to the curvature of the dental arch. The red circles indicate the distortion in the canine area.
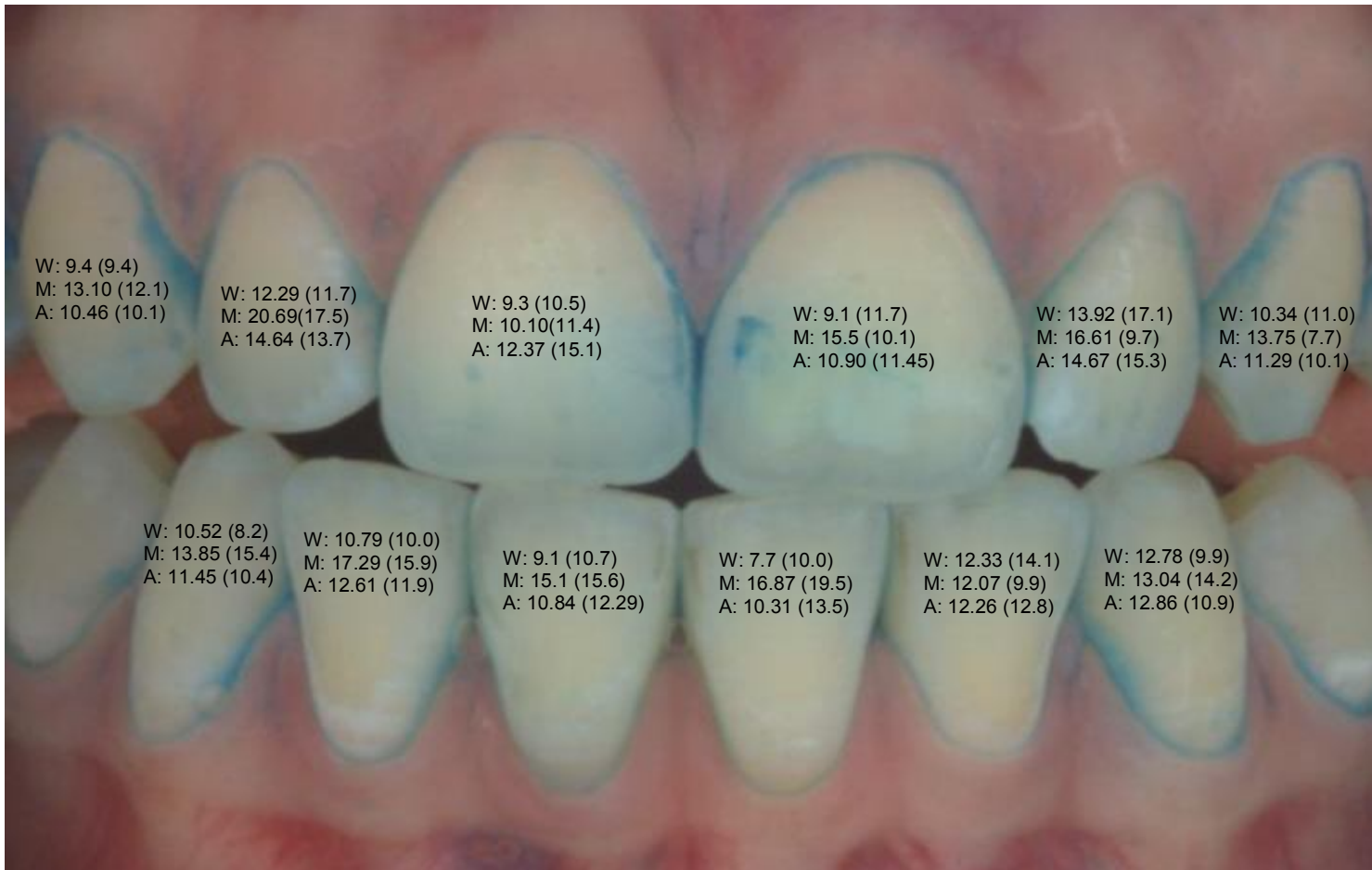
Figure 86 Mean PPI per gender (W=women, M=male) and per tooth (A=all). No statistical differences were found per gender or per tooth at p<0.05 (the S.D is in brackets).

Table 28 Paired samples t test per patient for the mean PPI scores in upper vs. lower and right vs. left teeth.

Patient	Upper		Lower			Right		Left		
	mean	S.D	mean	S.D	*p*	mean	S.D	mean	S.D	*p*
1	12.35	5.01	4.51	3.73	0.07	9.41	6.96	7.45	5.02	0.36
2	2.90	1.43	8.96	4.16	0.01*	6.35	5.25	5.51	3.66	0.39
3	10.42	8.06	15.69	12.49	0.23	10.65	7.04	15.45	13.20	0.34
4	0.75	0.58	0.57	0.61	0.62	0.48	0.46	0.84	0.66	0.16
5	15.34	8.03	18.15	5.97	0.51	15.93	6.92	17.56	7.45	0.71
6	33.29	13.50	31.88	8.10	0.59	33.02	6.30	32.15	14.45	0.85
7	6.84	3.01	3.72	2.81	0.08	5.42	3.15	5.14	3.58	0.85
8	20.37	12.34	6.39	2.15	0.03*	16.25	14.81	10.51	5.92	0.36
9	6.57	3.56	23.13	17.78	0.05	17.70	17.35	11.99	13.15	0.28
10	3.23	1.87	12.03	10.40	0.12	5.72	3.84	9.54	11.60	0.30
11	0.50	0.50	1.46	1.58	0.22	1.30	1.70	0.66	0.42	0.44
12	22.82	7.03	6.35	4.60	0.01*	15.15	12.69	14.02	8.44	0.77
13	5.63	5.02	2.82	2.60	0.21	5.67	4.77	2.78	2.98	0.29
14	3.76	3.67	2.86	1.44	0.67	3.13	1.03	3.49	3.86	0.85
15	1.08	0.95	0.21	0.21	0.09	0.58	0.69	0.71	0.96	0.81
16	9.21	8.21	5.40	3.82	0.39	8.78	8.49	5.83	3.65	0.48
17	12.18	4.11	13.31	4.77	0.69	14.97	4.59	10.53	2.75	0.07
18	5.59	4.01	18.07	6.64	0.01*	10.72	8.00	12.94	9.31	0.34
19	2.64	2.92	5.21	3.47	0.27	3.02	3.42	4.83	3.30	0.32
20	26.89	10.56	7.35	4.55	0.01*	13.85	8.11	20.39	16.43	0.18
21	11.70	6.59	17.85	6.93	0.26	16.03	7.12	13.52	7.73	0.46
22	31.79	18.17	25.30	11.14	0.39	22.77	13.86	34.32	14.40	0.26
23	16.03	9.25	32.64	7.69	0.01*	20.90	10.32	27.77	13.24	0.10
24	15.10	6.92	1.61	1.14	0.01*	5.84	4.87	10.87	10.92	0.18
25	32.86	20.84	27.71	12.98	0.63	38.06	18.63	22.51	11.24	0.14

*p< 0.05

6.3. Discussion

6.3.1. Images of complete dentures

Due to an increase in the life expectancy of the population it is likely that the demand for dentures in the elderly will remain (Petersen and Yamamoto, 2005) with 15 million potential denture wearers in the UK (Coulthwaite and Verran, 2007). Dentures return functionality and aesthetics to the patient and like natural teeth, can accumulate dental plaque (denture biofilm) and calculus (Connor et al., 1976, Felton et al., 2011) on their surface. As with dental plaque salivary glycoproteins are responsible for the initial bonding of bacteria to the denture (Abelson, 1981) which can cause denture stomatitis (candida) in the oral mucosa if it is not-removed (due to poor oral hygiene). The importance of the standardisation of the methods used to assess the efficiency of the denture cleansers has already been highlighted (Nikawa et al., 1999). Several methods for quantification of dental plaque on dentures have been developed and they can be classified in two groups: visual examination (using an ordinal scale in a similar way as the non quantitative methods for plaque detection on teeth), and quantitative indices (Jeganathan et al., 1996 , McCabe et al., 1996, Paranhos et al., 2004, Paranhos and Silva, 2004, Coulthwaite and Verran, 2009, Silva-Lovato et al., 2009, Paranhos et al., 2010). The latter are more reliable than the former as they eliminate the dependence on the examiner to score the extent of dental plaque and incorporate an interval scale or metric over which the measurements are reported (Coulthwaite and Verran, 2009).

In this study, quantification of dental plaque on dentures was done only on the labial surfaces of the teeth rather than using the different surfaces as described in most techniques (Tarbet, 1982, Keng and Lim, 1996).This was because in this work

staining of plaque on artificial teeth was used as a model to evaluate both the imaging techniques and the automated methods for dental plaque quantification prior the execution of the clinical trial which involved imaging of plaque on natural teeth. The reported methods for cleaning the denture show the variety of options available. Although the denture wearers who attend to the prosthetics clinic received a printed leaflet with advice on how to clean their dentures (rinse the denture after every meal, brush it with soap and cold water at least twice a day, soak the denture in alkaline hypochlorite-Dentural, Sterodent-for 20 minutes in the evening followed by a thoroughly rinse and brush of the denture under cold water and remove the denture from the mouth overnight while soaking it in cold water), it seems that the patients have adapted these instructions to their own convenience. While cleaning the CDs is required to prevent oral infections, there seems to be a weak evidence in the literature about the most effective method to achieve this (Jagger and Harrison, 1995). A few studies suggest that mechanical cleaning appear to provide better results in patients with good manual dexterity, than chemical cleaners alone (reviewed by de Souza et al., 2009). In the present study, the majority of the patients used Steradent with brushing (28.6%) or without it (21.4%) to clean their dentures, which shows the patients only follow half the instructions given by forgetting about the brushing. These results are in disagreement with other studies Peracini et al. (2010) found that all patients in his study (n=106) brushed their denture whilst Hoad-Reddick et al. (1990) found that the combination of brushing and soaking was the preferred method. Only 22.9% of the patients cleaned their dentures with the recommended frequency (at least twice a day), Dikbas et al. (2006) reported that 70% of their sample (n=234) cleaned their denture at least once a day which is a

similar result (68%) to the obtained in this study. These frequencies are lower than the reported in the literature (for the same toothbrushing frequency) which range from 79.1% to 99.09% (Hoad-Reddick et al., 1990, Nevalainen et al., 1997, De Castellucci Barbosa et al., 2008, Peracini et al., 2010). On average the denture wearers in this study had the same denture for 8.8 years which is almost 4 years more than the suggestions made by Catão et al. (2007) who proposed that dentures should be replaced every 5 years as both time and wear increase the acrylic porosity favouring plaque retention which then might lead to inflammation of the surrounding support tissues.

6.3.2. Images of dentures on a white background

Ideally, to quantify dental plaque on dentures, a coloured background that contrasts with the disclosing solution should be used (Paranhos and Silva, 2004). For the purpose of this study two different backgrounds (black and white) were used. Preliminary results obtained from the analysis of the DWB images showed that the plastic holder produced shadows between the denture and the background (white). This led to inaccuracies in the thresholding of the background and denture (Figure 87). To rectify this problem the segmentation of the denture was made by outlining its border by hand (see section 6.1.4.2-a) which added some undesirable subjectivity to the method. Additionally, although the method to threshold of dental plaque in the DWB worked well, no further attempts were made to segment the teeth into units because the human intervention had already introduced potential arbitrary steps into the design of an intended fully automated method. A novel aspect of this part of the study was the incorporation of a NBI filter to increase dental plaque contrast. As a solution to eliminate the shadows between the denture and the background the CDs

images were also obtained against a black background. Although the black background minimised the shadows it did not totally remove human intervention from the procedure. Table 29 presents the summary of the uses, advantages and disadvantages of the methods used to analyse the images of dentures in both backgrounds.

6.3.3. Images of dentures on a black background

The methods presented to segment the DBB images showed that computation of the tooth area and PPI for each individual tooth was possible with minimal human intervention. It may be argued that the procedure involved many steps increasing the analysis time as Coulthwaite and Veran concluded from their study on a computerised method to quantify dental plaque on dentures (Coulthwaite and Verran, 2009). However, ImageJ allows summarising the procedures by writing different macros for each action in the process with subsequent simplification of the method. In this study, independent macros were applied in a step like manner. Future research is needed to combine each of the individual macros as one single process and test its functionality.

Because of the background colour difference, the methods used to extract dental plaque in the DWB and the DBB were different. It was found that although simple, the plaque segmentation for the black images was not as straightforward as the method in the white images where no human intervention was needed (see 6.3.2) so the methodological design of future studies could take in to account alternate between backgrounds (black background for visible and white for NIB) within the same set of images.
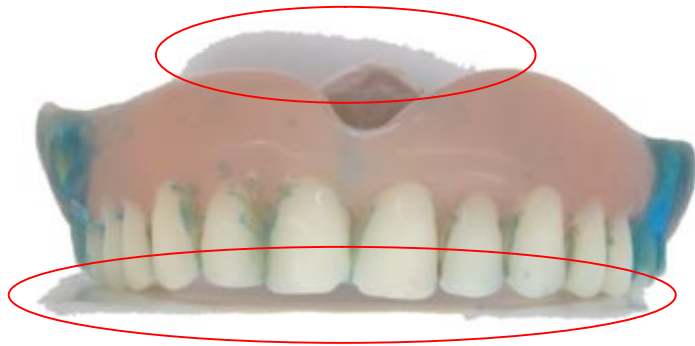
Visible image   Mask of the visible image

Figure 87 Aspect of the thresholded DWB image. Note the inaccuracy of the method due to shadows (encircled).

Table 29 Summary of the uses, advantages and disadvantages of the methods used to analyse the images of DWB and DBB.

Background	Dentures on a white background			Dentures on a black background		
Image	Visible	NBI filter	n-IR filter	Visible	NBI filter	n-IR filter
General comments	• Thresholding of denture done by hand			• More complex methodology • Segmentation of teeth into units was possible		
Use	• Segmentation of denture from background	• Dental plaque segmentation	Not used	• Segmentation denture from the background • Segmentation of teeth from denture • Teeth area separation into single units • Dental plaque segmentation	• Auxiliary image to separate denture from background	• Segmentation of denture from background • Elimination of excess pixels in the floor of dentures • Teeth area segmentation
Advantages	N/A	• Dental plaque segmentation straightforward	• Disclosed dental plaque is transparent	• Shadows between background & denture were minimised	None	• Disclosed dental plaque is transparent
Disadvantages	• Presence of shadows between plastic holder & background	None	Not used	N/A	None	• Borders (specially in the gingival region) difficult to threshold by computer

While it was shown that disclosing solutions are invisible under n-IR, these images presented a reduced definition especially in the area of the gingival margins. This deficiency was more evident in the images of dentures than in the ICT and complicated the localisation by the computer of the borders during the thresholding procedure. As a result the n-IR images were used only as an auxiliary in the segmentation procedure.

The variations in the PPI results per denture were translated into individual variations in their plaque accumulation pattern. However no differences were found among tooth type (e.g. canine, lateral, etc) in the dentures when the average PPI accumulated per tooth was analysed. This may indicate that in the dentures teeth in average tend to accumulate plaque homogenously according to their position in the denture arch. Reports available in the literature regarding to plaque accumulation on dentures are focused on plaque quantification on the fitting surface rather than in individual tooth surfaces with the fitting surface as the area with the highest percentage of plaque accumulation in comparison to those of the teeth (as a group) and palate (Keng and Lim, 1996, Coulthwaite and Verran, 2009). However, on dentures, when plaque quantification is focused on the teeth it only considers them as a group rather than as specific teeth as in the end dentures are all plastic. The calculation of the PPI per tooth in a denture takes into account the tooth size, giving a more precise estimation of the amount of plaque that a very specific site that the denture accumulates. This information may be used to determinate the amount of plaque that each tooth is contributing to the general dental plaque score and thus have a direct impact on the systemic health of the individual. Moreover, dental plaque accumulation on the teeth surfaces produces an unpleasant and unaesthetical

aspect therefore reporting plaque accumulation per tooth might help to indicate the places where more attention in the cleaning technique is required. Also, the results are expressed in a continuous scale and this enables a more precise method to measure the dental plaque removal capacities of the different commercially available cleaning products (e.g. chemical cleaners).

Finally, there were statistical differences in the tooth area (size) among teeth which is related to the individual variations in the anatomy and the size of the edentulous arch that requires different tooth sizes in each case. However, the teeth distribution in the dentures was symmetrical as no differences were found for the area (size) between teeth on either side of the denture.

6.3.4. Clinical Images

The methods used in this thesis to segment all images, including the ICT had several advantages, such as standardisation and light calibration of these images prior its analysis. Moreover, it was remarkable that no calibration of the examiner is required to quantify dental plaque with this technique. Moreover, both filters used (n-IR and NBI) are commercially available in photographic stores and can be applied to consumer goods. Additionally, ImageJ is an easy available open source programme and digital cameras are becoming a common and affordable technology due to the competitive market and the wide range of products now available.

The methods used in the analysis of the ICT were based on the segmentation of the DBB images where colour deconvolution was used. Improvements in the ICT methods were introduced and included the creation of unique subtractive colour vectors for the teeth, soft tissues and disclosed dental plaque. This approach provided more control over the segmentation procedures. The analysis of the ICT

images though colour deconvolution proved to be simple and quick to apply under variable conditions as the segmentation vectors can be modified according to the sample characteristics.

In image analysis, thresholding of an image is one of the most common processes and there is a variety of segmentation techniques and algorithms available. However, a single method that can be applied to all images all the time and in all situations does not exist (Fu and Mui, 1981, Young et al., 1998, Pham et al., 2000). The biggest difficulty in this study, when working with ICT, was segmenting the teeth into units. Other methods were tested before settling for the ABS snake as the final segmentation method. Thresholding of grey values used for the DBB (see section 6.1.4.2-b: part IV) together with skeletonisation of the image were tested, but neither method worked satisfactory for ICT. The ABS snake method is time consuming to use, but the author is confident that with increased interest on research focused on automated segmentation techniques and the rapid technological advances, this inconvenience will be reduced in the future.

In general, the methods to determine the tooth size (width) include the measurement of the crown's mesiodistal size in the arch measured on dental casts on either a digital image or manually. In the former the dental arch is digitalised while in the latter the measurements are done with the aid of a pair of Vernier callipers. These techniques are widely used in Orthodontics to diagnose malocclusions to detect discrepancies in the relationships between dental arch and teeth sizes. Studies have found a good correlation between the manual and the digital methods (Tomassetti et al., 2003, Paredes et al., 2006) although usually the inclusion criteria requires that

the arches present good alignment no considering the cases with dental anomalies in shape, attrition or gingival retraction.

In this study, the tooth area was measured from a digital image and no statistical differences were found in the teeth sizes between the right and left teeth per tooth or per gender. No studies with similar methodology were found in the literature therefore, the results from this study were compared against studies reporting the tooth size for the population. The general teeth sizes from this study presented smaller (up to 2mm) mesio-distal crown widths than the results from Schumacher et al. (1976) and Sterrett et al. (1999) studies. Moreover, the lack of statistical differences in the teeth sizes per gender from this work disagree with those from the literature where it is reported that men have larger teeth than women (Yap Potter, 1972, Arya et al., 1974, Hattab et al., 1996). These differences between the findings in this study and the reports in the literature may be attributed to distortion and magnification related to the visualisation of a 3D tooth in a 2D image (Botticelli et al., 2010) or to the fact that in this study, dental attrition and malocclusion were not considered exclusion criteria thus these factors together with tooth superimposion and consequent overlap in the images was not considered in the measurement of the final tooth dimension. These findings may lead to further research to investigate how well manual tooth dimension and computerised (digital pictures) measurements correlate.

6.3.5. Methods used to threshold dental plaque on clinical images

Two different approaches to extract dental plaque from the images were used: colour deconvolution and high pass filter with different algorithms (automated methods) to threshold dental plaque in each case. Both methods presented a high specificity

(mean 0.97±0.02 and 0.99±0.01) and a moderate sensitivity (mean 0.69±0.18 and 0.54±0.08) which means that both techniques identified correctly the non-plaque pixels but the identification of the plaque pixels was not as accurate. This may be related to the lack of sensitivity by the automated methods themselves or to discrepancies with the gold standard image traced by operator, without a way to know which the correct one was, reflecting in consequence the need to continue investigating for alternative methods to be used as gold standard where no human intervention is required.

When looking at the Euclidean distances to the ideal recorded by the two dental plaque thresholding approaches used (colour deconvolution or high pass filter), it is apparent that although differences were found between methods, the variations were more evident within individual images. Thresholding of image 25 showed the highest sensitivity and specificity (and the shortest distances to ideal) which may be explained by a thicker dental plaque distribution with better defined borders which may have facilitated its thresholding by both the operator and the machine (Figure 88). However only three images were used for the comparisons, therefore this might be investigated in the future using a larger sample. For the images analysed in this study, colour deconvolution with any of the three thresholding methods: MaxEntropy, RenyiEntropy or Yen showed the best results.
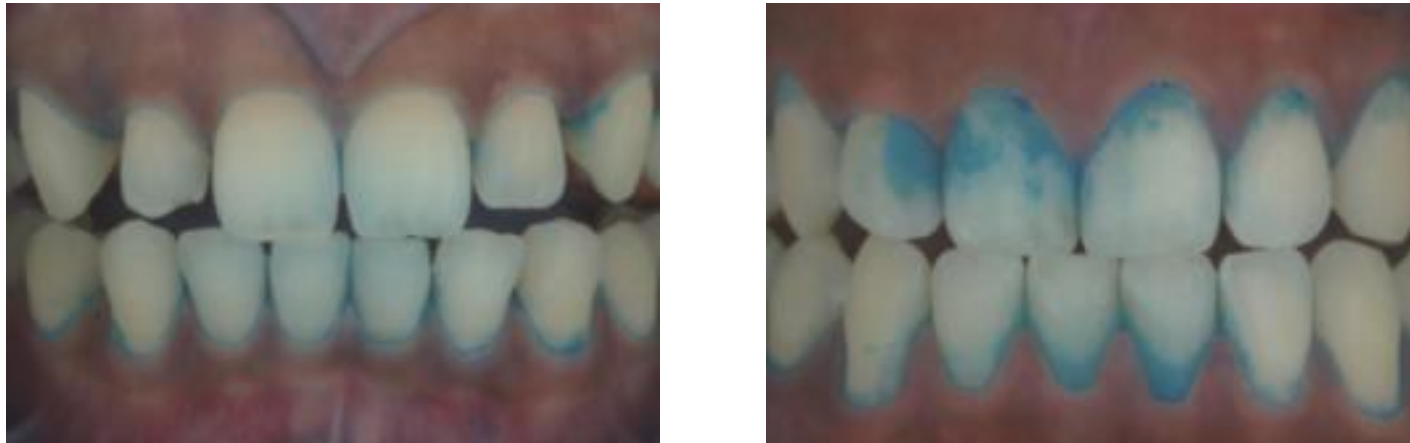
Figure 88 Two of the ICT used to compare between dental plaque segmentation methods. Notice that the image on

the right presented high amounts of dental plaque with well defined borders.

6.3.6. Intra-observer reliability of determination of dental plaque

Hand labelling of dental plaque was time consuming and susceptible to variations introduced by the operator possibly related to inaccuracies in the criteria used to define which plaque was and which was not. This may affect the final results however; hand outlining was used as the gold standard because no other method was available to do the comparisons with automated segmentation. In this study, the coefficient of variation for the intra-examiner reliability was 3.55%. This represents a high reliability with the measurements close to each other and suggests that hand outlining could be used as a gold standard in this study.

6.3.7. Comparison between automated and manual methods of dental plaque segmentation

It can be highlighted that the manual and automated methods are naturally not the same, because the manual ones are not likely to report each time the same score and precaution must be exercised as these methods are prone to the introduction of errors from the operator when outlining the images. However it was required to evaluate the agreement between methods. Moreover, because we are dealing with dental plaque accumulation, these results cannot be used to generalise which method is better than the other because each set of images is unique and might require a different segmentation method. Therefore it must be kept in mind that these results are only applicable to these particular images in this particular case. Further research is needed to develop more suitable methods to do the comparisons.

In this study the comparison between methods was done using the Bland-Altman test and a paired samples t-test instead of using correlation, this in concordance with the ideology from Bland-Altman (1983) who stated that correlation only measures the

relation between methods and not their agreement. A perfect agreement is only attained when all the points lie along the correlation line whilst a perfect correlation is achieved if the same points lie along **any** straight line.

When assessing agreement with the Bland-Altman test is expected that 95% of the differences between the variables tested (if normally distributed) will be within the limits of agreement which agrees with the findings of this study where only one point (6.7%) out of fifteen was outside the limits. Additionally, these results show that dental plaque area registered with any of the methods could lie within $116mm^2$ and $84mm^2$ and still be an acceptable agreement; however wide limits of agreement may be related to one (or both) methods having a poor precision. Observing the image that caused the outliner revealed that the disclosed dental plaque did not have well defined borders, with a very faint disclosure pattern. This may have provoked the differences between the operator labelling it as dental plaque (examiner error) or the machine which did not (Figure 89) and it is quite difficult to decide who was right. Finally, the statistical paired t-test did not show differences between methods which is consistent with the finding of the Bland-Altman plot however, the sample size is very small (n=15) and therefore might not have enough power to show any difference.

Figure 89 Differences in dental plaque segmentation between the manual (left) and automated (right) methods with the correspondent original image. It can also be seen that the dye when used in dentures gets inside the repairs.

6.3.8. Distortion in the anterior region

Image distortion has been associated with the transitional changes that occur when a 3D structure is represented in a 2D image and are reflected as variations in the magnification factor and superimposition of the structures (Quintero et al., 1999, Ladeira et al., 2010, Sakai, 2011). In a frontal image of the dental arches, the distortion due to the projection is larger for the canines due to their shape and position in the dental arch. Furthermore a frontal photograph conceals the distal surface of these teeth and most likely results in underestimation of plaque accumulation in these areas (Söder et al., 2003). Visualisation of the vestibular surfaces of the posterior teeth is even more complicated to visualise due to a gradual increase of the curvature along the arch.

6.3.9. Analysis of the differences in plaque accumulation

The segmentation methods presented in this study allowed the presentation of the results per tooth. Disclosed dental plaque is presented in a quantitative scale according to the number of pixels. These values are then transformed into area giving the final results although other measurements such as the area with plaque (not included), can be automatically calculated afterwards. Moreover, according to the literature there are more than 10^6 bacteria per mm^2 (Weiger et al., 1992, cited in Netuschil et al., 1995) in dental plaque, so if dental plaque extension is expressed in area mm^2 the amount of bacteria can be computed although this calculation is based only in two-dimensions. A limitation of quantifying dental plaque using conventional imaging techniques is that the computation of plaque thickness is not possible; therefore if dental plaque depth

quantification is desired, a more complex 3D technology (still under development) is required.

Although there are a few studies that report image analysis of dental plaque, the results from these studies were more focused on the reliability of the techniques (Söder et al., 1993, Smith et al., 2001) Only one study was found in the literature where the PPI per tooth was reported (Söder et al., 2003); although the images in this study were obtained through the digitalisation of pictures taken with a SLR camera.

The results from this study show individual differences in the mean PPI within subjects which agrees with the results from Söder et al. (2003). These variations are related to individual factors such as personal hygiene habits (e.g. toothbrushing frequency and smoking) and specific oral conditions that may favour plaque retention and in consequence accumulation (e.g. overhanging restorations). However no differences were noted in the PPI per tooth between genders. This disagrees with the findings from Shiau and Reynolds (2010) who stated that dental hygiene was poorer in males (who are also a higher risk of developing periodontal disease) than in females, which may be related to the fact that the sample in this study was not representative of the population as involved only dental students. In this study, although no differences were found between the mean general PPI for the upper teeth vs. the lower teeth; seven patients (28%) presented statistical differences when the mean PPI was compared within patients. These results agree with the results from Söder et al. (1993) but disagree with Furuichi et al. (1992), and Lilienthal et al. (2004) who found a higher accumulation of dental plaque in the mandibular teeth than in the maxillary ones. These differences may be associated with an independent more homogenous dental plaque distribution

between dental arches, to individual variations in the subjects representing the samples or to differences in the personal oral hygiene habits. These questions could not be answered in this study because the sample was not random an involved only dental students who may be more careful about their oral hygiene moreover it was by request that the volunteers suspended their oral hygiene for 48 hrs in order to accumulate dental plaque. Finally, the observation that dental plaque was equally distributed between left and right sides of the dental arch agrees with the results from Söder et al. (1993). No differences were found either between left and right plaque accumulation per tooth which may be related with the right-handedness of all the volunteers in the study.

6.4. Conclusions

A standardised method for dental plaque quantification with minimal human intervention has been presented. This work presents the basis for automated dental quantification describing each of the steps in the procedure, from image acquisition to interpretation of the results. Two different filters were introduced to aid in the analysis. Different segmentation methods in digital intraoral images and complete upper dentures are discussed with further analysis on their advantages and disadvantages in addition to the methods used to test their affectivity. Results from this study show that the methods used to analysis the images and to quantify dental plaque were easy to use, reliable, presented on a continuous scale and eliminated the dependence on the examiner to code dental plaque. Although still minor human interventions were required, with the rapid technological advances, fully automation is almost a reality.

Chapter 7
Reliability assessment of a dental plaque index

7.1. Introduction

Since plaque scoring was first introduced in the nineteen fifties (Ramfjord, 1956) most indices are based on operator observation and subsequent scoring. An examiner codes the numerical scores following their judgement on the area of the coronal part of the tooth covered by plaque. However, this approach introduces elements of subjectivity in the recording process. The variability of the results becomes more apparent when a number of examiners record the information, and even fully trained examiners may bring in an element of subjectivity. Therefore standardisation and evaluation of the reliability of scoring these clinical indices is required. The Quigley and Hein index modified by Turesky-QHT (Turesky et al., 1970) together with the Plaque Index of Silness and Löe, are the two indices recommended by the Council on Dental Therapeutics (1985) as methods to evaluate and measure the effectiveness of the chemotherapeutic products for the control of supragingival plaque and gingivitis. In this context image analysis based on photographs, drawings, charts or digital systems has been used to test the reliability of the methods used to quantify dental plaque (Ambjørnsen et al., 1984, Nordstrom et al., 1988, McCabe et al., 1996, Shaloub and Addy, 2000, Paranhos and Silva, 2004, Pretty et al., 2005, Kelly et al., 2008, Raggio et al., 2010).

The aim of this chapter was to assess the intra and inter-examiner reliability when the QHT index is used to score supragingival dental plaque on digital images.

7.2. Material and Methods

Three sets of digital images with plaque accumulation described earlier (60 images of complete upper dentures taken against a white background (DWB), 16 images of dentures taken against a black background (DBB) and 25 intraoral frontal-view clinical images (ICT) were used to assess the intra and inter-examiner reliability of the QHT index. Five pairs of the images of dentures were identical with only a variation in the background colour (either black or white). These images were allocated by their colour with the rest of the images without informing the volunteers of their presence.

The labial surfaces of the 6 anterior teeth (maxillary right to left canines) from the images of the CDs (both DWB and DBB) and the labial surfaces of the12 anterior teeth (maxillary and mandibular right to left canines) for the ICT were coded from 0 to 5 according to the QHT index. Three images (DWB -image 18: URC, ULL, and ULC and image 43: ULL and DBB-image 1: URC) had missing teeth (n=6) which were omitted from the statistical analysis.

The images for the dentures were assessed by 15 examiners divided into 10 qualified dentists (**QD**) and 5 final year dental students (**FYS**) whilst the ICT were assessed only by 14 examiners because one of the QD left work at the hospital by the time the scoring took place.

7.2.1. Images examination

The images were shown using numbered slides on a portable computer (Dell Inc, USA) with arrows indicating the position of the canines for easier identification on the image (examples are shown in Figures 90-92). Evaluation sheets with the teeth code and

image numbers (Table 30) were completed by the examiners. They were allowed to undertake the scoring in their own time but underwent no training or calibration prior to the start of the scoring session. The duration of the examination (in minutes) was recorded and used as a reference. At the start of the examination the coding of the QHT index was explained to the participants and each person had a reference diagram to refer to during the scoring process. No further instructions were given once the examination commenced. Both the DWB and the DBB images were scored together in one session and the ICT were assessed in an independent session to avoid bias related to the lapse of concentration because of the large amount of images (n=101). The scoring of the same set of images was performed twice with an interval of a week between scorings. All the procedures were supervised by the same investigator (the author).

7.2.2. Data analysis

The scores obtained from the examination were analysed with IBM SPSS "v.19.0". (IBM, NY, USA). Both the intra and inter-examiner reliability were determined with a Cohen's kappa (k) test (Cohen, 1960) statistic. The final kappa value was expressed in terms of the generalised kappa (Jackson, 1983) which was the result of averaging the examiners responses for each set of images (DWB, DBB and ICT). The kappa results were also expressed in groups according to the evaluation (1st and 2nd) and according to the examiners (all, QD and FYS).

Shannon's entropy (Shannon, 1948) was used to evaluate the degree of uncertainty in the scoring results using the formula:

$$H = -\sum p \log_2(p) \qquad\qquad \text{[Eq. 6.1]}$$

where,

H= is the entropy,

p= is the probability (p_i...p_n) of a score being recorded for a particular tooth. It

represents the total observations per code divided by the sum of all the codes.

Entropy here is considered to estimate the uncertainty (measured in bits) in the scoring.

It ranges from 0 (in the case where all the scorings agree) to a maximum of $\log_2(n)$

where n=6 (since there are 6 possible classes of scores) which is achieved in the case

that any score is equally likely. In summary, the larger the entropy the higher the

uncertainty (disorder, disagreement), regardless of whether the responses are correct or

not, or close to each other.

The responses were grouped into a) all examiners (AE), b) QD and c) FYS for the 1st

and 2nd evaluation. Both the tooth and the denture (image for the ICT) were used as

units. The values per denture/image represented the average uncertainty and were the

result of averaging the entropies for each tooth in the image (6 in the dentures and 12 in

the images from the CT). Descriptive statistics were performed, frequencies histograms

were plotted, and the normality of the scores was evaluated using the Kolmogorov-

Smirnov goodness of fit test (n>50) and the Shapiro-Wilk test (n<50) with a probability of

p > 0.05 (no difference).

Scatter graphs were used to compare the entropies for the QHT index scoring per tooth

and per denture between sets of images (AE, the QD and FYS) for the 1st and 2nd

evaluation. The comparisons were made a) per evaluation (1st and 2nd), b) per group

(QD against FYS) and c) per background colour (DWB against DBB) for the DWB and the DBB. Extra comparisons per background colour were made between evaluations (1st and 2nd) and between groups (QD and FYS) per denture and per tooth for the five identical pairs of images. These comparisons were performed with a paired t-test or an independent t-test when the distribution was normal (parametric) and the Wilcoxon signed-rank test (Wilcoxon, 1945) or the Mann-Whitney U test (Mann and Whitney, 1947) when the distribution was not so (non parametric). The comparisons made per groups are summarised in Figure 93 whilst Figure 94 shows the statistical analysis used in each case.

7.3. Results

The average evaluation time for the dentures (n=76) was 24.2, S.D.6 min. (1st evaluation) and 16.3, S.D.5 min (2nd evaluation) whilst for the ICT (n=25) it was 12.3, S.D.3.7 min (1st evaluation) and 13.4, S.D.4 min (2nd evaluation).

7.3.1. Cohen's Kappa

The magnitude values of kappa (proposed by Altman, 1991) for the generalised intra and inter-examiner reliability ranged between fair and moderate (Table 31) with similar kappa values among sets of images (all, DBW, DBB and ICT) and groups (QD and FYS). Overall, the intra-examiner agreement was higher (DWB, DBB, and ICT) than the inter-examiner agreement. Between sets of images, the DWB for all the examiners had the highest inter-examiner agreement (0.42, S.D. 0.05 versus DBB-0.33, S.D.0.09 and ICT-0.36, S.D.0.97) whilst the intra-examiner reliability presented a moderate agreement (*k* ranging from 0.52, S.D.0.15 to 0.54, S.D.0.07) in all three sets of images.
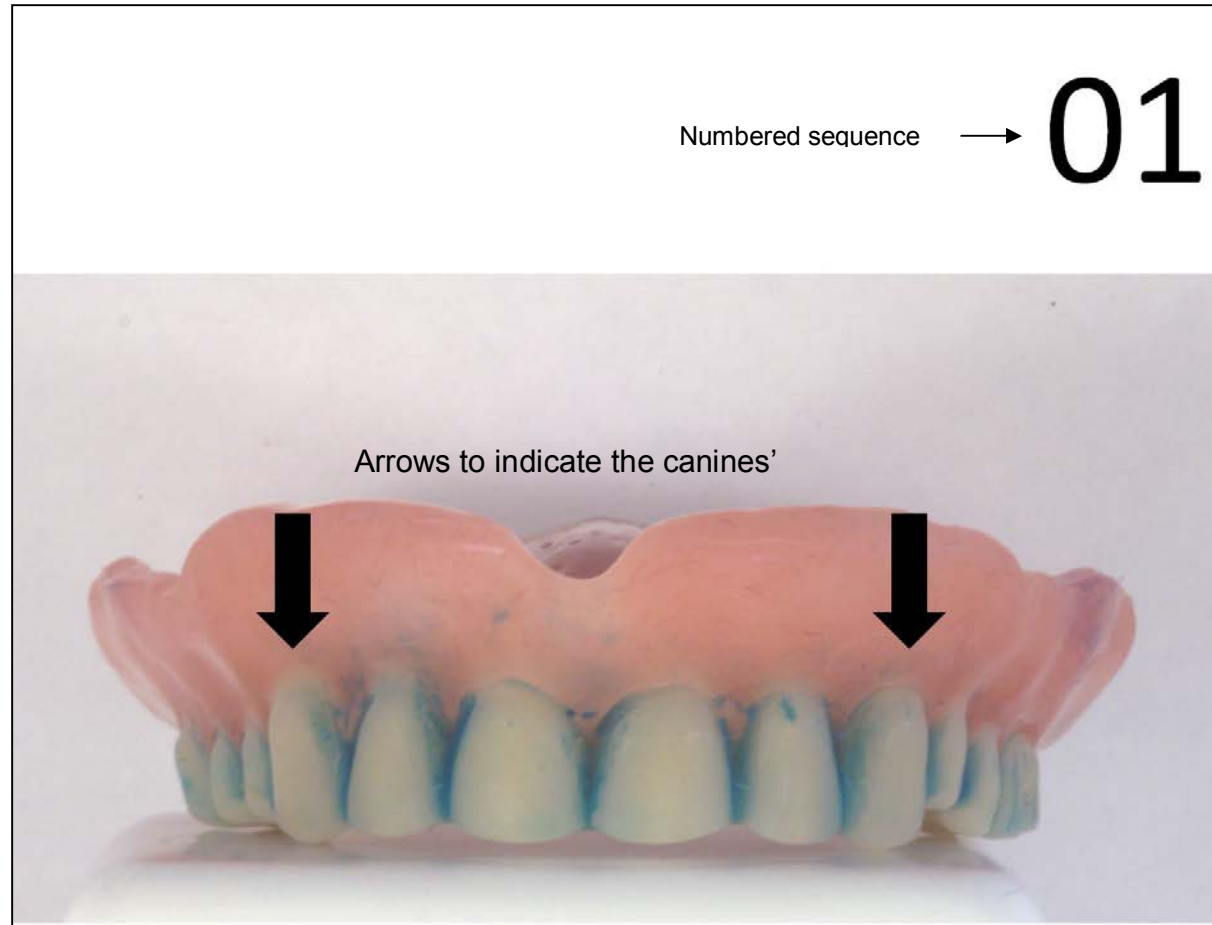
Figure 90 Upper complete denture on a white background inserted in a numbered slides presentation for the scoring of dental plaque.
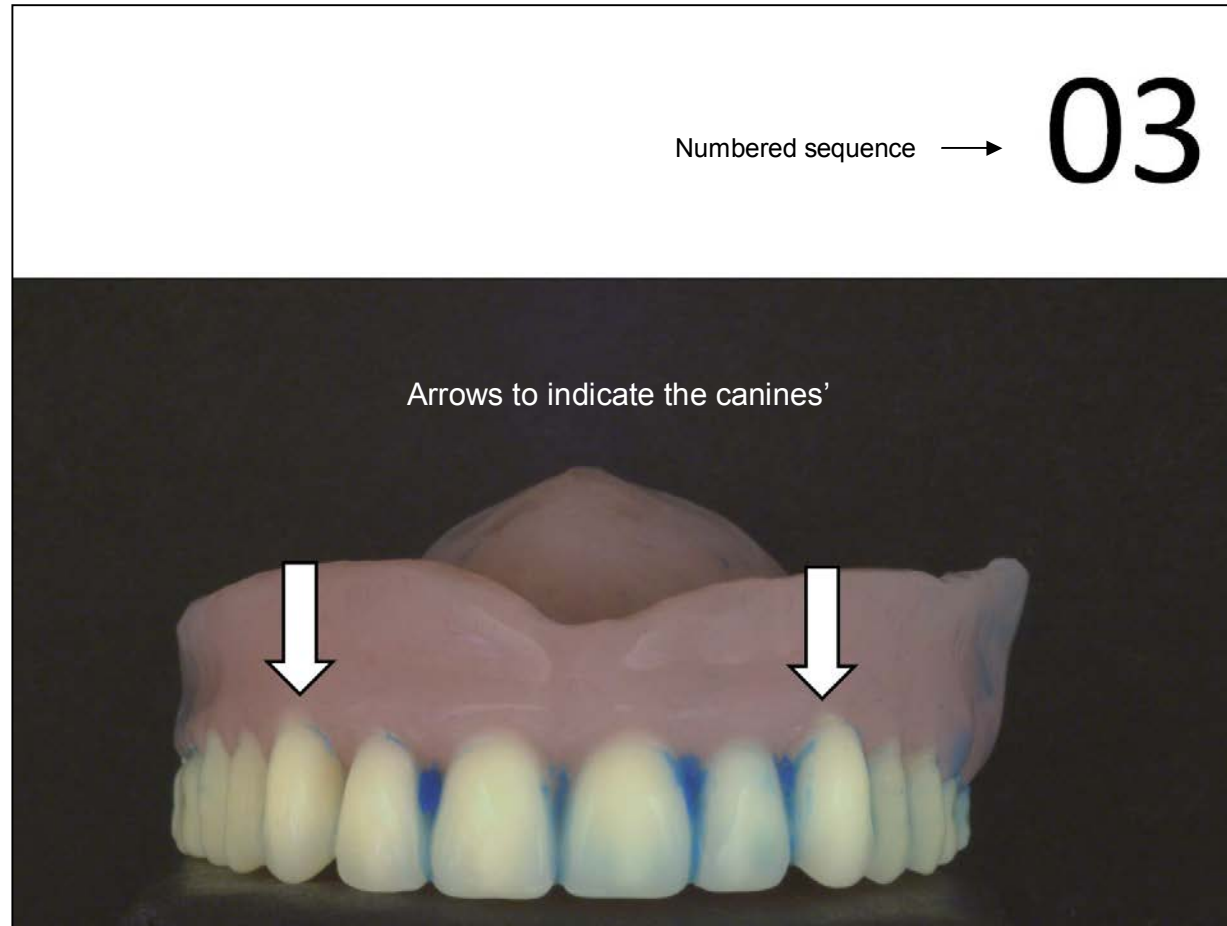
Figure 91 Upper complete denture on a black background inserted in a numbered slides presentation for the scoring of dental plaque.
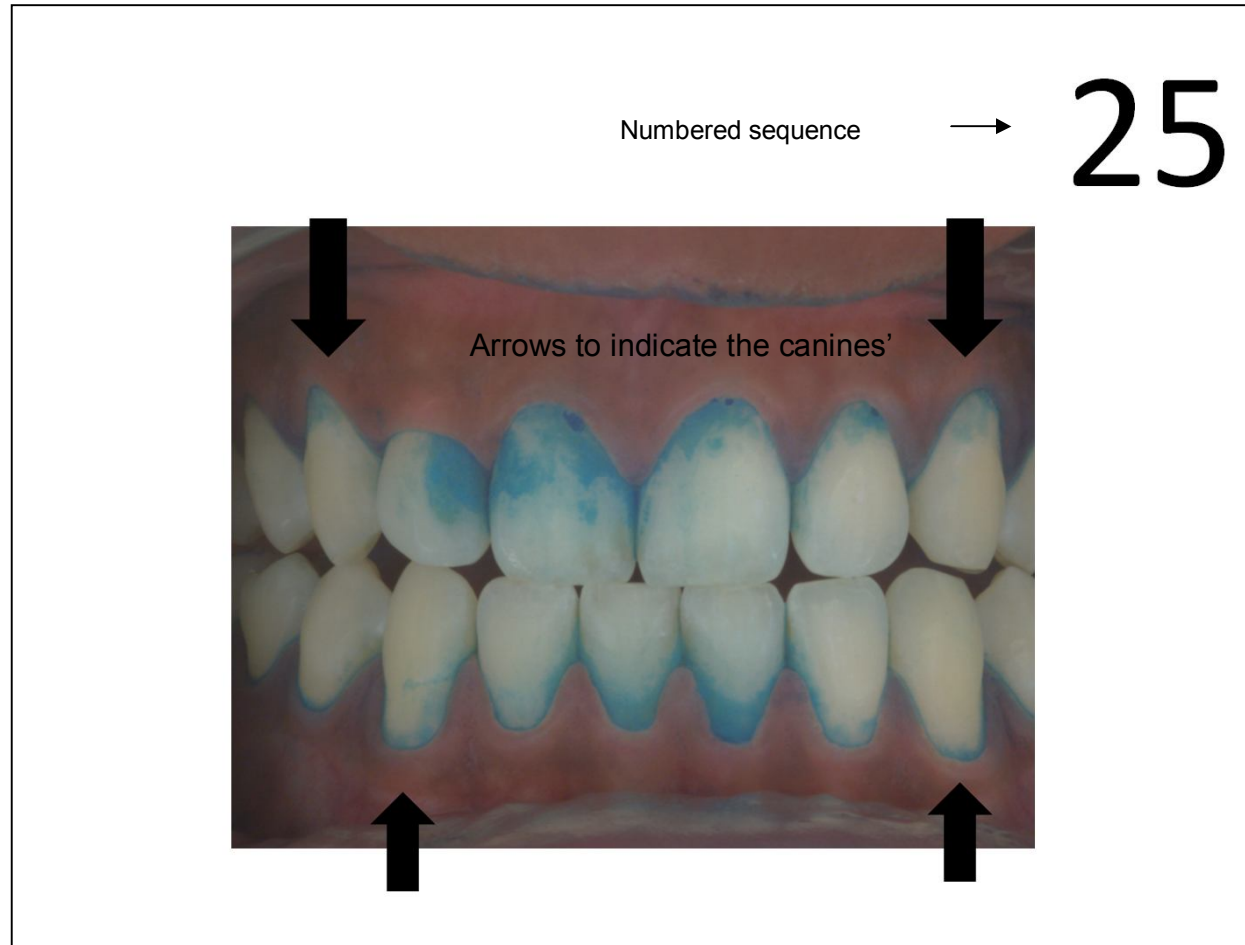
Figure 92 Intraoral image (from patients) inserted in a numbered slides presentation for the scoring of dental plaque.

Table 30 Questionnaire format used to code dental plaque. The same format was
repeated for the rest of the images. The schematisation of the code was
used as a reference.

ID: Time:

Date:
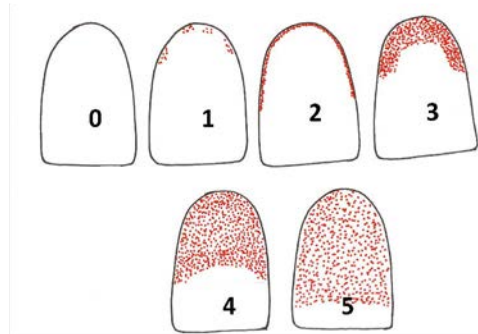
IMAGE 1					
Upper right canine	Upper right lateral	Upper right central	Upper left central	Upper left lateral	Upper left canine
Lower right canine	Lower right lateral	Lower right central	Lower left central	Lower left lateral	Lower left canine
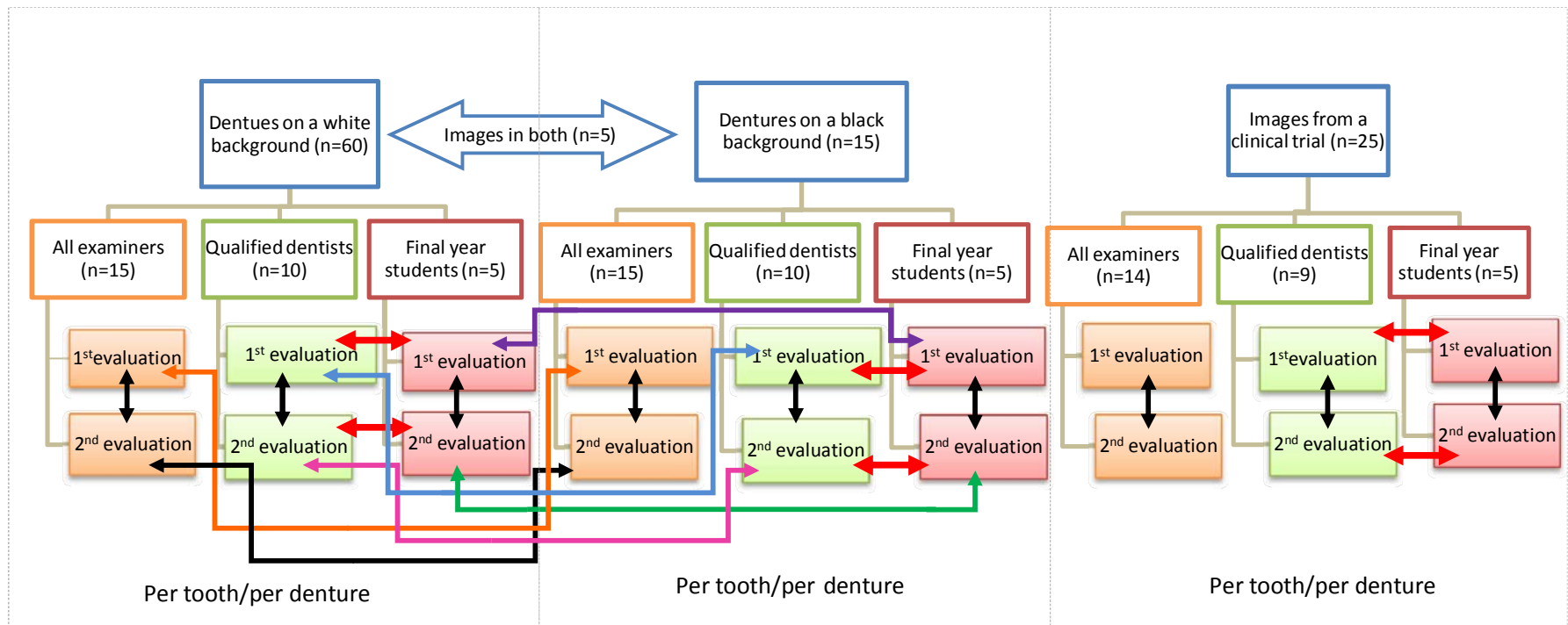
Figure 93 Diagram showing the combinations made for the comparisons between sets of images: DB, DBB and ICT, groups: QD, FYS, and 1st and 2nd evaluations.
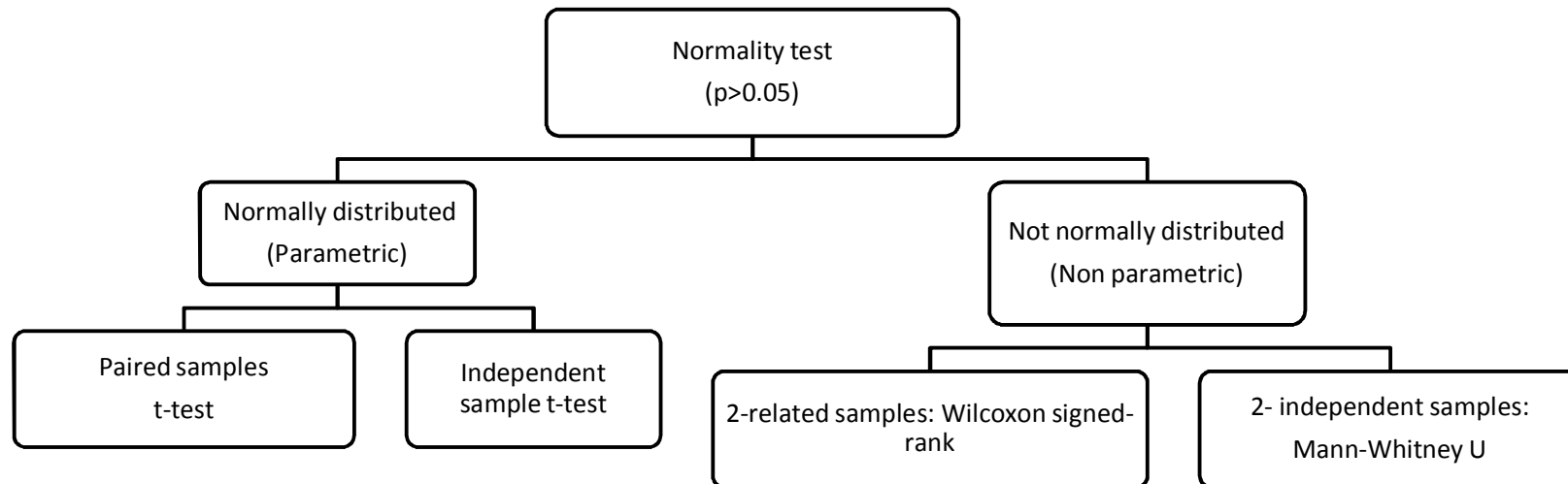
Figure 94 Statistical tests applied to the results of the Shannon's entropy per tooth and per denture depending on the

normality of the sample.

Table 31 Generalised Cohen's kappa for the intra-examiner and inter-examiner agreement dividing the sample into all examiners, qualified dentists and final year students when assessing the DWB, DBB and ICT images.

Images	Examiners	Inter-examiner	S.D	Intra-examiner	S.D.
Dentures on white background	All examiners (n=15)	0.42	0.05	0.54	0.07
	Students (n=5)	0.41	0.05	0.55	0.09
	Qualified dentists (n=10)	0.41	0.05	0.54	0.06
Dentures on black background	All examiners (n=15)	0.33	0.09	0.52	0.15
	Students (n=5)	0.37	0.08	0.53	0.16
	Qualified dentists (n=10)	0.33	0.09	0.52	0.16
Teeth from a clinical trial	All examiners (n=14)	0.36	0.10	0.53	0.10
	Students(n=5)	0.41	0.08	0.49	0.08
	Qualified dentists (n=9)	0.33	0.10	0.55	0.11

Values of kappa (Altman, 1991):<0.20 Poor, 0.21-0.40 Fair, 0.41-0.60 Moderate, 0.61-0.80 Good, 0.81-1.00 Very good

When comparing the QD versus FYS, the latter had a higher inter-examiner agreement for the DBB (k=0.37, S.D.0.08) and the ICT (k=0.41, S.D.0.08). For the intra-examiner agreement the differences were less pronounced with the QD performed better only in the assessment of the ICT (k=0.55, S.D.0.11 vs. 0.49, S.D.0.10). The individual inter and intra-examiner kappa values for the DWB, DBB and ICT are shown in Table 32 to 34.

7.3.2. Coding differences

Figure 95 shows an example of the degree of variation in the percentages of the reported codes given by all the examiners between the 1st and 2nd evaluation of four DWB. Code 1 (Separate flecks of plaque at the cervical margin) and 2 (a thin continuous band of plaque-up to 1 mm- at the cervical margin) showed the highest percentages per tooth in both the denture images: DWB (Figure 96) and DBB (Figure 97) whilst codes 2 and 3 (band of plaque wider than 1mm but covering less than one third or the crown) had the highest percentage for the ICT (Figure 98).

7.3.3. Shannon's entropy

The frequencies histograms for the Shannon's entropy per denture for all the examiners, 1st and 2nd evaluation, of the images from the three groups are shown in Figure 99. Individual histograms for the QD and FYS for the 1st and 2nd evaluation of the DWB (Figure 100) DBB (Figure 101) and ICT (Figure 102) are also shown. Tables 35 to 37 show the mean, standard deviation and the results from the normality test (per denture as well as per tooth) of the Shannon's entropy of all the images grouped as a) AE, b) QD and c) FYS for both evaluations. These show that the data "per denture" for all groups in the three sets of images (DWB, DBB and ICT) with exception of the FYS 2nd DWB evaluation were normally distributed whilst none

of the groups "per tooth" with exception of the 2nd evaluation for AE of the DBB had a normal distribution ($p>0.05$). Table 38 shows the descriptive statistics and the results from the normality test for the five paired images (same image on both white and black background). The summary of the statistical methods used for the images according to the results of the normality test per groups and per sample is presented in Figure 103.

The scatter graphs show the entropies of the QHT index scoring for AE comparing the 1st evaluation against the 2nd evaluation per denture and per tooth for the DWB (Figure 104), the DBB (Figure 105) and ICT (Figure 106). Scatter graphs comparing the entropies of QD against FYS for the 1st and 2nd evaluation per tooth and per denture for DWB (Figure 107), DBB (Figure 108) and ICT (Figure 109) are presented. Further comparisons between evaluations (1st vs. 2nd) for the QD and the FYS for DWB (Figure 110), DBB (Figure 111) and ICT (Figure 112) are also shown.

The results from the parametric and non parametric tests used to compare between groups per tooth and per denture are presented on Table 39 (DWB), Table 40 (DBB) and Table 41 (ICT). The results for the comparisons (per denture and per tooth) between backgrounds, for the DWB and DBB, from a) different samples (Table 42) and b) five identical images (Table 43) are presented.

Table 32 Individual Cohen's Kappa results from the intra-examiner (in bold) and inter-examiner agreement for AE when assessing the DWB. The underlined numbers show the qualified dentists.

		1	2	3	4	5	6	7	8	9	10	11	12	13	14	15
	1	*0.56*	0.38	0.39	0.36	0.41	0.47	0.37	0.35	0.36	0.44	0.30	0.38	0.48	0.34	0.45
	2		*0.55*	0.39	0.36	0.47	0.48	0.45	0.35	0.41	0.48	0.41	0.46	0.46	0.32	0.46
	3			*0.52*	0.46	0.34	0.44	0.40	0.42	0.35	0.42	0.40	0.39	0.44	0.37	0.44
	4				*0.57*	0.33	0.44	0.36	0.46	0.45	0.46	0.45	0.44	0.45	0.47	0.42
	5					*0.56*	0.50	0.40	0.37	0.47	0.44	0.34	0.46	0.44	0.31	0.44
Examiner	6						*0.71*	0.47	0.46	0.50	0.48	0.37	0.43	0.48	0.36	0.42
	7							*0.50*	0.38	0.47	0.40	0.43	0.43	0.45	0.40	0.45
	8								*0.50*	0.43	0.38	0.33	0.35	0.42	0.41	0.34
	9									*0.57*	0.45	0.36	0.44	0.47	0.37	0.41
	10										*0.51*	0.42	0.40	0.48	0.40	0.42
	11											*0.53*	0.35	0.40	0.41	0.42
	12												*0.39*	0.45	0.36	0.45
	13													*0.60*	0.39	0.50
	14														*0.48*	0.42
	15															*0.58*

(Examiner — column header spanning columns 1–15)

Values of kappa (Altman, 1991):<0.20 Poor, 0.21-0.40 Fair, 0.41-0.60 Moderate, 0.61-0.80 Good, 0.81-1.00 Very good

Table 33 Individual Cohen's Kappa results from the intra-examiner (in bold) and inter-examiner agreement for AE when assessing the DBB. The underlined numbers show the qualified dentists.

	Examiner														
Examiner	1	2	3	4	5	6	7	8	9	10	11	12	13	14	15
1	*0.78*	0.30	0.32	0.38	0.45	0.55	0.33	0.34	0.34	0.25	0.19	0.31	0.49	0.34	0.45
2		*0.43*	0.33	0.34	0.34	0.45	0.38	0.26	0.32	0.32	0.20	0.45	0.34	0.23	0.29
3			*0.62*	0.39	0.33	0.48	0.36	0.25	0.30	0.38	0.29	0.34	0.41	0.38	0.35
4				*0.36*	0.20	0.25	0.15	0.42	0.37	0.33	0.23	0.30	0.41	0.32	0.39
5					*0.63*	0.57	0.32	0.35	0.33	0.43	0.19	0.36	0.47	0.22	0.34
6						*0.78*	0.46	0.42	0.45	0.43	0.28	0.37	0.60	0.38	0.478
7							*0.45*	0.24	0.31	0.34	0.27	0.35	0.38	0.28	0.42
8								*0.43*	0.38	0.31	0.17	0.21	0.38	0.26	0.30
9									*0.53*	0.27	0.15	0.27	0.38	0.24	0.28
10										*0.42*	0.22	0.28	0.41	0.22	0.34
11											*0.26*	0.36	0.24	0.17	0.33
12												*0.58*	0.33	0.23	0.25
13													*0.70*	0.33	0.50
14														*0.40*	0.37
15															*0.49*

Values of kappa (Altman, 1991) :<0.20 Poor, 0.21-0.40 Fair, 0.41-0.60 Moderate, 0.61-0.80 Good, 0.81-1.00 Very good

Table 34 Individual Cohen's Kappa results from the intra-examiner (in bold) and inter-examiner agreement for AE when assessing the ITC. The underlined numbers show the qualified dentists.

	Examiner													
Examiner	1	2	3	4	5	6	7	8	9	10	11	12	13	14
1	*0.65*	0.47	0.34	0.40	0.39	0.26	0.35	0.28	0.45	0.26	0.25	0.27	0.28	0.35
2		*0.61*	0.47	0.42	0.31	0.30	0.42	0.31	0.42	0.32	0.20	0.32	0.41	0.38
3			*0.50*	0.52	0.41	0.38	0.49	0.34	0.48	0.35	0.21	0.36	0.40	0.47
4				*0.70*	0.51	0.38	0.52	0.26	0.55	0.43	0.12	0.48	0.42	0.50
5					*0.51*	0.35	0.41	0.30	0.46	0.34	0.19	0.37	0.23	0.43
6						*0.46*	0.41	0.29	0.47	0.35	0.25	0.31	0.35	0.42
7							*0.55*	0.36	0.51	0.40	0.23	0.46	0.42	0.49
8								*0.36*	0.40	0.26	0.28	0.28	0.28	0.29
9									*0.56*	0.35	0.28	0.35	0.33	0.45
10										*0.52*	0.13	0.37	0.33	0.42
11											*0.53*	0.17	0.13	0.17
12												*0.33*	0.34	0.38
13													*0.54*	0.38
14														*0.59*

Values of kappa (Altman, 1991): <0.20 Poor, 0.21-0.40 Fair, 0.41-0.60 Moderate, 0.61-0.80 Good, 0.81-1.00 Very good
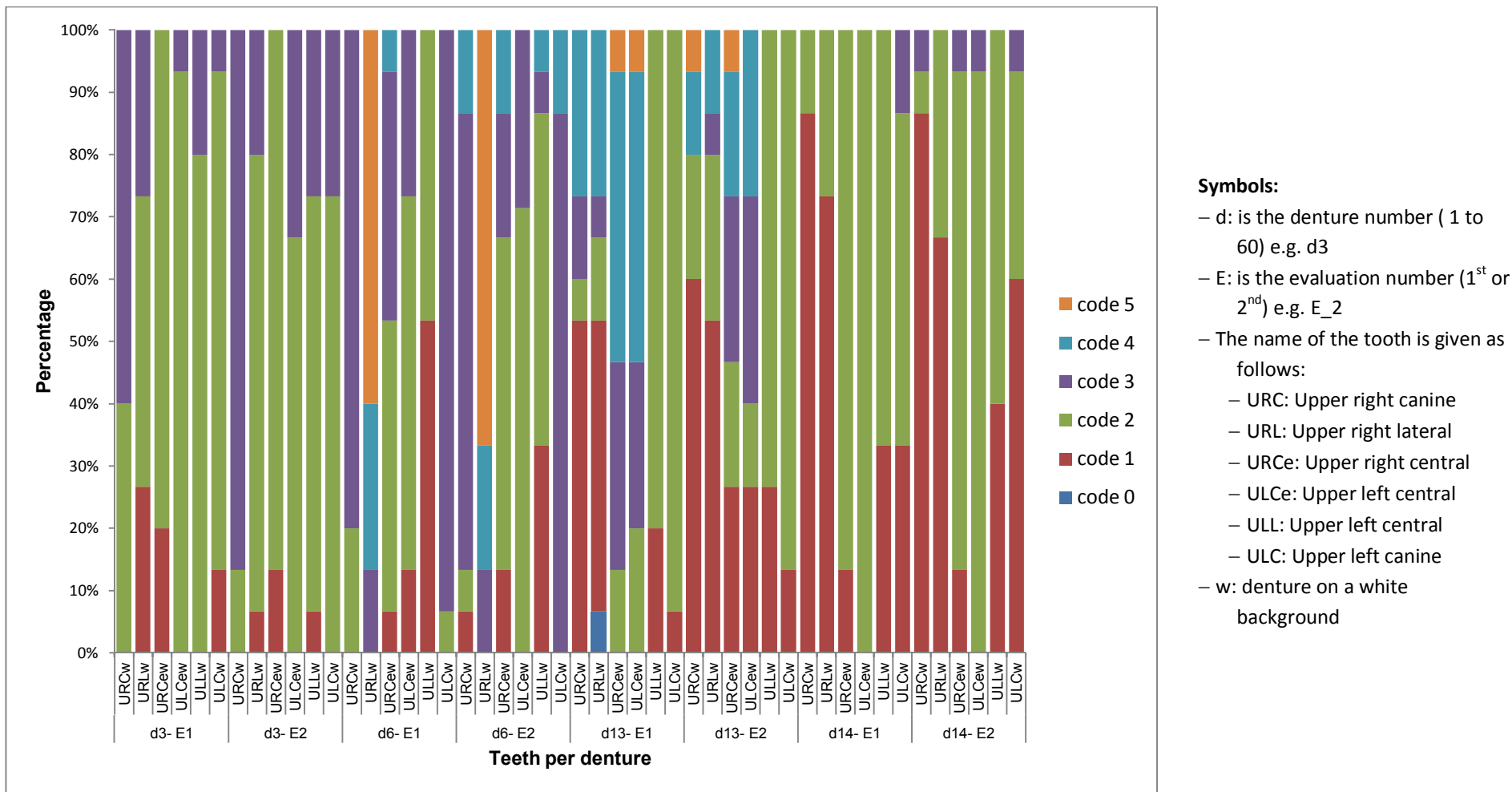
Figure 95 Example of the variations when recording the percentages per tooth for AE (n=15), in four DWB dentures, 1st and 2nd evaluation (one week later).
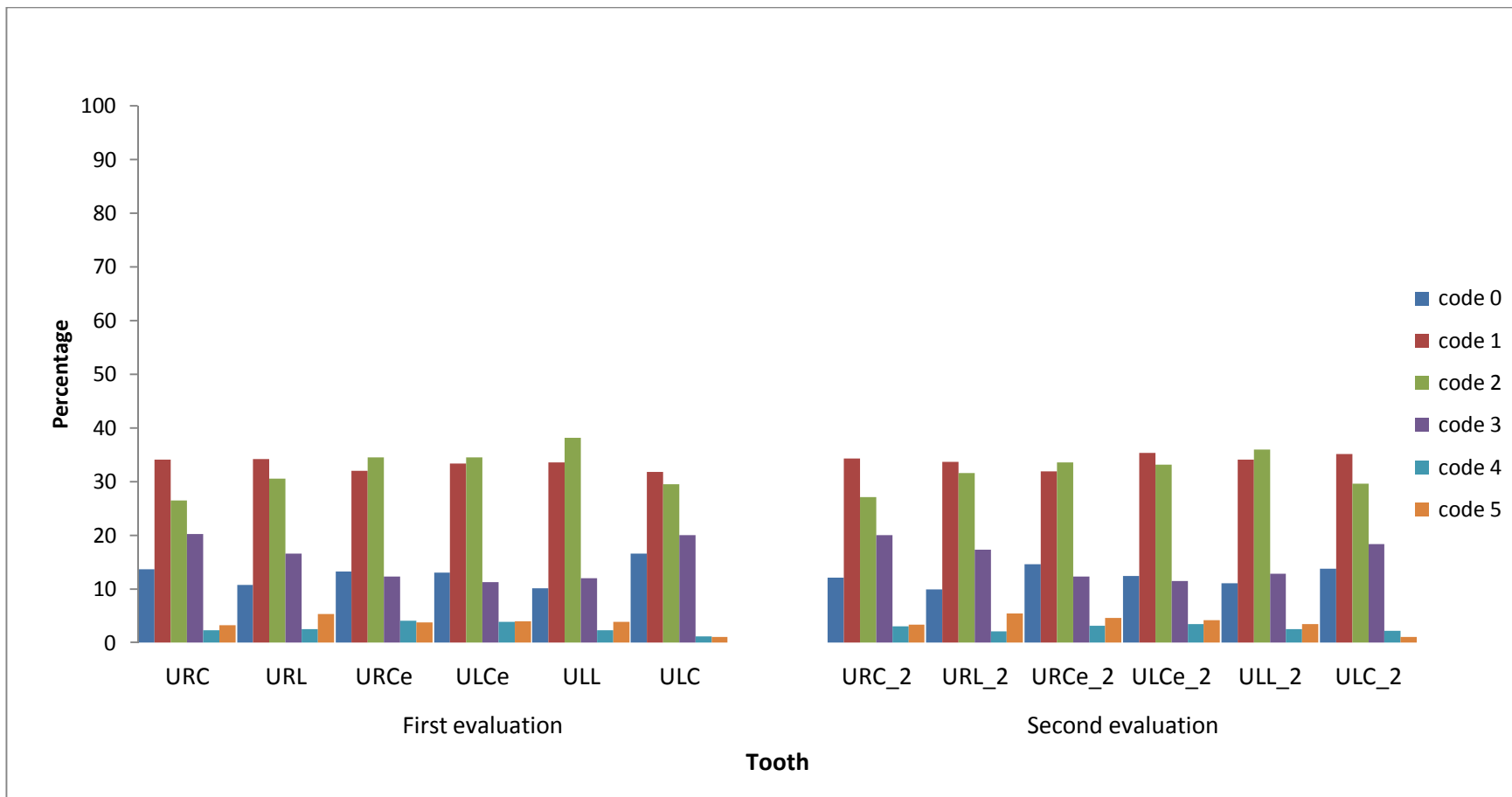
Figure 96 Percentage per code per tooth for the 1st (left) and 2nd (right) evaluation of images of DWB. All examiners (n=15).
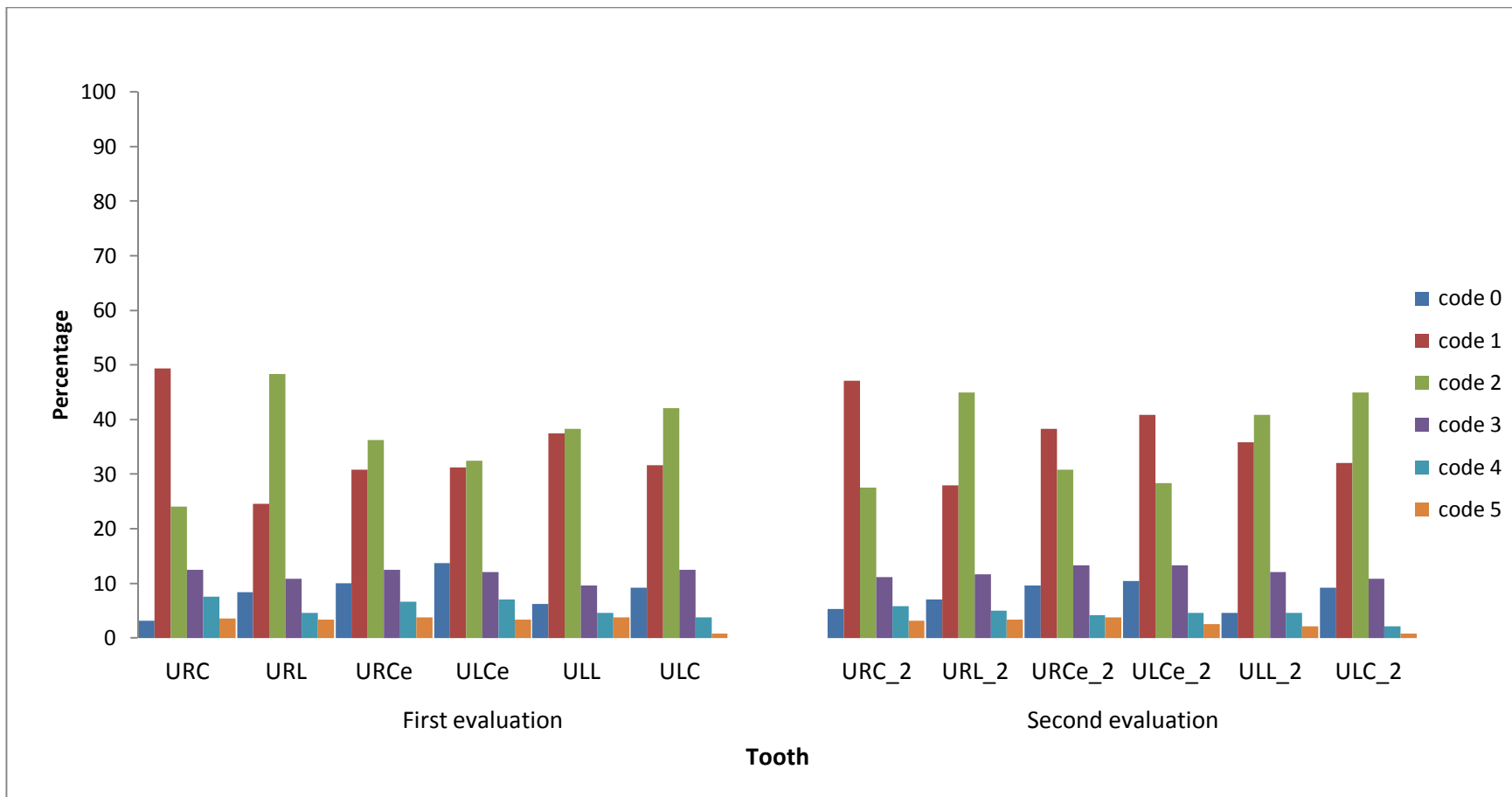
Figure 97 Percentage per code per tooth for the 1st (left) and 2nd (right) evaluation of images of DBB. All examiners (n=15).
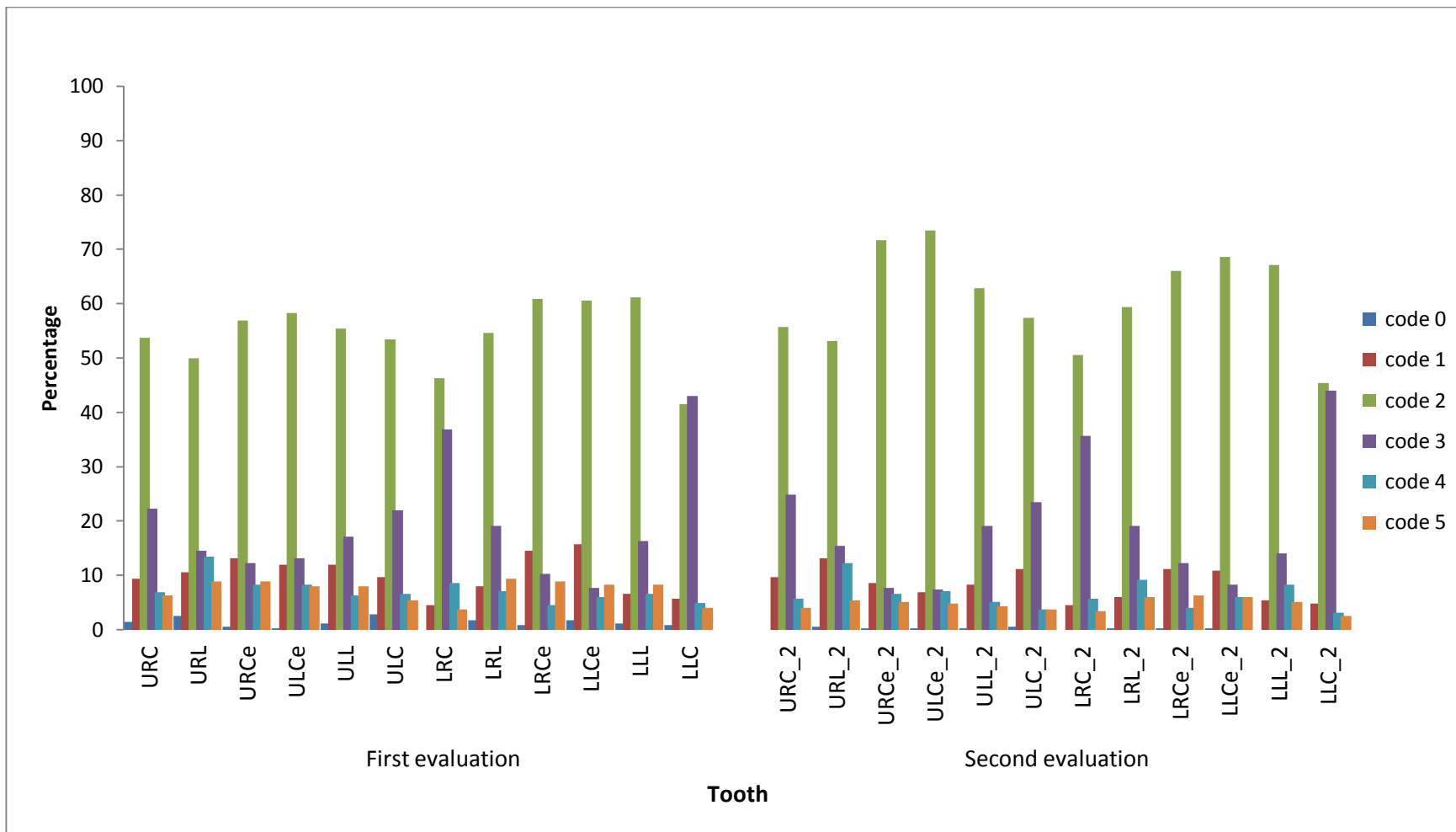
Figure 98 Percentage per code per tooth for the 1st (left) and 2nd (right) evaluation of ICT. All examiners (n=14).
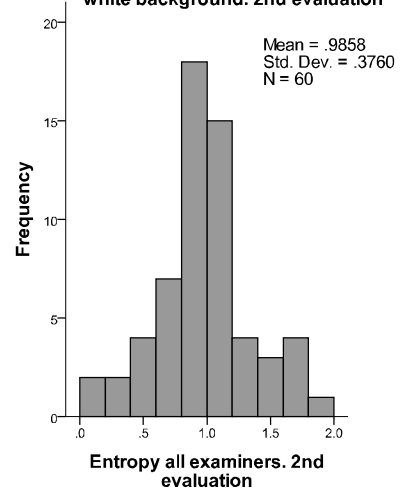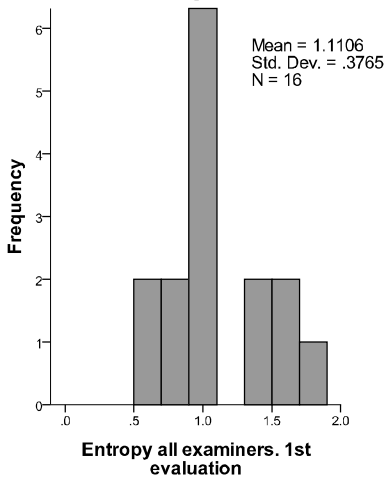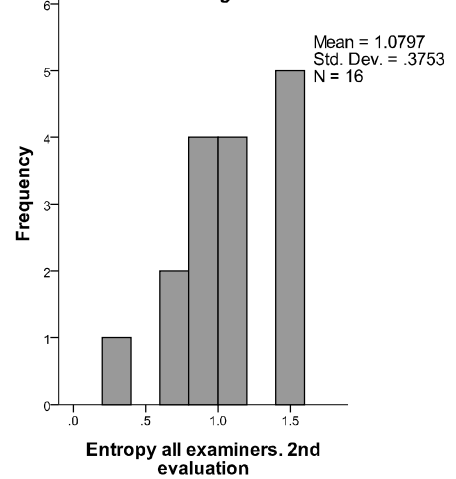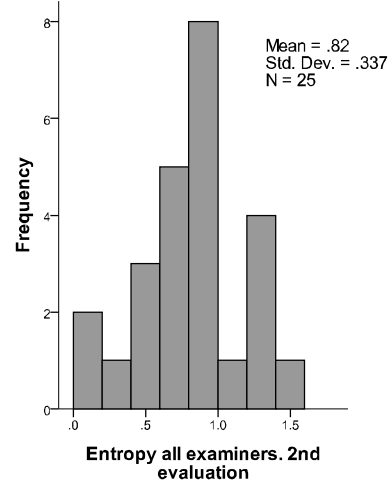
Figure 99 Histograms per denture for the Shannon's entropy for the 1st and 2nd evaluation; AE of DWB (upper row), DBB (middle row) and ICT (bottom row).
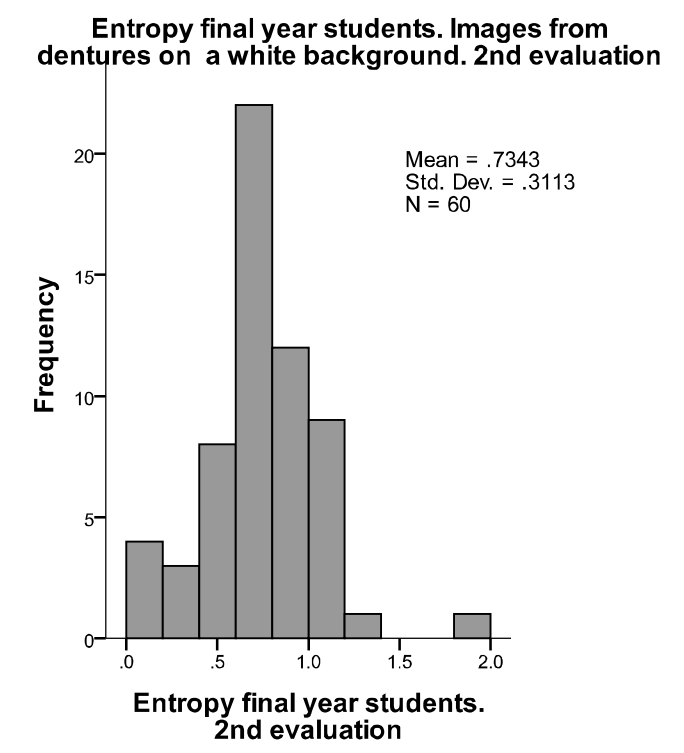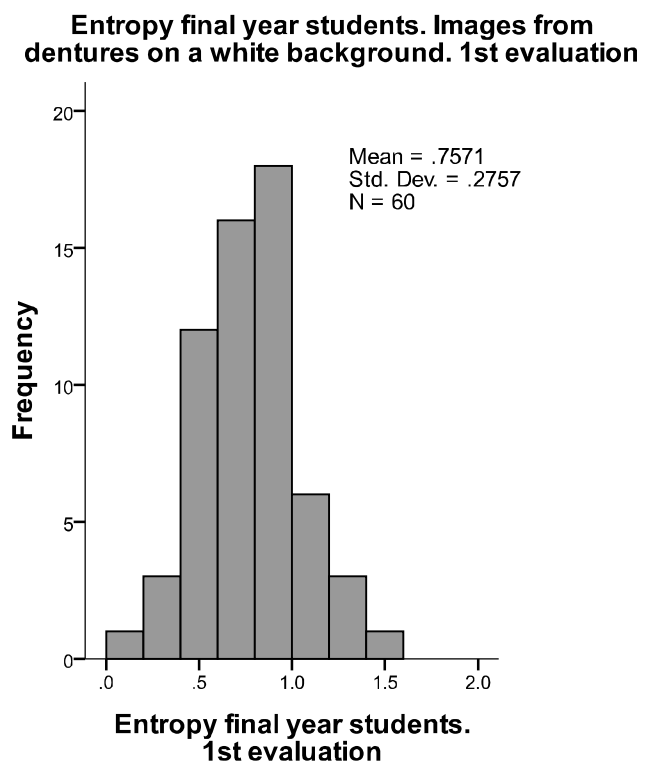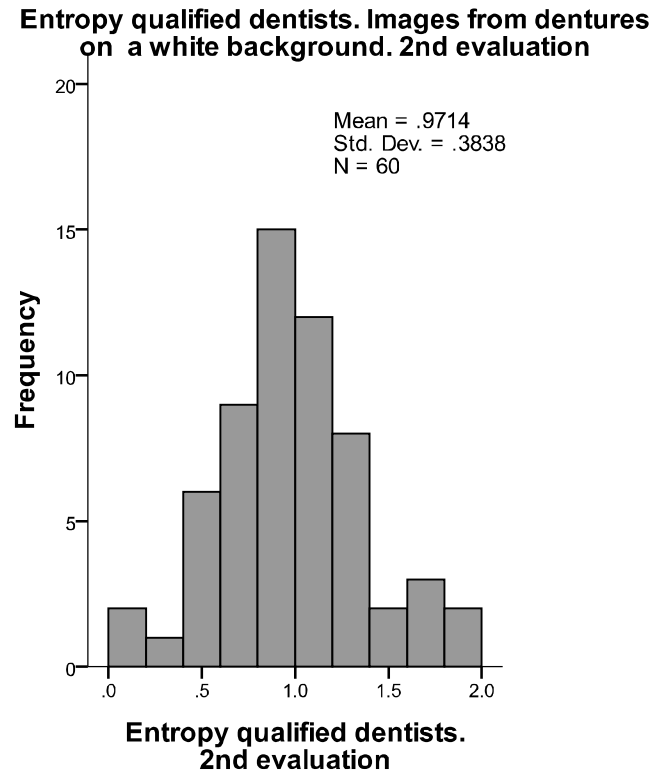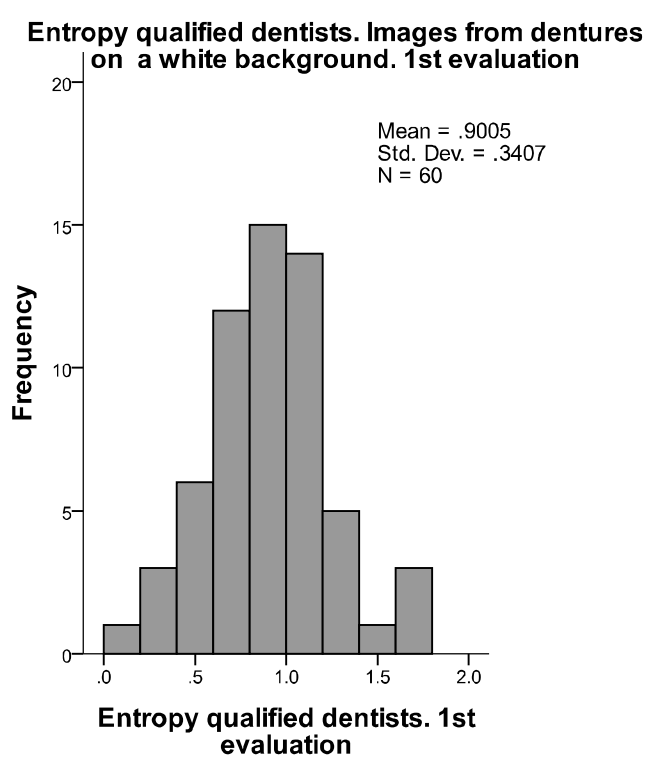
Figure 100 Histograms for the Shannon's entropy for the QD and the FYS. 1st and 2nd evaluation of the DWB.

Figure 101 Histograms for the Shannon's entropy for the QD and the FYS. 1st and 2nd evaluation of the DBB.

Entropy qualified dentists, per image. Images from a clinical trial. 1st evaluation
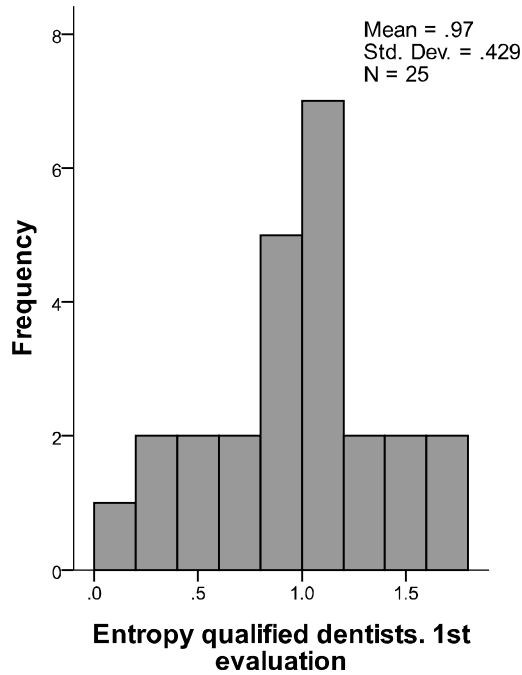
Mean = .97
Std. Dev. = .429
N = 25

Frequency

Entropy qualified dentists. 1st evaluation

Entropy qualified dentists, per image. Images from a clinical trial. 2nd evaluation
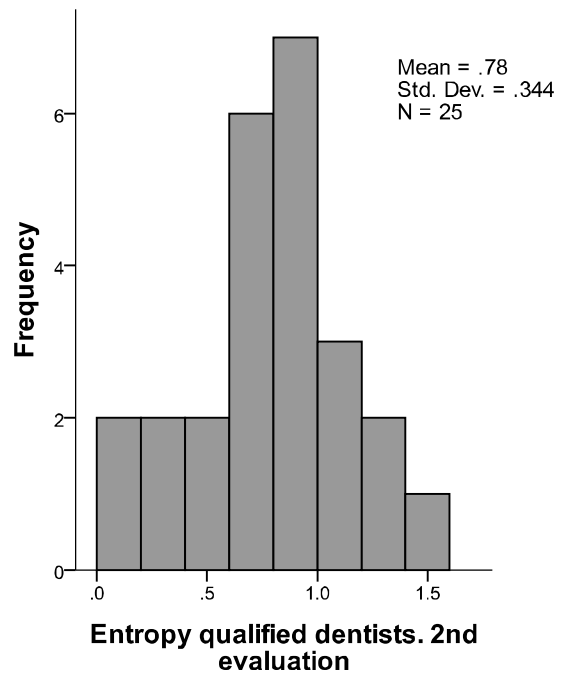
Mean = .78
Std. Dev. = .344
N = 25

Frequency

Entropy qualified dentists. 2nd evaluation

Entropy students, per image. Images from a clinical trial. 1st evaluation

Mean = .68
Std. Dev. = .265
N = 25

Frequency

Entropy students. 1st evaluation

Entropy students, per image. Images from a clinical trial. 2nd evaluation

Mean = .62
Std. Dev. = .266
N = 25

Frequency
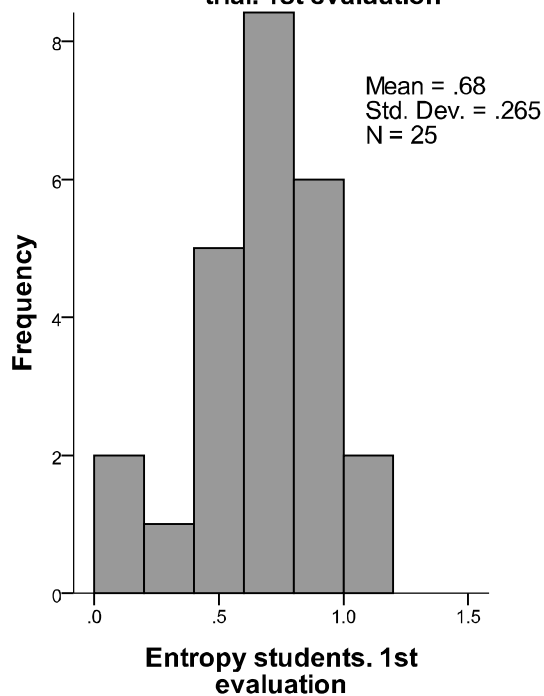
Entropy students. 2nd evaluation
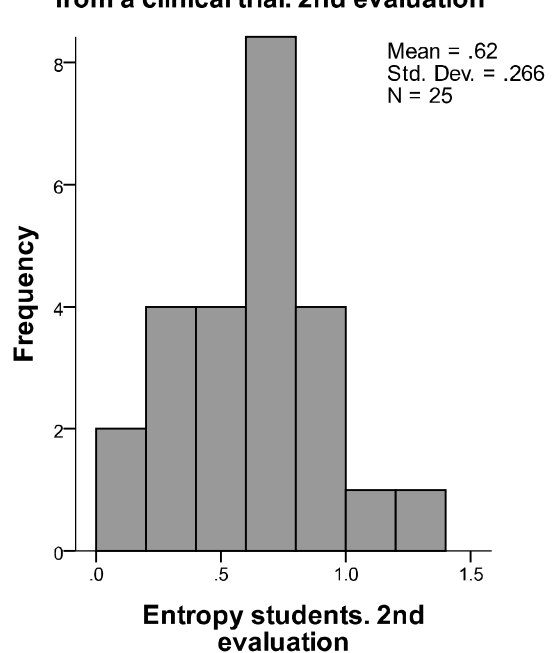
Figure 102 Histograms showing the results for the Shannon's entropy for the 1st and 2nd evaluation per image, for the QD and the FYS of ICT.

Table 35 Normality test, mean and standard deviation of the results of the Shannon's entropy of the DWB per denture and per tooth grouped in AE, QD and FYS for the 1st and 2nd evaluation.

Test	Group		Mean	S.D.	Normality value	p
Shapiro-Wilk	Per denture (n=60)	Entropy AE 1st evaluation	0.94	0.32	0.12	0.26
		Entropy AE 2nd evaluation	0.99	0.38	0.09	0.20
		Entropy QD. 1st evaluation	0.90	0.34	0.93	0.20
		Entropy QD. 2nd evaluation	0.97	0.38	0.07	0.20
		Entropy FYS. 1st evaluation	0.76	0.28	0.11	0.09
		Entropy FYS. 2nd evaluation	0.73	0.31	0.12	0.02*
Kolmogorov-Smirnov	Per tooth (n=356)	Entropy AE 1st evaluation	0.94	0.44	0.09	0.00*
		Entropy AE 2nd evaluation	0.98	0.49	0.78	0.00*
		Entropy QD. 1st evaluation	0.90	0.48	0.11	0.00*
		Entropy QD. 2nd evaluation	0.97	0.52	0.11	0.00*
		Entropy FYS. 1st evaluation	0.75	0.46	0.26	0.00*
		Entropy FYS. 2nd evaluation	0.73	0.48	0.25	0.00*

*p<0.05

Table 36 Normality test, mean and standard deviation of the results of the Shannon's entropy of the DBB per denture and per tooth grouped in AE, QD and FYS for the 1st and 2nd evaluation.

Test	Group		Mean	S.D.	Normality value	p
Shapiro-Wilk	Per denture (n=16)	Entropy AE 1st evaluation	1.11	0.38	0.93	0.26
		Entropy AE 2nd evaluation	1.08	0.38	0.95	0.52
		Entropy QD. 1st evaluation	1.12	0.42	0.93	0.21
		Entropy QD. 2nd evaluation	1.01	0.43	0.96	0.60
		Entropy FYS. 1st evaluation	0.76	0.26	0.97	0.79
		Entropy FYS. 2nd evaluation	0.83	0.30	0.91	0.10
Kolmogorov-Smirnov	Per tooth (n=95)	Entropy AE 1st evaluation	1.11	0.50	0.97	0.05
		Entropy AE 2nd evaluation	1.08	0.47	0.99	0.57
		Entropy QD. 1st evaluation	1.12	0.55	0.95	0.00*
		Entropy QD. 2nd evaluation	1.00	0.51	0.97	0.04*
		Entropy FYS. 1st evaluation	0.76	0.52	0.89	0.00*
		Entropy FYS. 2nd evaluation	0.83	0.53	0.88	0.00*

*p<0.05

Table 37 Normality test, mean and standard deviation of the results of the Shannon's entropy of the ICT per image and per tooth grouped in AE, QD and FYS for the 1st and 2nd evaluation.

Test	Group		Mean	S.D.	Normality value	p
Shapiro-Wilk	Per Image (n=25)	Entropy AE 1st evaluation	0.98	0.38	0.98	0.93
		Entropy AE 2nd evaluation	0.82	0.34	0.97	0.70
		Entropy QD. 1st evaluation	0.97	0.43	0.98	0.90
		Entropy QD. 2nd evaluation	0.78	0.34	0.97	0.70
		Entropy FYS. 1st evaluation	0.68	0.26	0.95	0.31
		Entropy FYS. 2nd evaluation	0.62	0.27	0.98	0.95
Kolmogorov-Smirnov	Per tooth (n=300)	Entropy AE 1st evaluation	0.98	0.52	0.98	0.00*
		Entropy AE 2nd evaluation	0.82	0.51	0.96	0.00*
		Entropy QD. 1st evaluation	0.97	0.58	0.96	0.00*
		Entropy QD. 2nd evaluation	0.78	0.55	0.94	0.00*
		Entropy FYS. 1st evaluation	0.68	0.48	0.86	0.00*
		Entropy FYS. 2nd evaluation	0.62	0.49	0.85	0.00*

*p<0.05

Table 38 Normality test, mean and standard deviation of the results of the Shannon's entropy of the identical images on dentures that were taken on both white and black background (n=5) per denture and per tooth grouped as AE, QD and FYS for the 1st and 2nd evaluation.

	Group	DWB				DBB			
		Mean	S.D.	Shapiro-Wilk	p	Mean	S.D.	Shapiro-Wilk	p
Per denture (n=5)	Entropy AE 1st evaluation	0.86	0.23	0.79	0.06	0.90	0.13	0.98	0.94
	Entropy AE 2nd evaluation	0.98	0.28	0.09	0.81	0.82	0.18	0.96	0.83
	Entropy QD. 1st evaluation	0.87	0.26	0.84	0.16	0.97	0.10	0.86	0.22
	Entropy QD. 2nd evaluation	0.98	0.27	0.93	0.59	0.74	0.31	0.96	0.84
	Entropy FYS. 1st evaluation	0.62	0.19	0.89	0.36	0.53	0.23	0.96	0.81
	Entropy FYS. 2nd evaluation	0.74	0.26	0.97	0.89	0.70	0.8	0.97	0.86
Per tooth (n=30)	Entropy AE 1st evaluation	0.86	0.33	0.91	0.16	0.90	0.29	0.88	0.00*
	Entropy AE 2nd evaluation	0.98	0.39	0.97	0.50	0.82	0.33	0.94	0.97
	Entropy QD. 1st evaluation	0.87	0.37	0.85	0.00*	0.97	0.32	0.90	0.10
	Entropy QD. 2nd evaluation	0.97	0.42	0.93	0.05*	0.74	0.39	0.01	0.17
	Entropy FYS. 1st evaluation	0.62	0.40	0.73	0.00*	0.53	0.45	0.81	0.00*
	Entropy FYS. 2nd evaluation	0.74	0.46	0.82	0.00*	0.70	0.44	0.83	0.00*

*p<0.05
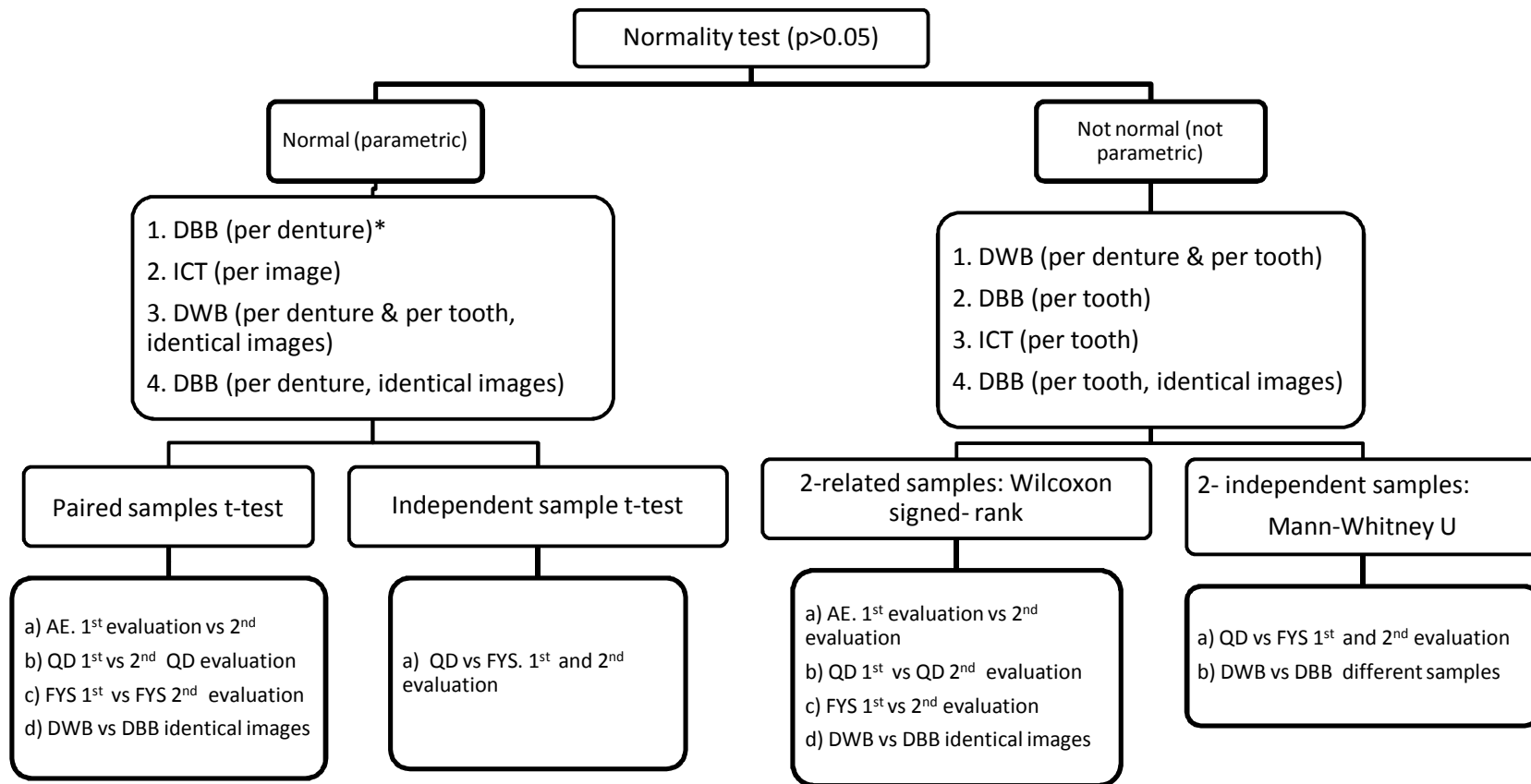
*This sample was analysed with non parametric tests because the distribution of its matching pair (DWB per denture) was not normal.

Figure 103 Summary of the statistical analysis method used, per group and per sample, for the images investigated in this study.
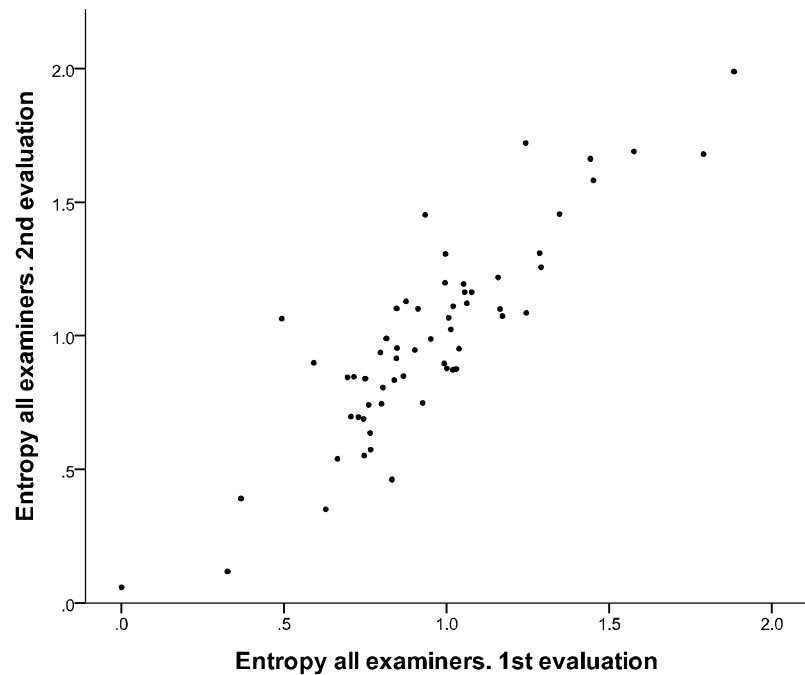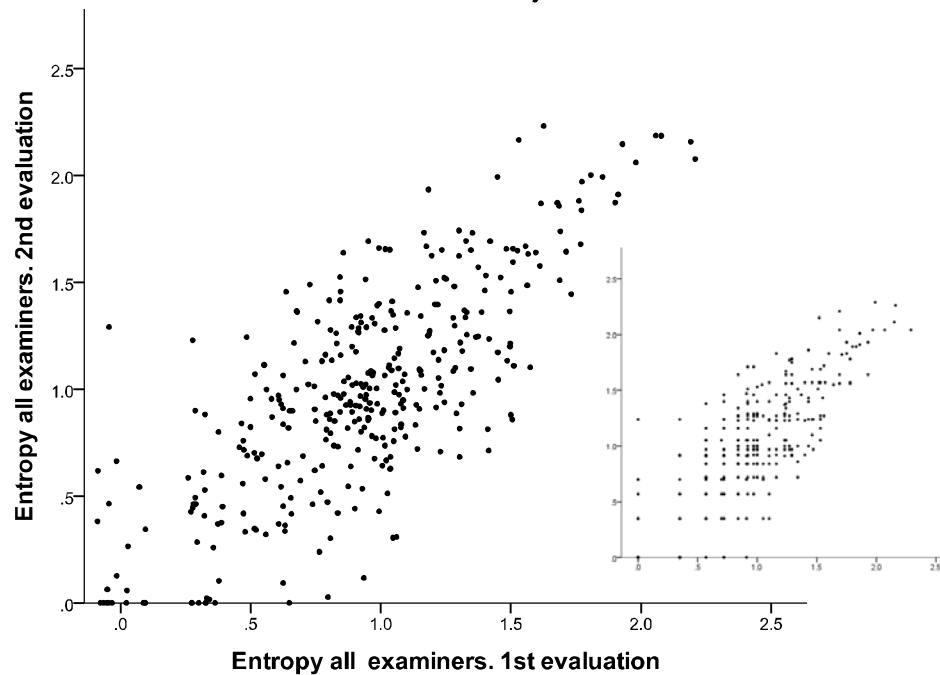
Figure 104 Shannon's entropy <u>per denture</u>- average (left) and <u>per tooth</u> (right) for results of the QHT index for AE between the 1st and 2nd evaluation of the DWB. Jitter was applied to the results per tooth (the small image on the right shows the plot without jitter).
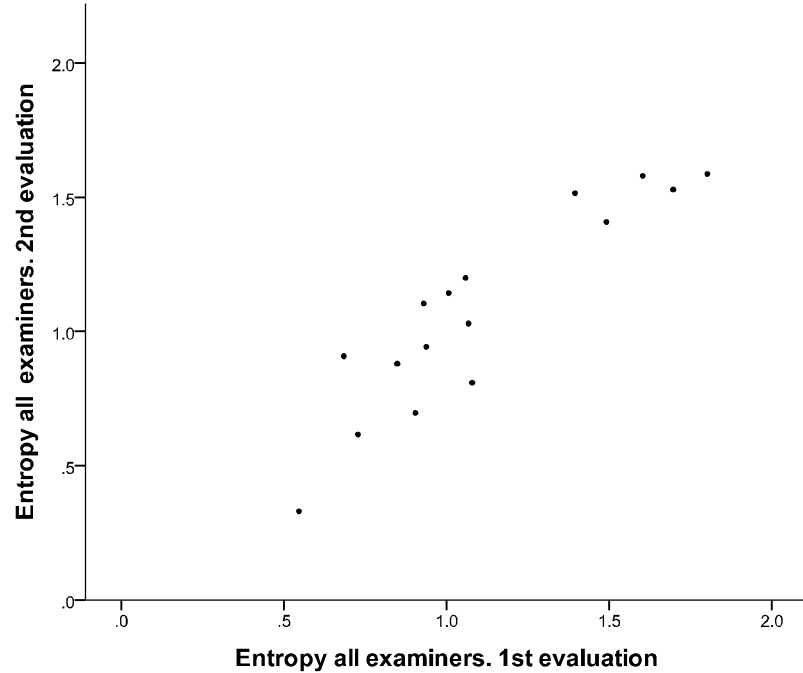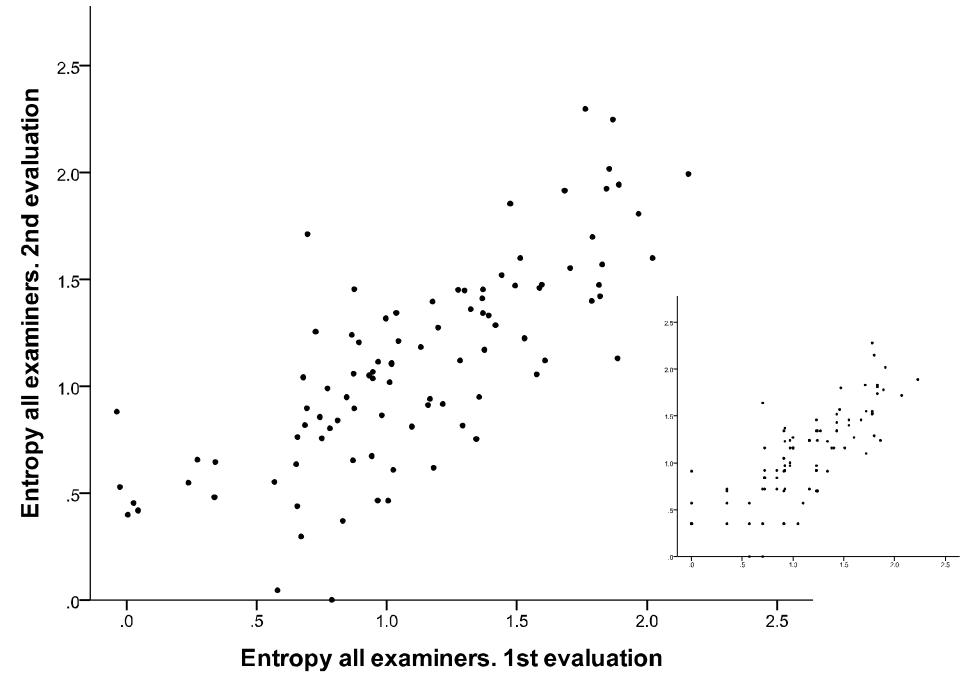
Figure 105 Shannon's entropy <u>per denture</u>- average (left) and <u>per tooth</u> (right) for results of the QHT index for AE between the 1st and 2nd

evaluation of the DBB. Jitter was applied to the results per tooth (the small image on the right shows the plot without jitter).
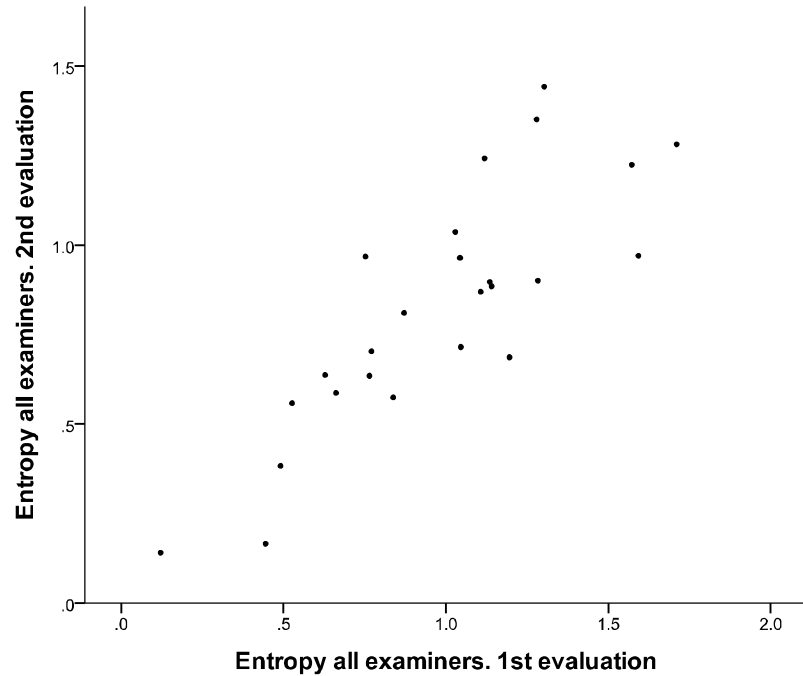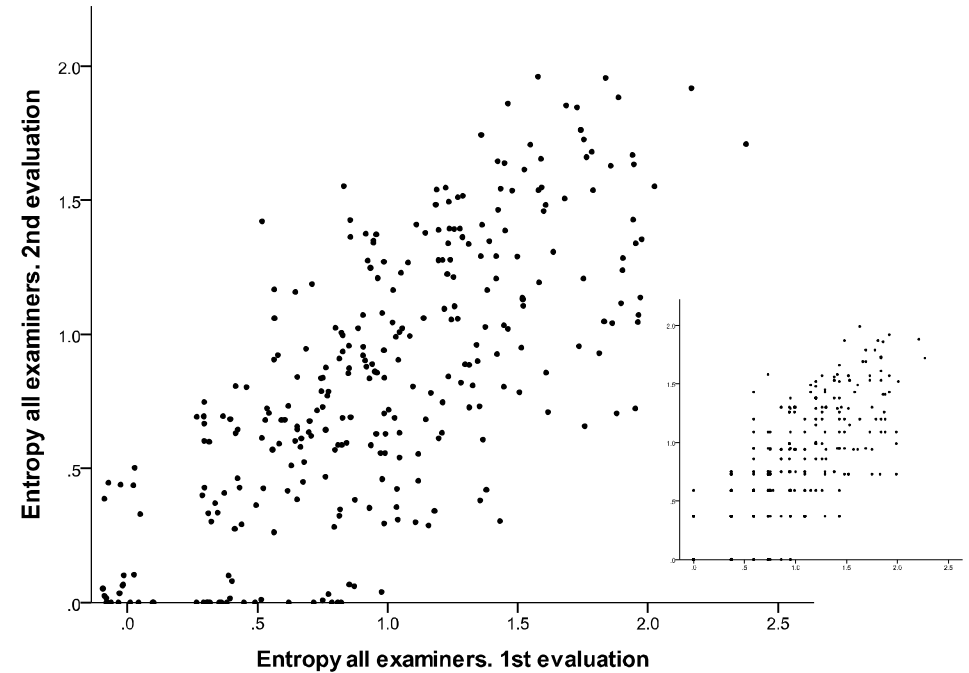
Figure 106 Shannon's entropy per denture- average (left) and per tooth (right) for results of the QHT index for AE between the 1st and 2nd evaluation of the ICT. Jitter was applied to the results per tooth (the small image on the right shows the plot without jitter).
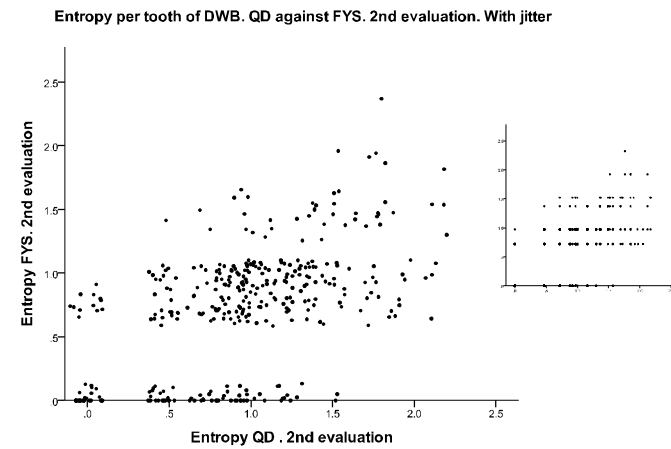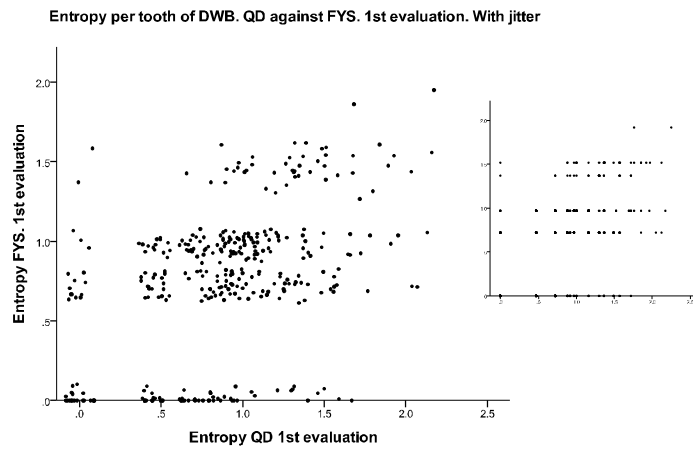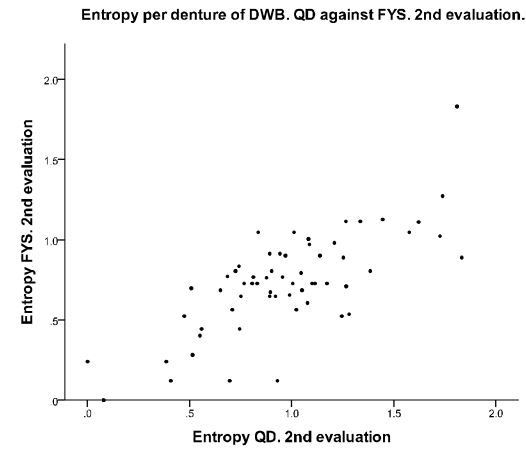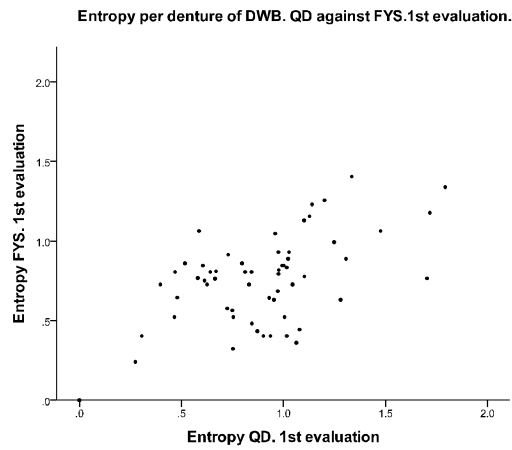
Figure 107 Shannon's entropy per denture (upper row) and per tooth (bottom row) for results of the QHT index on DWB between the QD against the FYS 1st (left) and 2nd evaluation (right). Jitter was applied to the results per tooth (the small image on the right shows the plot without jitter).
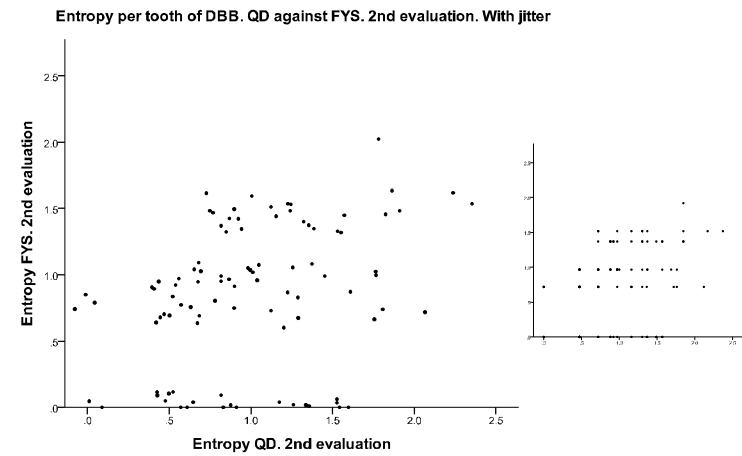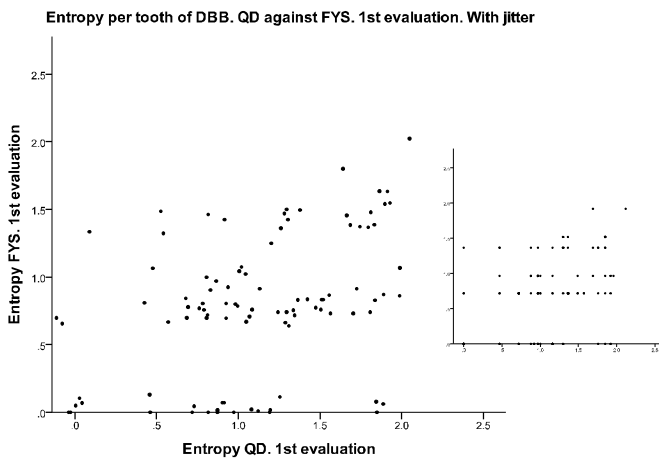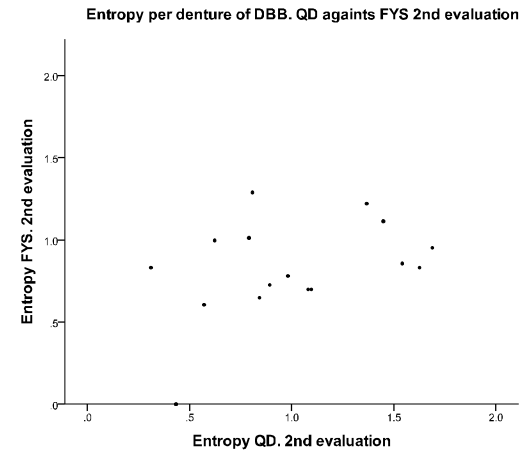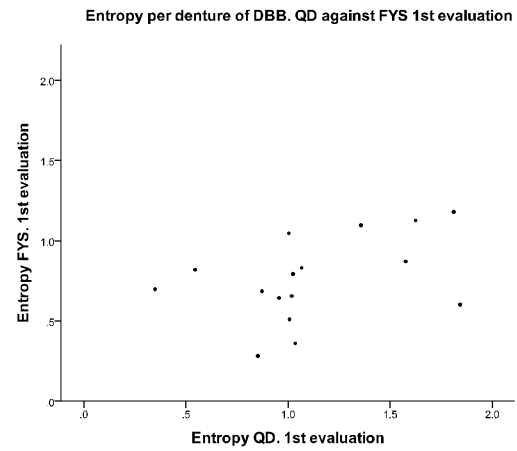
Figure 108 Shannon's entropy per denture (upper row) and per tooth (bottom row) for results of the QHT index on DBB between the QD against the FYS 1st (left) and 2nd evaluation (right). Jitter was applied to the results per tooth (the small image on the right shows the plot without jitter).
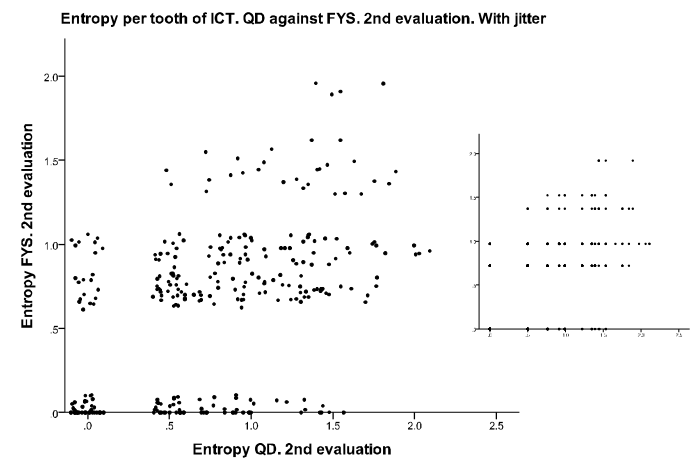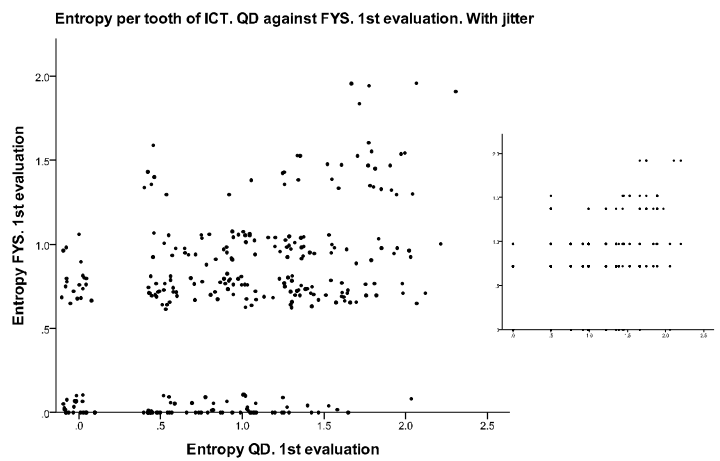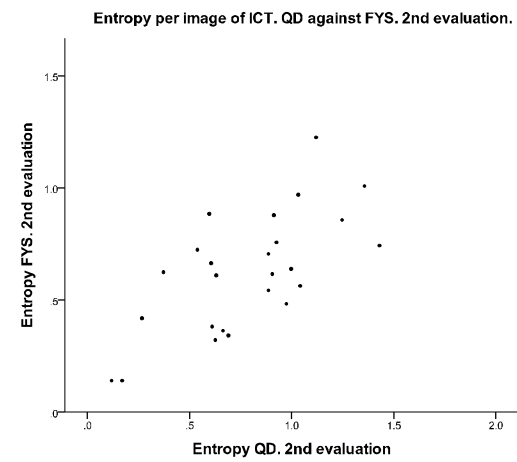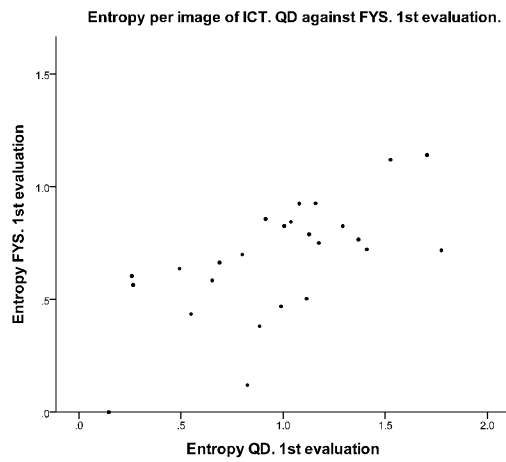
Figure 109 Shannon's entropy per denture (upper row) and per tooth (bottom row) for results of the QHT index of the ICT between QD against

FYS 1st (left) and 2nd evaluation (right). Jitter was applied to the results per tooth (the small image on the right shows the plot without

jitter).

279
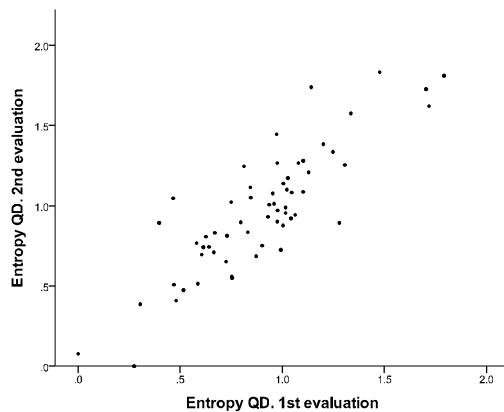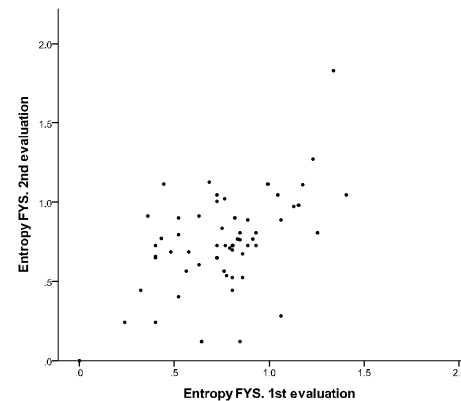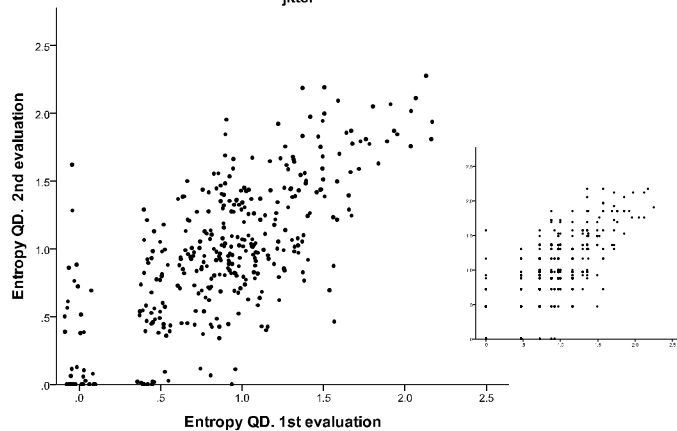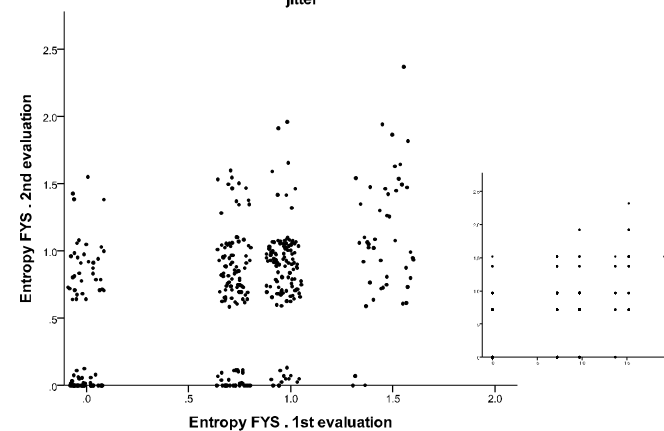
Figure 110 Shannon's entropy per denture (upper row) and per tooth (bottom row) for results of the QHT index of DWB for the QD 1st against 2nd evaluation (left) and the FYS 1st against 2nd evaluation (right). Jitter was applied to the results per tooth (the small image on the right shows the plot without jitter).
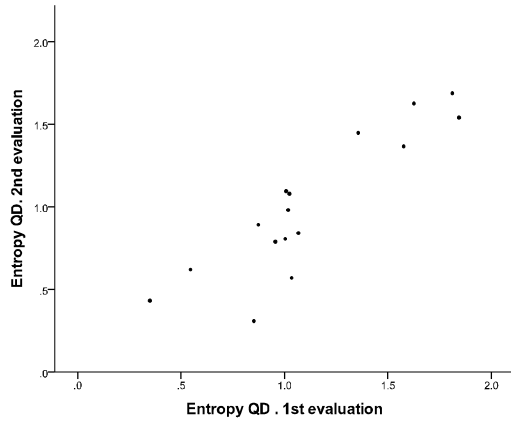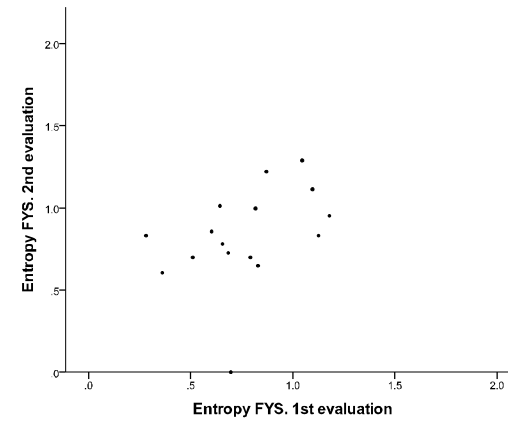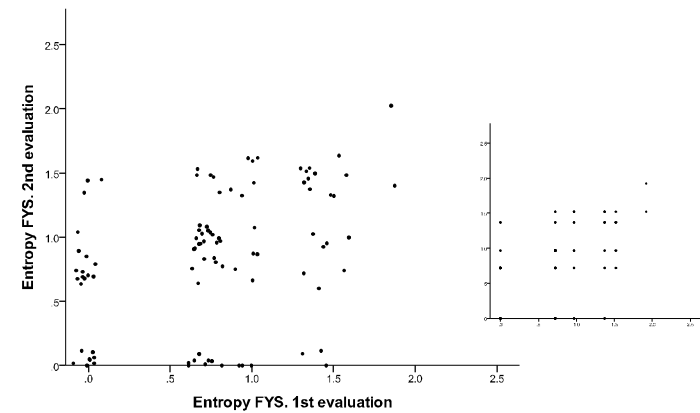
Figure 111 Shannon's entropy per denture (upper row) and per tooth (bottom row) for results of the QHT index of DBB for the QD 1st against 2nd evaluation (left) and FYS 1st against 2nd evaluation (right). Jitter was applied to the results per tooth (the small image on the right shows the plot without jitter).
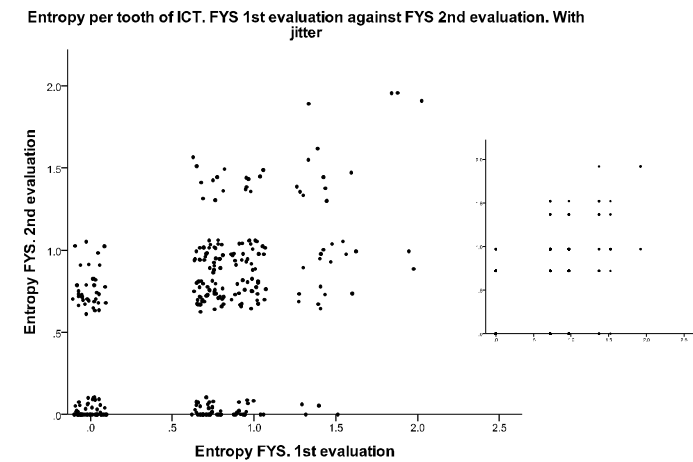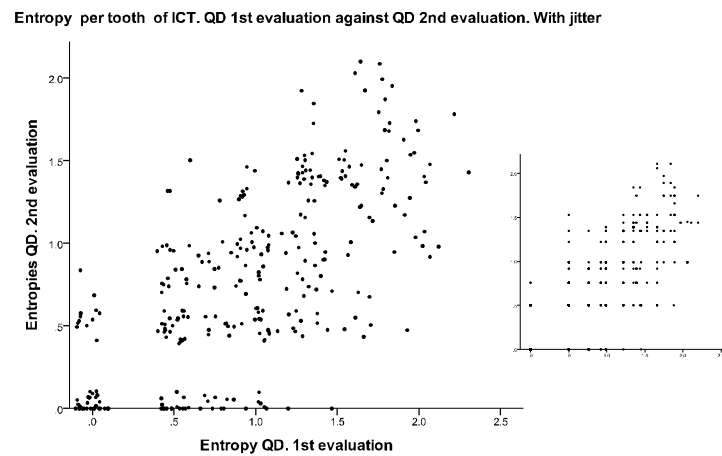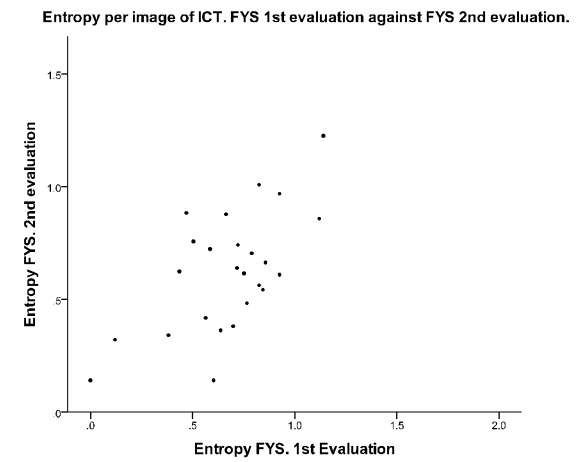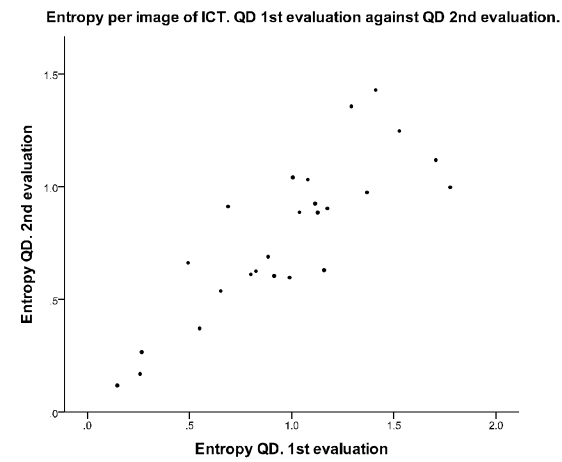
Figure 112 Shannon's entropy per denture (upper row) and per tooth (bottom row) for results of the QHT index of ICT for QD 1st against 2nd evaluation (left) and the FYS 1st against 2nd evaluation (right). Jitter was applied to the results per tooth (the small image on the right shows the plot without jitter).

Table 39 Results of the non parametric tests used to compare between groups per denture and per tooth of the DBW.

Groups	Unit	Entropy AE 2nd evaluation		Entropy QD. 2nd evaluation		Entropy FYS. 2nd evaluation		Entropy FYS. 1st evaluation		Entropy QD. 2nd evaluation	
		Wilcoxon signed- rank						Mann-Whitney U			
Test values		Z value	p	Z value	p	Z value	p	U value	p	U value	p
Entropy AE 1st evaluation	Per denture	-1.50	0.13								
	Per tooth	-2.30	0.02*								
Entropy QD. 1st evaluation	Per denture			-2.53	0.01*			1318.5	0.01*		
	Per tooth			-3.47	0.00*			55716	0.00*		
Entropy FYS. 1st evaluation	Per denture					-0.55	0.58				
	Per tooth					-0.79	0.43				
Entropy FYS. 2nd evaluation	Per denture									1100.5	0.00*
	Per tooth									49437	0.00*

*$p<0.05$

Table 40 Results of the non parametric tests used to compare between groups per denture and per tooth of the DBB.

Groups	Unit	Entropies per denture and per tooth. Dentures on a black background								
		Entropy AE 2nd evaluation		Entropy QD. 2nd evaluation		Entropy FYS. 2nd evaluation		Entropy FYS. 1st evaluation		Entropy QD. 2nd evaluation	
		Wilcoxon signed- rank						Mann-Whitney U			
Test values		Z value	p	Z value	p	Z value	p	U value	p	U value	p
Entropy AE 1st evaluation	Per denture	-0.72	0.47								
	Per tooth	-0.95	0.34								
Entropy QD. 1st evaluation	Per denture			-1.81	0.07			64.5	0.17		
	Per tooth			-2.83	0.01*			-4.22	0.00*		
Entropy FYS. 1st evaluation	Per denture					-1.19	0.23				
	Per tooth					-1.08	0.28				
Entropy FYS. 2nd evaluation	Per denture									101	0.31
	Per tooth									4069.5	0.16

*$p < 0.05$

Table 41 Results of the parametric and non parametric tests used to compare between groups per image and per tooth of ICT.

Groups	Unit	Entropy all 2nd evaluation		Entropy QD. 2nd evaluation		Entropy FYS. 2nd evaluation		Entropy FYS. 1st evaluation		Entropy QD. 2nd evaluation	
		Paired sample t-test						**Not paired sample t-test**			
Test values		Mean	*p*	Mean	*p*	Mean	*p*	Mean dif	*p*	Mean dif	*p*
Entropy AE 1st evaluation	Per Image	0.15	0.00*								
Entropy QD. 1st evaluation				0.19	0.00*			0.18	0.09		
Entropy FYS. 1st evaluation						0.05	0.28				
Entropy QD. 2nd evaluation										0.05	0.50
		Wilcoxon signed- rank						**Mann-Whitney U**			
U value		Z value	*p*	Z value	*p*	Z value	*p*	U value	*p*	U value	*p*
Entropy AE 1st evaluation	Per tooth	-6.43	0.00*								
Entropy QD. 1st evaluation				-6.81	0.00*			366838	0.00*		
Entropy FYS. 1st evaluation						-1.68	0.09				
Entropy QD. 2nd evaluation										42783	0.28

*p<0.05

Table 42 Results of the comparisons between the DWB against the DBB from different samples per tooth and per denture.

Entropies of DBB

Groups		AE 1st evaluation		AE 2nd evaluation		QD. 1st evaluation		QD 2nd evaluation		FYS 1st evaluation		FYS 2nd evaluation	
		Mann-Whitney U											
Test values		U value	p	U value	p	U value	p	U value	p	U value	p	U value	p
AE 1st evaluation	Per denture	359.5	0.13										
AE 2nd evaluation				412	0.39								
QD. 1st evaluation.						329	0.05						
QD. 2nd evaluation.								469.5	0.89				
FYS 1st evaluation.										477	0.97		
FYS. 2nd evaluation												10	0.25
AE 1st evaluation	Per tooth	14043	0.01*										
AE 2nd evaluation				15578	0.14								
QD. 1st evaluation.						12877	0.00*						
QD. 2nd evaluation.								177002	0.80				
FYS 1st evaluation.										16862.5	0.71		
FYS. 2nd evaluation.												15203	0.06

*$p<0.05$

286

Table 43 Results of the comparisons between the five pairs of identical images: DWB against DBB per tooth and per denture.

	AE 1st evaluation		AE 2nd evaluation		QD. 1st evaluation		QD 2nd evaluation		FYS 1st evaluation		FYS 2nd evaluation	
Entropies of DWB												
Paired t-test — Per denture												
Test values	Mean	p	Mean	p	Mean	p	Mean	p	Mean	p	Mean	p
AE 1st evaluation	0.40	0.71										
AE 2nd evaluation			-0.15	0.12								
QD. 1st evaluation.					0.10	0.49						
QD. 2nd evaluation.							-0.23	0.03*				
FYS 1st evaluation.									-0.08	0.17		
FYS. 2nd evaluation											-0.03	0.83
Wilcoxon signed- rank — Per tooth												
	Z	p	Z	p	Z	p	Z	p	Z	p	Z	p
AE 1st evaluation	-0.41	0.68										
AE 2nd evaluation			-2.73	0.01*								
QD. 1st evaluation.					-0.84	0.40						
QD. 2nd evaluation.							-2.87	0.04*				
FYS 1st evaluation.									-1.09	0.28		
FYS. 2nd evaluation.											-0.29	0.77

(Left axis label: Entropies of DBB)

*$p<0.05$

287

7.4. Discussion

Inter-examiner reliability refers to the consistency between examiners when using the same measuring method or instrument, whilst intra-examiner reliability refers to the self-performance consistency of a single observer (Dunn, 1992, Pretty and Maupome, 2004). When the reliability of dental plaque quantification is measured it is necessary that the plaque accumulation patterns remain stable, with little modification on the disclosure intensity during and between examinations, with the measurements taking place almost simultaneously. These conditions cannot be achieved using chair side recording unless some degree of bias is accepted. To avoid this, in this study a slide presentation of the digital images provided a permanent record of plaque distribution on the evaluated teeth which allowed the examinations to be made under similar controlled conditions. The main disadvantage of using photographs for assessing reliability is that a 3D world (tooth) is projected into 2 dimensions although, a good correlation (r=0.8) has been reported between dental plaque scores from a clinical evaluation and their corresponding matching images (Kelly et al., 2008).

The utilisation of dentures in this study was supported by the statement that dentures as natural teeth accumulate dental plaque and calculus (Connor et al., 1976, Felton et al., 2011), however completely different approaches are taken to locate plaque distribution in each case. Whilst in the case of epidemiological studies to measure periodontal disease, the surfaces of the teeth at risk of developing the disease need to be identified, in the studies on dentures little care is taken to locate the distribution of the dental plaque on dentures other than by surface (fitting, teeth) or type of surface (smooth vs. contoured). These studies are mainly focused on recognising

whether dental plaque is removed (or not) efficiently by a cleaning material from a certain surface. There is special emphasis placed on the areas of the denture that are in contact with the tissues such as the fitting surface (Tarbet, 1982, Keng and Lim, 1996), due to the strong relationship found between denture stomatitis (candida) and dental plaque accumulation (Nikawa et al., 1998, Gendreau and Loewy, 2011). Most of the indices used to quantify dental plaque on dentures have their origins in indices used for the same purpose in natural teeth. However, the intention of this investigation was to calculate the QHT index reliability and therefore the anterior teeth of the dentures provided a good model to assess plaque accumulation.

Due to the qualitative nature of the data, where dental plaque is graded in a numerical score that does not represent a quantity (thus a score of 2 is not twice the magnitude of a score of one), the statistical analysis needs to be a categorical tests (e.g. Fisher's exact test and odds ratio). However, reports in the literature were found like the ones by Fleiss et al. (1980), Marks et al. (1993) and Amini et al. (2009) where ordinal data was analysed as if they were quantitative by averaging the surfaces (per tooth) to obtain the score per "dentition/patient" using then parametrical tests (ANOVA) to compare the means of the results. Such an approach is incorrect (giving a numerical value to a variable does not make it quantitative), and whilst criticised, it appears to have remained in some literature.

Intra and inter-examiner agreement can be reported with the percentage of agreement (overall or in paired ratings), however when using this method, the agreement that may occur by pure chance is not taken into account (Hunt, 1986). Therefore, for this study it was decided to use the Cohen's kappa to measure both

the intra and inter-examiner agreement and the Shannon's entropy for the agreement in the pattern of probability of the data.

7.4.1. Cohen's Kappa

The presence of variability when using a subjective evaluation method it is usually expected due to the ambiguity of the index scale. However the generalised kappa for all the groups examined in the three sets of images, showed that the general agreement was not any higher than moderate. These results are lower than the agreement (k=0.62 or good) reported by Raggio et al. (2010) when dental plaque was quantified on bovine enamel blocks but correspond with the findings from Dababneh et al. (2002) who reported a low reproduction of the QHT index in an *in vitro* study. In this study, the moderate (or lower) agreement may be explained by the infinite variation in the distribution patterns of dental plaque. The examiner therefore needs to make unexpected decisions to classify dental plaque that may not "fit" into any of the criteria in the index coding. Three examples can illustrate the problems with unclear scoring criteria: a) dental plaque can be coded as either a code 2 (continuous band up to 1mm) or a code 3 (up to 1/3 of the clinical crown) depending where the examiner sets the 1mm limit, b) an isolated dental plaque deposit in a region different than the third near the gingival margin may receive different codes: either a code 0 (no plaque) if the examiner decides to ignore the deposits and focuses only on those near the gingival margin or a code1 (flecks) if the examiner considers that isolate deposits need to be coded as separate deposits or a code 4-5 if the plaque deposits are within the coronal extension of the crown and the examiner thinks that should code them accordingly. Vertical patterns in the distribution of

plaque might be also challenging as the index is designed to describe the accumulation horizontally.

An option to improve the results of the measurement of agreement is the use of a weighed kappa (Cohen, 1968), which is specially recommended when the code presents sequential values (e.g. 1, 2 and 3) as by doing so, more weight is placed on the large differences rather than on the smaller ones (Sim and Wright, 2005). This option was not used in this study because the weights are assigned arbitrarily with the risk of producing different weighted kappa values depending on the weighting scheme used.

In general, the reliability between examiners was lower than within examiners, which coincides with the results of Matthijs et al. (2001) who reported a good (k=0.70) intra-examiner agreement and no inter-examiner agreement when the QHT index was used to measure dental plaque on patients.

A high reliability within examiners means that the examiners are consistent with their answers but variations in the coding occur when the results are compared between examiners. This is corroborated by looking at the individual inter-agreement kappa where values as high as 0.78 (Table 33) or "good" agreement for one student and one clinician was registered. The presence of a better intra agreement may be explained by the occurrence of a systematic intra-examiner error (intra-examiner consistency), in which the examiner uses his/her own coding system consistently to quantify dental plaque which not necessarily coincides with the criteria used by the rest of the examiners (Birkeland and Jorkjend, 1975). A possibility to explain the lower inter-examiner agreement is the lack of training and calibration at the beginning of the study until higher agreement between the examiners was achieved according

to the recommendations of Eaton et al. (1997) where higher kappa scores were achieved when an intensive and constant training was given to the examiners. In this study no calibration or training procedures were given to duplicate the everyday conditions of a routine visit to the dentist where dental plaque accumulation is assessed.

Comparison of the results from the QD with those of the FYS, revealed that the FYS performed better than the QD in both inter (*k*=0.37 vs. 0.33-DBB and 0.41 vs. 0.33-ICT) and intra (k=0.55vs 0.54-DWB, 0.53 vs. 0.52-DBB) examiner agreement for all the sets of images (except the intra-agreement for the ICT where the QD performed better, and the DWB inter-agreement which both had the same results). These results disagree with the findings from Fleiss et al. (1980) and Shaloub and Addy (2000) who found no differences related to the experience of the examiners when assessing dental plaque with the QHT index and planimetry. The differences between QD and FYS encounter in this study may be related to various reasons. It may be that the results are due to the different sample size (the number of examiners was smaller for the FYS). Another possible explanation is that the QD were selected from a broad range of backgrounds with some of them specialised in a specific dental specialities (e.g. surgery) meanwhile the students were still undergoing training at the time of the study, and so their judgment may be more homogenous. It is interesting to note that the QD had better intra-examiner agreement for the ICT which may be related to the experience from the dentists when assessing patients. Further research is needed in this area to compare groups of students from different years to test whether the results change with the increase of their knowledge.

Originally the images were taken against different backgrounds (black and white) with the intention to facilitate the images segmentation (see Chapter 6). However, it was decided to use the images against both backgrounds to see whether the visualisation on one background was better than the other when assessing dental plaque. Green and Anderson (1956) observed that the use of the combination of different colours can speed up the visualisation when searching for information. This concept can be applied to visual presentations displayed on computer screens where an adequate contrast between foreground-background needs to be maintained for an easier reading (Hall and Hanna, 2004). Two tendencies exist about colour combinations used to present digital information, the studies that found that information is clearer when presented as a dark text on a light background (Buchner and Baumgartner, 2007, Greco et al., 2008) or white letters on a plain dark background (Dalal and Daver, 1996).

The results of this study for the inter-examiner agreement between sets dentures show that the DWB presented a higher kappa (0.42 ± 0.05) than DBB (0.33 ± 0.09) which may be linked to the contrast provided by the white background used. This finding was unexpected as it contradicts the general comments from the examiners when they finished the examination. They said that they felt that the black background provided a better visualisation of the dental plaque. Unfortunately no attempts were made to record these comments as it was thought that this might have been related to personal perception. It is suggested that in the future this information is recorded to compare between the perception and the results. The higher inter-examiner agreement of the DWB may have occurred as the DBB images were evaluated after the white examination and by that time the attention span of the

examiners became poor (after 24.2, S.D. 6 min and 16.3, S.D. 5 min for the 1st and 2nd evaluation).

7.4.2. Coding differences

For the four images represented in Figure 95, it is evident that the percentages of the differences between codes for the 1st examination were not the same for the 2nd, thus confirming the moderate intra-examiner agreement whilst the differences between dentures correlate with the inter-examiner agreement. The distribution of the percentages of the QHT index per code shows that majority of the dental plaque codes given to the ICT were between 2 and 3 which is the same range of codes found for an earlier study, that scored painted dental plaque on acrylic models (Dababneh et al., 2002). It was seen that majority of codes given to both the DWB and DBB were 1 and 2. The differences in the codes between ICT and dentures could be related simply to different distribution patterns between sets of images where natural teeth presented larger amounts of plaque. Another probability is that this could be a bias from the observers who might have assigned higher dental plaque codes to the ICT, however because of the design of this study where a "gold standard", does not exist; it is not possible to investigate this assumption further.

7.4.3. Shannon's entropy

The Shannon's entropy was first introduced in 1948 to predict information contained in messages in "bit" units. The Shannon's entropy has been applied in different fields to describe the uncertainty of occurrence of both DNA and protein sequences (Strait and Dewey, 1996, Schug et al., 2005), electroencephalographic amplitude when using an anaesthetic drug (Bruhn et al., 2001), and in patients with Alzheimer (Gomez and Hornero, 2010) .

In this study, the entropy was applied to the results from the answers when coding dental plaque. This theory is based on communication where the information on a message composed by successive symbols is not completely random and presents a statistical structure. A perfect transmission of the information is achieved when the value of the entropy is 0 because both the transmitter and the receiver are getting the same message. If this concept is applied to ordinal data derived from dental plaque quantification Shannon's entropy determines the heterogeneity of the responses between examiners when quantifying dental plaque. An entropy with a value of 0 equates to being "completely certain" or maximum agreement. Low entropies mean reduced uncertainty (more precise) whilst high entropy values represent the opposite. The maximum possible entropy in this study was 2.58. However the entropy has no concept of distance factor in the agreement (size of the disagreement), so it is possible to get the same entropy if 50% of the examiners score "0" and 50% score "1" (minimal disagreement) compared to 50% replying "0" and 50% "5" (greatest disagreement).

If good agreement between examiners was present the frequencies histograms (Figure 99-102) should shown a high frequency of small entropy values, however the results from the study for the three sets of images, groups and evaluations show that the entropy had a wide range of values with the means per group ranging from 0.62, ± 0.26 (FYS, ICT 2nd evaluation) to 1.12 ±90.42 (QD, DBB, 1st evaluation) which represents the variation in the examiners responses.

The scatter diagrams do not represent linear correlations due to the characteristics of the entropy. However, when comparing the entropies among groups if the results from the entropies (codes) were completely certain these would be clustered near the

X and Y zero regions. In presence of maximum uncertainty the values would be clustered at the top right hand corner of the graph. Therefore these diagrams should be only used as the visual representation of the comparisons between both sets of images and examiners. One possible correlation applicable to the entropies is that those images/dentures with higher entropies are the ones where it was more difficult to agree possible due to more complicated dental plaque patterns. However further research is needed to confirm this statement.

The scatter diagrams confirm the results from the histograms and show the variation between the scoring results which is denoted by the scattered pattern of the points. All the graphs (especially the values per tooth) also denote the presence of outliers which indicate that at that specific point one evaluation tended to present higher (or lower) values than the other.

Figure 107-112 (per tooth) presented horizontal patterns of distribution with existence of clustered values (e.g. Figure 110) which is related to human variation when coding dental plaque. Finally, the entropies per tooth also showed the existence of overlapped points which represent that some values were exactly the same for the two compared variables. Therefore in order be able to visualise these data points, some automated jitter was added to these graphs.

The results from the parametric and non parametric tests for the comparisons for the three sets of images (DWB, DBB and ICT) show that statistical significant differences ($p<0.05$ the entropies were different) occurred in the three sets of images without a recognised pattern on which groups of comparisons were more likely to present the difference. This could be explained by the existence of human variability in the scoring.

From the analysis of the results of the comparisons between the DWB and DBB from both identical and different images, it is apparent that the comparisons that resulted with statistical significant differences ($p < 0.05$) do not correspond to each other. In the case of the identical images, the differences were found in the comparisons per denture (QD 2nd) whilst in the group coming from different samples the differences were noticed in the comparisons per tooth (all 1st, QD 1st). However in general no differences between the entropies were found when comparing the backgrounds used for the images.

7.5. Conclusion

The results from this study showed that both the generalised intra and inter-examiner agreement when using the QHT was no better than moderate. Therefore fully automated methods for dental plaque quantification are indicated in order to reduce or eliminate those errors from either the examiners or the index itself. Where no other option is available to the QHT index as a method to determine dental plaque accumulation in dental research clinical trials or epidemiological studies then training and calibration of the examiners is necessary. This will maximise their reliability and thus increase the validity of the study. The Shannon's entropy was presented as an alternative method to compute the spread of the measurements when analysing the results from the QHT index (ordinal data).

Chapter 8
Future applications for the n-IR and UV

UV and n-IR imaging techniques broaden our knowledge of objects by unveiling features what cannot be perceived by the human eye. It has been investigated whether dental restorative materials as well as teeth present any fluorescent properties (Rüttermann et al., 2007, Hermanson et al., 2008, Bowers, 2010). In contrast, under n-IR light, enamel appears more transparent (Hirasuna et al., 2008). These characteristics have been exploited to assist in the detection of dental caries and demineralised lesions (Angmar-Mansson and ten Bosch, 2001, Bühler et al., 2005, Fried et al., 2005, De Josselin de Jong et al., 2009, Wu and Fried, 2009), dental plaque (Gwinnett and Ceen, 1978, Pretty et al., 2005), stains (Adeyemi et al., 2006) and fluorosis (Tranæus et al., 2001). This is not only of interest for characterisation of materials and pathological conditions but also of potential value in forensic applications such as victim identification from human remains. However a number of important questions remain unanswered:

• How do different dental materials appear under n-IR light?

• Is it possible to differentiate fillings from enamel/dentine using n-IR?

• Do digital images taken under UV have advantages over visible light for segmentation purposes? And if so, can this knowledge find and application in the forensics areas for dental biometrics (Marana et al., 2011) for determination of the size of dental restorations or identify dental cracks in the enamel?

As a preliminary attempt to answers some of these questions, digital images of 40 different dental materials: 35 composites, 4 glass ionomers and one amalgam (Table

44) were taken under both UV (2" Baader Venus U-filter, transmission peak from 300nm to 400nm and 395nm UV light source) and n-IR (Hoya 72 n-IR filter and IR spotlight module light source, 870-950nm) to determine their appearance under both lights. The preliminary results show that the dental materials under UV exhibit varying degrees of radiation absorption (appearing with various degrees of darkness, depending on the shade differences) whilst under n-IR all the materials look the same (Figure 113). Possibly these absorption patterns enable discrimination of brand and shades from unknown samples, although to which degree this might be accomplished still requires further research which is intended to develop as future work.
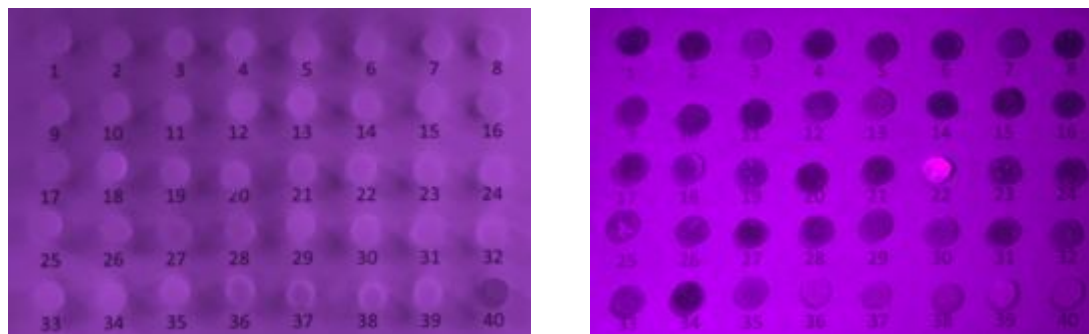
Figure 113 Appearance of different dental materials under a) n-IR (left) and b) UV (right)

Table 44 Dental materials, brands and manufacturers used in this study.

No	Shade	Type	Brand	No	Shade	Type	Brand
11	A	Artiste nanocomposite (enamel)	a	21	B2	Tetric ceram	b
2	A1	Tetric flow	b	22	B3		c
3	A1	Herculite unidose	c	23	B4	Glacier Dentine	e
4	A1	Artemis (enamel)	b	24	C1	Herculite unidose	c
5	A1	Tetric EvoCeram	b	25	C2	Herculite unidose	c
6	A2	Admira	d	26	C3	Herculite unidose	c
7	A2	Glacier Enamel	e	27	C4	Herculite unidose	c
8	A2	Artiste nanocomposite (dentin)	a	28	D2	Glacier Dentine	e
9	A2	Herculite unidose	c	29	D2	Herculite unidose	c
10	A2	Filtek Z250	f	30	D3	Herculite unidose	c
11	A3	Filtek Z250	f	31	D4	Herculite unidose	c
12	A3	Admira-Ormocer	d	32	Bleach	Tetric ceram	b
13	A3	Beautiful II	g	33	N/A	QuixFil universal	h
14	A3	Admira flow	d	34	A2	Clearfill Majestic aesthetic	i
15	A3	Premise flowable	c	35	B2	Clearfill Majestic aesthetic	i
16	A3.5	Glacier Enamel	e	36	A2	Chemfill	h
17	A3.5	Herculite unidose	c	37	A3	Chemfill	h
18	B1	Herculite unidose	c	38	A2	Ketack molar	f
19	B1	Glacier Enamel	e	39	A3	GC Fiji	j
20	B2	Majesty Aesthetic PLT	i	40	N/A	Amalgam	c

Brand code:

a) Petron clinical technologies

b) Ivoclar vivadent

c) Kerr

d) Voco

e) SDI

f) 3M ESPE

g) Shofu

h) Dentsply

i) Kuraray

j) CC corporation

Future work

- Investigate the advantages/disadvantages of the use of a green dye (complementary colour hue of red) to disclose dental plaque.

- Analysis of the remaining denture surfaces with comparison of the results.

- Creation and evaluation of a single process for quantification of dental plaque on digital images.

- Application of the methods presented in this thesis in clinical trials; testing dental plaque removal capabilities of the dental tools available.

- Testing of the sensitivity and specificity of the automated methods presented in this study when applied to clinical trials.

- Automated dental plaque quantification on digital images from patients on surfaces other than the labial surfaces of the anterior teeth.

- Investigate the application of n-IR and UV radiations in dental materials.

- Investigate the correlation between automated and manual methods when applied to measuring teeth sizes.

- Investigate plaque accumulation in orthodontic appliances.

General conclusions

The characteristics of an ideal index to quantify dental plaque are numerous; it should be cheap, simple and quick to use, reproducible, with high sensitivity and specificity, and be able to report the results in a continuous scale. Furthermore it should be flexible to allow its application on any patient and on any tooth surface. An index that fulfils all these conditions does not yet exist, however computerised, fully automated plaque indexes may solve some of the disadvantages with the currently available approaches. In this thesis a blue disclosing solution (Brilliant blue) was used to produce a good contrast between the disclosed dental plaque and the oral tissues. It was also showed that disclosed dental plaque is not visible on n-IR digital images and this is an advantage that can be exploited to obtain disclosed and non-disclosed images with minimal patient movement or imaging setup changes. The settings needed to obtain visible and n-IR images were determined, and the use of a second narrow interference band pass filter, tuned the absorption peak of the plaque dye, was investigated to increase the blue stained dental plaque contrast. These methods were used to acquire digital clinical images as well as images of complete upper dentures and several automated approaches for dental plaque quantification were investigated. The advantages and disadvantages of the different approaches were discussed together with the results from the plaque quantification. These methods proved relatively easy to use, reliable and eliminated the dependence on the examiner to code dental plaque, although minor human intervention was still required. Finally, to highlight the problem of reliability of the currently used indexes, the inter- and intra-examiner reliability measures of a common qualitative index for

dental plaque quantification (the Quigley and Hein modified by Turesky) were

investigated, and showed an agreement no better than "moderate".

 This further highlights the need of more quantitative and methodologies for the

assessment of dental plaque.

Appendices

Appendix I: Absorbance results for the λ1 and λ2 of both components in the two tone solution, the blue food colourant and the green food colourant.

Absorbance results for maxima light absorption wavelength (λ1) of the blue component (erioglaucine) of the two-tone solution.

Two-tone solution blue component: Erioglaucine (λ1)

Colour index: 42090				MW: 792.84	Formula: $C_{37}H_{34}N_2Na_2O_9S_3$		
Maxima light absorption wavelength: 630nm					Absorbance at 539nm **(λ1)**		
Sample	Concentration	Wavelength	Measurement 1	Measurement 2	Measurement 3	Average	S.D.
19	1.95E-07	539.00	0.01	0.01	0.00	0.01	0.00
18	3.91E-07	539.00	0.01	0.02	0.02	0.02	0.00
17	7.81E-07	539.00	0.01	0.01	0.01	0.01	0.00
16	1.17E-06	539.00	0.02	0.01	0.01	0.01	0.00
15	1.56E-06	539.00	0.02	0.02	0.01	0.02	0.00
14	2.34E-06	539.00	0.04	0.02	0.02	0.02	0.01
13	3.13E-06	539.00	0.03	0.03	0.04	0.03	0.00
12	4.69E-06	539.00	0.03	0.03	0.04	0.03	0.00
11	6.25E-06	539.00	0.04	0.04	0.04	0.04	0.00
10	9.38E-06	539.00	0.06	0.06	0.06	0.06	0.00
9	1.25E-05	539.00	0.07	0.08	0.07	0.07	0.00
8	1.88E-05	539.00	0.11	0.11	0.11	0.11	0.00
7	2.50E-05	539.00	0.14	0.14	0.14	0.14	0.00
6	3.75E-05	539.00	0.20	0.20	0.20	0.20	0.00
5	5.00E-05	539.00	0.26	0.27	0.27	0.27	0.00
4	7.50E-05	539.00	0.40	0.39	0.39	0.39	0.00
3	1.00E-04	539.00	0.49	0.49	0.49	0.49	0.00
2	1.50E-04	539.00	0.68	0.67	0.67	0.67	0.00
1	2.00E-04	539.00	0.93	0.93	0.93	0.93	0.00

Absorbance results for maxima light absorption wavelength (λ2) of the blue component (erioglaucine) of the two-tone solution.

Two-tone solution blue component: Erioglaucine (λ2)

| Sample | Concentration | Wavelength | Absorbance at 630nm (**λ2**) | | | | |
			Measurement 1	Measurement 2	Measurement 3	Average	S.D.
19	1.95E-07	630.08	0.02	0.02	0.02	0.02	0.00
18	3.91E-07	630.08	0.04	0.05	0.05	0.05	0.00
17	7.81E-07	630.08	0.07	0.07	0.07	0.07	0.00
16	1.17E-06	630.08	0.11	0.11	0.11	0.11	0.00
15	1.56E-06	630.08	0.14	0.14	0.14	0.14	0.00
14	2.34E-06	630.08	0.23	0.22	0.22	0.22	0.01
13	3.13E-06	630.08	0.28	0.28	0.28	0.28	0.00
12	4.69E-06	630.08	0.42	0.41	0.42	0.42	0.00
11	6.25E-06	630.08	0.53	0.53	0.53	0.53	0.00
10	9.38E-06	630.08	0.85	0.85	0.85	0.85	0.00
9	1.25E-05	630.08	1.03	1.03	1.03	1.03	0.00
8	1.88E-05	630.08	1.55	1.55	1.55	1.55	0.00
7	2.50E-05	630.08	1.90	1.90	1.90	1.90	0.00
6	3.75E-05	630.08	2.39	2.39	2.39	2.39	0.00
5	5.00E-05	630.08	2.50	2.52	2.52	2.51	0.01
4	7.50E-05	630.08	2.60	2.59	2.58	2.59	0.01
3	1.00E-04	630.08	2.59	2.60	2.61	2.60	0.01
2	1.50E-04	630.08	2.65	2.64	2.62	2.64	0.02
1	2.00E-04	630.08	2.62	2.65	2.68	2.65	0.03

Absorbance results for the maxima light absorption wavelength (λ1) of the red component (phloxine B) of the two-tone solution.

Two-tone solution red component: Phloxine B (λ1)

Colour index: 45410				Formula: $C_{20}H_2Br_4Cl_4Na_2O_5$			
Maxima light absorption wavelength: 539nm				MW: 829.64			
				Absorbance at 539nm **(λ1)**			
Sample	Concentration	Wavelength	Measurement 1	Measurement 2	Measurement 3	Average	S.D.
19	1.95E-07	539.00	0.02	0.03	0.02	0.02	0.00
18	3.91E-07	539.00	0.04	0.03	0.04	0.04	0.00
17	7.81E-07	539.00	0.05	0.04	0.04	0.04	0.00
16	1.17E-06	539.00	0.08	0.08	0.08	0.08	0.00
15	1.56E-06	539.00	0.09	0.09	0.08	0.09	0.00
14	2.34E-06	539.00	0.16	0.15	0.15	0.15	0.00
13	3.13E-06	539.00	0.17	0.17	0.17	0.17	0.00
12	4.69E-06	539.00	0.29	0.29	0.29	0.29	0.00
11	6.25E-06	539.00	0.36	0.36	0.35	0.36	0.00
10	9.38E-06	539.00	0.56	0.56	0.56	0.56	0.00
9	1.25E-05	539.00	0.69	0.69	0.69	0.69	0.00
8	1.88E-05	539.00	1.09	1.09	1.09	1.09	0.00
7	2.50E-05	539.00	1.34	1.33	1.33	1.33	0.00
6	3.75E-05	539.00	1.89	1.89	1.89	1.89	0.00
5	5.00E-05	539.00	2.01	2.01	2.00	2.01	0.00
4	7.50E-05	539.00	2.14	2.15	2.15	2.15	0.00
3	1.00E-04	539.00	2.17	2.17	2.17	2.17	0.00
2	1.50E-04	539.00	2.23	2.23	2.23	2.23	0.00
1	2.00E-04	539.00	2.26	2.26	2.26	2.26	0.00

Absorbance results for the maxima light absorption wavelength (λ2) of the red component (phloxine B) of the two-tone solution.

Two-tone solution red component: Phloxine B (λ2)

| Sample | Concentration | Wavelength | Absorbance at 630nm **(λ2)** | | | | |
			Measurement 1	Measurement 2	Measurement 3	Average	S.D.
19	1.95E-07	630.08	0.00	0.00	0.00	0.00	0.00
18	3.91E-07	630.08	0.00	0.00	0.01	0.00	0.00
17	7.81E-07	630.08	0.00	0.00	0.00	0.00	0.00
16	1.17E-06	630.08	0.00	0.00	0.00	0.00	0.00
15	1.56E-06	630.08	0.00	0.00	0.00	0.00	0.00
14	2.34E-06	630.08	0.01	0.01	0.00	0.01	0.00
13	3.13E-06	630.08	0.00	0.00	0.00	0.00	0.00
12	4.69E-06	630.08	0.00	0.00	0.00	0.00	0.00
11	6.25E-06	630.08	0.01	0.01	0.00	0.01	0.00
10	9.38E-06	630.08	0.00	0.01	0.00	0.00	0.00
9	1.25E-05	630.08	0.00	0.01	0.00	0.00	0.00
8	1.88E-05	630.08	0.01	0.00	0.00	0.00	0.00
7	2.50E-05	630.08	0.01	0.00	0.00	0.00	0.00
6	3.75E-05	630.08	0.01	0.01	0.02	0.01	0.00
5	5.00E-05	630.08	0.01	0.01	0.00	0.01	0.00
4	7.50E-05	630.08	0.01	0.01	0.01	0.01	0.00
3	1.00E-04	630.08	0.02	0.02	0.01	0.02	0.00
2	1.50E-04	630.08	0.02	0.02	0.02	0.02	0.00
1	2.00E-04	630.08	0.04	0.04	0.05	0.04	0.00

Absorbance results for the maxima light absorption wavelength (λ1) of the blue component (erioglaucine) of the blue food colourant.

Blue food colourant solution blue component: Erioglaucine (λ1)

Colour index: 42090

Maxima light absorption wavelength: 630nm

Formula: $C_{37}H_{34}N_2Na_2O_9S_3$

MW: 792.84

Absorbance at 516nm (**λ1**)

Sample	Concentration	Wavelength	Measurement 1	Measurement 2	Measurement 3	Average	S.D.
19	1.95E-07	516.13	0.01	0.01	0.00	0.01	0.00
18	3.91E-07	516.13	0.01	0.02	0.02	0.02	0.00
17	7.81E-07	516.13	0.01	0.01	0.01	0.01	0.00
16	1.17E-06	516.13	0.01	0.01	0.01	0.01	0.00
15	1.56E-06	516.13	0.01	0.01	0.01	0.01	0.00
14	2.34E-06	516.13	0.03	0.01	0.01	0.02	0.01
13	3.13E-06	516.13	0.02	0.02	0.03	0.02	0.00
12	4.69E-06	516.13	0.02	0.02	0.02	0.02	0.00
11	6.25E-06	516.13	0.02	0.02	0.02	0.02	0.00
10	9.38E-06	516.13	0.03	0.03	0.03	0.03	0.00
9	1.25E-05	516.13	0.03	0.04	0.04	0.04	0.00
8	1.88E-05	516.13	0.05	0.05	0.05	0.05	0.00
7	2.50E-05	516.13	0.06	0.06	0.06	0.06	0.00
6	3.75E-05	516.13	0.09	0.09	0.08	0.09	0.00
5	5.00E-05	516.13	0.12	0.12	0.12	0.12	0.00
4	7.50E-05	516.13	0.17	0.16	0.16	0.16	0.00
3	1.00E-04	516.13	0.19	0.20	0.19	0.19	0.00
2	1.50E-04	516.13	0.27	0.27	0.27	0.27	0.00
1	2.00E-04	516.13	0.37	0.37	0.36	0.37	0.00

Absorbance results for the maxima light absorption wavelength (λ2) of the blue component (erioglaucine) of the blue food colourant.

Blue food colourant solution blue component: Erioglaucine (λ2)

Sample	Concentration	Wavelength	Absorbance at 630nm (λ2)				
			Measurement 1	Measurement 2	Measurement 3	Average	S.D.
19	1.95E-07	630.08	0.02	0.02	0.02	0.02	0.00
18	3.91E-07	630.08	0.04	0.05	0.05	0.05	0.00
17	7.81E-07	630.08	0.07	0.07	0.07	0.07	0.00
16	1.17E-06	630.08	0.11	0.11	0.11	0.11	0.00
15	1.56E-06	630.08	0.14	0.14	0.14	0.14	0.00
14	2.34E-06	630.08	0.23	0.22	0.22	0.22	0.01
13	3.13E-06	630.08	0.28	0.28	0.28	0.28	0.00
12	4.69E-06	630.08	0.42	0.41	0.42	0.42	0.00
11	6.25E-06	630.08	0.53	0.53	0.53	0.53	0.00
10	9.38E-06	630.08	0.85	0.85	0.85	0.85	0.00
9	1.25E-05	630.08	1.03	1.03	1.03	1.03	0.00
8	1.88E-05	630.08	1.55	1.55	1.55	1.55	0.00
7	2.50E-05	630.08	1.90	1.90	1.90	1.90	0.00
6	3.75E-05	630.08	2.39	2.39	2.39	2.39	0.00
5	5.00E-05	630.08	2.50	2.52	2.52	2.51	0.01
4	7.50E-05	630.08	2.60	2.59	2.58	2.59	0.01
3	1.00E-04	630.08	2.59	2.60	2.61	2.60	0.01
2	1.50E-04	630.08	2.65	2.64	2.62	2.64	0.02
1	2.00E-04	630.08	2.62	2.65	2.68	2.65	0.03

Absorbance results for the maxima light absorption wavelength (λ1) of the red component (carmoisine) of the blue food colourant.

Blue food colourant solution red component: Carmoisine (λ1)

Colour index: 14720   Formula: $C_{20}H_{12}N_2Na_2O_7S_2$

Maxima light absorption wavelength: 516nm   MW: 502.44

Absorbance at 516nm **(λ1)**

Sample	Concentration	Wavelength	Measurement 1	Measurement 2	Measurement 3	Average	S.D.
19	1.95E-07	516.13	0.00	0.00	0.00	0.00	0.00
18	3.91E-07	516.13	0.00	0.00	0.00	0.00	0.00
17	7.81E-07	516.13	0.01	0.01	0.01	0.01	0.00
16	1.17E-06	516.13	0.02	0.02	0.02	0.02	0.00
15	1.56E-06	516.13	0.03	0.03	0.03	0.03	0.00
14	2.34E-06	516.13	0.05	0.05	0.05	0.05	0.00
13	3.13E-06	516.13	0.05	0.05	0.05	0.05	0.00
12	4.69E-06	516.13	0.08	0.08	0.08	0.08	0.00
11	6.25E-06	516.13	0.11	0.11	0.11	0.11	0.00
10	9.38E-06	516.13	0.17	0.17	0.17	0.17	0.00
9	1.25E-05	516.13	0.23	0.22	0.22	0.22	0.00
8	1.88E-05	516.13	0.34	0.34	0.34	0.34	0.00
7	2.50E-05	516.13	0.45	0.44	0.44	0.44	0.00
6	3.75E-05	516.13	0.68	0.68	0.67	0.68	0.00
5	5.00E-05	516.13	0.87	0.89	0.87	0.88	0.01
4	7.50E-05	516.13	1.33	1.33	1.33	1.33	0.00
3	1.00E-04	516.13	1.69	1.68	1.68	1.68	0.00
2	1.50E-04	516.13	2.31	2.32	2.30	2.31	0.01
1	2.00E-04	516.13	2.51	2.50	2.48	2.50	0.01

Absorbance results for the maxima light absorption wavelength (λ2) of the red component (carmoisine) of the blue food colourant.

Blue food colourant solution red component: Carmoisine (λ2)

| Sample | Concentration | Wavelength | Absorbance at 630nm **(λ2)** | | | | |
			Measurement 1	Measurement 2	Measurement 3	Average	S.D.
19	1.95E-07	630.08	0.00	0.00	0.00	0.00	0.00
18	3.91E-07	630.08	-0.01	-0.01	-0.01	-0.01	0.00
17	7.81E-07	630.08	-0.01	-0.01	-0.01	-0.01	0.00
16	1.17E-06	630.08	0.00	-0.01	0.00	0.00	0.00
15	1.56E-06	630.08	0.00	0.00	0.00	0.00	0.00
14	2.34E-06	630.08	0.01	0.00	0.00	0.00	0.00
13	3.13E-06	630.08	-0.01	-0.01	-0.01	-0.01	0.00
12	4.69E-06	630.08	0.00	0.00	-0.01	0.00	0.00
11	6.25E-06	630.08	0.00	0.00	-0.01	0.00	0.00
10	9.38E-06	630.08	0.00	-0.01	-0.01	0.00	0.00
9	1.25E-05	630.08	0.00	0.00	0.00	0.00	0.00
8	1.88E-05	630.08	0.00	0.00	0.00	0.00	0.00
7	2.50E-05	630.08	0.00	0.00	0.00	0.00	0.00
6	3.75E-05	630.08	0.00	0.00	0.00	0.00	0.00
5	5.00E-05	630.08	0.00	0.02	0.00	0.01	0.01
4	7.50E-05	630.08	0.00	0.00	0.00	0.00	0.00
3	1.00E-04	630.08	0.01	0.00	0.00	0.00	0.00
2	1.50E-04	630.08	0.01	0.01	0.01	0.01	0.00
1	2.00E-04	630.08	0.01	0.01	0.01	0.01	0.00

Absorbance results for the maxima light absorption wavelength (λ1) of the blue component (lisamine green) of the green food colourant.

Green food colourant solution blue component: Lisamine Green (λ1)

Colour index: 44090

Formula: $C_{27}H_{25}N_2NaO_7S_2$

Maxima light absorption wavelength: 632nm

MW: 576.62

Absorbance at 426nm **(λ1)**

Sample	Concentration	Wavelength	Measurement 1	Measurement 2	Measurement 3	Average	S.D.
19	1.95E-07	426.10	0.00	0.00	0.00	0.00	0.00
18	3.91E-07	426.10	0.01	0.01	0.01	0.01	0.00
17	7.81E-07	426.10	0.00	0.00	0.00	0.00	0.00
16	1.17E-06	426.10	0.00	0.00	0.00	0.00	0.00
15	1.56E-06	426.10	0.02	0.01	0.01	0.01	0.01
14	2.34E-06	426.10	0.01	0.01	0.01	0.01	0.00
13	3.13E-06	426.10	0.02	0.02	0.02	0.02	0.00
12	4.69E-06	426.10	0.02	0.02	0.02	0.02	0.00
11	6.25E-06	426.10	0.03	0.03	0.03	0.03	0.00
10	9.38E-06	426.10	0.05	0.05	0.05	0.05	0.00
9	1.25E-05	426.10	0.07	0.07	0.07	0.07	0.00
8	1.88E-05	426.10	0.10	0.10	0.10	0.10	0.00
7	2.50E-05	426.10	0.13	0.13	0.13	0.13	0.00
6	3.75E-05	426.10	0.20	0.20	0.20	0.20	0.00
5	5.00E-05	426.10	0.26	0.26	0.26	0.26	0.00
4	7.50E-05	426.10	0.38	0.38	0.38	0.38	0.00
3	1.00E-04	426.10	0.51	0.51	0.51	0.51	0.00
2	1.50E-04	426.10	0.75	0.75	0.75	0.75	0.00
1	2.00E-04	426.10	1.01	1.01	1.01	1.01	0.00

Absorbance results for the maxima light absorption wavelength (λ2) of the blue component (lisamine green) of the green food colourant.

Green food colourant solution blue component: Lisamine Green (λ2)

Sample	Concentration	Wavelength	Measurement 1	Measurement 2	Measurement 3	Average	S.D.
				Absorbance at 632nm (**λ2**)			
19	1.95E-07	632.17	0.01	0.01	0.01	0.01	0.00
18	3.91E-07	632.17	0.03	0.03	0.03	0.03	0.00
17	7.81E-07	632.17	0.06	0.06	0.06	0.06	0.00
16	1.17E-06	632.17	0.09	0.09	0.09	0.09	0.00
15	1.56E-06	632.17	0.13	0.13	0.13	0.13	0.00
14	2.34E-06	632.17	0.19	0.19	0.19	0.19	0.00
13	3.13E-06	632.17	0.25	0.25	0.26	0.25	0.00
12	4.69E-06	632.17	0.39	0.39	0.39	0.39	0.00
11	6.25E-06	632.17	0.52	0.52	0.52	0.52	0.00
10	9.38E-06	632.17	0.78	0.78	0.78	0.78	0.00
9	1.25E-05	632.17	1.03	1.03	1.03	1.03	0.00
8	1.88E-05	632.17	1.51	1.51	1.51	1.51	0.00
7	2.50E-05	632.17	1.94	1.95	1.94	1.95	0.00
6	3.75E-05	632.17	2.48	2.47	2.48	2.48	0.01
5	5.00E-05	632.17	2.66	2.67	2.64	2.66	0.01
4	7.50E-05	632.17	2.72	2.70	2.76	2.73	0.03
3	1.00E-04	632.17	2.79	2.81	2.80	2.80	0.01
2	1.50E-04	632.17	2.86	2.90	2.89	2.88	0.02
1	2.00E-04	632.17	2.91	2.89	2.89	2.90	0.01

Absorbance results for the maxima light absorption wavelength (λ1) of the yellow component (tartrazine) of the green food colourant.

Green food colourant solution yellow component: Tartrazine (λ1)

MW: 534.37

Formula: $C_{16}H_9N_4Na_3O_9S_2$

Maxima light absorption wavelength: 426nm

Absorbance at 426nm **(λ1)**

Sample	Concentration	Wavelength	Measurement 1	Measurement 2	Measurement 3	Average	S.D.
18	3.91E-07	426.10	0.01	0.01	0.01	0.01	0.00
17	7.81E-07	426.10	0.01	0.01	0.01	0.01	0.00
16	1.17E-06	426.10	0.02	0.03	0.02	0.02	0.00
15	1.56E-06	426.10	0.03	0.02	0.03	0.03	0.00
14	2.34E-06	426.10	0.03	0.04	0.03	0.03	0.00
13	3.13E-06	426.10	0.06	0.05	0.06	0.06	0.00
12	4.69E-06	426.10	0.08	0.07	0.07	0.08	0.00
11	6.25E-06	426.10	0.12	0.12	0.12	0.12	0.00
10	9.38E-06	426.10	0.16	0.16	0.16	0.16	0.00
9	1.25E-05	426.10	0.32	0.32	0.31	0.32	0.00
8	1.88E-05	426.10	0.48	0.48	0.47	0.48	0.00
7	2.50E-05	426.10	0.62	0.62	0.62	0.62	0.00
6	3.75E-05	426.10	0.91	0.91	0.91	0.91	0.00
5	5.00E-05	426.10	1.20	1.20	1.20	1.20	0.00
4	7.50E-05	426.10	1.66	1.66	1.67	1.66	0.01
3	1.00E-04	426.10	1.96	1.97	1.96	1.96	0.00
2	1.50E-04	426.10	2.13	2.12	2.13	2.13	0.01
1	2.00E-04	426.10	2.18	2.18	2.15	2.17	0.01

Absorbance results for the maxima light absorption wavelength (λ2) of the yellow component (tartrazine) of the green food colourant.

Green food colourant solution yellow component: Tartrazine (λ2)

Sample	Concentration	Wavelength	Absorbance at 632nm (λ2)				
			Measurement 1	Measurement 2	Measurement 3	Average	S.D.
18	3.91E-07	632.17	0.00	0.00	0.00	0.00	0.00
17	7.81E-07	632.17	0.00	0.00	0.00	0.00	0.00
16	1.17E-06	632.17	-0.01	-0.01	0.00	0.00	0.00
15	1.56E-06	632.17	-0.01	-0.01	-0.01	-0.01	0.00
14	2.34E-06	632.17	0.00	0.00	0.00	0.00	0.00
13	3.13E-06	632.17	0.00	-0.01	-0.01	-0.01	0.00
12	4.69E-06	632.17	0.00	0.00	0.00	0.00	0.00
11	6.25E-06	632.17	0.00	0.00	0.00	0.00	0.00
10	9.38E-06	632.17	0.00	0.00	0.00	0.00	0.00
9	1.25E-05	632.17	0.00	0.00	0.00	0.00	0.00
8	1.88E-05	632.17	0.01	0.01	0.01	0.01	0.00
7	2.50E-05	632.17	0.01	0.01	0.01	0.01	0.00
6	3.75E-05	632.17	0.01	0.00	0.00	0.01	0.00
5	5.00E-05	632.17	0.00	0.01	0.00	0.00	0.00
4	7.50E-05	632.17	0.01	0.01	0.01	0.01	0.00
3	1.00E-04	632.17	0.00	0.00	0.00	0.00	0.00
2	1.50E-04	632.17	0.00	0.00	0.00	0.00	0.00
1	2.00E-04	632.17	0.01	0.01	0.01	0.01	0.00

Appendix II: Formulas used in the determination of the amount of colour added to the two-tone disclosing solution, blue and green food colourant.

Two-tone dye

Solution	Concentration	Absorbance	
		at 539	at 630
Two-tone	?	0.76	0.85

To obtain ε the following formula was applied.

$$A = \varepsilon c l$$

Where:

A= absorbance

ε= extinction coefficient

c=concentration

l=path length (1cm)

$\varepsilon_{blue\ 539} = 4715.2$ $\varepsilon_{blue\ 630} = 80219$

$\varepsilon_{red\ 539} = 55625$ $\varepsilon_{red\ 630} = 0$

$$A_{total} = A_{blue} + A_{red}$$

Two-tone$_{539}$: $0.76 = (\varepsilon_{blue\ 539})(c_{blue\ 539})(l) + (\varepsilon_{red\ 539})(c_{red\ 539})(l)$

Two-tone$_{630}$: $0.85 = (\varepsilon_{blue\ 630})(c_{blue\ 630})(l) + (\varepsilon_{red\ 630})(c_{red\ 630})(l)$

Substituting values into the equation:

Two-tone$_{539}$: $0.76 = (4715.2)(c_{blue\ 539}) + 55625(c_{red\ 539})$

Two-tone$_{630}$: $0.85 = (80219)(c_{blue\ 630}) + 0$

Solving the equation for $c_{blue\ 630}$:

$c_{blue\ 630}$= 0.85 / 80219

$c_{blue\ 630}$= 1.06×10^{-5} mol/dm^{-3}

$c_{red\ 630}$= **0 mol/dm^{-3}**

Substituting these values in the equation, as the concentration of $c_{blue\ 539}$ and

$c_{blue\ 630}$ is the same at both wavelengths:

Two-tone$_{539}$: 0.76= (4715.2) ($c_{blue\ 539}$) +55625 ($c_{red\ 539}$)

Two-tone$_{539}$: 0.76= (4715.2) (1.06×10^{-5} mol/dm^{-3}) +55625 ($c_{red\ 539}$)

$c_{red\ 539}$= **1.28×10^{-5} mol/dm^{-3}**

Then:

Two-tone$_{630}$: 1.06×10^{-5} mol/dm^{-3}

Two-tone$_{539}$= 1.28×10^{-5} mol/dm^{-3}

Converting molar concentration to mass concentration

Blue: moles= mass / RMV

      RMV:792.84

1.06×10^{-5} mol/dm^{-3}= mass / 792.84g/mol

mass = (1.06×10^{-5} mol/dm^{-3})(792.84 g/mol)

mass= **8.40×10^{-3} dm^{-3}**

To find the ratio of the masses:

Blue + Red= **8.40×10^{-3} + 1.06×10^{-2}= 0.019**

Red: moles= mass / RMV

      RMV: 829.64

1.28×10^{-5} mol/dm^{-3}= mass / 829.64 g/mol

mass= (1.28×10^{-5} mol/dm^{-3})(829.64)g/mol

mass= **1.06×10^{-2} dm^{-3}**

Blue= 8.40×10^{-3} / 0.019= **44.2%**

Red= 1.06×10^{-2} / 0.019 = **55.8%**

Blue food colourant

Solution	Concentration	Absorbance	
		at 516	at 630
Blue food colourant	?	0.05	0.49

$\varepsilon_{blue\ 516}$= 1891.6　　　　　　$\varepsilon_{blue\ 630}$= 84214

$\varepsilon_{red\ 516}$= 17753　　　　　　$\varepsilon_{red\ 630}$= 0

$$A_{total}= A_{blue}+A_{red}$$

Blue food colourant$_{516}$: 0.05= ($\varepsilon_{blue\ 516}$) ($c_{blue\ 516}$) (l) + ($\varepsilon_{red\ 516}$) ($c_{red\ 516}$) (l)

Blue food colourant$_{630}$: 0.49= ($\varepsilon_{blue\ 630}$) ($c_{blue\ 630}$) (l) + ($\varepsilon_{red\ 630}$) ($c_{red\ 630}$) (l)

Substituting values into the equation:

Blue food colourant$_{516}$: 0.05= (1891.6) ($c_{blue\ 516}$) + 17753 ($c_{red\ 516}$)

Blue food colourant$_{630}$: 0.49= (84214) ($c_{blue\ 630}$) + 0

Solving the equation for $c_{blue\ 630}$:

$c_{blue\ 630}$= 0.49 / 84214

$c_{blue\ 630}$= 5.8×10^{-6} mol/dm^{-3}

$c_{red\ 630}$= **0 mol/dm^{-3}**

Substituting these values in the equation, as the concentration of $c_{blue\,516}$ and $c_{blue\,630}$ is the same at both wavelengths:

Blue food colourant$_{516}$: $0.05 = (\varepsilon_{blue\,516})\,(c_{blue\,516})\,(l) + (\varepsilon_{red\,516})\,(c_{red\,516})\,(l)$

Blue food colourant$_{516}$: $0.05 = (1891.6)\,(5.8 \times 10^{-6}\ mol/dm^{-3}) + 17753\,(c_{red\,516})$

$c_{red\,516} =$ **$2.20 \times 10^{-6}\ mol/dm^{-3}$**

Then:

Blue food colourant$_{630} =$ **$5.8 \times 10^{-6}\ mol/dm$**$^{-3}$

Blue food colourant$_{516} =$ **$2.20 \times 10^{-6}\ mol/dm$**$^{-3}$

Converting molar concentration to mass concentration

Blue: moles= mass / RMV   Red: moles= mass / RMV

      RMV:792.84   RMV:502.44

$5.8 \times 10^{-6}\ mol/dm^{-3} =$ mass $/\ 792.84\ g/mol$ $2.20 \times 10^{-6}\ mol/dm^{-3} =$ mass $/\ 502.44\ g/mol$

mass $= (5.8 \times 10^{-6}\ mol/dm^{-3})(\ 792.84\ g/mol)$ mass $= (2.20 \times 10^{-6}\ mol/dm^{-3})(\ 502.44\ g/mol)$

mass **$= 4.60 \times 10^{-3}\ g/dm$**$^{-3}$ mass **$= 1.11 \times 10^{-3}\ g/dm$**$^{-3}$

To find the ratio of the masses.

Blue + red $= 4.6 \times 10^{-3} + 1.11 \times 10^{-3} = 5.7 \times 10^{-3}$

Blue $= (4.60 \times 10^{-3} /\ 5.7 \times 10^{-3})\ 100 =$ **80.6%**

Red $= (1.11 \times 10^{-3} / 5.7 \times 10^{-3})\ 100 =$ **19.4%**

Green food colourant

Solution	Concentration	Absorbance	
		at 426	at 632
Green food colourant	?	0.14	0.13

$\varepsilon_{blue\ 426} = 5303.4$ $\varepsilon_{blue\ 632} = 81414$

$\varepsilon_{yellow\ 426} = 23076$ $\varepsilon_{yellow\ 632} = 0$

$$A_{total} = A_{blue} + A_{yellow}$$

Green food colourant$_{426}$: $0.14 = (\varepsilon_{blue\ 426})(c_{blue\ 426})(l) + (\varepsilon_{yellow426})(c_{yellow\ 426})(l)$

Green food colourant$_{632}$: $0.13 = (\varepsilon_{blue\ 632})(c_{blue\ 632})(l) + (\varepsilon_{yellow\ 632})(c_{yellow\ 632})(l)$

Substituting values into the equation for $c_{blue\ 632}$:

Green food colourant$_{426}$: $0.14 = (5303.4)(c_{blue\ 426}) + (23076)(c_{yellow\ 426})$

Green food colourant$_{632}$: $0.13 = (81414)(c_{blue\ 632}) + 0$

Solving the equation:

$c_{blue\ 632} = 0.13/81414$

$c_{blue\ 632} = 1.5 \times 10^{-6}$ mol /dm^{-3}

$c_{red\ 632} =$ **0 mol /dm^{-3}**

Substituting these values in the equation, as the concentration of $c_{blue\ 632}$ and $c_{yellow4\ 26}$ is the same at both wavelengths:

Green food colourant$_{426}$: 0.14= (5303.4) ($c_{blue\ 426}$) + (23076) ($c_{yellow\ 426}$)

Green food colourant$_{426}$: 0.14= (5303.4) (1.5×10^{-6} mol /dm^{-3}) + (23076) ($c_{yellow\ 426}$)

$c_{yellow\ 426}$= **5.72×10^{-6} mol /dm^{-3}**

Then:

Green food colourant$_{632}$: **1.5×10^{-6} mol/dm**$^{-3}$

Green food colourant$_{426}$: **5.72×10^{-6} mol/dm**$^{-3}$

Converting molar concentration to mass concentration

Blue: moles= mass / RMV   Yellow: moles= mass / RMV

RMV:576.62   RMV:534.37

1.5×10^{-6} mol/dm^{-3}= mass / 576.62 g/mol 5.72×10^{-6} mol/dm^{-3} =x/534.37 g/mol

mass =(5.72×10^{-6} mol/dm^{-3})(534.37 g/mol)

mass =(1.5×10^{-6} mol/dm^{-3})(576.62 g/mol)

mass = **8.65^{-4} g/dm**$^{-3}$ mass = **3.06×10^{-3} g/dm**$^{-3}$

To find the ratio of the masses.

Blue + Yellow= 8.65×10^{-4} + 3.06×10^{-3}= 3.92×10^{-3}

Blue= 8.65×10^{-4}/3.92×10^{-3}) 100= **22.1%**

Yellow= (3.06×10^{-3}/ 3.92×10^{-3}) 100= **77.9%**

Appendix III: Calculation of the concentration of the disclosing solution to be used for patients

The blue component of the two tone disclosing solution was ordered from The Arnott & Co Limited (Surrey, UK), a company certified to sell dyes for human consumption (purity) and a stock solution (A) with a concentration of 1.06×10^{-2} mol / dm^{-3} was mixed (1/1000) with distilled water to create a solution with a final volume of100ml. Its absorbance at a λ_{max} at 630nm was 1.16. This result was a higher than the absorbance from the Erioglaucine used for dentures (0.85). The difference could be related to an inaccuracy of: a) the machine, b) the operator while mixing the powder, c) the operator while making the dilution or d) to a different purity of the dye. To test the hypothesis of the error due to an inaccuracy in the machine two solutions (concentration 1.06×10^{-5} mol/dm^{-3}) that were previously used and for which their absorbance was known were randomly selected and their absorbance was measured three times at 630 nm and compared against the known values. The results showed a variation of 0.03 (known absorbance 0.88, S.D.0.0 and 0.55, S.D.0.0 vs. measured absorbance 0.91, S.D.0.0 and 0.56, S.D.0.0). Therefore it was concluded that the machine registered the absorbance accurately.

To test the error related to the inaccuracy of the operator while mixing the powder a new stock solution (B) with a concentration of 1.06×10^{-2} mol/dm^{-3} was mixed and diluted 1/1000 in the same way as the previously used stock solution (a known absorbance). Its absorbance was measured three times and compared against the solution with a known absorbance. A variation of 0.02 (stock solution A 1.28, S.D.0.1 vs. Stock solution B 1.26, S.D.0.0) was found which rejects the possibility of an error while mixing the powder.

The error related to an inaccuracy from the operator while mixing the dilutions was tested by using the stock solution A to make a new dilution (1/1000) and measuring its absorbance. This value was compared against the absorbance of the known dilution and the results showed a variation of 0.03 Stock A, dilution one 1.26±0.0, dilution two 1.23±0.0) which rejected the possibility of an error while preparing the dilutions.

The last option was to verify the purity of the dye. Thirteen serial dilutions were made from the stock solution A with a dilution factor of 1:2. Their absorbance was measured and the mean and standard deviation were calculated. The obtained data (dilutions 9 to 13) were plotted in excel and a calibration curve (absorbance vs. concentration) was obtained.
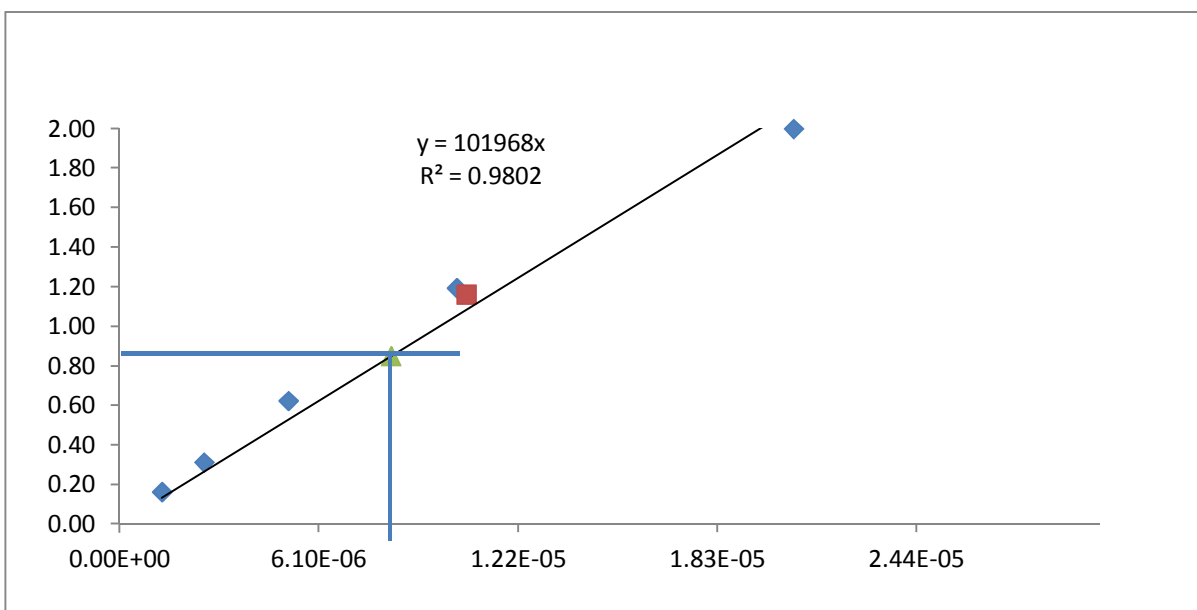
The regression line was used to deduct that for an absorbance of 0.85 with the dye for humans it is necessary to mix a solution with a concentration of 8.3×10^{-2} mol/dm^{-3}. As a final step, to verify this founding a new solution was mixed (0.66g/100ml of distilled water) and a dilution of 1/1000 was made. Its absorbance was measured fining an absorbance value of 0.83, S.D.0.0.

The concentration of the same dye varies between both companies and applications. For this investigation a dye suitable for human consumption was needed therefore the concentration at a known absorbance was calculated. For an absorbance of 0.85 with the Erioglaucine from Thew Arnott & Co a concentration of 8.3×10^{-2} mol / dm^{-3} is needed. The table below summarises the findings.

dye	percentage	Absorbance	Concentration	In 1L	In 100ml
Sigma	70.5%	0.85	1.06×10^{-2} mol / dm^{-3}	8.4 g/L	0.84g
patients	85%	0.85	8.3×10^{-2} mol / dm^{-3}	6.6g/L	0.66g
	85%	1.16	1.06×10^{-2} mol / dm^{-3}	8.4 g/L	0.84g

Formulas used:

$y = 101968x$

$0.85 = 101968x$

$x = 8.3 \times 10^{-6}$ mols

moles = mass/RMV

RMV = 792.84g

8.3×10^{-6} mols $= x/792.84$

$x = (8.3 \times 10^{-6}$ mols$) (792.84)$

Appendix IV: Ethical approval

Appendix V: Macros used in ImageJ for the analysis of the images

Correction of the visible, red and n-IR images (with chart)-Black background

```
// Opens the directory. Corrects and saves visible image.
//Opens red image, duplicates it, saves it in 8-bits. Opens a copy of that image and makes RGB stack saving only
the red channel.
//Opens the n-IR image, makes the RGB stack and saves only the red channel.
/Stacks the 4 images and saves them.

//first image is DSC_0001
dir1 = getDirectory("Choose Source Directory");
photoIndex=39;

image1="DSC_00"+photoIndex+".NEF";
print(dir1);
run("DCRaw Reader...", "open=["+dir1+image1+ "] white=None read=[8-bit non-linear] interpolation=[0 - High-
speed, low-quality bilinear]");
a=getTitle();
a1=substring(a, 0, lengthOf(a)-4); // strip the ".tiff"
waitForUser("Draw line from black to white");
 //makeLine(2391, 66, 477, 69);
run("Chart White Balance", "chart=[Small Macbeth ColourChecker Chart] include");
selectWindow(a);
saveAs("Tiff", dir1+a1+"visible.tif");
close();
photoIndex++;
numString = "00"+photoIndex;
numString= substring(numString, lengthOf(numString)-4, lengthOf(numString));
image2= substring(image1, 0, lengthOf(image1)-8)+numString+".NEF";
run("DCRaw Reader...", "open=["+dir1+image2+ "] white=None read=[8-bit non-linear] interpolation=[0 - High-
speed, low-quality bilinear]");
a=getTitle();
a2=substring(a, 0, lengthOf(a)-4); // strip the ".tiff"
run("Duplicate...", "title=red8bits");
run("8-bit");
saveAs("Tiff", dir1+a2+"red8bits.tif");
close();
selectWindow(a);
run("RGB Stack");
setSlice(1);
run("Duplicate...", "title=red");
saveAs("Tiff", dir1+a2+"red");
close();
selectImage(a);
close();
// change this!
//open("/home/gabriel/ImageJ/plaque/examples/DSC_0023nir8bitshotspot_scaled.tif");
open("C:\\Documents and Settings\\Jocelyn\\My Documents\\My Pictures\\PictureProject\\Pictures of
dentures\\apatients black backwground\\hotspotf22black bw\\DSC_0023nir8bitshotspot_scaled.tif");
photoIndex++;
numString = "00"+photoIndex;
numString= substring(numString, lengthOf(numString)-4, lengthOf(numString));
image3= substring(image1, 0, lengthOf(image1)-8)+numString+".NEF";
run("DCRaw Reader...", "open=["+dir1+image3+ "] white=None read=[8-bit non-linear] interpolation=[0 - High-
speed, low-quality bilinear]");
a=getTitle();
a3=substring(a, 0, lengthOf(a)-4); // strip the ".tiff"
selectImage(a);
run("RGB Stack");
setSlice(1);
run("Duplicate...", "title=nir");
selectImage("nir");
imageCalculator("Subtract", "nir","DSC_0023nir8bitshotspot_scaled.tif");
```

```
saveAs("Tiff", dir1+a3+"nir.tif");
close();
selectImage(a);
close();
selectImage("DSC_0023nir8bitshotspot_scaled.tif");
close();
open(dir1+a1+"visible.tif" );
open(dir1+a2+"red8bits.tif" );
open(dir1+a2+"red.tif" );
open(dir1+a3+"nir.tif" );
run("Images to Stack", "name=Stack title=[] use");
saveAs("Tiff", dir1+"Stack"+a1+".tiff");
close();
```

Correction of the visible, red and n-IR images (with chart)-White background

```
//Opens the directory. Corrects and saves visible image.
//Opens red image, duplicates it, saves it in 8-bits. Opens a copy of that image and makes RGB stack saving only
the red channel.
//Opens the n-IR image, makes the RGB stack and saves only the red channel.
/Stacks the 4 images and saves them.


//first image is DSC_0001
dir1 = getDirectory("Choose Source Directory");
photoIndex=39;
image1="DSC_00"+photoIndex+".NEF";
print(dir1);
run("DCRaw Reader...", "open=["+dir1+image1+ "] white=None read=[8-bit non-linear] interpolation=[0 - High-
speed, low-quality bilinear]");
a=getTitle();
a1=substring(a, 0, lengthOf(a)-4); // strip the ".tiff"
waitForUser("Draw line from black to white");
 //makeLine(2391, 66, 477, 69);
run("Chart White Balance", "chart=[Small Macbeth ColorChecker Chart] include");
selectWindow(a);
saveAs("Tiff", dir1+a1+"visible.tif");
close();
photoIndex++;
numString = "00"+photoIndex;
numString= substring(numString, lengthOf(numString)-4, lengthOf(numString));
image2= substring(image1, 0, lengthOf(image1)-8)+numString+".NEF";
run("DCRaw Reader...", "open=["+dir1+image2+ "] white=None read=[8-bit non-linear] interpolation=[0 - High-
speed, low-quality bilinear]");
a=getTitle();
a2=substring(a, 0, lengthOf(a)-4); // strip the ".tiff"
run("Duplicate...", "title=red8bits");
run("8-bit");
saveAs("Tiff", dir1+a2+"red8bits.tif");
close();
selectWindow(a);
run("RGB Stack");
setSlice(1);
run("Duplicate...", "title=red");
saveAs("Tiff", dir1+a2+"red");
close();
selectImage(a);
close();
// change this!
//open("/home/gabriel/ImageJ/plaque/examples/DSC_0023nir8bitshotspot_scaled.tif");
open("C:\\Documents and Settings\\Jocelyn\\My Documents\\My Pictures\\PictureProject\\Pictures of
dentures\\apatients black backwground\\hotspotf22black bw\\DSC_0023nir8bitshotspot_scaled.tif");
photoIndex++;
numString = "00"+photoIndex;
numString= substring(numString, lengthOf(numString)-4, lengthOf(numString));
```

```
image3= substring(image1, 0, lengthOf(image1)-8)+numString+".NEF";
run("DCRaw Reader...", "open=["+dir1+image3+ "] white=None read=[8-bit non-linear] interpolation=[0 - High-
speed, low-quality bilinear]");
a=getTitle();
a3=substring(a, 0, lengthOf(a)-4); // strip the ".tiff"
selectImage(a);
run("RGB Stack");
setSlice(1);
run("Duplicate...", "title=nir");
selectImage("nir");
imageCalculator("Subtract", "nir","DSC_0023nir8bitsshotspot_scaled.tif");
saveAs("Tiff", dir1+a3+"nir.tif");
close();
selectImage(a);
close();
selectImage("DSC_0023nir8bitsshotspot_scaled.tif");
close();
open(dir1+a1+"visible.tif" );
open(dir1+a2+"red8bits.tif" );
open(dir1+a2+"red.tif" );
open(dir1+a3+"nir.tif" );
run("Images to Stack", "name=Stack title=[] use");
saveAs("Tiff", dir1+"Stack"+a1+".tiff");
close();
```

Hot spot elimination-DBB

//It is necessary to change manually the image number.

```
imageCalculator("Subtract create", "DSC_0003nir8bits.tif","DSC_0023nir8bitsshotspot.tif");
selectWindow("Result of DSC_0003nir8bits.tif");
run("Save", "save=[C:\\Documents and Settings\\Jocelyn\\My Documents\\My
Pictures\\PictureProject\\111\\DSC_0003nir8bitscorrected.tif]");
close();
selectWindow("DSC_0003nir8bits.tif");
close();
```

Hot spot elimination-DWB

//It is necessary to change manually the image number.

```
//run("Calculator Plus", "i1=DSC_0021nir8bits.tif i2=F22(DSC_0057)-ir.tif operation=[Divide: i2 = (i1/i2) x k1 + k2]
k1=200 k2=0 create");
//run("Save", "save=[C:\\Documents and Settings\\Jocelyn\\My Documents\\My
Pictures\\PictureProject\\111\\DSC_0021correctedby200.tif]");
//close();
//selectWindow("DSC_0021nir8bits.tif");
//close();
```

Images comparisons: Sensitivity and specificity

//compares the 0's and 1's mask vs. the 2's and 4's. Gives specificity and sensitivity. It is necessary to indicate the image number.

```
//meth=newArray("Default", "Huang", "Intermodes", "IsoData", "Li", "MaxEntropy", "Mean", "MinError(I)",
"Minimum", "Moments", "Otsu", "Percentile", "RenyiEntropy", "Shanbhag", "Triangle", "Yen");
```

```
//image 08
//imageCalculator("Add create", "visible_44-cropped_handdrawn-mask.tif", "thresolding_default_bluevisiblevsred-
mask-0044");
```

```
imageCalculator("Add create", "visible_59-cropped_handdrawn-mask.tif", "thresolding_huang_bluevisiblevsred-2-
mask-0059");
```

```
print ("huang59B\tTN\tFP\tFN\tTP\tTNR\tTPR\tACC\tPPV\tNPV\tFDR\tMCC");
```

```
nBins = 256;

getHistogram(values, counts, nBins);
  TN=counts[2];
  FN=counts[3];
  FP=counts[4];
  TP=counts[5];
N=TN+FP;
P=TP+FN;
TNR=TN/N;
TPR=TP/P;
ACC=(TP+TN) / (P+N);
PPV=TP/(TP+FP);
NPV=TN/(TN+FN);
FDR=FP/(FP+TP);
//MCC=((TP)(TN)-(FP)(FN))/(raiz)PNP'N'
MCC=(TP*TN-FP*FN)/(sqrt((TP+FP)*(TP+FN)*(TN+FP)*(TN+FN)));

rename("Result-visible59hand-vs-huang-2");

run("Save");

print ("*
"+"\t"+TN+"\t"+FP+"\t"+FN+"\t"+TP+"\t"+TNR+"\t"+TPR+"\t"+ACC+"\t"+PPV+"\t"+NPV+"\t"+FDR+"\t"+MCC);
```

Smooth ROI3

```
for (j=0;j<100;j++){
run("Properties...", "origin="+(getWidth()/2)+","+(getHeight()/2));
getSelectionCoordinates(x, y);
run("Select None");
makeSelection("polygon", x, y);
l=x.length;
nx=newArray(l);
ny=newArray(l);
for (i=1;i<l-1;i++){
 nx[i]=round(((x[i-1]+x[i]+x[i+1])/3)+random-0.5);
 ny[i]=round(((y[i-1]+y[i]+y[i+1])/3)+random-0.5);
}
nx[0]=round(((x[l-1]+x[0]+x[1])/3)+random-0.5);
ny[0]=round(((y[l-1]+y[0]+y[1])/3)+random-0.5);
nx[l-1]=nx[0];
ny[l-1]=ny[0];
run("Select None");
makeSelection("polygon", nx, ny);
run("Properties...", "origin=0,0");}
```

Appendix VI: Diagnostic Sciences Group of the IADR Student award.

List of references

ABELSON, D. 1981. Denture plaque and denture cleansers *The Journal of Prosthetic dentistry,* 45**,** 376-379.

ADAMS, R. & BISCHOF, L. 1994. Seeded region growing. *IEEE Transactions on Pattern Analysis and Machine Intelligence,* 16**,** 641-647.

ADDY, M., RENTON-HARPER, P. & MYATT, G. 1998. A plaque index for occlusal surfaces and fissures. Measurement of repeatability and plaque removal. *Journal of Clinical Periodontology,* 25**,** 164-168.

ADDY, M., WILLIS, L. & MORAN, J. 1983. Effect of toothpaste rinses compared with chlorhexidine on plaque formation during a 4-day period. *Journal of Clinical Periodontology,* 10**,** 89-99.

ADEYEMI, A. A., JARAD, F. D., PENDER, N. & HIGHAM, S. M. 2006. Comparison of quantitative light-induced fluorescence (QLF) and digital imaging applied for the detection and quantification of staining and stain removal on teeth. *Journal of Dentistry,* 34**,** 460-466.

AINAMO, J. & BAY, I. 1975. Problems and proposals for recording gingivitis and plaque. *Internationa Dental Journal,* 25**,** 229-235.

ALTMAN, D. G. 1991. *Practical statistics for medical research,* London, Chapman and Hall.

ALTMAN, D. G. & BLAND, J. M. 1983. Measurements in medicine: The analysis of method comparison studies. . *The Statistician,* 32**,** 307-317.

AMAECHI, B. T. & HIGHAM, S. M. 2002. Quantitative light-induced fluorescence: A potential tool for general dental assessment. *Journal of Biomedical Optics,* 7**,** 7-13.

AMBJØRNSEN, E., RISE, J. & HAUGEJORDEN, O. 1984. A study of examiner errors associated with measurement of dental plaque. *Acta Odontologica Scandinavica,* 42**,** 183-191.

AMBJØRNSEN, E., VALDERHAUG, J., NORHEIM, P. W. & FLØYSTRAND, F. 1982. Assessment of an additive index for plaque accumulation on complete maxillary dentures. *Acta Odontologica Scandinavica,* 40**,** 203-208.

AMINI, P., ARAUJO, M. W. B., WU, M.-M., CHARLES, C. A. & SHARMA, N. C. 2009. Comparative antiplaque and antigingivitis efficacy of three antiseptic mouthrinses: a two week randomized clinical trial. *Brazilian Oral Research,* 23**,** 319-325.

ANDREY, P. & BOUDIER, T. 2006. Adaptive active contours (snakes) for the segmentation of complex structures in biological images.

ANGMAR-MANSSON, B. & TEN BOSCH, J. J. 2001. Quantitative light-induced fluorescence (QLF): a method for assessment of incipient caries lesions. *Dentomaxillofacial Radiology,* 30**,** 298-307.

ANGMAR-MASSON, B. & TEN BOSCH, J. J. 1987. Optical methods for the detection and quantification of caries. *Advances in Dental Reseach,* 1**,** 14-20.

ANNARATONE, M. & RUSCELLO, C. 2006. Digital Infrared Photography. Part one. Available: http://www.infraredphoto.eu/Site/GentleIntro1.html [Accessed September 2011].

ANUSAVICE, K. J. 2005. Present and Future Approaches for the Control of Caries. *Journal of Dental Education,* 69**,** 538-554.

ARYA, B. S., SAVARA, B. S., THOMAS, D. & CLARKSON, Q. 1974. Relation of sex and occlusion to mesiodistal tooth size. *American Journal of Orthodontics,* 66**,** 479-486.

AXELSSON, P. 2000. *Diagnosis and risk prevention of dental caries,* Chicago, Quintessence Publishing Co, Inc.

BANKMAN, I. N. 2000. Handbook of medical imaging. Processing and analysis. San Diego, USA: Academic Press.

BARAK, S., OETTINGER-BARAK, O., OETTINGER, M., MACHTEI, E. E., PELED, M. & OHEL, G. 2003. Common Oral Manifestations During Pregnancy: A Review. *Obstetrical & Gynecological Survey,* 58**,** 624-628.

BASS, C. C. 1954. An effective method of personal oral hygiene. *Journal of the Louisiana Medical Society,* 106**,** 100-112.

BAY, I., KARDEL, K. M. & SKOUGAARD, M. R. 1967. Quantitative evaluation of the plaque-removing ability of different types of toothbrushes. *Journal of Periodontology,* 38**,** 526-533.

BENGEL, W. 2002. *Mastering dental photography,* Berlin, Quintessenz-Verlags-GmbH.

BENSON, B. J., HENYON, G., GROSSMAN, E., MANDOKI, S. & SHARMA, N. C. 1993. Development and verification of the proximal/marginal plaque index. *Journal of Clinical Dentistry,* 4**,** 14-20.

BERGSTRÖM, J. 1980. Photogrammetric registration of dental plaque accumulation in vivo. *Acta Odontologica Scandinava,* 39**,** 275-284.

BERRY, E. 2008. *A practical approach to medical imaging processing,* Florida, Taylor and Francis group.

BIRKELAND, J. M. & JORKJEND, L. 1975. The influence of examination on the assessment of the intra-examiner error by using the Plaque and Gingival index systems. *Community Dentistry and Oral Epidemiology,* 3**,** 214-216.

BLAND, J. M. & ALTMAN, D. G. 1986. Statistical methods for assessing agreement between two methods of clinical measurement. *The Lancet,* 307-310.

BLOCK, P. L., LOBENE, R. R. & DERDIVANIS, J. P. 1972. A two-tone dye test for dental plaque. *Journal of Periodontology,* 43**,** 423-426.

BONFERRONI, C. E. 1937. *Teoria statistica delle classi e calcolo delle probabilita. Volume in Onore di Ricarrdo dalla Volta,* Florence, Italy: Universita di Firenza.

BOTTICELLI, S., VERNA, C., CATTANEO, P. M., HEIDMANN, J. & MELSEN, B. 2010. Two- versus three-dimensional imaging in subjects with unerupted maxillary canines. *The European Journal of Orthodontics*.

BOWERS, M. 2010. *Forensic Dental Evidence: An investigator's handbook*, Elsevier Ltd.

BRAND, R. W. & ISSELHARD, D. E. 1994. *Anatomy of orofacial structures,* St. Louis Missouri, Mosby.

BRATTHALL, D. 2005. Estimation of global DMFT for 12-year-olds in 2004. *International Dental Journal,* 55 370-372.

BROWN, L. J., JOHNS, B. A. & WALL, T. P. 2002. The economics of periodontal diseases. *Periodontology 2000,* 29**,** 223-234.

BROWN, S. B. 1980. *An introduction to spectroscopy for biochemists.,* London, Academic Press.

BRUHN, J., LEHMANN, L. E., RÖPCKE, H., BOUILLON, T. W. & HOEFT, A. 2001. Shannon Entropy Applied to the Measurement of the Electroencephalographic Effects of Desflurane. *Anesthesiology,* 95**,** 30-35.

BUCHNER, A. & BAUMGARTNER, N. 2007. Text – background polarity affects performance irrespective of ambient illumination and colour contrast. *Ergonomics,* 50**,** 1036-1063.

BUDTZ-JØRGENSEN, E. 1979. Materials and methods for cleaning dentures. *Journal of Prosthetic Dentistry,* 42**,** 619-623.

BÜHLER, C. M., HNGAOTHEPPITAK, P. & FRIED, D. 2005. Imaging of occlusal dental caries (decay) with near-IR light at 1310nm. *Optics Express,* 13**,** 573-579.

BURGER, W. & BURGE, M. J. 2008. *Digital image processing: An algorithmic introduction using Java*, Springer.

CARIDE, E. & MEISS, A. 1981. Simple method for preparation of disclosing solutions using food coloring. Evaluation of its worth in prevention and treatment in dentistry. *Revista de la Asociación Odontológica Argentina,* 69**,** 349-352.

CARRANZA, F. A. & NEWMAN, M. G. 1996. *Clinical Periodontology.* , W B Saunders Company.

CARTER, K., LANDINI, G. & WALMSLEY, A. D. 2004. Automated quantification of dental plaque accumulation using digital imaging. *Journal of Dentistry,* 32**,** 623-8.

CARVALHO, J. C., EKSTRAND, K. R. & THYLSTRUP, A. 1989. Dental plaque and caries on occlusal surfaces of first permanent molars in relation to stage of eruption. *Journal Dental Research,* 68**,** 773-779.

CASIGLIA, J. M., MIROWSKI, G. W. & FLOWERS, F. 2009. Oral manifestations of systemic diseases. *Medscape reference*.

CATÃO, C., RAMOS, I., SILVA--NETO, J., DUARTE, S., BATISTA, A. & DIAS, A. 2007. Eficiência de substâncias químicas na remoção do biofilme em próteses totais. *Revista de Odontologia da UNESP,* 36**,** 53-60.

CHAPPLE, I. & GILBERT, A. 2002a. How does plaque cause disease? . *Understanding periodontal diseases: Assessment and diagnostic procedures in practice.* Quintessence Publishing Co. Inc.

CHAPPLE, I. & GILBERT, A. 2002b. *Understanding periodontal diseases: Assessment and diagnostic procedures in practice,* London, Quintessentials Publishing Co. Ltd.

CHILTON, N. W., DIDIO, A. & ROTHNER, J. T. 1962. Comparison of the clinical effectiveness of an electric and a standard toothbrush in normal individuals. *The Journal of the American Dental Association,* 64**,** 777-782.

CLAYDON, N. & ADDY, M. 1995. The use of planimetry to record and score the modified Navy index and other area-based plaque indices. A comparative toothbrush study. *Journal of Clinical Periodontology,* 22**,** 670-673.

COE, C. & WESTON, W. 2010. Creative DSLR photography: the ultimate creative work.: University of Birmingham (electronic resource).

COFFIN, D. 1997. *DCRaw* [Online]. Boston. Available: http://www.cybercom.net/~dcoffin/dcraw/ [Accessed September 2011].

COHEN, D. W., STOLLER, N. H., CHACE, R., JR. & LASTER, L. 1972. A comparison of bacterial plaque disclosants in periodontal disease. *Journal of Periodontology,* 43**,** 333-338.

COHEN, J. 1968. Weighted kappa: Nominal scale agreement provision for scaled disagreement or partial credit. *Psychological Bulletin,* 70**,** 213-220. .

COHEN, K. 1960. A coefficient agreement for nominal scales. . *Education and Psychological measurement,* 1960**,** 37-47.

CONNOR, J. N., SCHOENFELD, C. M. & TAYLOR, R. L. 1976. Study of In Vivo Plaque Formation. *Journal of Dental Research,* 55**,** 481-488.

CONSUMERS' ASSOCIATION AND HODDER & STOUGHTON 1988. *Understanding Additives. Which? ,* London, UK, Books.

COONTZ, E. J. 1983. The effectiveness of a new oral hygiene device on plaque removal. *Quintessence International Dental Digest,* 14**,** 739-742.

COULTHWAITE, L., PRETTY, I. A., SMITH, P. W., HIGHAM, S. M. & VERRAN, J. 2009. QLF is not readily suitable for in vivo denture plaque assessment. *Journal of Dentistry,* 37**,** 898-901.

COULTHWAITE, L. & VERRAN, J. 2007. Potential pathogenic aspects of denture plaque. *British Journal of Biomedical Science,* 64**,** 180-189.

COULTHWAITE, L. & VERRAN, J. 2009. Evaluation of in vivo denture plaque assessment methods. *British Dental Journal,* 207**,** E12; discussion 282-283.

COUNCIL OF DENTAL THERAPEUTICS 1985. Guidelines for acceptance of chemotherapeutic products for the control of supragingival dental plaque and gingivitis. *Journal of the American Dental Association,* 112**,** 529-532.

DABABNEH, R. H., KHOURI, A. T., SMITH, R. G. & ADDY, M. 2002. Correlation and examiner agreement between a new method of plaque scoring and a popular established plaque index, modelled in vitro. *Journal of Clinical Periodontology,* 29**,** 1107-1111.

DALAL, M. D. & DAVER, B. M. 1996. Computer generated slides: a need to curb our enthusiasm. *British Journal of Plastic Surgery,* 49**,** 568-571.

DANISH, M. Year. Teeth Segmentation and Feature Extraction for Odontological Biometrics. *In:* STEPHEN, D. W. & CHRISTOPH, B., eds., 2010. 323-328.

DAVIES, R. M. & DAVIES, G. M. 2005. Periodontal disease and general health. *Dental Update,* 32**,** 438-442.

DAWES, C. 2003. What is the critical pH and why does a tooth dissolve in acid? *Journal of the Canadian Dental Association,* 69**,** 722-724.

DE CASTELLUCCI BARBOSA, L., FERREIRA, M. R. M., DE CARVALHO CALABRICH, C. F., VIANA, A. C., DE LEMOS, M. C. L. & LAURIA, R. A. 2008. Edentulous patients' knowledge of dental hygiene and care of prostheses. *Gerodontology,* 25**,** 99-106.

DE JOSSELIN DE JONG, E., HIGHAM, S. M., SMITH, P. W., VAN DAELEN, C. J. & VAN DER VEEN, M. H. 2009. Quantified light-induced fluorescence, review of a diagnostic tool in prevention of oral disease. *Journal of Applied Physics,* 105**,** 102031-102037.

DE MENT, J. & CULBERTSON, R. 1951. Comparative photography in dental science. *Dental Radiography and Photography,* 24**,** 28-35.

DE SOUZA, R. F., DE FREITAS OLIVEIRA PARANHOS, H., LOVATO DA SILVA, C. H., ABU-NABA'A, L., FEDOROWICZ, Z. & GURGAN, C. A. 2009. Interventions for cleaning dentures in adults. *Cochrane Database of Systematic Reviews*

DEBROUX, S. T., MCCAUL, K. K., SHIMAMOTO, S. & BROOKS, M. J. 2007. Infrared Photography. Available: htpp:

www.neiai.org/index.php?option=com_docman&task=doc_download&gid=28&Itemid=54 De Broux ST, Forensic Photography III [Accessed September 2011].

DEMENT, J. & CULBERTSON, R. 1951. Comparative photography in dental science. *Dental Radiography and Photography* 24**,** 28-34.

DIFFEY, B. L. 2002. Sources and measurement of ultraviolet radiation. *Methods,* 28**,** 4-13.

DIKBAS, I., KOKSAL, T. & CALIKKACAOGLU, S. 2006. Investigation of the cleanliness od dentures in a university hospital. *International Journal of Prosthodontics,* 19**,** 294-298.

DOMBRET, B., MATTHIJS, S. & SABZEVAR, M. M. 2003. Interexaminer reproducibility of ordinal and interval-scaled plaque indices. *Journal of Clinical Periodontology,* 30**,** 630-5.

DORLAND'S, D. N. 1988. *Illustrated Medical Dictionary,* Philadelphia, USA, WB Saunders College Publishing.

DOYLE, W. 1962. Operation useful for similarity-invariant pattern recognition. *Journal of the Association for Computing Machinery,* 9**,** 259-267.

DUNN, G. 1992. Review papers : Design and analysis of reliability studies. *Statistical Methods in Medical Research,* 1**,** 123-157.

EATON, K. A., RIMINI, F. M., ZAK, E., BROOKMAN, D. J. & NEWMAN, H. N. 1997. The achievement and maintenance of inter-examiner consistency in the assessment of plaque and gingivitis during a multicentre study based in general dental practices. *Journal of Clinical Periodontology,* 24**,** 183-188.

ELLIOT, J. R., BOWERS, M. G., CLEMMER, B. A. & ROVELSTAD, G. H. 1972. Evaluation of an oral physiotherapy center in the reduction of bacterial plaque and periodontal disease. *Journal of Periodontology,* 4**,** 221-224.

FDI 1984. The prevention of dental caries and periodontal disease. *International Dental Journal,* 34**,** 141-158.

FEHRENBACH, M. J. & HERRING, S. W. 2007. *Illustrated anatomy of the head and neck,* Canada, Saunders Elevier.

FEJERSKOV, O. & KIDD, E. A. M. V. 2008. *Dental caries: the disease and its clinical management,* Oxford., Blackwell Munksgaard.

FELTON, D., COOPER, L., DUQUM, I., MINSLEY, G., GUCKES, A., HAUG, S., MEREDITH, P., SOLIE, C., AVERY, D. & CHANDLER, N. D. 2011. Evidence-based guidelines for the care and maintenance of complete dentures. *The Journal of the American Dental Association,* 142**,** 1S-20S.

FISHMAN, S., CANCRO, L. P., PRETARA-SPANEDDA, P. & JACOBS, D. 1987. Distal mesial plaque index: a technique for assessing dental plaque about the gingival. *Dental Hygiene* 61**,** 404-409.

FISHMAN, S. L. 1979. Design studies to evaluate plaque control agents. *Journal of Dental Research,* 58**,** 2389-2395.

FISHMAN, S. L. 1986. Current status of indices of plaque. *Journal of Clinical Periodontology* 13**,** 371-374.

FLEISS, J. L., CHILTON, N. W. & PARK, M. H. 1980. Inter- and intra-examiner variability in scoring supragingival plaque: II. Statistical analysis. *Pharmacology and Therapeutics in Dentistry,* 5**,** 5-9.

FOOD ADDITIVES AND INGREDIENTS ASSOCIATION & CENTRE., A. T. C. I. E. 2008. *Understanding Food Additives'* [Online]. Available:

www.Understandingfoodadditives.Org/Pages/Ch6p1.Htm, [Accessed September 2011].

FOOD STANDARDS AGENCY. 2010. Current EU approved additives and their E Numbers. Available: Www.Food.Gov.Uk/ [Accessed April 2011].

FREEMAN, H. S. & OETERS, A. T. 2000. Colorants for non textile applications. *Color additives for foods, drugs and cosmetics.* Elsevier Science.

FRIED, D., FEATHERSTONE, J. D. B., DARLING, C. L., JONES, R. S., NGAOTHEPPITAK, P. & BÜHLER, C. M. 2005. Early caries imaging and monitoring with near-infrared light. *Dental Clinics of North America,* 49**,** 771-793.

FU, K. S. & MUI, J. K. 1981. A survey on image segmentation. *Pattern Recognition,* 13**,** 3-16.

FURUICHI, Y., LINDHE, J., RAMBERG, P. & VOLPE, A. R. 1992. Patterns of de novo plaque formation in the human dentition. *Journal of Clinical Periodontology,* 19**,** 423-433.

GALLAGHER, I. H., FUSSELL, S. J. & CUTRESS, T. W. 1977. Mechanism of action of a two-tone plaque disclosing agent. *Journal of Periodontology,* 48**,** 395-396.

GEDLING, C. 2009. *RE: Standards Agency. Novel foods, additives, and supplements division.*

GENDREAU, L. & LOEWY, Z. G. 2011. Epidemiology and Etiology of Denture Stomatitis. *Journal of Prosthodontics,* 20**,** 251-260.

GIBSON, H. L. 1973. *Medical photography: clinical Ultraviolet and infrared. ,* Rochester N.Y., Eastman Kodak company.

GILLINGS, B. R. 1977. Recent developments in dental plaque disclosants. *Australian Dental Journal,* 22**,** 260-266.

GILMORE, N. D. & CLARK, R. E. 1975. Comparison of wet weight of plaque and a plaque index. *Journal Dental Research,* 54**,** 422.

GLASBEY, C. A. 1993. An analysis of histogram-based thresholding algorithms. *CVGIP: Graphical Models and Image Processing* 55**,** 532-537.

GOMEZ, C. & HORNERO, R. 2010. Entropy and complexity analysis in Alzheimer's disease: An MEG study *The Open Biomedical Engineering Journal,* 4**,** 223-235.

GRANT, D. A., STERN, I. B. & LISTGARTEN, M. A. 1988. *Periodontics*, The C.V. Mosby Company.

GRECO, M., STUCCHI, N., ZAVAGNO, D. & MARINO, B. 2008. On the Portability of Computer-Generated Presentations: The Effect of Text-Background Color Combinations on Text Legibility. *Human Factors: The Journal of the Human Factors and Ergonomics Society,* 50**,** 821-833.

GREEN, B. F. & ANDERSON, L. K. 1956. Color coding in a visual search task. *Journal of Experimental Psychology,* 51**,** 19-24.

GREEN, J. & VERMILLON, J. 1960. The Oral Hygiene Index- A Method for classifying oral hygiene status. *The Journal of the American Dental Association,* 61**,** 29-35.

GREEN, J. & VERMILLON, J. 1964. The simplified oral hygiene index. *The Journal of the American Dental Association,* 68**,** 7-13.

GREEN, J. C. 1967. The Oral Hygiene Index- Development and Uses. *Journal of Periodontology,* 38**,** 53-63.

GWINNETT, A. J. & CEEN, R. F. 1978. An ultraviolet photographic technique for monitoring plaque during direct bonding procedures. *American Journal of Orthodontics,* 73**,** 178-186.

HAGIWARA, A., SANO, M., ICHIHARA, T., YOSHINO, H., MIYATA, E., TAMANO, S., AOKI, H., YUKAWA, C., KODA, T., NAKAMURA, M. & SHIRAI, T. 2003. Four week oral toxicity study of 1-Carboxy-5,7-Dibromo-6-Hydroxy-2,3,4-Trichloroxanthone (HXCA), An impurity of phloxine B in F344 rats. *The Journal of Toxicological Sciences,* 28**,** 445-453.

HALL, A. & GIRKIN, J. M. 2004. A Review of Potential New Diagnostic Modalities for Caries Lesions. *Journal of Dental Research,* 83**,** C89-C94.

HALL, R. & HANNA, P. 2004. The impact of web page text-background color combinations on readability, retention, aesthetics, and behavioral Intention. *Behaviour and Information Technology,* 23**,** 183-195.

HAMMOND, J. H. 1981. *The Camera Obscura. A Chronicle.,* Bristol, Taylor & Francis, Inc.

HANCOCK, E. B. & WIRTHLIN, M. R., JR. 1977. An evaluation of the Navy Periodontal Screening Examination. *Journal of Periodontology,* 48**,** 63-66.

HANSSEN, M. 1984. *E for Additives. The complete E number guide* Wellingborough, Northamptonshire., Thorsons Publishers Limited.

HARRAP, G. J. 1974. Assessment of the effect of dentifrices on the growth of dental plaque. *Journal of Clinical Periodontology,* 1**,** 166-174.

HARRIS, O. & GARCIA-GODOY, F. 1999. *Primary Preventive Dentistry*, USA: Appleton and Lange.

HATTAB, F. N., AL-KHATEEB, S. & SULTAN, I. 1996. Mesiodistal crown diameters of permanent teeth in jordanians. *Archives of Oral Biology,* 41**,** 641-645.

HEFFERREN, J. J., COOLEY, R. O., HALL, J. B., OLSEN, N. H. & LYON, H. W. 1971. Use of ultraviolet illumination in oral diagnosis. *Journal of American Dental Association,* 82**,** 1353-1360.

HERMANSON, A. S., BUSH, M. A., MILLER, R. G. & BUSH, P. J. 2008. Ultraviolet Illumination as an Adjunctive Aid in Dental Inspection*. *Journal of Forensic Sciences,* 53**,** 408-411.

HIRASUNA, K., FRIED, D. & DARLING, C. L. 2008. Near-infrared imaging of developmental defects in dental enamel. *Journal of Biomedical Optics,* 13**,** 044011.

HOAD-REDDICK, G., GRANT, A. A. & GRIFFITHS, C. S. 1990. Investigation into the cleanliness of dentures in an elderly population. *The Journal of Prosthetic Dentistry,* 64**,** 48-52.

HOPE, C. K. & WILSON, M. 2006. Biofilm structure and cell vitality in a laboratory model of subgingival plaque. *Journal of Microbiological Methods,* 66**,** 390-398.

HOTZ, P., GUGGENHEIM, B. & SCHMID, R. 1972. Carbohydrates in pooled dental plaque. *Caries Research,* 6**,** 103-121.

HUANG, L. K. & WANG, M. J. 1995. Image thresholding by minimizing the measures of fuzzines. *Pattern Recognition,* 28**,** 41-51.

HUNT, R. J. 1986. Percent Agreement, Pearson's Correlation, and Kappa as Measures of Inter-examiner Reliability. *Journal of Dental Research,* 65**,** 128-130.

HUTCHINSON, I. & WILLIAMS, P. 1999. Digital Cameras. *Journal of Orthodontics,* 26**,** 326-331.

IRELAND, R. 2006. Dental caries and pulpitis. *Clinical textbook of dental hygiene and therapy.* Blackwell Munksgaard, a Blackwell Publishing Company.

JACKSON, P. L. 1983. An easy to use BASIC program for agreement amongst many raters. *British Journal of Clinical Psychology,* 22**,** 145-156.

JAGGER, D. C. & HARRISON, A. 1995. Denture cleansing--the best approach. *Br Dent J,* 178**,** 413-417.

JAREK, S. 2011. Seeded Region Growing (ImageJ Plugin).

JEGANATHAN, S., THEAN, H. P., THONG, K. Y., CHAN, Y. C. & SINGH, M. 1996 A clinically viable index for quantifying denture plaque. *Quintessence international* 27**,** 569-573.

JENKINSON, H. F. & LAMONT, R. J. 2005. Oral microbial communities in sickness and in health. *Trends in Microbiology,* 13**,** 589-595.

KANG, J. Y., LI, X., QINGXIAN, L., LIU, J. Z. & MIN, L. Q. 2006. Dental plaque quantification using cellular neural network-based image segmentation. *Lecture notes in control and information sciences,* 345**,** 797-802.

KANG, J. Y., MIN, L. Q., LUAN, Q. X., LI, X. & LIU, J. Z. Year. Dental plaque classification using FCM-based classification in HIS color space. *In:* Proceedings on the 2007 international conference on Wavelet Analysis and Pattern recognition 2-4 Nov. 2007 Beijing, China. 78-81.

KAPUR, J., N,, SAHOO, P. K. & WONG, A. C. K. 1985. A New Method for Gray-Level Picture Thresholding Using the Entropy of the Histogram. *Graphical Models and Image Processing,* 29**,** 273-285.

KATAYAMA, T., SUZUKI, T. & OKADA, S. 1975. Clinical observation of dental plaque maturation. Application of oxidation-reduction indicator dyes. *Journal of Periodontology,* 46**,** 610-613.

KELLY, A., ANTONIO, A. G., MAIA, L. C., LUIZ, R. R., VIANNA, R. B. & QUINTANILHA, L. E. 2008. Reliability assessment of a plaque scoring index using photographs. *Methods of Information in Medicine,* 47**,** 443-447.

KELLY, M., STEELE, J., NUTALL, N., BRADNOCK, G., MORRIS, J., NUNN, J., PINE, C., PITTS, N., TREASURE, E. & WHITE, D. 2000. Adult Dental health Survey-Oral Health in the United Kingdom 1998. *London: the stationary office*.

KENG, S. & LIM, M. 1996. Denture plaque distribution and the effectiveness of a perborate-containing denture cleanser. *Quintessence International,* 27**,** 341-345.

KIDD, E. A. M. 2005. *Essentials of dental caries,* New York, Oxford University Press.

KIESER, J. B. & WADE, A. B. 1976. Use of food colourants as plaque disclosing agents. *Journal of Clinical Periodontology,* 3**,** 200-207.

KITTLER, J. & LLINGWORTH, J. 1986. Minimum error thresholding. *Pattern Recognition,* 19**,** 41-47.

LADEIRA, D. B. S., CRUZ, A. D. D., ALMEIDA, S. M. D. & BÓSCOLO, F. N. 2010. Evaluation of the panoramic image formation in different anatomic positions. *Brazilian Dental Journal,* 21**,** 458-462.

LAINE, M. A. 2002. Effect of pregnancy on periodontal and dental health. *Acta Odontologica Scandinavica,* 60**,** 257-264.

LANG, N. P., ATTSTRÖM, R. & HARALD, L. 1998. Assessments of periodontal health and disease. *Proceedings of the European workshop on mechanical plaque control.* Switzerland: Quintessence Publishing Co. Inc.

LANG, N. P., CUMMING, B. R. & LOE, H. 1973. Toothbrushing frequency as it relates to plaque development and gingival health. *Journal of Periodontology,* 44**,** 396-405.

LANG, N. P., OSTERGAARD, E. & LOE, H. 1972. A fluorescent plaque disclosing agent. *Journal of Periodontal Research,* 7**,** 59-67.

LEVINKIND, M., OWENS, J., MOREA, C., ADDY, M., LANG, N. P., ADAIR, R. & BARTON, I. 1999. The development and validation of an occlusal site-specific plaque index to evaluate the effects of cleaning by tooth brushes and chewing gum. *Journal of Clinical Periodontology,* 26**,** 177-182.

LI, C. H. & LEE, C. K. 1993. Minimum Cross Entropy Thresholding *Pattern Recognition,* 26**,** 617-625.

LI, C. H. & TAM, P. K. S. 1998. An Iterative Algorithm for Minimum Cross Entropy Thresholding. *Pattern Recognition Letters,* 18**,** 771-776.

LILIENTHAL, B., AMERENA, V. & GREGORY, G. 2004. An epidemiological study of chronic periodontal disease. *Archives of Oral Biology,* 10**,** 553-566.

LINDHE, J., AXELSSON, P. & TOLLSKOG, G. 1975. Effect of proper oral hygiene on gingivitis and dental caries in Swedish schoolchildren. *Community Dentistry and Oral Epidemiology,* 3**,** 150-155.

LÖE, H. 1967. The Gingival Index, the Plaque Index and the Retention Index Systems. *Journal Periodontology,* 38**,** Suppl:610-616.

LÖE, H. & KLEINMAN, D. V. 1986. Mechanical Oral Hygiene practices. *Dental Plaque Control Measures and Oral Hygiene Practices: Proceedings from A State-Of-The-Science Workshop* IRL Press Ltd.

LOVATO, C., OLIVEIRA, H. & ITO, I. 2002. Biofilm disclosing agents in complete denture: clinical and antimicrobial evaluation. *Pesquisa Odontologica Brasileira,* 16**,** 270-275.

MAGER, D. L., XIMENEZ-FYVIE, L. A., HAFFAJEE, A. D. & SOCRANSKY, S. S. 2003. Distribution of selected bacterial species on intraoral surfaces. *Journal of Clinical Periodontology,* 30**,** 644-654.

MAHESHWARI, A. & KUMAR, M. 2011. Photographic implication and basis of camera lens. *Annals and Essences of Dentistry,* 3**,** 95-99.

MANDEL, L. D. 1974. Indices for measurement of soft accumulations in clinical studies of oral hygiene and periodontal disease *Journal of Periodontal Research* 9**,** 7-30.

MANN, H. B. & WHITNEY, D. R. 1947. On a Test of Whether one of Two Random Variables is Stochastically Larger than the Other. *Annals of Mathematical Statistics,* 18**,** 50-60.

MANSON, J. D. 1986. *Periodontics,* London, Kimpton Medical Publications.

MANSON, J. D. & ELEY, B. M. 2000. *Outline of Periodontics* Butterworth-Heinemann.

MARANA, A. N., BARBOZA, E. B., PAPA, J. P., HOFER, M. & OLIVEIRA, D. T. 2011. Dental Biometrics for Human Identification. *Dental Biometrics for Human Identification, Biometrics - Unique and Diverse Applications in Nature, Science, and Technology***,** 41-56.

MARKS, R. G., MAGNUSSON, I., TAYLOR, M., CLOUSER, B., MARUNIAK, J. & CLARK, W. B. 1993. Evaluation of reliability and reproducibility of dental indices. *Journal of Clinical Periodontology,* 20**,** 54-58.

MARSH, P. D. 1992. Microbiological Aspects of the Chemical Control of Plaque and Gingivitis. *Journal of Dental Research,* 71**,** 1431-1438.

MARSH, P. D. 1994. Microbial ecology of dental plaque and its significance in health and disease. *Advances in Dental Research,* 8**,** 263-271.

MARSH, P. D. 2003. Plaque as a biofilm: pharmacological principles of drug delivery and action in the sub- and supragingival environment. *Oral Diseases,* 9**,** 16-22.

MATTHIJS, S., SABZEVAR, M. M. & ADRIAENS, P. A. 2001. Intra-examiner reproducibility of 4 dental plaque indices. *Journal of Clinical Periodontology,* 28**,** 250-254.

MCCABE, J. M., MURRAY, D., KELLY, J. L. & KELLY, P. J. 1996. A method for scofing denture plaque. *European Journal of Restorative Dentistry,* 4**,** 59-64.

MCCANN, D., BARRETT, A., COOPER, A., CRUMPLER, D., DALEN, L., GRIMSHAW, K., KITCHIN, E., LOK, K., PORTEOUS, L., PRINCE, E., SONUGA-BARKE, E., WARNER, J. O. & STEVENSON, J. 2007. Food additives and hyperactive behaviour in 3-year-old and 8/9-year-old children in the community: a randomised, double-blinded, placebo-controlled trial. . *Lancet,* 370**,** 1560-1567.

MCCARTY, G. A. 1976. Intraoral infrared color photography of radiotherapy patients. *Journal of Prosthetetic Dentistry,* 35**,** 327-331.

MCCRACKEN, G. I., HEASMAN, L., STACEY, F., STEEN, N., DE-JAGER, M. & HEASMAN, P. A. 2002a. Testing the efficacy of 2 prototype brush heads for a powered toothbrush: refining the model. *Journal of Clinical Periodontology,* 29**,** 42-7.

MCCRACKEN, G. I., JANSSEN, J., STEEN, N., DE-JAGER, M. & HEASMAN, P. A. 2002b. A clinical evaluation of a novel data logger to determine compliance with the use of powered toothbrushes. *Journal of Clinical Periodontology,* 29**,** 838-843.

MCCRACKEN, G. I., PRESHAW, P. M., STEEN, I. N., SWAN, M., DE-JAGER, M. & HEASMAN, P. A. 2006. Measuring plaque in clinical trials: index or weight? *Journal of Clinical Periodontology,* 33**,** 172-6.

MOUNT, G. J. 2005. Defining, Classifying, and Placing Incipient Caries Lesions in Perspective. *Dental Clinics of North America,* 49**,** 701-723.

NASSAU, K. 1998. *Fundamentals of colour science in Colour for science, art and technology,* The Netherlands, Elsevier science BV.

NETUSCHIL, L., PREISLER, R. & BRECX, M. 1995. Plaque bacteria counts and vitality during clorhexidine Meridol and Listerine mouthrinses. *European Journal of Oral Sciences,* 103**,** 355-361.

NEVALAINEN, M. J., NÄRHI, T. O. & AINAMO, A. 1997. Oral mucosal lesions and oral hygiene habits in the home-living elderly. *Journal of Oral Rehabilitation,* 24**,** 332-337.

NHS & DEPARTMENT OF HEALTH. 2011. National expenditure data. *Programme budgeting tools and data* [Online]. Available: http://www.dh.gov.uk/en/Managingyourorganisation/Financeandplanning/Programmebudgeting/DH_075743#_2 [Accessed September 2011].

NIKAWA, H., HAMADA, T. & YAMAMOTO, T. 1998. Dentrure plaque- past and recent concerns. Review. . *The Journal of Dentistry,* 26**,** 299-304.

NIKAWA, H., HAMADA, T., YAMASHIRO, H. & KUMAGAI, H. 1999. A review of in vitro and in vivo methods to evaluate the efficacy of denture cleansers. *International Journal of Prosthodontics,* 12**,** 153-159.

NORDIC, C. O. M. 2002. Food Additives in Europe. *TemaNord.*

NORDSTROM, N., PAIKOFF, E., ULDRICKS, J., SOLT, C., BURCHS, J. & BECK, F. M. 1988. Testin reliability of plaque and gingival indices. Two methods. *Journal of Periodontology,* 59**,** 270-273.

NUTTALL, N. M., STEELE, J. G., PINE, C. M., WHITE, D. & PITTS, N. B. 2001. Adult dental health survey: The impact of oral health on people in the UK in 1998. *Br Dent J,* 190**,** 121-126.

O'DOWD, L. K., DURHAM, J., MCCRACKEN, G. I. & PRESHAW, P. M. 2010. Patients' experiences of the impact of periodontal disease. *Journal of Clinical Periodontology,* 37**,** 334-339.

O'LEARY, T. J., DRAKE, R. B. & NAYLOR, J. E. 1972. The plaque control record. *Journal of Periodontology,* 43**,** 38.

OECD, H. D. 2010. Health at a Glance 2010-OECD indicators. Available: http://www.oecd.org/document/14/0,3343,en_2649_33929_16502667_1_1_1_37407,00.html.

OTSU, N. 1979. A threshold selection method from gray-level histograms. *IEEE Trans. Sys., Man., Cyber,* 9**,** 62-66.

PAGE, R. C. 1986. Gingivitis. *Journal of Clinical Periodontology,* 13**,** 345-355.

PARAHITIYAWA, N. B., SCULLY, C., LEUNG, W. K., YAM, W. C., JIN, L. J. & SAMARANAYAKE, L. P. 2010. Exploring the oral bacterial flora: current status and future directions. *Oral Diseases,* 16**,** 136-145.

PARANHOS, H. D. F. O., LOVATO DA SILVA, C. H., DE SOUZA, R. F. & PONTES, K. M. D. F. 2010. Evaluation of three indices for biofilm accumulation on complete dentures. *Gerodontology,* 27**,** 33-40.

PARANHOS, H. D. F. O. & SILVA, C. H. L. D. 2004. Comparative study of methods for the quantification of biofilm on complete dentures. *Brazilian Oral Research,* 18**,** 215-223.

PARANHOS, H. F. O., LOVATO DA SILVA, C. H. & CRUZ, P. C. 2004. Metodos de quantificacao de biofilme em protese total: Revisao da literatura. *Revista de Odontologia da UNEST,* 33**,** 203-201.

PAREDES, V., GANDIA, J. L. & CIBRIAN, R. 2006. Determination of Bolton tooth-size ratios by digitization, and comparison with the traditional method. *The European Journal of Orthodontics,* 28**,** 120-125.

PAVIA, D., LAMPMAN, G. M. & KRIZ, G. S. 1996. *Introduction to Spectroscopy,* Philadelphia USA, Sauders College Publishing.

PAVIA, D., LAMPMAN, G. M. & KRIZ, G. S. 2001. *Introduction to Spectroscopy,* USA.

PERACINI, A., ANDRADE, I. M. D., PARANHOS, H. D. F. O., SILVA, C. H. L. D. & SOUZA, R. F. D. 2010. Behaviors and hygiene habits of complete denture wearers. *Brazilian Dental Journal,* 21**,** 247-252.

PETERSEN, P. E. 2003. The World Oral Health Report 2003: continuous improvement of oral health in the 21st century - the approach of the WHO Global Oral Health Programme. . *Community Dental Oral Epidemiology 2003* [Online], 31(suppl. 1). Available:

http://www.who.int/oral_health/media/en/orh_report03_en.pdf [Accessed September 2011].

PETERSEN, P. E. & KAWAND, S. 2009. World Health Organisation global oral health strategies for oral health promotion and disease prevention in the twenty-first century. . *Präv Gesundheitsf,* 4**,** 100-104.

PETERSEN, P. E. & YAMAMOTO, T. 2005. Improving the oral health of older people: the approach of the WHO Global Oral Health Programme. *Community Dentistry and Oral Epidemiology,* 33**,** 81-92.

PHAM, D., XU, C. & PRINCE, J. 2000. Current methods in medical image segmentation. *Annual Review of Biomedical Engineering,* 2**,** 315-337.

PIHLSTROM, B. L., MICHALOWICZ, B. S. & JOHNSON, N. W. 2005. Periodontal diseases. *The Lancet,* 366**,** 1809-1820.

PITTS, N. & HARKER, R. 2005. Obvious decay experience: Children's dental health in the United Kingdom 2003 *Office for National Statistics, London*.

PLÜSS, E. M., ENGELBERGER, P. R. & RATEITSCAK, K. H. 1974. Effect of chlorhexidine on dental plaque formation under periodontal pack *Journal of Clinical Periodontology* 2**,** 136-142.

PODSHADLEY, A. G. & HALEY, J. V. 1968. A method for evaluating oral hygiene performance. *Public Health Reports,* 83**,** 259-64.

PRETTY, I. A., EDGAR, W. M. & HIGHAM, S. M. 2004. A study to assess the efficacy of a new detergent free, whitening dentifrice in vivo using QLF planimetric analysis. *British Dental Journal,* 197**,** 561-6; discussion 551.

PRETTY, I. A., EDGAR, W. M., SMITH, P. W. & HIGHAM, S. M. 2005. Quantification of dental plaque in the research environment. *Journal of Dentistry,* 33**,** 193-207.

PRETTY, I. A. & MAUPOME, G. 2004. A closer look at diagnosis in clinical dental practice: part 1. Reliability, validity, specificity and sensitivity of diagnostic procedures. *Journal of Canadian Dental Association,* 70**,** 251-255.

PREWITT, J. M. S. & MENDENLSOHN, M. L. 1966. The analysis of cell images. *Annals of New York Academy of Sciences,* 128**,** 1035-1053.

QUIGLEY, G. A. & HEIN, J. W. 1962. Comparative cleansing efficiency of manual and power brushing *Journal of the American Dental Association* 65**,** 26-29.

QUINTERO, J. C., TROSIEN, A., HATCHER, D. & KAPILA, S. 1999. Craniofacial imaging in orthodontics: Historical perspective, current status, and future developments. *The Angle Orthodontist,* 69**,** 491-506.

RAGGIO, P. D., BRAGA, M. M., RODRIGUES, J. A., FREITAS, P. M., IMPARATO, J. C. & MENDES, F. 2010. Reliability and discriminatory power of methods for dental plaque quantification. *Journal of Applied Oral Sciences,* 18**,** 186-193.

RAMFJORD, S. 1956. Indices for prevalence and incidence of periodontal disease *Journal of Periodontology* 30**,** 51-59.

RASBAND, W. & LANDINI, G. 2004. *Calculator Plus, ImageJ* [Online]. Available: http://rsbweb.nih.gov/ij/plugins/calculator-plus.html [Accessed September 2011].

RASOOLY, R. 2005. Expanding the bactericidal action of the food color additive phloxine B to gram-negative bacteria. *FEMS Immunology & Medical Microbiology,* 45**,** 239-244.

RASOOLY, R. 2007. Phloxine B, a versatile bacterial stain. *FEMS Immunology & Medical Microbiology,* 49**,** 261-265.

REISINE, S. T. 1985. Dental health and public policy: the social impact of dental disease. *American Journal of Public Health,* 75**,** 27-30.

REKOLA, M. & SCHEININ, A. 1977. Quantification of dental plaque through planimetric analysis. *Scandinavian Journal of Dental Research,* 85**,** 51-55.

RIDLER, T. W. & CALVARD, S. 1978. Picture thresholding using an iterative selection method. *IEEE Transactions on Systems, Man and Cybernetics,* 8**,** 630-632.

RUIFROK, A. C. & JOHNSTON, D. A. 2001. Quantification of histochemical staining by color deconvolution. *Analitical and Quantitative Cytology and Histology,* 23**,** 291-299.

RUSS, J. C. 1995. *The image Processing handbook,* Florida, CRC Press, Inc.

RUSTOGI, K. N., CURTIS, J. P., VOLPE, A. R., KEMP, J. H., MCCOOL, J. J. & KORN, L. R. 1992. Refinement of the Modified Navy Plaque Index to increase plaque scoring efficiency in gumline and interproximal tooth areas. *Journal of Clinical Dentistry,* 3**,** C9-12.

RÜTTERMANN, S., RITTER, J., RAAB, W. H. M., BAYER, R. & JANDA, R. 2007. Laser-induced fluorescence to discriminate between a dental composite resin and tooth. *Dental Materials,* 23**,** 1390-1396.

SAFETY OFFICER IN PHYSICAL CHEMISTRY. 2010. Safety data for methylene blue. *The Physical and Theoretical chemistry laboratory, Oxford University, chemical and other safety information* [Online]. Available: http://msds.chem.ox.ac.uk/ME/methylene_blue.html [Accessed September 2011].

SAGEL, P. A., LAPUJADE, P. G., MILLER, J. M. & SUNBERG, R. J. 2000. Objective quantification of plaque using digital image analysis. *Monograms of Oral Science,* 17**,** 130-143.

SAKAI, N. 2011. *Comparison between tooth mesiodistal angulation measurements from constructed panoramic images and three dimensional volumentric images.* Master of Science, University of Southern California.

SAXER, U. P. & YANKELL, S. L. 1997. Impact of improved toothbrushes on dental diseases. *Quintessence International,* 28**,** 513-525.

SCHUG, J., SCHULLER, W.-P., KAPPEN, C., SALBAUM, J. M., BUCAN, M. & STOECKERT, C. 2005. Promoter features related to tissue specificity as measured by Shannon entropy. *Genome Biology,* 6**,** R33.

SCHUMACHER, G. H., SCHMIDT, H. & RICHTER, W. 1976. *Anatomie und Biochemie der Zähne*, G. Fischer.

SEYMOUR, G. J., FORD, P. J., CULLINAN, M. P., LEISHMAN, S. & YAMAZAKI, K. 2007. Relationship between periodontal infections and systemic disease. *Clinical Microbiology and Infection,* 13**,** 3-10.

SEYMOUR, R. A. & HEASMAN, P. A. 1992. *Drug, diseases and the periodontium,* New York, Oxford University Press.

SEZGIN, M. & SANKUR, B. 2004. Survey over Image Thresholding Techniques and Quantitative Performance Evaluation. *Journal of Electronic Imaging,* 13**,** 146-166.

SGAN-COHEN, H. D. 2005. Oral hygiene: past history and future recommendations. *International Journal of Dental Hygiene,* 3**,** 54-58.

SHALOUB, A. & ADDY, M. 2000. Evaluation of accuracy and variability of scoring-area-based plaque indices. *Journal of Clinical Periodontology,* 27**,** 16-21.

SHANBHAG & ABHIJIT, G. 1994. Utilization of information measure as a means of image thresholding". *CVGIP: Graphical Models and Image Processing,* 56**,** 414-419.

SHANNON, C. E. 1948. A mathematical theory of communication. *Bell system technical journal,* 27**,** 379-423, 627-656.

SHIAU, H. J. & REYNOLDS, M. A. 2010. Sex Differences in Destructive Periodontal Disease: A Systematic Review. *Journal of Periodontology,* 81**,** 1379-1389.

SHICK, R. S. & ASH, M. M. 1961. Evaluation of the vertical method of toothbrushing *Journal of Periodontology* 32**,** 346-353.

SILNESS, J. & LOE, H. 1964. Periodontal Disease in Pregnancy. II. Correlation between Oral Hygiene and Periodontal Condition. *Acta Odontologica Scandinava,* 22**,** 121-135.

SILVA-LOVATO, C. H., TOTTI, A. M. G., PARANHOS, H. F. O. & TOTTI, V. G. 2009. Evaluation of a Computerized Method for Denture Biofilm Quantification: Inter-Examiner Reproducibility. *Journal of Prosthodontics,* 18**,** 332-336.

SIM, J. & WRIGHT, C. 2005. The kappa statistic in reliability studies: use, interpretatio , and sample size requirements. *Physical Therapy Journal,* 85**,** 257-268.

SIMON, R. 2003. Adverse reactions to food additives. *Current Allergy and Asthma Reports,* 3**,** 62-66.

SKINNER, F. H. 1914. The prevention of pyorrhea and dental caries by oral prophylaxis *Dental Cosmos* 56**,** 293-309.

SKOOG, D. A., WEST, D. M. & HOLLER, F. J. 1994. *Analytical Chemistry: An introduction,* USA, Saunders College Publishing.

SMITH, R. N., BROOK, A. H. & ELCOCK, C. 2001. The quantification of dental plaque using an image analysis system: reliability and validation. *Journal of Clinical Periodontology,* 28**,** 1158-1162.

SMITH, R. N., RAWLINSON, A., LATH, D., ELCOCK, C., WALSH, T. F. & BROOK, A. H. 2004. Quantification of dental plaque on lingual tooth surfaces using image analysis: reliability and validation. *Journal of Clinical Periodontology,* 31**,** 569-573.

SMITH, R. N., RAWLINSON, A., LATH, D. L. & BROOK, A. H. 2006. A digital SLR or intra-oral camera: preference for acquisition within an image analysis system for measurement of disclosed dental plaque area within clinical trials. *Journal of Periodontal Research,* 41**,** 55-61.

SÖDER, B., JOHANNSEN, A. & LAGERLÖF, F. 2003. Percent of plaque on individual tooth surfaces and differences in plaque area between adjacent teeth in healthy adults. *International Journal of Dental Hygiene,* 1**,** 22-28.

SÖDER, P. O., JIN, L. J. & SODER, B. 1993. Computerized planimetric method for clinical plaque measurement. *Scandinavian Journal of Dental Research,* 101**,** 21-25.

SPLIETH, C. H. & NOURALLAH, A. W. 2006. An occlusal plaque index. Measurements of repeatability, reproducibility, and sensitivity. *American Journal of Dentistry,* 19**,** 135-137.

STAUDT, C. B., KINZEL, S., HASSFELD, S., STEIN, W., STAEHLE, H. J. & DORFER, C. E. 2001. Computer-based intraoral image analysis of the clinical plaque removing capacity of 3 manual toothbrushes. *Journal of Clinical Periodontology,* 28**,** 746-752.

STERRETT, J. D., OLIVER, T., ROBINSON, F., FORTSON, W., KNAAK, B. & RUSSELL, C. M. 1999. Width/length ratios of normal clinical crowns of the maxillary anterior dentition in man. *Journal of Clinical Periodontology,* 26**,** 153-157.

STOOKEY, G. K. 2004. Optical Methods—Quantitative Light Fluorescence. *Journal of Dental Research,* 83**,** C84-C88.

STOOKEY, G. K. 2005. Quantitative light fluorescence: a technology for early monitoring of the caries process. *Dental Clinics of North America,* 49**,** 753-70.

STRAIT, B. J. & DEWEY, T. G. 1996. The Shannon information entropy of protein sequences. *Biophysical Journal,* 71**,** 148-155.

TAN, A. E. 1981. Disclosing agents in plaque control: a review. *Journal of the Western Society of Periodontology Periodontal Abstracts,* 29**,** 81-86.

TARBET, W. J. 1982. Denture plaque: Quiet destroyer. *The Journal of Prosthetic Dentistry,* 48**,** 647-652.

TEN CATE, J. M. 2006. Biofilms, a new approach to the microbiology of dental plaque. *Odontology,* 94**,** 1-9.

TETLEY, C. & YOUNG, S. 2007. Digital Infrared and ultraviolet imaging Part 1: Infrared. *Journal of Visual Communication,* 30**,** 162-171.

THE EUROPEAN COMMISSION FOR FOOD SAFETY. 1994. *Food additives and flavourings* [Online]. Available: http://ec.europa.eu/food/fs/sfp/flav_index_en.html [Accessed September 2011].

THE NHS INFORMATION CENTRE, D. A. E. C. T. 2010. Adult Dental Health Survey 2009 –first release. *The Health and Social Care Information Centre* [Online]. Available: http://www.ic.nhs.uk/webfiles/publications/007_Primary_Care/Dentistry/dentalsurvey09/Adult_Dental_Health_Survey_2009_FirstRelease.pdf [Accessed September 2011].

THE NHS INFORMATION CENTRE, D. A. E. C. T. 2011. Adul Dental Health Survey 2009-2: disease and related disorders- a report from the Adult Dental Health Survey 2009. *The Health and Social Care Information Centre.*

THOMAS, M. J. 1996. *Ultraviolet and visible spectroscopy,* West Sussex, England, John Wiley & Sons Ltd.

TOMASSETTI, J. J., TALOUMIS, L. J., DENNY, J. M. & FISCHER, J. 2003. A comparison of 3 computerized bolton tooth-size analysis with a commonly used method. *The Angle Orthodontist,* 7**,** 351-357.

TRANÆUS, S., HEINRICH-WELTZIEN, R., KÜHNISCH, J., STÖSSER, L. & ANGMAR-MÅNSSON, B. 2001. Potential Applications and Limitations of Quantitative Light-induced Fluorescence in Dentistry. *Medical Laser Application,* 16**,** 195-204.

TRANÆUS, S., SHI, X.-Q. & ANGMAR-MÅNSSON, B. 2005. Caries risk assessment: methods available to clinicians for caries detection. *Community Dentistry and Oral Epidemiology,* 33**,** 265-273.

TRAPP, L. D., NOBLE, W. H., NAVARRO, R. & GREEN, E. 1975. Objective quantification method for measuring in vivo accumulated dental plaque. *Journal Dental Research,* 54**,** 164-167.

TSAI, W. 1985. Moment-preserving thresholding: a new approach. *Computer Vision, Graphics, and Image Processing,* 29**,** 377-393.

TURESKY, S., GILMORE, N. D. & GLICKMAN, I. 1970. Reduced plaque formation by the chloromethyl analogue of victamine C. *Journal of Periodontology,* 41**,** 41-43.

URAGO, A. 1991. *Ageing changes of the oral tissues,* Tokio, Japan, Quintessence Publishing.

US DEPARTMENT, O. H. A. H. S. 2000. Oral Health in America: A Report of the Surgeon General.

VAN DER WEIJDEN, G. A., TIMMERMAN, M. F., NIJBOER, A., LIE, M. A. & VAN DER VELDEN, U. 1993. A comparative study of electric toothbrushes for the effectiveness of plaque removal in relation to toothbrushing duration. Timerstudy. *Journal of Clinical Periodontology,* 20**,** 476-481.

VANDER HAEGHEN, Y. 2007. *C4Real, realistic, web-ready sRGB pictures from your digital camera* [Online]. Available: http://www.c4real.biz/Introduction.aspx [Accessed June 2011].

VENKATARAMAN, K. 1952. *The chemistry of synthetic dyes,* New York, USA., Academic Press INC.

VERRAN, J. & ROCLIFFE, M. D. 1986. Feasibility of using automatic image analysis for measuring dental plaque in situ. *Journal of Dentistry,* 14**,** 11-3.

VERRAN, J. A. 1986. Patient classification in ambulatory care. *Nurs Econ,* 4**,** 247-51.

VETTER, J. P. 1992. *Medical photography,* Boston, USA, Butterworth-Heinemann.

WAITE, J. G. & YOUSEF, A. E. 2009. Chapter 3 Antimicrobial Properties of Hydroxyxanthenes. *In:* ALLEN, I. L., SIMA, S. & GEOFFREY, M. G. (eds.) *Advances in Applied Microbiology.* Academic Press.

WALL, S., KAZAHAYA, K., BECKER, S. S. & BECKER, D. G. 1999. Thirty-Five Millimeter versus Digital Photography: Comparison of Photographic Quality and Clinical Evaluation. *Facial plast Surg,* 15**,** 101,109.

WEIGER, R., NETUSCHIL, L. & BRECX, M. 1992. Comparison of early human dental plaque formation on vestibular and approximal enamel surfaces *in situ*. *The Journal of the Western Society of Periodontology,* 4**,** 101-104.

WILCOXON, F. 1945. Individual Comparisons by Ranking Methods. *Biometrics Bulletin,* 1**,** 80-83.

WILLIAMS, R. 1984. *Medical photography study guide,* Lancaster, MTP Press Limited.

WILLIAMS, R. & WILLIAMS, G. 2002. Medical and scientific photography: an oline resource for doctors, scientists and students. Available: http://www.msp.rmit.edu.au/index.html [Accessed September 2011].

WILSON, J., FIRNHABER, R. & KUTCHER, M. J. 1992. Computer-aided analysis of intraoral ulcerative lesions. *Oral Surgery, Oral Medicine, Oral Pathology,* 74**,** 393-399.

WITHEY, D. J. & KOLES, Z. J. 2008. A review of medical image segmentation: Methods and available software. *International Journal of Bioelectromagnetism,* 10**,** 125-148.

WOLFFE, G. N. 1976. An evaluation of proximal surface cleansing agents. *Journal of Clinical Periodontology,* 3**,** 148-156.

WONG, C. H. & WADE, A. B. 1985. A comparative study of effectiveness in plaque removal by Super Floss and waxed dental floss. *Journal of Clinical Periodontology,* 12**,** 788-795.

WOOTTON, R., SPRINGALL, D. R. & POLAK, J. M. 1995. *Image analysis in histology: conventional and confocal microscopy.,* Cambridge, Postgraduate medical science, Cambridge University Press.

WORLD HEALTH ORGANIZATION, T. 2010. National health accounts.

WU, J. & FRIED, D. 2009. High contrast near-infrared polarised reflectance images of demineralization on tooth buccal and occlusal surfaces at λ=1310nm. *Lasers in Surgery and Medicine,* 41**,** 208-213.

YANG, J. & DUTRA, V. 2005. Utility of Radiology, Laser Fluorescence, and Transillumination. *Dental Clinics of North America,* 49**,** 739-752.

YAP POTTER, R. H. 1972. Univariate Versus Multivariate Differences in Tooth Size According to Sex. *Journal of Dental Research,* 51**,** 716-722.

YEGANEH, S., LYNCH, E., JOVANOVSKI, V. & ZOU, L. 1999. Quantification of root surface plaque using a new 3-d laser scanning method. *Journal of Clinical Periodontology* 26**,** 692-697.

YEGANEH, S., ZOU, L., JOVANOVSKI, V. & LYNCH, E. 1995. A novel method of three-dimensional quantification of plaque in vivo. *Journal Dental Research* 75**,** 124.

YEN, J. C., CHANG, F. J. & CHANG, S. 1995. A New Criterion for Automatic Multilevel Thresholding", 4 *IEEE Transactions on Image Processing* 4**,** 370-378.

YOUNG, A. R. 2006. Acute effects of UVR on human eyes and skin. *Progress in Biophysics and Molecular Biology,* 92**,** 80-85.

YOUNG, I. T., GERBRANDS, J. & VAN VLIET, L. 1998. *Fundamentals of Image Processing,* Delf, Delft University of Technology.

ZACK, G. W., ROGERS, W. E. & LATT, S. A. 1977. Automatic measurement of sister chromatid exchange frequency. *Journal of Histochemistry and Cytochemistry,* 25**,** 741-753.